

Innate immune activity in endometrial epithelial cells: implication for female fertility



Trinity College Dublin
Coláiste na Tríonóide, Baile Átha Cliath
The University of Dublin

**This thesis is submitted to The University of Dublin for the
degree of Doctor of Philosophy (Ph. D.)**

By

Federica Giangrazi, B.Sc., M.Sc.

School of Biochemistry and Immunology

Trinity College Dublin

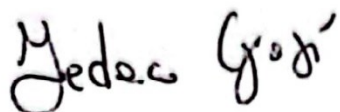
2023

Supervisors: Prof. Cliona O'Farrelly and Dr. Louise E. Glover

I declare that this thesis has not been submitted as an exercise for a degree at this or any other university and it is entirely my own work.

I agree to deposit this thesis in the University's open access institutional repository or allow the Library to do so on my behalf, subject to Irish Copyright Legislation and Trinity College Library conditions of use and acknowledgement.

I consent to the examiner retaining a copy of the thesis beyond the examining period, should they so wish (EU GDPR May 2018).

A handwritten signature in black ink, appearing to read "Federica Giangrazi". The signature is written in a cursive style with some stylized letters.

Federica Giangrazi

2022

General Abstract

The maternal local immune system is key to a successful pregnancy. Maternal immunity is required to initiate pregnancy related processes, whilst controlling and being active against any infections or malignancies that may occur. For these reasons, imbalanced immune activity in the endometrium can severely impact on pregnancy outcomes.

A master regulator of mucosal immunity is IL-17A, a cytokine produced by immune cells in response to bacterial and fungal infections. This pro-inflammatory cytokine induces epithelial and stromal cells to secrete antimicrobial peptides (AMPs), chemokines and matrix metalloproteases, responsible for infection clearance. IL-17A is also linked to several immune-mediated diseases such as psoriasis, arthritis, multiple sclerosis, where its highly pro-inflammatory signature is responsible for the symptomatology associated with these diseases, making this cytokine an excellent therapeutic target. The possible roles of IL-17A in female reproductive tract are poorly explored. It has been previously shown that women with unexplained infertility who failed to sustain a successful pregnancy after Assisted Reproductive Technologies (ART) showed higher level of IL-17A, both in the endometrium and systemically in blood circulation, therefore we aimed to explore the role of this cytokine in female fertility.

The IL-17 cytokines, IL-17A - IL-17F, share similar structures and functions. We hypothesized that IL-17A and the other cytokines belonging to the same family might have evolved functions related to female fertility in mammalian clades. To investigate this, synteny mapping, Multiple Sequence Alignment (MSA) and phylogeny were applied to the IL-17s belonging to representative species of the three mammalian clades (eutherian, metatherian and prototherian), confirming the similarities in the genomic organisation and in the protein sequences of all mammalian IL-17s. Furthermore, analysis of fertility-related datasets showed an upregulation of IL-17A transcript in metatherian pregnancy stages corresponding to placentation, whereas in eutherian mammals IL-17D expression is increased during placentation. Analyses also demonstrated upregulation of IL-17B and IL-17D in endometriosis, recurrent

implantation failure (RIF) and unexplained infertility when compared with healthy women, further emphasising a role for IL17 in female reproductive immunity.

The main producers of IL-17A are classically thought to be lymphoid populations such as T_H17, $\gamma\delta$ T-cells or ILC3 cells. Having shown that IL-17A was increased in our cohort of women with unexplained fertility, immune cell gene signature analysis of bulk RNA-seq from endometrial biopsies revealed that immune cell populations were similar in women with successful and unsuccessful pregnancies. We therefore hypothesised that endometrial epithelial cells were responsible for production of IL-17A in endometrial tissue from women with unexplained infertility. We focused initially on the Ishikawa immortalised endometrial epithelial cell line. Treatment of these cells with bacterial lipopolysaccharide (LPS) or the synthetic analogue of viral double stranded RNA virus poly(I:C) induced upregulation of IL-17A mRNA. IL-12B which in conjunction with IL-23A stimulates activation of ROR γ t, the transcription factor responsible for IL17 transcription, was also induced and flow cytometry confirmed ROR γ t protein positive staining in Ishikawa cells. Stimulation with recombinant IL-17A induced increased expression of AMPs and *CXCL8* in both Ishikawa cells and primary human endometrial epithelial cells (hEECs), obtained from endometrial biopsies.

Since IL-17A is produced in response to bacterial infections, we explored the uterine microbial composition in women with unexplained infertility from our study cohort. Bacterial DNA was extracted from endometrial biopsies taken from our cohort of women and subjected to 16S sequencing. This analysis identified a more diverse microbiome in the women with unsuccessful pregnancy outcome, with *Corynebacterium spp.* and *Prevotella spp.* significantly higher in those women. Given that a greater microbial diversity in bacterial vaginosis results in increased SCFAs, we wondered what effect SCFA might have on endometrial cells. Butyrate treatment of Ishikawa and hEECs cells induced increased expression of AMPs, cytokines such as *TNF α* and *IL-17A*, and chemokines, *CXCL8*. Butyrate treatment led also to the production of IL-17A, IL-8 and *TNF α* protein levels, confirming the ability of non-immune cells to produce IL-17A. By using selective inhibitors of HIF1 α and Nf- κ B, we demonstrated that these two pathways seem to be involved in butyrate induction of cytokines, chemokines and AMPs. Analysis of a chromatin immuno-precipitation (ChIP)-seq database identified a

butyrylation binding site upstream of the *IL-17A* gene, which also seemed to be confirmed by performing ChIP on Ishikawa cells treated with butyrate.

A role for IL-17A and butyrate in implantation was explored using models recapitulating the window of implantation. The changes induced during the window of implantation were mimicked by treating cells with progesterone with or without IL-17A. The presence of IL-17A during the maturation of epithelial cells seems to not impact on their receptivity, given that markers of endometrial receptivity such as *SPP1* and *ITGAV* show no changes in expression when IL-17A is added to the progesterone. However, IL-17A slightly reduced expression of stromal decidualisation markers such as *PRL* or *SPP1*. Butyrate seems to facilitate stromal cells decidualisation, as can be seen by the increase in *PRL* and *IGFBP1* expression when butyrate is added to the decidualisation media. Also, butyrate was shown to drive endometrial receptivity markers, as it can be noticed a significantly increased Expression of *SPP1* and *ITGAV* is significantly increase. *IL-15* and *LIF*, which are two markers used for detecting the window of implantation are also induced by butyrate in epithelial cells, but are decreased by butyrate in stromal cells.

In summary, we present evidence that IL-17A and other cytokines belonging to the same family, have roles in female fertility and that their expression is dysregulated in fertility complications. Furthermore, we find that endometrial epithelial cells contribute to local mucosal immune activity by producing IL-17A, contributing to a pro-inflammatory environment which is detrimental to fertility. Women who are not able to conceive despite ART had a different endometrial microbiome, which is likely to alter local metabolite environment. Among the stimulants that induce IL-17A production by endometrial epithelial cells in FRT is butyrate, a metabolite derived from microbial species, that can potentially regulate IL-17A expression by epigenetic modification. Also, high butyrate levels during endometrium maturation are associated with increased stromal cell decidualisation and epithelial receptivity markers. The mechanisms regulating the first stages of pregnancy are complex thus, further investigation on the local microbiome-induced immune mechanisms may provide novel therapeutic targets to improve female fertility.

Acknowledgments

I would first like to thank my two amazing supervisors: Prof. Cliona O'Farrelly and Dr. Louise Glover. Their collaboration for my supervision has been outstanding and they both were extremely supportive and honest throughout these years.

Cliona has welcomed me in her laboratory with so much enthusiasm, which she has kept for the entire duration of my PhD. I am very grateful of having had the opportunity to work in her group and to learn from her so much, not only from a scientific point of view, but also as a personal growth stimulated by such a wise and cultured person.

Louise also has been a great supervisor, giving me many practical hints from her experience on multiple techniques and helping me getting into the reproductive field from a medical point of view, also considering the patients' standpoint.

This PhD project would not have been possible without the help of Prof. Aoife McLysaght. She guided me in a very difficult moment and introduced me to Cliona, allowing me to pursue my PhD. I will be forever grateful for her help and guidance.

I would like to thank all the past and present members of the combined COF-FJS lab. They have been my second family considering how much time and fun moments we shared together throughout these years. Among others, special thanks go to Jamie and Mihai, our lab twins which are always ready for deep scientific conversation and cool project ideas, while preparing silly gags and pranks. I would also like to thank Mag and Sarah S., my COF ladies with which I spent so many enjoyable moments together and I have learnt so much, from understanding the weird ordering system in Trinity to the best practice in qPCR setup.

I cannot not mention Simone, who has supported me for these years in so many ways: celebrating the joys with me, standing on my side during tough moments, feeding me when I got home late from the lab, making me laugh when I was overstressed. He was a very patient director, making sure I could make this PhD happen by helping me behind the scenes, and I am very thankful for this.

I would also like to thank my parents for being my very first fans, supporting me since my first steps in science. They always believed in me and, at the same time, helped me seeing things from a practical standpoint, to compensate my daydreamer attitude. Despite the physical distance between us, they always find the way to share with me all the good and bad moments and I am very grateful for their constant support.

A big thank goes to all the technical staff in Trinity Biomedical Sciences Institute and all the other Professors who have helped me learning new approaches and setting up protocols. I would also like to thank all my friends which have always been present and made sure I would have a great time while doing my PhD.

Last, but not least, I would like to thank all the patients who kindly enrolled in the project and agreed to provide the endometrial biopsies.

Table of contents

General Abstract	3
Acknowledgments.....	6
Table of contents	8
List of figures.....	12
List of tables	14
Abbreviations	15
Chapter 1. General Introduction.....	17
1.1 <i>Anatomy and physiology of the female reproductive tract</i>	17
1.1.1 Ovaries.....	18
1.1.2 Fallopian tube	18
1.1.3 Uterus and endocervix	19
1.1.4 Cervix.....	20
1.1.5 Vagina	21
1.2 <i>Mucosal immune system in the female reproductive tract</i>	21
1.2.1 Immune cells involved in the mucosal activity in FRT	22
1.2.1.a Professional Antigen Presenting Cells (APCs)	22
1.2.1.b Neutrophils.....	23
1.2.1.c Innate Lymphoid Cells (ILCs)	24
1.2.1.d Natural killer (NK) cells	24
1.2.1.e T lymphocytes	25
1.3 <i>IL-17 family of cytokines and receptors</i>	26
1.3.1 Family members and signalling pathways activated	27
1.3.1.a IL-17A-IL-17RA signalling pathway	27
1.3.1.b IL-17RB signalling pathway.....	30
1.3.1.c IL-17RC signalling	30
1.3.1.d IL-17RD signalling	30
1.3.1.e IL-17RE signalling.....	31
1.3.2 Downstream gene targets of each IL-17.....	31
1.3.2.a IL-17A.....	31
1.3.2.b IL-17B.....	32
1.3.2.c IL-17C.....	32
1.3.2.d IL-17D	33
1.3.2.e IL-25.....	33
1.3.2.f IL-17F.....	33
1.4 <i>Sources of IL-17s cytokines</i>	34
1.4.1 Immune cells production of IL-17s	34
1.4.2 Non-immune cellular source for IL-17s	35
1.4.3 Transcription factors responsible for IL-17s transcription.....	35
1.5 <i>IL-17s in Health and disease</i>	37
1.5.1 Roles in inflammation.....	37
1.5.2 Roles in health complications.....	39
1.5.3 Therapies targeting IL-17 pathway	41
1.6 <i>Role of inflammation in pregnancy</i>	42
1.6.1 Mediators required in early pro-inflammatory stage	42
1.6.2 Immunosuppressive stage throughout gestation.....	42
1.6.3 Inflammatory signals required for parturition.....	43
1.7 <i>Balance between “good” inflammation and “bad” inflammation in fertility</i>	44

1.8 Roles of IL-17s in female fertility and in pregnancy complications	45
1.8.1. Fertility complications	46
1.8.2. Pregnancy-related complications	48
1.9 Anti IL-17A therapies for female fertility	52
1.10 The microbiome in female reproductive tract	53
1.10.1. Vaginal microbiota	53
1.10.2 Uterine microbiota	54
1.11 Changes in the microbiota during pregnancy	55
1.12 The impact of microbiome in fertility	56
1.13 Epithelial cells: roles in defence and as mediators of microbiome and host interaction	58
1.13.1 Barrier function	59
1.13.2 Pattern Recognition Receptor expression	59
1.13.3 Antigen presentation	61
1.13.4 Antimicrobial peptides (AMPs) secretion	61
1.13.5 Cytokine and chemokine secretion	62
1.14 Overall Rationale and Aims	63
Chapter 2. Materials and Methods	66
2.1 PATIENT RECRUITMENT	66
2.1.2. Subjects for primary epithelial and stromal cell isolation	66
2.1.3. Subjects for the 16S-sequencing and immune cell abundance estimation	67
2.2 COMPUTATIONAL BIOLOGY TECHNIQUES	68
2.2.1 Databases	68
2.2.2 Identification of IL-17 proteins	69
2.2.2.a Search using Genome Browsers for IL-17 proteins	69
2.2.2.b Reciprocal Best Hits analysis	69
2.2.3 Protein analysis	70
2.2.3.a Multiple sequence alignment	70
2.2.3.b Phylogenetic analysis	70
2.2.3.b Protein modelling	70
2.2.4 Genetic analysis of IL-17 genes between mammals	73
2.2.4.a Identification of IL-17 genes	73
2.2.4.b Identification of gene conservation using synteny	73
2.2.5 Transcriptomic analysis and cell population abundance estimation	74
2.2.5.a Transcriptomic analysis	74
2.2.5.a Immune cell abundance estimation from a bulk RNA-seq dataset	75
2.2.6 ChIP-seq analysis	77
2.2.7 Peak identification in the corresponding human sequence	77
2.3 WET LABORATORY TECHNIQUES	78
2.3.1 Immortalised cell culture	78
2.3.2 Primary endometrial epithelial and stromal cell isolation	79
2.3.3 Hormonal treatment to induce endometrial receptivity	81
2.3.3.a Decidualisation model in primary hESCs	81
2.3.3.b Receptivity model in Ishikawa cells	81
2.3.4 Viability assays	82
2.3.5 Gene silencing	82
2.3.6 Chromatin Immuno-Precipitation (ChIP)	83
2.3.7 RNA-extraction and cDNA generation	85
2.3.8 qPCR	87
2.3.8.a Primer design and optimisation	87
2.3.8.b qPCR	89
2.3.8.c ChIP-qPCR	91
2.3.8.d Determination of cell markers for primary hEEC and hESCs and Ishikawa cells	93
2.3.9 Immunocytochemistry staining for epithelial and stromal cell markers	95
2.3.10 Flow cytometry	96

2.3.11 Enzyme-linked immunosorbent assay (ELISA).....	98
2.3.12 SDS-gel protein electrophoresis, western blotting and membrane staining.....	98
2.3.12.a SDS-gel protein electrophoresis	98
2.3.12.b Western blotting	99
2.3.12.c Immunostaining.....	99
2.3.13 16S-sequencing	100
2.3.13.a Bacterial DNA extraction	100
2.3.13.b 16S sequencing and data analysis	100
2.3.13 Statistical analysis.....	100
Chapter 3: Evolution of IL-17 family of cytokines and possible roles in placentation .	102
3.1 INTRODUCTION	102
3.1.1 Organization of mammalian groups.....	102
3.1.2 Characteristics of mammalian pregnancy	103
3.1.2.a Embryonic development in fertilised eggs	103
3.1.2.b Maternal recognition of pregnancy.....	103
3.1.2.c Placentation.....	104
3.1.2.d Partuition.....	105
3.1.3 Involvement of immune response in mammalian pregnancy	106
3.1.4 Evolution of mammalian pregnancy.....	107
3.1.5 Involvement of IL-17s in inflammatory diseases.....	108
3.1.7 Involvement of IL-17s in mammalian pregnancy and fertility.....	108
3.2 HYPOTHESIS AND AIMS	109
3.3 RESULTS	110
3.3.1 IL-17s genes are conserved and syntenic among mammals	110
3.3.2 IL-17s protein are conserved in the three mammalian clades with high percentage identity.	112
3.3.3 IL-17F in prototherian is significantly different from the human ortholog in terms of amino acid composition in the important residues and 3D protein structure.	115
3.3.4 IL-17s are differentially expressed in female reproduction and fertility.	122
3.4 DISCUSSION.....	126
Chapter 4: IL-17A production by endometrial epithelial cells.....	130
4.1 INTRODUCTION	130
4.2 HYPOTHESIS AND AIMS	134
4.3 RESULTS	135
4.3.1 Immune cell population estimation in bulk RNA-sequencing identifies similarities between the two groups.....	135
4.3.2 LPS has little effect on endometrial epithelial cells.....	138
4.3.3 Endometrial epithelial cells produce IL-17A upon stimulation with viral ligands.....	139
4.3.4 ROR γ t signalling is present in endometrial epithelial cells.....	142
4.3.5 IL-17A induces a pro-inflammatory mucosal signature in endometrial epithelial cells	146
4.4 DISCUSSION.....	150
Chapter 5: The uterine microbiome and the microbial metabolite butyrate stimulate pro-inflammatory responses in the human female reproductive tract	155
5.1 INTRODUCTION	155
5.1.1 Microbial-derived metabolites in the FRT	155
5.1.1.a Lactic acid	155
5.1.1.b Short chain fatty acids.....	155
5.1.2 Bacterial species producing SCFAs	156
5.1.3 Mechanisms of SCFAs modulation on immunity.....	158
5.1.3.a Anti-inflammatory and protective actions in the gut	158
5.1.3.b Pro-inflammatory actions in the vagina	160
5.1.4 Crosstalk between mucosal responses and the microbiome.....	162

5.2 HYPOTHESIS AND AIMS	163
5.3 RESULTS	164
5.3.1 <i>A different microbiome is present in the biopsies from unsuccessful pregnancy women</i>	164
5.3.2 <i>Lactobacillus spp. abundance correlates with serum level of IL-17A</i>	166
5.3.3 <i>SCFAs induce a pro-inflammatory response in endometrial epithelial cells</i>	171
5.3.4 <i>Effect of butyrate stimulation on Nf-κB pathway in Ishikawa cells</i>	178
5.3.5 <i>Assessment of HIF1α pathway activation during butyrate stimulation</i>	180
5.3.6 <i>Assessment of epigenetic control induced by butyrate in endometrial epithelial cells</i>	182
5.3.7 <i>Butyrate does not activate S100A9 through IL-17A signalling pathway</i>	185
5.4 DISCUSSION	189
Chapter 6: Defining the impact of IL-17A and butyrate during the window of implantation	194
6.1 INTRODUCTION	194
6.1.1 <i>Changes induced in the endometrium during the window of implantation</i>	194
6.1.1.a Epithelial cell receptivity	194
6.1.1.b Stromal cell decidualisation	197
6.1.2 In vitro models of the window of implantation	198
6.2 HYPOTHESIS AND AIMS	199
6.3 RESULTS	200
6.3.1 <i>IL-17A does not impact on endometrial epithelial receptivity</i>	200
6.3.2 <i>Effect of IL-17A on endometrial stromal cell decidualisation</i>	202
6.3.3 <i>Butyrate enhances endometrial epithelial receptivity and stromal decidualisation</i>	204
6.4 DISCUSSION	209
Chapter 7: General discussion and future perspectives	214
7.1 GENERAL DISCUSSION	214
7.2 FUTURE PERSPECTIVES	223
Chapter 8: References	228
Appendix	252
I. LIST OF MATERIALS, REAGENTS AND EQUIPMENT USED IN THE STUDY	252
II. ETHICAL STATEMENT FOR THE HUMAN SAMPLE COLLECTION	260
<i>Ethical statement approval for collecting biopsies to obtain hEEC and hESC cells</i>	260
<i>Ethical statement approval for collecting biopsies from the ART cohort</i>	261
III. WRITTEN CONSENT FORMS FOR HUMAN SAMPLE AUTHORISATION	262
<i>Written consent form for biopsies authorisation to obtain hEEC and hESC cells</i>	262
<i>Written consent form for collecting biopsies from the ART cohort</i>	263

List of figures

<i>Figure 1.1. Anatomy of the human female reproductive tract.</i>	17
<i>Figure 1.2. The Menstrual cycle in the FRT.</i>	20
<i>Figure 1.3. IL-17 family of cytokine and receptors.</i>	29
<i>Figure 1.4. Cells producing IL-17 family members.</i>	37
<i>Figure 1.5. Mechanism of IL-17A in clearing infection at mucosal sites.</i>	38
<i>Figure 1.6. Immune events involved in pregnancy.</i>	44
<i>Figure 1.7. Changes in endometrial immune cells and in the microbiota induced by the menstrual cycle.</i>	55
<i>Figure 1.8. Functions of FRT epithelial cells in fighting infections.</i>	58
<i>Figure 2.1. Conserved regions in the human genome corresponding to the peak identified in the ChIP-seq analysis.</i>	78
<i>Figure 2.2. Procedure to obtain primary human endometrial epithelial and stromal cells.</i>	80
<i>Figure 2.3. Expression of cell markers in the cell models used in the study.</i>	94
<i>Figure 2.4. ICC staining for epithelial and stromal cell markers.</i>	96
<i>Figure 2.5. Gating strategy used in the study.</i>	97
<i>Figure 3.1. Phases of mammalian pregnancy.</i>	106
<i>Figure 3.2. Synteny maps indicating IL-17 gene location in metatherian, prototherian and human genomes.</i>	111
<i>Figure 3.3. The evolutionary history of IL17s in mammals.</i>	113
<i>Figure 3.4. Multiple Sequence Alignments (MSA) of eutherian, metatherian and prototherian IL-17A and IL-17F.</i>	117
<i>Figure 3.5. IL-17A and F protein structures in mammals.</i>	121
<i>Figure 3.6. Involvement of IL-17 family members in pregnancy stages and placentation.</i>	124
<i>Figure 4.1. Overview of the sampling strategy and the technologies used in our study in the unexplained infertility cohort.</i>	130
<i>Figure 4.2. Overview of the RNA-seq results from our preliminary study</i>	132
<i>Figure 4.3. Immune cell composition of the endometrial samples from successful and unsuccessful pregnancies.</i>	136
<i>Figure 4.4. Immune cell markers in the RNA-seq result from the successful and unsuccessful pregnant endometrial biopsies.</i>	137
<i>Figure 4.5. Expression of IL-17 in endometrial epithelial cells upon LPS stimulation.</i>	139
<i>Figure 4.6. IL-17A expression is increased by simulated viral infection in Ishikawa cells.</i>	141
<i>Figure 4.7. Influence of LPS on pathways upstream of IL-17A production.</i>	143

<i>Figure 4.8. Activation of RORγt signalling in Ishikawa cells treated with poly(I:C).</i>	144
<i>Figure 4.9. Ishikawa cells express RORγt protein.</i>	145
<i>Figure 4.10. A response characteristic of mucosal inflammation is activated in endometrial epithelial cells by IL-17A.</i>	148
<i>Figure 4.11. rIL-17A treatment increases IL-17A expression in endometrial epithelial cells.</i>	149
<i>Figure 5.1. Immunomodulatory roles of short chain fatty acids (SCFAs) in the gut and vagina.</i>	161
<i>Figure 5.2. Controls for the 16S sequencing results.</i>	165
<i>Figure 5.3. Women who failed to establish a successful pregnancy after ART show a different endometrial microbiome.</i>	168
<i>Figure 5.4. Correlation between endometrial bacterial composition and circulating IL-17A protein levels.</i>	170
<i>Figure 5.5. Treatment of Ishikawa cells with SCFA and lactate activates S100A AMPs.</i>	173
<i>Figure 5.6. Butyrate induces a pro-inflammatory response in Ishikawa cells.</i>	174
<i>Figure 5.7. Butyrate induces IL-17A production in Ishikawa cells.</i>	176
<i>Figure 5.8. Butyrate and pro-inflammatory mucosal response in hEEC cells.</i>	177
<i>Figure 5.9. Influence of butyrate on Nf-κB activation and inhibition of Nf-κB pathway.</i>	179
<i>Figure 5.10. Impact of Butyrate on HIF1α pathway and S100A9 and IL-8 expression.</i>	181
<i>Figure 5.11. A region 15kb upstream IL-17A TSS is butyrylated in mouse round spermatids.</i>	183
<i>Figure 5.12. ChIP performed on Ishikawa cells suggests that two regions 15kb upstream IL-17A TSS could be butyrylated.</i>	184
<i>Figure 5.13. Silencing of IL-17 receptors does not prevent S100A9 expression increase induced by butyrate.</i>	187
<i>Figure 6.1. Molecules and processes associated to the window of implantation</i>	196
<i>Figure 6.2. IL-17A does not affect endometrial epithelial receptivity markers.</i>	201
<i>Figure 6.3. IL-17A treatment affects stromal cells decidualisation.</i>	203
<i>Figure 6.4. Butyrate enhances the epithelial expression of markers associated with endometrial receptivity.</i>	205
<i>Figure 6.5. Butyrate enhances stromal decidualisation markers but decreases LIF and IL-15.</i>	207
<i>Figure 6.6. IL-17A impairs embryo implantation by decreasing decidualisation.</i>	211
<i>Figure 6.7. Effects of excessive IL-17A and butyrate during the window of implantation.</i>	213
<i>Figure 7.1. Proposed model associated with dysbiosis and inflammation in the FRT.</i>	222
<i>Figure 7.2. IL-17A staining is mainly localised within stromal cells in endometrial biopsies.</i>	224

List of tables

<i>Table 1.1. IL-17 family in human diseases.</i>	40
<i>Table 1.2. Roles of IL-17s in fertility complications.</i>	48
<i>Table 1.3. Roles of IL-17s in pregnancy-related complications.</i>	50
<i>Table 2.1. General characteristics of the participants from which primary cells were obtained.</i>	67
<i>Table 2.2. General characteristics of the microbiome study cohort.</i>	68
<i>Table 2.3. NCBI or Ensembl IDs relative to IL-17 family members present in chosen organisms.</i>	72
<i>Table 2.4. Public datasets analysed in the study.</i>	76
<i>Table 2.5. Seeding densities used for the study.</i>	79
<i>Table 2.6. Sequence details of siRNAs used in the study.</i>	83
<i>Table 2.7. Primers used in the study.</i>	88
<i>Table 2.8. CHIP-qPCR primers used in the study.</i>	92
<i>Table 3.1. Reciprocal best hits analysis results.</i>	115
<i>Table 3.2. Non-identical residues in metatherian and prototherian IL-17A and F.</i>	118
<i>Table 3.3. Non-identical residues in metatherian and prototherian IL-17B to IL-25.</i>	119
<i>Table 3.4. Involvement of IL-17 family members in pregnancy stages.</i>	123
<i>Table 3.5. Involvement of IL-17 family members in human female reproduction and fertility complications.</i>	125
<i>Table 5.1. Bacterial species responsible for production of the more abundant SCFAs in the gut and FRT.</i>	157
<i>Table I.1: General reagents used with manufacturer details</i>	252
<i>Table I.2: Cell culture treatments</i>	255
<i>Table I.3: Antibodies and kits used</i>	256
<i>Table I.4: Materials used with manufacturer details.</i>	257
<i>Table I.5: Equipment used with manufacturer details.</i>	258
<i>Table I.6: Software used with manufacturer details or website.</i>	258

Abbreviations

ACT-1: Nf- κ B activator 1	MHC: Major histocompatibility complex
AMPs: Anti-Microbial Peptides	MMPs: Matrix metalloproteases
AP1: Activator Protein 1	MRCA: Most recent common ancestor
APC: Antigen Presenting cells	MS: Multiple sclerosis
AS: Ankylosing Spondylitis	MSA: Multiple sequence alignment
BV: Bacterial Vaginosis	NETs: Neutrophil extracellular traps
βhCG: beta human Chorionic Gonadotropin	Nf-κB: Nuclear Factor κ B
c/EBPβ: CCAAT Enhancer Binding Protein β	NLRs: NOD-like Receptors
CCL20: C-C Motif Chemokine Ligand 20	NMH: National Maternity Hospital
cGAS: cyclic GMP-AMP Synthase	NOS: Nitric Oxide Synthase
COX: Cyclooxygenase	Nrf2: Nuclear factor erythroid 2-related factor 2
CVL: Cervicovaginal Lavage	P4: Progesterone
CXCL1: C-X-C Motif Chemokine Ligand 1	PAMP: Pathogen-Associated Molecular Pattern
CXCL8: C-X-C Motif Chemokine Ligand 8	PBMCs: Peripheral Blood Mononuclear cells
DAMP: Damage-Associated Molecular Pattern	PCOS: Polycystic Ovary Syndrome
DC: Dendritic cells	PE: Preeclampsia
dNK: decidual NK cells	PGE2: Prostaglandin E2
DSC: Decidual Stromal cells	PRL: Prolactin
E2: Estradiol	PRRs: Pattern Recognition Receptors
ESHRE: European Society of Human Reproduction and Embryology	RA: Rheumatoid Arthritis
FRT: Female Reproductive Tract	RIF: Recurrent Implantation Failure
FSH: Follicle Stimulating Hormone	RLRs: RIG-I-Like Receptors
G-CSF: Granulocyte-Colony Stimulating Factor	RORγt: Retinoid Orphan Receptor gamma t
GM-CSF: Granulocyte Macrophages-Colony Stimulating Factor	ROS: Reactive Oxygen Species
GPR: G-Protein coupled Receptors	SCFAs: Short Chain Fatty Acids
hEEC: human Endometrial Epithelial cells	SCJ: Squamocolumnar junction
hESC: human Endometrial Stromal cells	SEFIR: SEF/IL-17R Motif

HDAC: Histone Deacetylases	SLE: Systemic Lupus Erythematosus
HIF1α: Hypoxia Inducible Factor 1 Subunit α	SLPI: Secretory Leukocyte Protease Inhibitor
IBD: Inflammatory Bowel Diseases	SPP1: Secreted Phosphoprotein 1 (Osteopontin)
IFN: Interferon	STING: Stimulator Of Interferon Response CGAMP Interactor
IgA: Immunoglobulin A	TAK: TGF-Beta Activated Kinase
IGFBP1: Insulin Like Growth Factor Binding Protein 1	TCR: T-cell receptor
IHC: Immunohistochemistry	TGF-β: Transforming Growth Factor Beta
Iκk: Inhibitor of Nuclear Factor Kappa B Kinase	T_H cells: T helper cells
ILCs: Innate Lymphoid cells	TILL: TIR-like loop
IL-17A: Interleukin 17A	TNFα: Tumour Necrosis Factor α
iNKT: Invariant natural killer T cells	TLRs: Toll-Like Receptors
ITGAV: Integrin subunit alpha V	TRAF: TNF Receptor Associated Factor
IVF: <i>In Vitro</i> Fertilisation	T_{REG}: regulatory T-cells
LPS: lipopolysaccharide	TSH: Thyroid Stimulating Hormone
LH: Luteinizing hormone	TSS: Transcription starting site
MAIT: Mucosal associated invariant T-cells	UI: Unexplained Infertility
MAPK: Mitogen-Activated Protein Kinase	uNK: uterine NK cells
MCP1: Monocyte Chemotactic Protein 1	VEGF: Vascular Endothelial Growth Factor
MCT: Monocarboxylate Transporter	WAP: whey acidic protein
MFC: Merrion Fertility Clinic	WOI: Window of Implantation

Chapter 1. General Introduction

1.1 Anatomy and physiology of the female reproductive tract

The human female reproductive tract (FRT) comprises several organs showing a very diverse anatomy and physiological roles. Furthermore, sex hormones, such as oestrogen and progesterone, are responsible for changes occurring cyclically during the menstrual cycle. The component of the FRT are: ovaries, fallopian tubes, uterus and vagina. Often, the ovaries, fallopian tubes and uterus are referred as upper FRT, whereas the vagina is referred as lower FRT, with the cervix acting as a barrier between these two compartments (**Figure 1.1**).

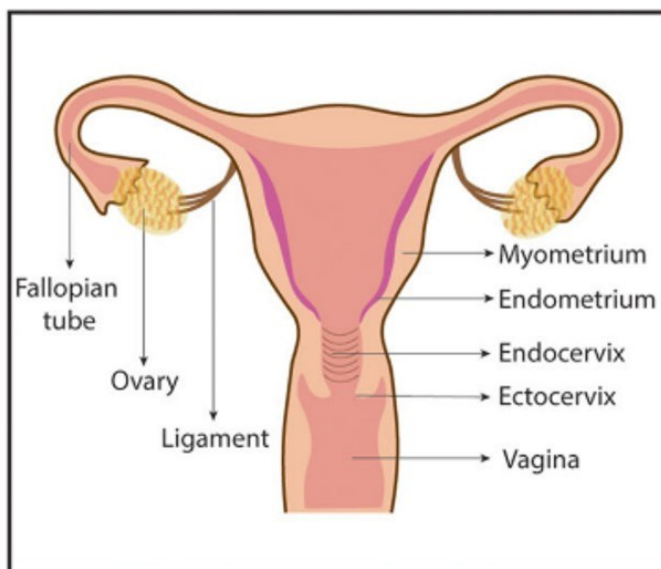


Figure 1.1. Anatomy of the human female reproductive tract. The human female reproductive tract consists in ovaries, which are held by the ligament and project into the fallopian tubes. The uterus is composed by the endometrium and the muscular myometrium. The cervix is the portion that separates the uterus from the vagina and it is divided in endocervix and ectocervix. Figure taken from (1).

1.1.1 Ovaries

Ovaries are almond-shaped glands formed by an outer cortex which surrounds the follicles containing the oocytes and an inner medulla containing interstitial cells, fibrous tissue, blood vessels and nerves. The main functions of ovaries are the development and release of mature oocyte and the production of sex hormones (oestrogen, or E2, and progesterone, or P4,) (Figure 1.2) (1). The oocyte develops from the follicles which are present in great number in the ovaries since birth and consist of immature gamete cells which arrested their development at the stage of meiosis I. After reaching sexual maturity, the Follicle Stimulating Hormone (FSH) from the pituitary gland stimulates follicle activation and maturation. This process starts the follicular phase in the menstrual cycle, during which follicles enlarge and migrate from the medulla toward the outer surface of the ovary. In the meantime, interstitial cells produce androgens which are transformed in oestrogen and progesterone by the granulosa cells, which surround the developing follicle. At the end of the follicular phase, which lasts 14 days, only one or two follicles mature and release the oocyte into the fallopian tube to allow fertilisation (1). This process is also known as ovulation and is stimulated by a peak of the Luteinizing Hormone (LH) deriving from the pituitary gland, also called LH surge (2). For the remaining 14 days of the menstrual cycle, the follicle who was ruptured and expelled the oocyte, also called corpus luteum, keeps producing progesterone in response to the stimulation with LH. This phase is also known as luteal phase. Progesterone is secreted in high quantity in order to help developing the fertilised oocyte into an embryo. If, at the end of the luteal phase the oocyte has not been fertilised, the corpus luteum involutes and stops producing progesterone, causing the shedding of the uterine lining known as menstruation, starting another cycle of follicle maturation .

1.1.2 Fallopian tube

The fallopian tube, also called oviduct, is a duct that connects the ovaries with the uterus. It is lined with a mucous layer and the end close to the ovaries is funnel shaped and presents finger-like branches called fimbriae (1). This region is called infundibulum and is required to catch and channel the oocyte once expelled from the follicle. In the

fallopian tube also occurs the sperm migration, a process that is helped by the secretion of the mucosal cells required to keep viable both the sperm and the oocyte. The mucosal lining cells of the oviduct are also ciliated, to help the movement of the oocyte and the sperm and allow fertilisation. Fertilisation happens in the fallopian tube and then the fertilised egg moves into the uterus thanks to the cilia and to peristaltic movement of the fallopian tube (1). If the oocyte has not been fertilised, it moves to the uterus where it will be secreted during the menstruation.

1.1.3 Uterus and endocervix

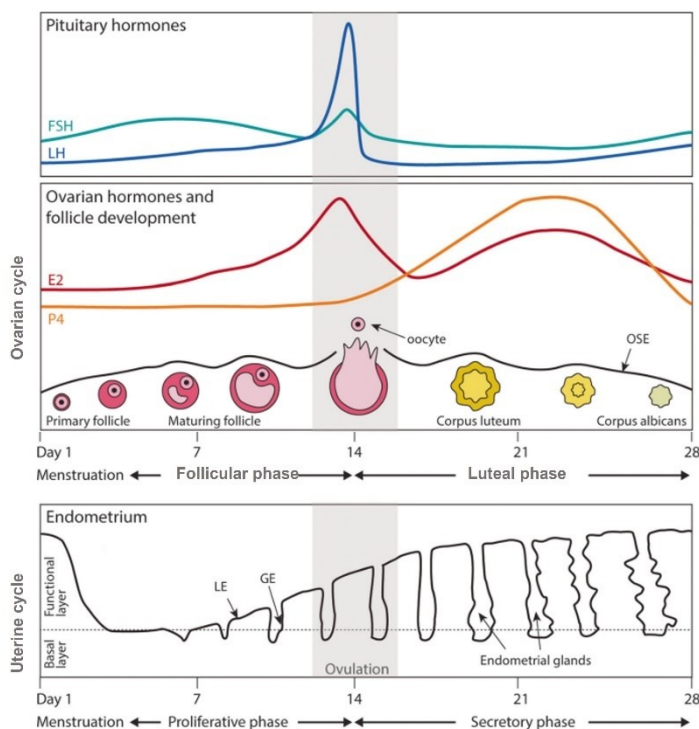
This muscular organ is connected to the fallopian tubes in the upper region, named also fundus, and to the lower FRT with the cervix. The internal lining of the internal uterine cavity is the endometrium, a single columnar layered epithelium and is surrounded by a thick smooth muscular layer named myometrium (1). Due to the stimulation with sex hormones, the endometrium is subject to cyclic changes that form the uterine cycle, which happens at the same time as the ovarian cycle ([Figure 1.2](#)). During the follicular phase of the ovarian cycle, the oestrogen (particularly 17- β -Estradiol) stimulates the growth of the epithelial layer in the endometrium, which increases his thickness. Similarly, also the stromal cells undergo proliferation and spiral arteries forms. This phase is also known as proliferative phase and lasts until ovulation (2). During this phase, the mucus lining the endometrium becomes more fluid to accommodate sperm motility. After ovulation, it starts the secretory phase, which happens at the same time as the luteal phase and lasts 14 days. The changes induced in the endometrium during this phase are dominated by progesterone. This hormone stimulates the endometrial epithelial cells to stop proliferating and developing as glandular secretory cells, able to produce more mucous secretions. If the oocyte is fertilised, it develops as an embryo which reaches the endometrium and invade the thick epithelial layer for implantation, stimulated by the constant production of progesterone by the corpus luteum. If fertilisation has not occurred, the corpus luteum stops producing sex hormones. The drop in sex hormones levels causes the start of the third phase of the uterine cycle which are menses. Without the stimulation of sex hormones, the thick epithelium cannot be maintained, and it is therefore shed together with artherial blood from the spiral

arteries. This phase lasts for up to 5 days, after which another cycle restarts with the proliferative phase (2).

1.1.4 Cervix

The cervix is the region linking the uterus with the vagina and acts as a physical barrier for preventing vaginal bacteria and external pathogens to reach the uterus. It is divided into two regions, the endocervix, which is continuous with the uterus, and the ectocervix, which projects into the vagina (1). The endocervix shows the columnar epithelium as in the endometrium, whereas the ectocervix shows a squamous epithelium. The junction between these two epithelia creates the squamocolumnar junction (SCJ). In certain conditions, hormonal dysregulation or infections can cause replacement with the glandular epithelium with the squamous metaplasia, a phenomenon called Transformation zone (TZ), which is one of the causes leading to cervical cancer (1). The cervix undergoes cyclical changes throughout the menstrual cycle under the influence of sex hormones. It has been demonstrated indeed that the overall width and length of the cervix is greatest in the follicular phase of the menstrual cycle (3). Also, during ovulation the mucus lining the cervix changes his consistency to help sperm passage (3).

Figure 1.2. The Menstrual cycle in the FRT. The hormones deriving from the pituitary gland (FSH and LH) direct the changes induced during the ovarian (central panel) and uterine cycle (bottom panel). In the ovarian cycle, the ovaries are responsible for the maturation of the follicles to release a mature oocyte during ovulation, as well as producing the sex hormones oestrogen (E2) and progesterone (P4). Meanwhile, in the uterine cycle the endometrium undergoes proliferation first and then epithelial cells develop a



and LH) direct the changes induced during the ovarian (central panel) and uterine cycle (bottom panel). In the ovarian cycle, the ovaries are responsible for the maturation of the follicles to release a mature oocyte during ovulation, as well as producing the sex hormones oestrogen (E2) and progesterone (P4). Meanwhile, in the uterine cycle the endometrium undergoes proliferation first and then epithelial cells develop a

glandular phenotype to welcome the developing embryo. If fertilisation does not occur, menstruation takes place, starting a new cycle. On the right is displayed the FRT structure, with all the compartments highlighted. LE: luminal epithelium; GE: glandular epithelium; OSE: ovarian surface epithelium. Adapted from (1).

1.1.5 Vagina

Vagina corresponds to the lower region of the FRT and connects the vulva to the uterine cervix. This channel is elastic and distensible and displays a nonkeratinized stratified squamous epithelium (1). Given its direct connection with the outer space, this region displays a unique microbiota responsible for lactic acid production and is colonised by many immune cells to prevent pathogen infections.

1.2 Mucosal immune system in the female reproductive tract

Like the gut and all other mucosal sites, the FRT is characterised by a system that allow to tolerate commensal bacterial whilst protecting from pathogen infections. This system is named mucosal response or mucosal immunity and is composed by physical barriers to prevent infections as well as epithelial and immune cells activation to clear pathogen invasion (4). To avoid activation of the immune responses against the symbiotic microbiome, the commensal bacteria are known to tailor the mucosal response to maintain immune tolerance for the healthy microbiota component (5). Similarly, the immune response in the FRT must tolerate the semen as well as the semi-allogenic embryo for the establishment of a correct pregnancy (6). As described earlier on, there is a different microbial component between the lower and the upper FRT and, both the microbiome and immune compartments, have been shown to change under the influence of sex hormones during the menstrual cycle ([Figure 1.7](#)) (7). Therefore, mucosal immunology of the FRT is very complex. The following sections will briefly explain the mechanism mediated by immune cells and by non-immune cells in fighting infections in the FRT mucosal sites.

1.2.1 Immune cells involved in the mucosal activity in FRT

1.2.1.a Professional Antigen Presenting Cells (APCs)

During infections, microbial derived molecules are internalised by cells able to process them and present to lymphocytes to trigger their activation against the right antigens. These abilities are possessed by Antigen Presenting Cells (APCs), which include dendritic cells (DCs), macrophages and B cells as professional APCs (8). Within vaginal mucosa have been identified four subsets of APCs: **cervicovaginal Langerhans cells (cvLCs)**, **CD14⁺DCs**, **CD14⁻DCs**, and **CD14⁺ macrophages** (9). cvLCs are located within the cervico-vaginal epithelium, whereas the other three subsets can be found in the subepithelial lamina propria. All the four subsets can induce a pro-inflammatory T_H1 response, but only CD14⁻DCs and cvLCs have been found to induce a T_H2 response (9, 10). In mouse, which shows a similar organisation of vaginal APCs, cvLCs change their location during oestrus cycle, with an higher abundance of cvLCs in the vaginal epithelium during diestrus and late metestrus (corresponding to the luteal phase) and very few during oestrus and early metestrus (corresponding to the ovulatory phase) (11).

In non-pregnant endometrium macrophages cannot be identified however, during the secretory phase of the menstrual cycle are formed **lymphoid aggregates** containing a core of B-cells surrounded by CD8⁺ T-cells with an external circle of macrophages (12). The function of these structures is still not clear, however it is possible that they act as sensory stations to recognize infections and limit their systemic spread during menstruation, when endometrial epithelium barrier disrupts and the organism would be more sensitive to infections (6). Furthermore, the macrophages that are found in non-pregnant endometrium secrete angiogenic factors as well as anti-inflammatory mediators, characteristic of M2 subtype macrophages (13). During menstruation it can be observed an increased recruitment of macrophages as well as their activation in secreting endometrial repair molecules, to help restore endometrial integrity (14).

In pregnant endometrium, decidual DCs have been shown to inhibit uNK cell cytotoxicity and stimulate pro-angiogenic factor for spiral arteries formation (15). Additionally, **decidual macrophages**, which are grouped in two phenotypes CD11c^{hi} and CD11c^{lo}, secrete anti-inflammatory molecules such as IL-10 and TFG-β to induce tolerance for the

foetus, as well as inducing pro-angiogenic factors to facilitate the remodelling of blood vessel during placentation (16, 17). Similarly, **B-cells** show positive effects during pregnancy since in pre-term labour were found reduced levels of B-cells impairing the production of progesterone-induced blocking factor 1 (PIBF1), which seems to lower inflammatory responses (18).

1.2.1.b Neutrophils

These polymorphonuclear cells belong to the innate arm of the immune response and are involved in the first line of defence against infection for their neutralising and killing abilities (19). They are indeed able to phagocyte pathogens, as well as killing them by producing reactive oxygen species (ROS), bactericidal enzymes or through the formation of neutrophil extracellular traps (NETs), formed by extrusion of their chromatin loaded with lytic enzymes (19). Neutrophils represent approximately 10% of the immune cells present in the cervix, but they show a very low concentration in the endometrium, with exception for the pre-menstrual phase, where they increase up to 15% of the total immune cells (20). Neutrophils have been indeed shown to be among the initiator of menstruation via induction of endometrium remodelling through secretion of matrix metalloproteases (MMPs) (21). Neutrophil recruitment in the endometrium is regulated by sex-hormones and is facilitated by progesterone but severely inhibited by oestrogen (22). The absence of neutrophils during the ovulatory phase, when oestrogen levels are high, is also required to avoid excessive semen degradation to ensure fertilisation (22).

In pregnancy, there is an increase recruitment of neutrophils in the decidua through IL-8 and they are shown to secrete pro-angiogenic factors (23). An even higher increase in neutrophils in uterine tissue and in the cervix can be observed during parturition, either at term or preterm. In this phase, more IL-8 is produced leading to the recruitment of neutrophils, which in turn secrete MMPs and cytokines, responsible for the pro-inflammatory environment and for the remodelling processes needed for parturition (23).

1.2.1.c Innate Lymphoid Cells (ILCs)

This group comprises five subsets of lymphoid cells which belong to the innate arm of the immune response. The cells belonging to this group derive from different developmental pathways and show also different actions: NK cells, ILC1, ILC2, ILC3, and lymphoid tissue inducer (LTi) cells (24). In human endometrium and decidua have been identified **ILC3**, which are highly pro-inflammatory and are characterised by the expression of RORC and IL-22 genes (25, 26).

1.2.1.d Natural killer (NK) cells

NK cells are the most studied subset of innate lymphoid cells in the uterus, also named uNK, and can be found in several phenotypes: the more common CD3⁻ CD56^{bright} CD16⁻, as well as a more immature phenotype CD34⁻ CD117⁺ CD94⁻ capable of expressing RORC and IL-22 (4, 27). NK cells are strictly regulated by the menstrual cycle and by progesterone, showing very few cells during the proliferative phase within the stromal compartment, but they start proliferating after ovulation until menstruation. In this phase, NK cells can reach up to the 30-40% of the lymphocytes infiltrating in the decidua, which explains their name decidual NK cells or dNK, and acquire a characteristic phenotype CD56^{bright} CD16⁻ KIR⁺ CD9⁺ (20, 28). Contrarily to circulating NK cells, dNK cells show poor cytotoxicity, caused by impaired degranulation and release of IFN- γ (29). In addition, dNK cells sustain pregnancy processes by secreting pro-angiogenic factors (VEGF) as well as tissue remodelling molecules, such as stromal derived factor-1 (SDF-1) and IFN- γ -inducing protein 10 (IP10) (30). Due to their ability in recognising self and non-self antigens, uNK cells have also an important role in tolerating foetal-derived tissues. In normal conditions, cells expressing a non-self MHC would be recognised by activating NK-cell receptors, leading to the degranulation, and killing of non-self cells. uNK cells showed increased expression of inhibitory receptors, such as CD94/NKG2A which shows increased binding affinity than the corresponding activating receptor CD94/NKG2C (28). Given that the foetus and the foetal-derived tissue carry two haplotypes of MHC, one maternal and one paternal, is possible that uNK cells are educated in tolerating the allogenic antigens via the activation of the inhibitory NKG2A receptor binding to maternal antigens (28, 31). Due to all these processes mediated by uNK cells, their

dysregulation is closely associated with fertility-related pathologies and complications (32-34).

1.2.1.e T lymphocytes

Several populations of T lymphocytes have been identified in the FRT mucosa. An important function is played in mucosal immunity by **tissue resident memory T-cells (T_{RM})**, which are found to be abundant in the endometrium and are particularly enriched during the window of implantation (35). Despite T_{RM} cells can derive from both CD4⁺ and CD8⁺ T-cells, the most abundant population found in human decidua is of CD8⁺ lineage. dT_{RM} cells have been found to be able to secrete in high amounts both antimicrobial cytokines, TNF α and IFN- γ , as well as anti-inflammatory cytokines, IL-4 and TGF- β , displaying the capability of both protecting the mucosa from infections whilst being able to maintain a tolerogenic environment for sustaining the pregnancy (36). Other T-cells associated with mucosal defence are **Mucosal-associated invariant T (MAIT) cells**. These cells are characterised by the expression of a semi-invariant chain in their TCR, thus can recognise several microbial-derived metabolites (37). MAIT cells are abundant in the FRT and display different functions if compared to the circulating ones indeed, when challenged by bacterial infections, they produce mainly IL-17A and IL-22, whereas their circulating counterparts produce mainly IFN- γ , TNF and granzyme B (38). During the first trimester of pregnancy, MAIT cell can be identified in the decidua in low amounts and their expression of granzyme B is much lower than in the circulating counterparts whereas immune checkpoint markers, such as PD-1, show an increased expression, in agreement with the tolerogenic environment needed for the early stages of embryo development (39). Regarding the conventional T-cells, both **CD4⁺ and CD8⁺ T** cells can be found in the lower FRT, in a 40:60 proportion respectively (6). Vaginal CD8⁺ T cells are highly cytotoxic against pathogens and can quickly respond to subsequent infections thanks to the T_{RM}. The vaginal CD4⁺ T-cells display the typical range of differentiation in the four main T helper subtypes (6). It has been already mentioned the formation in the endometrium of the lymphoid aggregates in which CD8⁺ T-cells are abundant and ready to respond in case of infection. However, during the secretory phase the cytotoxicity activity of endometrial CD8⁺ T-cells is shown to be decreased, probably because under influence of sex hormones (40). During pregnancy the main

CD4⁺ T cell subsets in the decidua are Treg and T_H2, which show an anti-inflammatory phenotype to guarantee foetal tolerance (41-43).

1.3 IL-17 family of cytokines and receptors

IL-17A has been extensively studied for its central roles in host mucosal defence against infections (44). These roles also appeared to be shared by the other five members of the IL-17 cytokine family, which are named from IL-17B through IL-17F. However, the other IL-17 cytokines have not been extensively studied. These cytokines show a variable percentage identity between them, with IL-17A and IL-17F being the closest and IL-17E (also known as IL-25) as the most divergent from IL-17A (45). What characterises these cytokines is the presence of five conserved cysteines involved in the formation of a cystine-knot structure, which is similar to the one found in growth factors and dimeric hormones (46). The active form of IL-17 cytokines is generated by dimerization through disulphide bond interactions, either as homodimers or heterodimers, however only IL-17A and IL-17F are known to form the heterodimer (47). In particular, IL-17F/F and IL-17A/F are dimers produced by activated CD4⁺ T-cells (47). These cytokines activate downstream signalling pathways through interaction with dedicated dimeric receptors. IL-17RA and IL-17RC were the first to be discovered (48, 49) and are responsible for binding IL-17A and IL-17F(50), however they show different affinities for them, with higher affinity for IL-17A/A > IL-17A/F > IL-17F/F, which can explain why the dimers show different potency in stimulating pro-inflammatory signals (51, 52). IL-17RB can bind both IL-17B or IL-25 (53), while IL-17RE binds to IL-17C (54). The ligand for IL-17RD is still unknown to date, despite it has been shown to be the most ancient member of the family, with homologues in lampreys (55). These receptors are expressed ubiquitously in the human body and the main cell types who respond to IL-17A and IL-17A/F are epithelial cells, endothelial cells, macrophages and dendritic cells (56).

1.3.1 Family members and signalling pathways activated

The IL-17R are characterised by fibronectin-like extra-cytoplasmatic domain and they all share a SEFIR (SEF/IL-17) domain in the cytoplasmatic domain, which is distantly related to the toll-IL-1 receptor (TIR) domain, shown in Toll-like receptors and IL-1 receptors (57). However, the SEFIR domain lacks the region needed for interacting with TIR-based proteins, but IL-17RA has been shown to possess a TIR-like loop (TILL) which enables it to interact with, ACT1, another protein which shares the SEFIR domain (57, 58). Thus IL-17RA is required for downstream signalling pathway activation ([Figure 1.3](#)) and is required by IL-17RC, IL-17RB, IL-17RD and IL-17RE dimerization (56), although evidences of independent signalling pathways have also been also observed for those receptors (59, 60).

1.3.1.a IL-17A-IL-17RA signalling pathway

Once ACT1 binds to the IL-17RA, then it recruits TNFR associated Factor 6 and 3 (TRAF6 and TRAF3), leading to the activation of Nf- κ B signalling pathway. Additionally, IL-17RA shows a C/EBP β activation domain (CBAD), responsible for activation of C/EBP β and C/EBP δ , as well as MAPKs/AP-1 (50, 61). The outcome for the signalling pathway activation is the transcription of chemokines, cytokines, anti-microbial peptides and matrix metalloproteases (56), which are extremely important for clearing the infection in the mucosal sites and restore the homeostasis. Studies have highlighted how IL-17A per se is a weak cytokine and chemokine inducer through Nf- κ B signalling pathway (62). However, IL-17A can yet induce a potent pro-inflammatory response through enhancing mRNA stability (63). mRNA stability is increased by certain RNA binding proteins such as tristetraprolin, however IL-17A seems to act independently from this molecule (64). IL-17A mediated mRNA stabilisation is instead achieved through ATC1-MAPK pathway, but it does not require TRAF6 (56, 62, 65). Several studies have highlighted how IL-17A treatment induces mRNA stabilisation of its target mRNA, especially cytokines and chemokines such as IL-6, IL-8, CXCL1 (64-67).

In addition to this canonical signalling pathway, also other pathways have been discovered to require the interaction of IL-17 with other ligands (68-70). For example, stimulation of the osteoblastic cell line MC-3T3 with IL-17A and Tumor Necrosis Factor

α (TNF- α) results in increased IL-6 expression via C/EBP δ activation (68). IL-17A signalling can also activate ERK pathway in conjunction with growth factors. In an intestinal dysbiosis model basic fibroblast growth factor (FGF2), secreted by T_{reg} cells, synergise with IL-17A, secreted by T_H17 cells, and leads to ERK pathway activation to induce intestinal epithelial cells proliferation and wound-healing processes (70). ERK pathway activation is obtained by ACT1 binding preferentially to IL-17RA-IL-17RC, thus releasing its suppressive effect on ERK activation through FGF2 (70). IL-17A activates ERK5 also in chemically induced carcinogenesis model in keratinocytes stimulated with carcinogenetic chemicals 7,12-dimethylbenz[a]anthracene (DMBA) and the pro-inflammatory phorbol ester 12-O-tetradecanoylphorbol 13-acetate (TPA), leading to cell proliferation and tumorigenesis (71). Also, a PAMP stimuli such as Candidalysin, a pore-forming peptide secreted by hyphal-stage *Candida albicans*, was shown to potentiate IL-17 signalling in human buccal epithelial cells by activating c-Fos dependent secretion of pro-inflammatory cytokines (69).

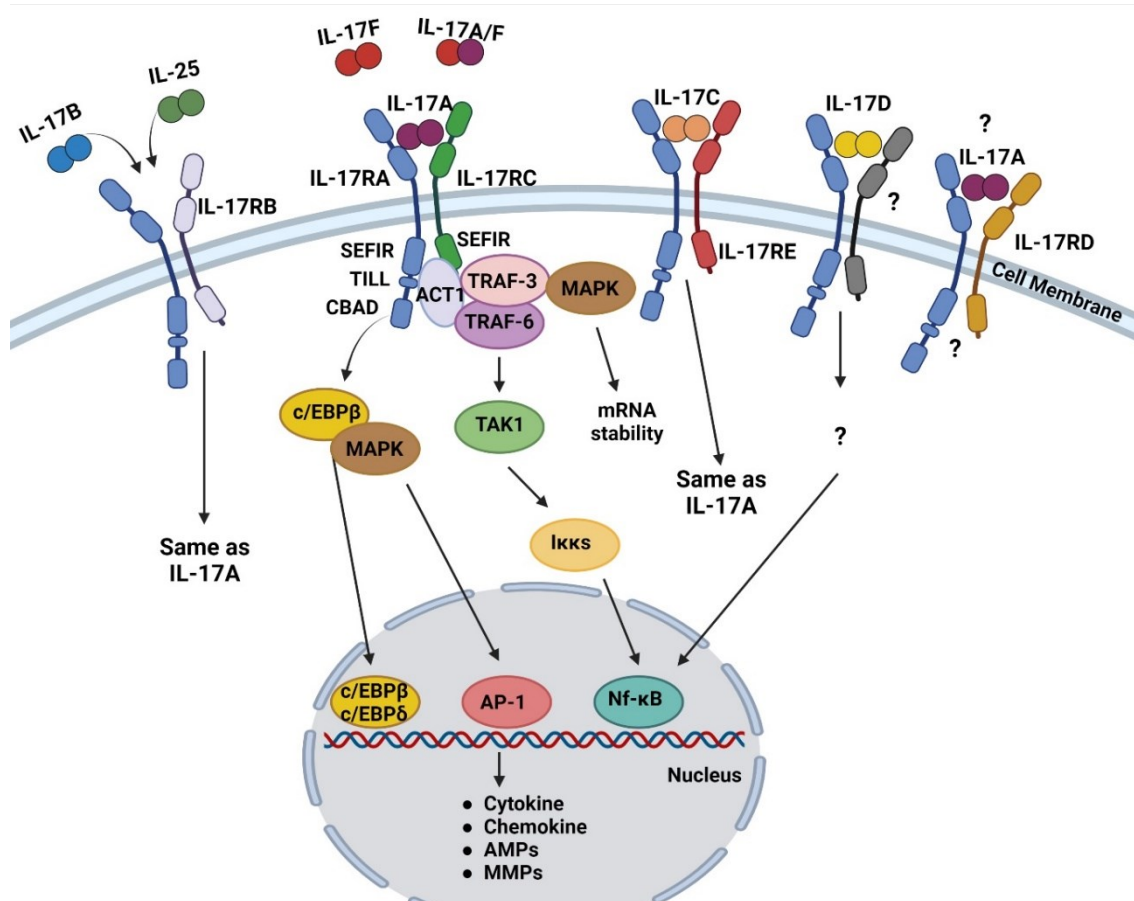


Figure 1.3. IL-17 family of cytokine and receptors. The six members of IL-17 cytokine family (IL-17A to IL-17F) are shown together with their dimeric receptors (IL-17RA to IL-17RE). All the receptor bind dimeric cytokines and encode for the SEF/IL-17R (SEFIR) domain in their cytoplasmic tail. IL-17RA shows two additional domains: a TIR-like loop (TILL) domain and a C/EBPβ activation domain (CBAD). IL-17RA is thought to be required for downstream IL-17A/F pathway activation through interacting with ACT-1 via its SEFIR-TILL domain. Then, TRAF3 and TRAF6 are recruited leading to activation of Nf-κB via TAK1 and Iκks inactivation of IκB. Alternatively, TRAF3 can lead to mRNA stability through MAPKs activation. Whereas through the CBAD domain c/EBPβ can be activated, leading to the activation of the transcription factor c/EBPβ and c/EBPδ and AP-1 through mediation with MAPKs. These three transcription factors lead to the expression of genes coding for cytokines, chemokines, antimicrobial peptides (AMPs) and matrix metalloproteases (MMPs). The receptor complexes containing IL-17RB and IL-17RE activate the same pathway as the IL-17RA-RC complex. It is not well established yet the pathway downstream IL-17D, neither the receptor complex, however it has been shown to activate Nf-κB. IL-17RD is thought to bind IL-17A, however its downstream activation has not been investigated.

1.3.1.b IL-17RB signalling pathway

IL-17RB is responsible for binding IL-17B (72) and IL-25 (73) but the signalling pathway activated downstream the two cytokines seems quite different. It seems that IL-17RA can bind the IL-25-IL-17RB pre-formed complex, but evidence is missing if this is happening for IL-17B-IL-17RB complex (52). IL-17RB shows an additional TRAF6 binding domain in its cytoplasmatic tail, which leads to activation of Nf- κ B independently of IL-17RA (59). Furthermore, the SEFIR domain in the cytoplasmatic tail of IL-17R receptor can bind ACT1, since mice lacking ACT1 fail to respond to IL-25 *in vivo* (74, 75). Thus, IL-17RB signalling pathway leads to the same pathway activation as IL-17RA, with Nf- κ B and MAPK/AP-1. Additionally, IL-25 has been shown to activate NFATc1 (nuclear factor of activated T cells, cytoplasmatic 1) and JUNB (76).

1.3.1.c IL-17RC signalling

IL-17RC forms the receptor responsible for IL-17A and IL-17F interaction (75, 77). Differently from IL-17RA, which shows a 100-fold higher affinity for IL-17A (52), IL-17RC binds both IL-17F and IL-17A with same high affinity (77). Recent studies highlighted that IL-17RC can form complexes with IL-17F and IL-17A in a 2:1 ratio, and that IL-17F preferentially binds IL-17RC than IL-17RA (60). This finding suggests activation of the downstream signalling pathway without IL-17RA involvement (60) however, this is only confirmed to happen in IL-17RA^{-/-} mouse fibroblasts complemented with human IL-17RC (49). The signalling pathway activated downstream IL-17RC is the same as IL-17RA (51).

1.3.1.d IL-17RD signalling

IL-17RD was shown to bind IL-17A by dimerizing with IL-17RA (78). In the same publication, IL-17RD mutant lacking the intracellular domain suppresses the IL-17A mediated signalling because of the impossibility to interact with TRAF6 (78). IL-17RD can be found in evolutionarily distant species and it seems to have similar functions as Toll from *Drosophila melanogaster*. Indeed, in zebrafish and frog development IL-17RD was shown to control embryonic dorsoventral polarity by binding to FGFR1 and FGFR2 and blocking the downstream FGF signalling which leads to RAS-MAPK and PI3K activation (79). Also in human IL-17RD can bind FGFR1, leading to inhibition of ERK pathway

activation and blocking proliferation, although the mechanism by which this is mediated is not well characterised yet (80, 81).

1.3.1.e IL-17RE signalling

IL-17RE binds to IL-17C, however the details of the pathway downstream are to date still missing (50). This receptor is widely expressed in the body and is particularly highly expressed in some tumours, which has led to suggest for a mitogenic role, given that it was shown to mediate RAS/MAPK pathway activation through ERK1/2 (54).

1.3.2 Downstream gene targets of each IL-17

1.3.2.a IL-17A

As mentioned, IL-17A stimulate a pro-inflammatory signature with induction of Nf- κ B-dependent cytokines and chemokines such as IL-6, IL-8, G-SCF, GM-CSF (82), CXCL1 and MCP1 (83). Secretion of these immune-mediators is needed for activation and recruitment of neutrophils and monocytes in the site of IL-17A release (84). Other target genes activated upon IL-17A stimulations are antimicrobial peptides (AMPs). These are small molecules belonging to the innate arm of the immune system, constituted by at least two positively charged residues with an acidic pH (85). This feature enables them to bind to the negatively charged membranes of bacteria, mycobacteria, fungi, and enveloped viruses mediating their direct killing (85). There are several classes of AMPs and IL-17A was shown able to induce several types such as β -defensins, S100 proteins and lipocalin2 (LCN2) (56, 86). Other genes belonging to the IL-17A target signature are matrix metalloproteases such as MMP1 and MMP9, thus confirming that IL-17A can also mediate wound healing processes (56, 87). Furthermore, there are other target genes induced by IL-17A which are expressed only in certain compartments. For example, it was shown that IL-17A plays an important role for maintenance of epithelial barrier integrity in gut, lungs and CNS by inducing occludin (*Ocln*) and mucins (56, 88, 89). During disseminated *Candida albicans* infection in the kidney, IL-17A was shown to activate the Kallikrein (Klk)-kinin system by increasing Klk1 production, exerting protective functions in preventing apoptosis in renal cells caused by the infection (90).

In the context of *C. albicans* infection in the oral mucosa, IL-17A regulates expression of histatins which, alongside AMPs, can resolve the infection by direct killing of the yeast and preventing it to bind to the oral epithelium (91). Furthermore, IL-17A treatment of hepatocytes and smooth muscle cells resulted in production of acute phase C-reactive protein (CRP), pointing out a role for IL-17A in mediating systemic inflammation and atherosclerosis (92).

1.3.2.b IL-17B

Differently from IL-17A, the roles of IL-17B are not clear and seem to be cell-type specific. IL-17B alone does not induce IL-6 secretion in synovial fibroblasts (93) but, stimulation in conjunction with TNF α , restores the ability to produce IL-6 and G-CSF (94). Similarly in a pneumonia model IL-17B cannot induce IL-8 protein secretion by lung fibroblasts, but this ability is present in bronchial epithelial cells and it is mediated by Akt-p38 MAPK, ERK and Nf- κ B (95). In the monocytic cell line THP1, IL-17B induced production of TNF α and IL-1 β , but production of other cytokines such as IL-6, IL-1 α or G-CSF was not observed (93). In HeLa cells, Chinese Hamster Ovary (CHO) cells or 293T cells *in vitro* treatment with recombinant human IL-17B did not show induction of cytokines either mRNA or proteins (96), but in 3T3 cells and peritoneal exudate cells was observed production of pro-inflammatory cytokines IL-1 α , IL-6, IL-23 (97).

1.3.2.c IL-17C

IL-17C signals through the IL-17RA-IL-17RE dimer, with IL-17RE being responsible for the specific binding for this cytokine (98). IL-17C induces a pro-inflammatory response in epithelial cells of mucosal sites, which also express the receptors for this cytokine, thus showing an autocrine signalling process (99). When a microbial infection occurs at mucosal sites, IL-17C is produced by epithelial cells and it leads to activation of expression of pro-inflammatory target genes: AMPs such as S100A family and defensins, cytokines and chemokines such as IL-1 β , G-CSF and IL-8, and pro-inflammatory molecules (99). Among the target genes induced by IL-17C signalling, are also occludin, claudin-1 and claudin-4, who are involved in restoring tight junctions needed for epithelial barrier integrity (100). Furthermore, both in epithelial cells and in immune

cells IL-17C has been shown to induce IL-17A production, thus showing how family members of the IL-17 family can regulate each other expression (101, 102).

1.3.2.d IL-17D

IL-17D is the least studied member of the family and recently studies on lamprey have highlighted how IL-17D interacts with IL-17RA in B-like cells and leads to IL-8, BCL6 and BCAP increased expression (103). Human endothelial HUVEC cells treated with IL-17D showed increased expression of IL-6, IL-8 and GM-CSF via Nf- κ B (104). Whilst production of IL-17D upon bacterial stimulation is still not clear (105) other reports have linked IL-17D with antiviral and antitumor effects (106). Indeed, in viral infections or carcinogenesis models, cells are shown to activate a stress response through Nrf2, which can activate the transcription of IL-17D (106). Using *il-17d*^{-/-} mice models has confirmed how this cytokine is fundamental for viral clearance, as well as mediating NK-cells recruitment and activation to favour tumour regression, however the details of the pathway involved in such mechanisms are not clear (106).

1.3.2.e IL-25

This member of the family stands out for its type-2 immunity activation in the context of helminth infection and allergy. A study using a model of helminth infection has highlighted how IL-25 is produced by tuft cells and activates ILC2 to produce IL-13, leading to epithelial progenitors remodelling to expand tuft cells, resulting in a circuit to expand both these cell populations (107). Among the gene target activated by the interaction with IL-25 and IL-17RB/RA are IL-6, TGF- β , G-CSF in mouse myeloma cells (59), as well as Th2 cytokines such as IL-4, IL-5, IL-13 in various organs of rIL-25 treated mice (108). In the same model, was also observed recruitment of plasma cells and eosinophils.

1.3.2.f IL-17F

IL-17F is the most similar cytokine to IL-17A in terms of structure and signalling pathway activated. These two cytokines are indeed co-expressed on linked genes and produced by the same immune cell subsets that produce IL-17A (109). Furthermore, IL-17F can form homo- and heterodimers with IL-17A and use the same dimeric IL-17RA-IL-17RC

receptor leading to the same signalling pathway activation but with different strength, with IL-17A/F dimer being the intermediate and the IL-17F/F homodimer being the weakest (110). Thus, the genes that are activated under IL-17F signalling are the same as for IL-17A.

1.4 Sources of IL-17s cytokines

1.4.1 Immune cells production of IL-17s

In mammals IL-17A is classically assumed to be produced by lymphoid cells. It has been linked to a subset of CD4⁺ T-cells, called T_H17s, which was discovered to be activated with IL-23 in the absence of IFN- γ or IL-4, leading to the secretion of IL-17 (111). Since that discovery, T_H17 differentiation from naïve CD4⁺ T-cells is now known to be induced by several stimuli, such as IL-1 β and TNF, or IL-21 and TGF- β , or IL-6, IL-1 β and IL-23 (112, 113). Recently, other lymphoid cell subsets have been identified as IL-17A producers if stimulated with IL-1 β , IL-23 or microbe-derived products (**Figure 1.4**), such as: $\gamma\delta$ T cells (114); tissue resident memory cells (T_{RM}) (115); cytotoxic CD8⁺ T cells able to produce IL-17, named T_C17 cells (116); mucosal associated invariant T cells (MAIT)(38). Additionally, immune cells belonging to the innate arm of the immune response secrete IL-17A, such as invariant Natural Killer T cells (iNKT) (117), NK cells (118), Paneth cells (119) innate lymphoid cells type 3 (ILC3) and neutrophils (120, 121). The other IL-17s are also secreted mainly by immune cells, although slightly different subsets are the source (**Figure 1.4**): IL-17F is produced by the same subsets as IL-17A (122), whereas IL-25 is produced by mast cells, eosinophils, basophils and T_H2 cells, thus promoting a type 2 immune response after fungal infection (108, 122, 123). IL-25 can be produced by immune cells, particularly is produced by dendritic cells in the context of atopic dermatitis, in which a strong type 2 immunity activation is observed (124). IL-17D mRNA is expressed at basal conditions in resting CD4⁺ T-cells and in resting CD19⁺ B-cells but it is not detectable in the activated counterparts (104). Also in non-mammalian species, such as teleosts, IL-17 family homologs are shown to be expressed in hemocytes, which are the teleosts counterpart for macrophages (125). Furthermore, the IL-17A/F1 which is homologue to IL-17A, was shown to induce CXCL8, IL-6 and IL-1 β expression in the

grass carp, showing that the immunomodulatory activation induced by this cytokine appeared a long time ago (126).

1.4.2 Non-immune cellular source for IL-17s

Production of IL-17s by mammalian non-immune cells had also been observed, particularly for IL-17B, IL-17C and IL-17D (**Figure 1.4**). IL-17B protein production - as well as IL-17A - was observed in chondrocytes during healing processes after one week from fracture had occurred (127) and northern blot analysis and immune histochemistry (IHC) demonstrated the spinal cord and neurones as a site where IL-17B is produced in basal conditions (128). IL-17C has been shown to be produced by a broad range of epithelial cells (101, 129) and keratinocytes, where it is shown to activate mucosal responses (98), as well as dampening excessive inflammation induced by dextran sodium sulphate-induced colitis (99). IL-17D mRNA has been shown to be broadly expressed in the body, especially in non-immune cell compartments such as brain, adipose tissue, lung, kidney, heart, skeletal muscle, pancreas, placenta (104). IL-25 can be produced by non-immune cells, particularly is produced by intestinal Tuft cells when stimulated by protozoan derived succinate (130) and also keratinocytes have been shown to secrete IL-25 protein in psoriatic lesions (131). Also, the transcript for IL-25 is enhanced in lung epithelial cells upon allergens stimulation (76) and is present in brain capillary endothelial cells, where it helps maintaining the blood brain barrier (132). IL-17F protein can be produced by intestinal epithelial cells in the aggravation of ulcerative colitis inflammation induced by *Fusobacterium nucleatum* infection (133). There is no evidence of production of IL-17A by non-immune cells (45) in mammals. However, these cytokines, including IL-17A/F which is an IL-17A and IL-17F homolog from several marine species including vertebrates teleosts and invertebrates such as mollusks, are shown to have a higher expression in gills, intestine, head kidney or gonads if compared to blood or hemocytes, (134, 135). This finding highlights how the mucosal associated activity of these cytokine is ancient and maintained over time.

1.4.3 Transcription factors responsible for IL-17s transcription

The transcription factor responsible for IL-17A and IL-17F production in all immune cell subsets studied so far is RAR-related orphan receptor- γ t and $-\alpha$ (ROR γ t and ROR α), with

ROR γ t is a more potent inducer of IL-17A and F transcription (136, 137). Indeed, studies using ROR γ t inhibitors have highlighted how blockade of this transcription factor leads to impaired T_H17 differentiation and no IL-17A production (138). However, the transient use of an oral ROR γ t inhibitor GSK805 upon enteric *Citrobacter rodentium* infection in mice was shown to block T_H17-dependent inflammation, but failed to block ILC3-dependent immunity, thus highlighting how diverse cell types might rely differently on this transcription factor for IL-17A production (139).

Other modulators for IL-17A production have the ability of induce ROR γ t expression, such as NF- κ B, Runt-related transcription factor 1 (Runx1) and hypoxia-inducible factor 1 (HIF-1). c-Rel was shown to bind ROR γ t promoter and experiments using knock-out mice has demonstrated how their pro-inflammatory experimental autoimmune encephalomyelitis (EAE) profile is milder if compared to wild type littermates due to lack of *RORc* expression, the gene coding for ROR γ t, and consequently less T_H17 cells maturation (140). In T_H17 cells has also been shown that Runx1 increases the expression of ROR γ t and mediates this cell subset maturation and IL-17A production (141). The metabolic sensor HIF1 enhances T_H17 maturation upon hypoxic conditions by inducing ROR γ t transcription and helping ROR γ t binding to IL-17A promoter via interaction with p300 (142).

It seems that ROR γ t expression is not limited to immune cells. Looking at the human protein atlas database (<https://www.proteinatlas.org/>) is possible to see the mRNA expression of *RORc* in other cell types such as epithelial cells (glandular, squamous or specialised), endocrine cells and muscle cells from various organs.

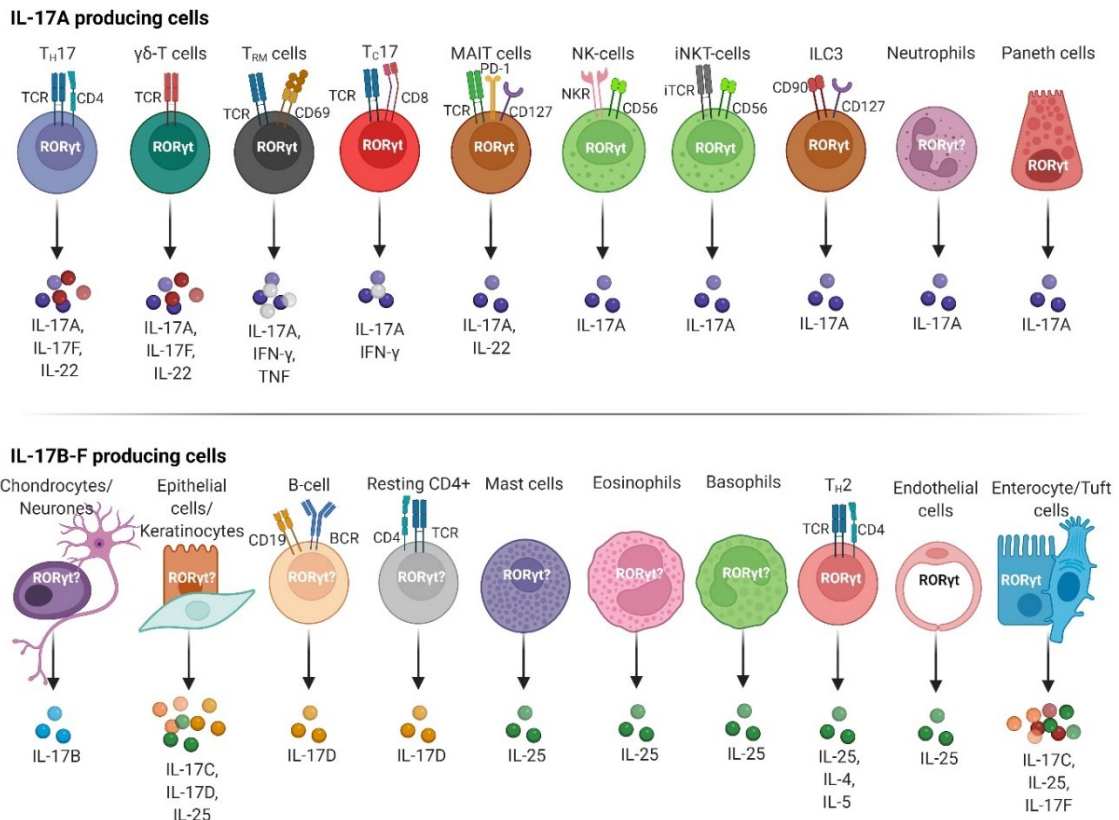


Figure 1.4. Cells producing IL-17 family members. IL-17A is mainly produced by immune cell subsets belonging both to the adaptive arm (T_H17, γδ-T cells, T_{RM} cells, T_C8 cells) or to the innate arm of the immune system (MAIT cells, NK cells, iNKT cells, ILC3, neutrophils and Paneth cells). IL-17B to IL-17F are produced by both immune and non-immune cells.

1.5 IL-17s in Health and disease

1.5.1 Roles in inflammation

IL-17 family of cytokines are important players in mucosal immunity. They activate pro-inflammatory responses, mainly in non-immune cells such as epithelial, stromal cells and macrophages. It seems that IL-17A/F have a broad spectrum of activity and that the other members of the family are more cell-type or organ specific (45). Almost all IL-17s mediate responses against bacterial and fungal infections, such as *Candida*, *Klebsiella* and *Bordetella* species (114, 115, 143). The role for these cytokines in bacterial and fungal infection is extremely important, as it can be noticed how drastic are the effects of genetic mutation in the IL-17 signalling pathway in the severity of mucocutaneous

Candida infections (144). The exception for IL-17 members having a role in bacterial and fungal protection is IL-25, which is instead involved in helminth and allergy-induced inflammation (107), and IL-17D which seems to have a role for viral infection clearance (106).

In the context of inflammation, IL-17s mediate neutrophil attraction to the site of infection by inducing chemokines and myeloid-activating cytokines such as IL-6 and G-CSF (59, 82, 99, 104) (Figure 1.5). For IL-25 we can also observe T_H2 inducing cytokines production, leading to B-cell activation (108). In addition to immune-cell recruitment and activation, IL-17s also stimulate non-immune cells in clearing the infection by inducing AMPs. Various classes of AMPs are produced in response to each IL-17 family member: β -defensins, S100 proteins, lipocalin2 (56, 86, 99). These molecules can resolve infection by direct killing of microbes, as well as further modulating the immune cells by exerting chemotactic and immunomodulatory activities (145). IL-17A and F also induce wound-healing responses through secretion of MMPs (56, 87). Another way IL-17s protect from infection is by mediating epithelial barrier integrity via the tight junction proteins occludin, claudin-1 and claudin-4 (88, 100).

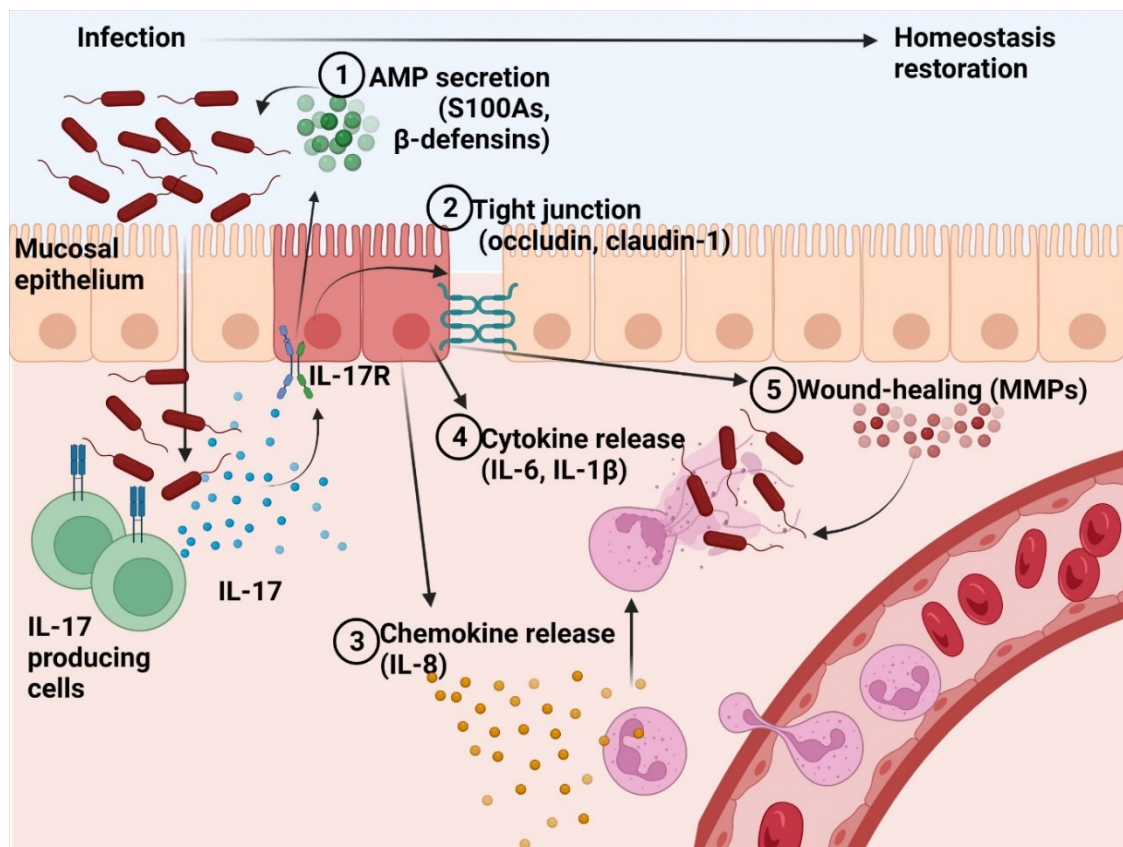


Figure 1.5. Mechanism of IL-17A in clearing infection at mucosal sites. During an infection, IL-17A producing cells produce IL-17A which stimulates non-immune cells (such as epithelial, stromal cells and macrophages) via IL-17R. The stimulation induces target genes expression and comprises: ① Secretion of antimicrobial peptides (AMPs) with microbicidal and immunomodulatory activities; ② Restoration of mucosal membrane integrity via induction of tight-junction forming proteins; ③ Secretion of chemokines to attract immune cells, such as neutrophils, to the site of infection; ④ Secretion of cytokines to activate immune cells; ⑤ Activation of wound-healing response in order to restore homeostasis and heal the site via matrix metalloproteases (MMPs) release.

1.5.2 Roles in health complications

As already indicated, IL-17s are pro-inflammatory molecules secreted in infection settings, however when their activation becomes dysregulated and chronic, this contributes to **immune pathologies** onset. There are several inflammatory pathologies linked to inappropriate IL-17A/F signalling pathway activation, such as psoriasis, ankylosing spondylitis (AS), rheumatoid arthritis (RA), inflammatory bowel disease (IBD) and multiple sclerosis (MS) (122, 146). In all these pathologies, we can observe a dichotomous nature of these cytokines having both protective and pathogenic roles. Indeed, in both the skin and the gut IL-17A/F are crucial for host protection against infections (88, 144), yet its chronic activation leads to inflammatory skin diseases and IBD (147, 148). It is possible to note in [Table 1.1](#) a difference in the highly pro-inflammatory cytokines IL-17A, IL-17B, IL-17C and IL-17F, which are actively associated with the pro-inflammatory symptomatology characteristic of autoimmune diseases. This is mainly caused by the release of cytokine and chemokines which leads to immune cells recruitment and activation as well as excessive wound-healing processes mediated by matrix metalloproteases release (45, 122, 146). On the other hand, IL-17D and IL-25 are instead associated with fewer autoinflammatory diseases and they show a milder, if not anti-inflammatory, effect given that they compete for the IL-17RA and IL-17RB receptors with the pro-inflammatory family members (149, 150) ([Table 1.1](#)).

	Autoinflammatory diseases		Cancer and other diseases	
IL-17s	Disease	Reference	Disease	Reference
IL-17A	RA	(151)	Skin cancer	(163, 164)
	Psoriatic Arthritis	(152)	Multiple Myeloma	(165)
	AS	(153)	Autism	(166)
	Psoriasis	(154)		
	IBD	(155, 156)		
	MS	(157)		
	Brain Ischemia	(158)		
	Epilepsy	(159)		
	Obesity	(160, 161)		
	Atherosclerosis	(162)		
IL-17B	Coeliac disease	(167)	Pancreatic cancer	(169)
	RA	(94)	Lung cancer	(169)
	Pneumonia	(95)	Breast cancer	(169)
	SLE	(168)	Gastric cancer	(170)
IL-17C	Psoriasis	(154)	Colorectal cancer	(173)
	Atherosclerosis	(171)	Lung cancer	(174)
	Inflammatory	(172)		
	Glomerulonephritis			
IL-17D	RA	(175)		
IL-25	Asthma	(176)	Hepatocellular carcinoma	(177)
	Atopic dermatitis	(176)		
	IBD (anti-inflammatory role)	(150)		
IL-17F	RA	(151, 178)		
	Psoriasis	(154)		
	IBD	(133)		

Table 1.1. IL-17 family in human diseases. RA, Reumatoid Arthritis; Ankylosing Spondylitis, AS; Inflammatory Bowel Disease, IBD; Multiple Sclerosis, MS; Systemic Lupus Erythematosus, SLE.

Sustained and prolonged pro-inflammatory stimuli are often associated with **tumorigenesis**, thus also the members of the IL-17 family have been associated with several malignancies (Table 1). One of the mechanisms linked to tumorigenesis is the pro-proliferative stimulation that IL-17, especially IL-17A, have on epithelial cell growth, which has been linked to skin cancer (164). Another way IL-17s promote tumorigenesis is through the induction of angiogenic factors and matrix remodelling molecules such as MMPs (179). Again, IL-17D and IL-25 show an anti-tumoral behaviour. IL-17D has been shown to favour tumour regression through NK cells recruitment (106). The role of IL-25 is instead more controversial. This molecule is associated with anti-tumour processes such as eosinophils and B-cell attraction to tumour xenografts sites (180) and apoptosis induction in human mammary glands cancer cells (181). Other reports have shown that IL-25 is linked to poor prognosis on Hepatocellular carcinoma and have clarified how IL-25 induces tumorigenesis through activation of pro-tumorigenic M2 macrophages (177).

1.5.3 Therapies targeting IL-17 pathway

Given the important role played by IL-17A in many pro-inflammatory diseases monoclonal antibodies have been developed to block it. Currently there are several antibodies that block IL-17A signalling and are used in autoinflammatory diseases such as psoriasis, ankylosing spondylitis and rheumatoid arthritis. Secukinumab and ixekizumab bind IL-17A, whereas brodalumab is active in neutralising IL-17RA (146). Other biologics are useful in such pathologies since they target IL-23 or IL-12, the upstream molecules responsible in IL-17A production: ustekinumab, mirikizumab, brazikumab, risankizumab, tildrakizumab, guselkumab (146). However, despite IL-17 and IL-17RA blocking antibodies are extremely effective in psoriasis, they show limited efficacy and lead to worsening symptoms in other inflammatory diseases such as Crohn's disease (182, 183), this is possibly due to the loss of the beneficial role that IL-17A plays maintaining the gut epithelial barrier function (88). Furthermore, it has been noted an increased risk of fungal infections, such as candidiasis, in patients using IL-17A neutralising therapies (184). Thus, a fine tuning of IL-17A pathway could be more productive than completely abolishing it in certain pathologies.

1.6 Role of inflammation in pregnancy

The immune system and inflammation in general are pivotal for the correct establishment and progression of pregnancy (Figure 1.6) (185-187). Three main phases can be identified during pregnancy: an early phase in which embryo implants and placentation occurs, an intermediate phase in which the foetus grows and, lastly, the parturition of the newborn. At all of these stages a different involvement of immune cells and immune-related molecules can be observed, creating pro-inflammatory environments for the early pregnancy establishment and parturition (185-187). Between these two stages, an immunosuppressive stage occurs, this is characterised by immune tolerance establishment (185-187).

1.6.1 Mediators required in early pro-inflammatory stage

As already indicated in the decidualization section, decidual cells secrete cytokines to communicate with the immune cells and to direct correct implantation (188). After implantation, the maternal decidua undergoes drastic changes for the formation of the placenta, which is the maternal-foetal communication interface. For correct placentation, the embryo erodes the decidual stroma and connects to the spiral arteries which are also subject to remodelling. These processes are mediated by embryonic-derived cells and by maternal immune cells. dNK and decidual macrophages with M1 phenotype produce VEGF and promote remodelling of the decidual stroma. Furthermore, dNK cells produce IL-8 and CXCL10, which directs embryo implantation (185). Other cells involved in embryo implantation are ILC3s, which produce IL-17, IL-22 and TNF α , responsible for neutrophil recruitment (187).

1.6.2 Immunosuppressive stage throughout gestation

Pregnancy is a complex process in which the maternal immune system encounters and tolerates the foetus, which is a semiallogenic graft, since it shares only half of its genome with the mother, while the remaining half is of paternal origin. dNK cells have an important role in being able to tolerate foetal antigens (28, 31), especially under the stimulation of decidual stromal cells which blunts the cytotoxic activity of those immune

cells through IL-15 stimulation (188). Furthermore, the tolerogenic environment is also mediated by the increase in regulatory T-cells (T_{REG}), which is stimulated by oestrogen (187). To further maintain this tolerance, anti-inflammatory cytokines such as IL-10 and TGF β are secreted, which stimulates further maturation of TREG and anti-inflammatory decidual macrophages of M2 phenotype (185). Decidual macrophages are also involved in foetal growth through secretion of angiogenic factors and matrix metalloproteases, as well as removing apoptotic trophoblast cells which would cause pro-inflammatory immune cell activation (185).

1.6.3 Inflammatory signals required for parturition

At the end of the pregnancy, a pro-inflammatory environment associated with parturition is induced. The main cell types involved in such process are neutrophils and macrophages. These cells infiltrate the decidua and start secreting matrix metalloproteinases, IL-6, TNF and nitric oxide (NOS) (187). Inflammation is also induced by the progressive accumulation of damage associated molecular pattern (DAMPs) from the foetal membranes which undergo senescence (189). The release of pro-inflammatory cytokines activates prostaglandin release, which are responsible for cervix ripening and labor induction (189).

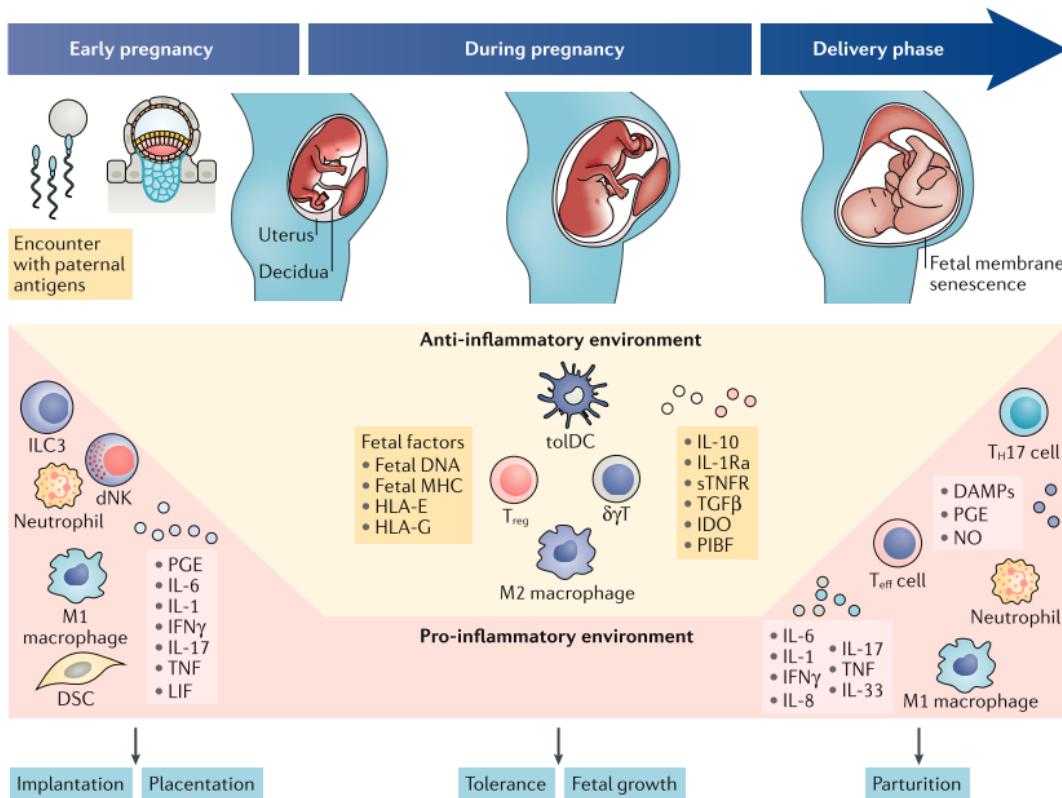


Figure 1.6. Immune events involved in pregnancy. The three main immune events required during pregnancy are illustrated. A first pro-inflammatory activation is required for embryo implantation and placentation. It is then followed by an anti-inflammatory environment sustained throughout all pregnancy in order to establish tolerance for the fetus and allow its growth. Finally, a pro-inflammatory environment is required again for parturition. DAMP, damage-associated molecular pattern; dNK cell, decidual natural killer cell; DSC, decidual stromal cell; IDO, indoleamine 2,3-diogxygenase; IL-1Ra, IL-1 receptor antagonist; ILC3, type 3 innate lymphoid cell; LIF, leukaemia inhibitory factor; NK, natural killer; NO, nitric oxide; PGE, prostaglandin; PIBF, progesterone-induced blocking factor ; sTNFR, soluble TNF receptor; TGFβ, transforming growth factor β; T_{eff} cell effector T cell; T_H17 cell, T helper 17 cell; toIDC, tolerogenic dendritic cell; T_{REG}, regulatory T cell; γδT, γδ T cell. Image from (187).

1.7 Balance between “good” inflammation and “bad” inflammation in fertility

Given the involvement of the immune response in pregnancy, whenever there is an imbalance of the inflammatory activation it leads to pregnancy complications. For

example, certain subsets of uNK cells have been associated with endometriosis (32, 190) and a decrease in the number of dNK cells is shown in women with unexplained infertility (185). A more cytotoxic phenotype is displayed by dNK cells which have been associated with several pregnancy complications such as pre-eclampsia, recurrent spontaneous abortion and recurrent implantation failure (34). There are fewer T_{REG} cells and they are also shown to be less functional in women with pre-eclampsia (186). An excessive inflammation activation, especially at an earlier timepoint, is associated with pre-term birth (189).

At the same time, the maternal immune system must be active against possible pathogens that can cause infections. Indeed infections during pregnancy can cause miscarriage and still birth, thus it is fundamental for the maternal immune system to be active against infection (191).

It is then important for each immune mediator involved in pregnancy process to be activated and inactivated in the right amount and time, making it obvious that there is a delicate balance between positive actions exerted by the immune mediators, but this can turn to be a negative action, if they act in an unbalanced manner.

1.8 Roles of IL-17s in female fertility and in pregnancy complications

A role for IL-17 cytokines in female fertility has not been recognised yet, even though this dichotomy between beneficial and pathogenic roles is indicated. As for other mucosal sites, IL-17s are expressed in the female reproductive tract (FRT) to clear infections from pathogenic insults such as *Chlamydia* and *Candida* (192, 193). In the FRT IL-17s seem also to have additional roles beyond their classical pro-inflammatory mucosal immunity. In the very early stages of pregnancy establishment, IL-17A and IL-25 are required for trophoblast implantation and decidual cell proliferation (194, 195). Furthermore, IL-17A mRNA was shown to be expressed in the Choriocarcinoma cell line JEG-3, where it increases progesterone secretion (196) and it is also increased during the third trimester in women, suggesting that this cytokine might play a role throughout pregnancy and in labour (197). Indeed, it has been found a decrease in circulating levels

of IL-17A in women 24 hours after they had a spontaneous abortion during their first trimester, whereas in healthy pregnant women the IL-17A levels were found to be higher (198). Similarly, some studies have divided endometrial T_H17 cells into different subsets depending on their secretion of IL-4 and IL-22 in addition to IL-17A, which are named T_H17/T_H2, T_H17/T_H0 and T_H17/T_H1 (199, 200). T_H17/T_H2 and T_H17/T_H0 subsets are beneficial for pregnancy establishment, as they are required for trophoblast implantation due to their production of IL-4 (199, 200). Conversely, T_H17/T_H1 cells, which secrete IL-22 but not IL-4, correlate with unexplained recurrent abortion (199, 200).

Alongside these beneficial roles, IL-17s have also been linked to pathogenic processes found in several female fertility and pregnancy-related complications, which are summarised in [Table 1.2](#) and [Table 1.3](#). For better understanding of the role of IL-17s in each pathology, they will be briefly summarised for each complication.

1.8.1. Fertility complications

Endometriosis: this is a complex disease characterised by retrograde invasion of endometriotic stromal cells in the peritoneal cavity, which is unfortunately commonly found in 10% of reproductive age women (201). These cells are under oestrogen influence and are characterised by chronic inflammatory processes (201). The dogma regarding the aetiologic factor leading to endometriosis is retrograde menstruation, where during menstruation endometrial cells reach the peritoneum through the fallopian tubes. However studies have now confirmed that retrograde menstruation is a common process which occurs in 76-90% of women, even in those not presenting endometriosis (202). It is now well established that multiple processes contribute to this disease, such as genetic mutations and inflammation (201). Indeed it can be observed an increased inflammation and immune cell activation in women affected by endometriosis (202). Women who display endometriosis often experience infertility, which is mainly caused by the hyperactivation of the inflammatory responses associated with this pathology (201). IL-17A has an active role in endometriosis progression by inducing proliferation in endometriotic stromal cells (203).

Furthermore, IL-17A induces endometriotic stromal cells to secrete pro-inflammatory cytokines (IL-6, G-CSF and IL-1 β) and chemokines (IL-8) as well as inducing blood vessel formation through induction of angiogenic factors (V-EGF), thus helping the endometriotic lesions in proliferation and growth (204). IL-17F also has been associated with an increased inflammatory signature in endometriosis with induction of IL-8 and COX2 (205). In the case of endometriosis, IL-25 seems to also contribute to the pathogenesis, since its levels are found to be upregulated in endometriotic lesions (206).

Polycystic Ovary Syndrome: this is an endocrine-metabolic syndrome which is caused by inheritable genetic mutations and is characterised by distinct hormonal abnormalities (207). This pathology is also linked to other metabolic dysfunctions such as obesity and diabetes (207). IL-17A and IL-17F are found to be increased in the circulation of women affected by PCOS, whereas IL-25 is significantly decreased and shows a positive correlation with IL-17A increase (208, 209). In an Iranian cohort it was also identified a significant correlation with the prevalence of the GG allele in the IL-17A SNP rs2275913 in PCOS affected women (210).

Unexplained Infertility: unexplained infertility is diagnosed when there is failure to conceive after 12 months of attempts with unprotected intercourse and excluding any medical conditions that may cause infertility in both the partners (211). The most common causes of unexplained infertility is undiagnosed endometriosis and uterine abnormalities (211). Unexplained infertility is closely associated with defects in endometrial receptivity, therefore embryo implantation is the step that is mostly affected by this condition. The endometrium becomes receptive in the mid-luteal phase (around day 19-23), where the high progesterone levels induce stromal cell decidualisation as well as modulate the maternal immune system to prepare for embryo implantation (188). Studies performed on women with unexplained infertility have identified significant increase in IL-17A in blood samples collected during the mid-luteal phase (212, 213). IL-17A is also found to be increased in cervical mucus and in endometrial biopsies of women diagnosed with UI, suggesting that IL-17A has a negative impact on pregnancy outcome (213).

IL-17s	Disease	Finding	Reference
IL-17A	Endometriosis	IL-17A induces IL-8 and COX-2 and has proliferative effects in endometriotic stromal cells	(203)
		IL-17A creates pro-inflammatory environment and V-EGF leading to endometriosis	(204)
	PCOS	Circulating IL-17A levels are increased in PCOS patients	(208, 209)
		G allele and GG genotype of rs2275913 SNP in IL-17A is higher in PCOS	(210)
	Unexplained infertility	Increased systemic and local IL-17A and increased pathway activation in UI	(212-214)
IL-25	Endometriosis	Increased IL-25 levels in the peritoneum from patients with endometriosis	(206)
	PCOS	Decreased circulating levels of IL-25 in PCOS patients which negatively correlates with IL-17A	(209)
IL-17F	Endometriosis	IL-8 and COX2 increase leading to pro-inflammatory environment	(205)
	PCOS	Circulating IL-17F levels are increased in PCOS patients	(209)

Table 1.2. Roles of IL-17s in fertility complications. Unexplained infertility, UI; Polycystic Ovary Syndrome, PCOS.

1.8.2. Pregnancy-related complications

Pregnancy loss: Under this category fall all the complications leading to pregnancy interruption before 20 weeks gestation and that does not involve an external intervention (215). These complications are sometimes referred using multiple names such as (spontaneous) miscarriage or spontaneous abortion and, in case the pregnancy loss repeats for more than three times, it is referred as recurrent spontaneous abortion, recurrent miscarriage or recurrent spontaneous miscarriage (215). The causes leading

to pregnancy loss are multiple, and the principal ones are chromosomal abnormalities, uterine abnormalities or maternal infections, among others (215). Several reports have highlighted how, throughout all pregnancy stages, the maternal immune response plays an important role for the correct foetus growth (185, 186). In the context of pregnancy loss, T_H17 cells and the consequent IL-17A protein are found to be increased, thus pointing out to an unbalanced pro-inflammatory signature that is not compatible for maintenance of a healthy gestation (216-219). Some studies, performed in Egyptian and Iranian women, have highlighted some single nucleotide polymorphisms (SNPs) in IL-17A and IL-17F genes that are associated with recurrent pregnancy loss, even though those two studies have found conflicting results regarding IL-17F SNPs, where one study has found it to be positively associated with RLP, whereas the other study says that it is linked to decreased risk of RPL (220, 221). IL-25, on the other hand, seems to have a protective role against pregnancy losses. Indeed this cytokine is found to be reduced in women with recurrent miscarriage and, treatment with 1,25 vitamin D₃, increases IL-25 which in turn is able to reduce T_H17 frequency as well as the IL-17A protein produced in women with unexplained recurrent spontaneous abortion (222, 223).

Pre-eclampsia: this condition is identifiable after 20-weeks of gestation and is characterised by hypertension in the placenta which often leads to multi-organ dysfunction in the mother (224). Among the causes leading to pre-eclampsia can be found increased maternal age, maternal comorbidities, and defective placentation, which results in incorrect spiral artery transformation and leads to hypoxia and ischemia (224). Several reports have identified increased levels of IL-17A being associated with pre-eclampsia due to its pro-inflammatory signature and neutrophils chemoattraction (225-227). Furthermore, studies blocking IL-17A signalling, either with siRNA or with neutralising antibodies, have been shown to ameliorate the symptoms (228, 229). However, a study conducted in rat who were given rIL-17A during pregnancy, has highlighted how this induced significant increase in the mean arterial pressure leading to placental hypertension, but was not sufficient *per se* in causing PE (230). IL-25 again seems to have a protective role with its anti-inflammatory function. In normal pregnancies IL-25 levels increase during the third trimester, but in pre-eclampsia it can be noticed a significant decrease in IL-25 (231). The decrease in IL-25 is associated with

a decrease in anti-inflammatory M2 macrophages (232). It seems that in pre-eclampsia there are some epigenetic mechanisms regulating IL-17s expression, since were identified IL-17F, IL-25 and IL-17A genes being hypomethylated in omental arteries (227). Hypomethylation in Jurkat cells resulted in increased IL-25 and IL-17F expression but failed to modulate IL-17A secretion (227).

Recurrent Implantation Failure: this term refers to the cases when there are at least three failed cycles of in vitro fertilisation-embryo transfer (IVF-ET) with a good quality embryo (233). Also in this case the causes leading to RIF are multiple and complexes and comprise maternal age, genetic factors as well as immunological factors (233). Again, in this complication the levels of IL-17A are found increased, leading to a pro-inflammatory signature (234).

Pre-term labour: pre-term labour is defined when delivery happens before 37 weeks of gestation (235). Among the risk factors for this conditions can be found vaginal and intrauterine infections, sexually transmitted infections, uterine abnormalities and shortened cervix (235). In the context of chorioamnionitis, a disease closely associated with preterm labour, IL-17A levels are increased and correlate with increased IL-8 levels, thus pointing out a possible involvement of IL-17A in neutrophil enrichment, which is a characteristic of this pathology (236).

IL-17s	Disease	Finding	Reference
IL-17A	Pregnancy loss	Increased T _H 17 and less T _{REG} in women with RPL	(216-218)
		Increased IL-17A ⁺ cells in decidua and increased neutrophils in abortion cases	(219)
		Less IL-17A ⁺ cells in menstrual blood in women with URSA	(237)
		Progesterone reduces IL-17A production, which is associated with recurrent spontaneous miscarriage	(238, 239)
		IL-17A SNP rs2275913 is associated with increased risk of RPL	(221)

		Decreased circulating IL-17A levels in women after spontaneous abortion if compared to healthy pregnancies	(198)	
		T _H 17/ T _H 2/IL-22+ and T _H 17/ T _H 0/IL-22+ cells producing IL-4 are needed for implantation, whereas expansion of T _H 17/ T _H 1 /IL-22+ cells, which lack of IL-4, leads to URSA	(199, 200)	
	PE		Increased IL-17A leads to PE	(225, 226)
			Blocking IL-17A signalling prevents PE	(228, 229)
			Metabolic syndrome induces inflammation leading to increased IL-17A and PE	(238)
			IL-17A supplementation alone during gestation causes placental hypertension but not PE	(230)
			IL-17A is hypomethylated in PE and IL-17A treatment induces neutrophil chemotactic molecules expression	(227)
	RIF	Increased IL-17A and T _H 17 in RIF patients with metabolic syndrome	(234)	
	Preterm Labour	Increased IL-17A in Chorioamnionitis, leading to TNF- α -mediated inflammation	(236)	
	Endometritis	Shift towards pro-inflammatory cytokine milieu caused by IL-17A, increased in endometritis	(239)	
IL-17C	Stress	IL-17C found among immune markers for maternal stress however, is not associated with stress	(240)	
IL-25	Pregnancy loss	Reduced IL-25 expression in recurrent miscarriage	(222)	
		1,25VitD3 increased IL-25 expressions and reduced IL-17A expression in URSA	(223)	

	PE	IL-25 supplementation ameliorates pre-eclampsia in Rats via M2 macrophages maturation	(232)
		IL-25 is hypomethylated in PE, which increases its expression	(227)
		IL-25 increases in third trimester, but not in PE where it decreases, preventing embryo proliferation and invasion	(231)
IL-17F	Pregnancy loss	IL-17F SNP rs763780 shows significantly different allele frequencies in women with RPL	(220)
		SNP rs763780 found to be associated with decreased risk of RPL in another cohort	(221)
	PE	IL-17F is hypomethylated in PE, which increases its expression	(227)

Table 1.3. Roles of IL-17s in pregnancy-related complications. Unexplained infertility, UI; Recurrent Pregnancy Loss, RPL; Unexplained Recurrent Spontaneous Abortion, URSA; Pre-eclampsia, PE; Recurrent Implantation Failure, RIF; Polycystic Ovary Syndrome, PCOS.

1.9 Anti IL-17A therapies for female fertility

More insights regarding the use of anti-IL-17A antibodies during pregnancy are now appearing to be released, especially in studies where women affected by psoriasis, psoriatic arthritis and ankylosing spondylitis continue their medication throughout pregnancy. The current recommendations for treatment of those pathologies around pregnancy are to discontinue the therapy until breastfeeding (241) and, in all the studies mentioned, all the participants have discontinued their therapy before the third trimester. Both secukinumab and ustekinumab have been shown to cross the placenta and can be found in the offspring circulation, but there is no evidence of teratogenesis or increased risk of pregnancy complications (242-244). Also ixekizumab should be able to cross the placenta, as shown in preclinical studies performed in cynomolgus monkeys (245), however it is shown to be not harmful to the foetus or the mother (246). Some

studies conducted in rat models of pre-eclampsia have used recombinant IL-17RC infusion at day 14 of pregnancy to block IL-17A signalling and resulted in improvement of hypertension, oxidative stress and less cytolytic NK cells (247, 248).

1.10 The microbiome in female reproductive tract

Despite being thought of being a sterile compartment for a very long period, the female reproductive tract is now known to be colonised by commensal bacterial species forming a local microbiome. Since the female reproductive tract is characterised by different compartments with different functions and physical structures, the microbiome found in those compartments is also extremely variable.

1.10.1. Vaginal microbiota

The vaginal microbiota has been extensively studied, given it was believed to be the only non-sterile compartment of the FRT due to its connection with the outer world. The predominant genus found in healthy women is dominated by the Firmicutes *Lactobacillus spp.* (249, 250), with four main distinct microbiota community types dominated by different species: *L. iners*, *L. crispatus*, *L. gasseri* and *L. jenesii* (249). Another microbiota community type was also identified with a predominant abundance of anaerobic organisms, such as *Prevotella*, *Gardnerella*, *Aerococcus*, *Dialister*, *Atopobium*, *Megasphaera*, *Peptoniphilus*, *Sneathia*, *Finnegoldia*, and *Mobiluncus* (249). In this fifth group, *Lactobacillus iners* and *L. crispatus* can still be detected, but they do not represent the most abundant species (249).

Studies performed on microbial composition through menstrual cycle had identified changes in the vaginal microbiome, with increased *Garnerella spp.* and decrease of *Lactobacillus spp.* at menses (251, 252). Steroid hormones have been found to modulate microbial species composition. Oestrogen stimulates vaginal epithelium production of glycogen, which fuels *Lactobacilli*, leading to increased lactobacilli composition in the middle of the menstrual cycle when oestrogen peaks (253).

1.10.2 Uterine microbiota

The composition of the upper FRT microbiota displays a lower consensus among research groups. Firstly, the microbiome in the endometrium has only recently been investigated, due to the old belief that this was a sterile compartment. It is estimated that the bacterial load in the endometrium is much lower than the one found in the vagina, with approximately 100-10000 times lower biomass (250, 254). Studies focusing on the microbiome present in the endometrium show discrepancies in the phyla identified. There are some reports in which even the endometrial microbiome was found to be dominated solely by *Lactobacillus spp.* (254-256), other reports, on the other hand, have reported a different microbial composition with an higher abundance of non-lactobacilli genus (250, 257, 258). These reports display different genera being highly abundant in the endometrium, with *Flavobacterium* in one study (257) and *Pseudomonas*, *Acinetobacter*, *Vagococcus*, *Sphingobium* in the other study (250). Thus, a eubiotic endometrial microbiome has not been identified yet, due to differences in the microbiome composition found in different studies (259). The possible reasons for these discrepancies could be ethnicity as well as different dietary habits of the participants and sample collection, all factors that are known to contribute to modulate the microbiome (260, 261). There have been also other reports in which no microbiome was identified in the maternal side of the placenta by sampling trough caesarean section (262, 263), thus suggesting that the endometrium could not be colonised by a microbiome.

Another debate regards the modulation of the endometrial microbiome through menstrual cycle. Some studies revealed changes in the microbial species colonising the endometrium between the proliferatory and the mid-secretory phases, with increase in *Propionibacterium acnes* and decrease in *Sphingobium* app. and *Gardnerella vaginalis* (Figure 1.7) (250, 258). Other reports show that the microbiome does not change through menstrual cycle (255, 256). It is possible that steroid hormones impact on endometrial microbiome. In a pilot study performed on a cohort of women subjected to controlled ovarian stimulation and progesterone supplementation was reported a decrease in *Lactobacilli* and an increase in *Prevotella* and *Aptobium* abundance, as well as increased in bacterial biodiversity (264).

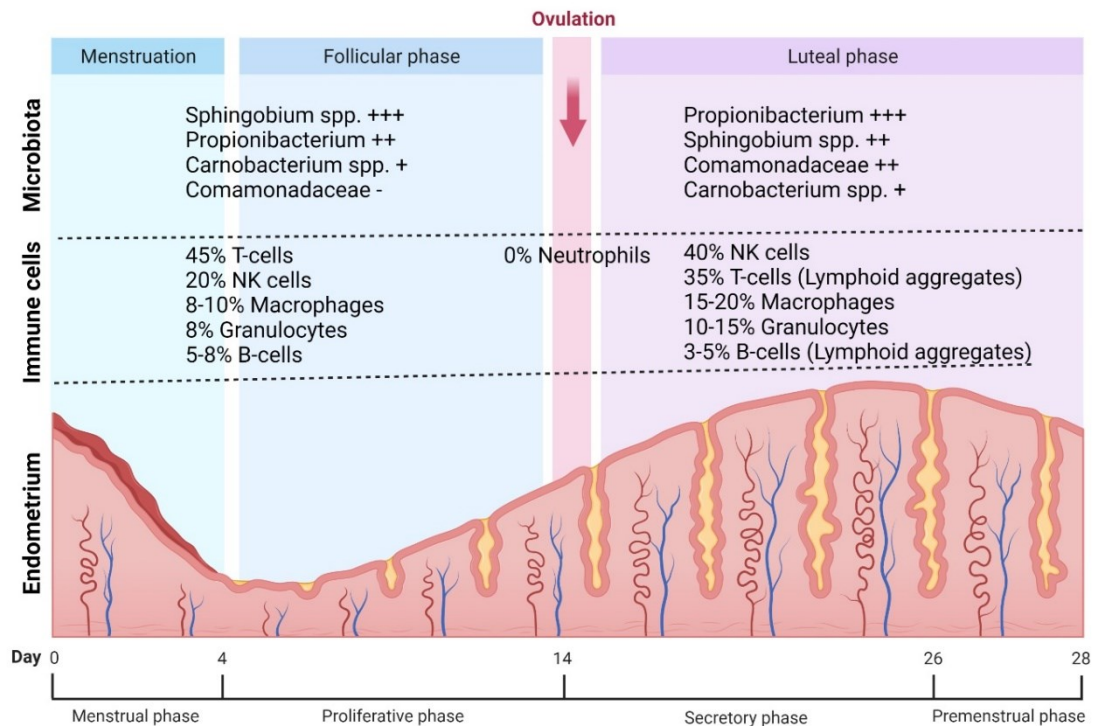


Figure 1.7. Changes in endometrial immune cells and in the microbiota induced by the menstrual cycle. During the menstrual cycle the sex hormones drive changes in the endometrium, immune cells and microbiota. The microbiota composition seems stable during the cycle, with changes in abundance between *Sphingobium* spp. and *Propionibacterium* between the proliferative and the secretory phase. The secretory phase seems to be characterised by an increased microbial proliferation. The immune cells change greatly during the menstrual cycle. T-cells are the most abundant cell type during the proliferative phase, but their percentage decreases greatly in the secretory phase, where they can be found mainly in lymphoid aggregates, together with B-cells. It has been reported absence of neutrophils during the ovulatory phase, probably to avoid semen degradation. NK cells percentages are significantly increased during the secretory phase, where they have been associated with spiral arteries formation and decidualisation. +/- represents the relative abundance of microorganisms. Figure adapted from (4).

1.11 Changes in the microbiota during pregnancy

Similar to the local immune milieu and the physical epithelial/stromal tissue structures, the microbiome is also modified during pregnancy.

The vaginal microbiome evolves by converting to a lower diversity microbiome, dominated by a single *Lactobacillus* specie. Indeed, studies have shown how, even women showing the anaerobic-dominated microbiome, during pregnancy they convert it into a *Lactobacillus*-dominant (265-267).

Little is known about changes in endometrial microbiome during pregnancy, some microbial species have been identified in maternal-foetal compartments and amniotic fluid and colonising the placenta(268).The placental microbiome described in these studies is characterised by prevalence of *Proteobacteria*, *Actinobacteria*, *Firmicutes*, *Bacteroidetes*, *Tenericutes*, and *Fusobacteria* phyla, which are more similar to the oral microbiome, rather than to the endometrial or vaginal one (269). Indeed it have been proposed three different exposure routes for the foetus to microbial species: ascension from the vagina, haematogenous from the oral cavity and the third route is linked to the gut microbiome (268). The exposure of the foetus to maternal microbiome seem to play important roles in ensuring correct development as well as inducing tolerance for commensal bacterial species, improving post-natal development as well (270).

Other studies have reported on the other hand that the placenta does not contain a microbiome, considering that when they performed their analysis they could only identify species used as a positive control in the sample, but not other bacteria (262, 263). One study identified *Streptococcus agalactiae* as a pathogen present in the maternal side of the placenta which is associated to fatal sepsis if it reaches the foetus (262).

1.12 The impact of microbiome in fertility

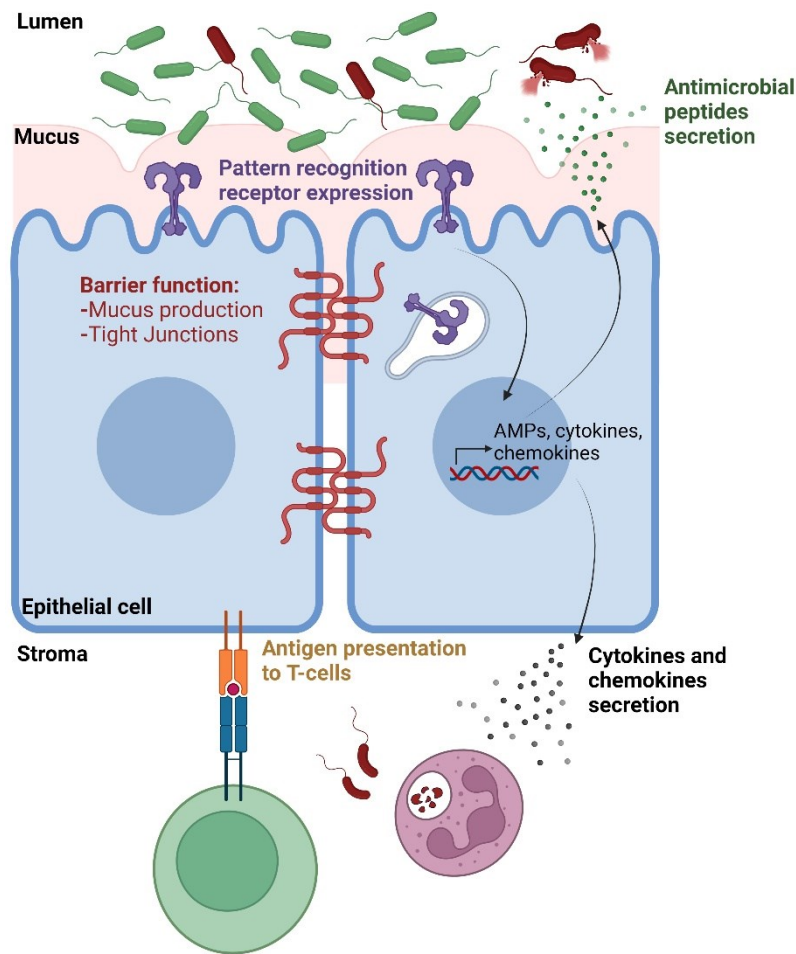
The processes involved in female fertility and reproduction are extremely complex and involve a crosstalk between the specialised endometrium/stromal compartment and the surrounding environment, including the microbiome.

In the lower reproductive tract, *Lactobacilli* have been shown to play important roles in maintaining eubiosis by producing lactic acid and bacteriocins, which can prevent pathogens infection by lowering the pH (271) and by direct killing (272), respectively.

Furthermore, Lactobacilli are involved in promoting tolerance against commensal bacterial by stimulating a weak pro-inflammatory response (273). When the optimal microbiome composition is altered, such as in the case of bacterial vaginosis, the lactobacilli dominance is lost and anaerobic opportunistic species, such as *Gardnerella*, *Prevotella*, *Mobiluncus* and *Megasphaera* increase their expression and induce a pro-inflammatory environment through secretion of short chain fatty acid (SCFA) (273). Vaginal dysbiosis, associated with lower abundance of Lactobacilli and an higher diversity in microbial species abundance has been associated with fertility complications such as infertility (274), higher miscarriage rates (275), higher risk or preterm birth (266) and poor reproductive outcomes (276). There are some studies suggesting that *Lactobacillus* dominance in the vaginal microbiome can be used as a positive prediction factor for successful IVF treatment (277), however not all studies agree in a positive correlation between vaginal microbiome and IVF outcome (278).

Regarding the upper FRT, since there is not yet a consensus on the composition of the healthy microbiome, is still uncertain what are the roles of endometrial microbiome and fertility. A distinct microbiome has also been identified to be associated with the pathology of endometriosis, with increased levels of Proteobacteria, *Enterobacteriaceae*, *Streptococcus*, and *E. coli* (250, 256). Is possible that this dysbiosis is causing the pro-inflammatory environment that is associated with endometriosis or *vice versa* (256). Similar to the vaginal microbiome, the loss of Lactobacilli predominance has been reported to negatively impact in implantation and pregnancy rates (255, 257). In these studies, *Gardnerella* and *Streptococcus* abundance seems to negatively impact on pregnancy establishment and live birth rate (255, 279). Conversely, a study showed that women presenting dysbiotic endometrium with 0% *Lactobacillus* content had pregnancy rates comparable to women showing the eubiotic lactobacillus- dominated endometrium (280). The authors of this study commented this result by suggesting that maybe the presence of a particular specie or set of species might have a bigger impact in pregnancy outcomes, rather than looking at a discriminatory *Lactobacillus* versus non-*Lactobacillus* microbiome at the genus level (280).

Figure 1.8. Functions of FRT epithelial cells in fighting infections. Epithelial cells located within the FRT mucosa possess multiple functions to prevent and clear infections from pathogenic bacteria (red).



Epithelial cells located within the FRT mucosa possess multiple functions to prevent and clear infections from pathogenic bacteria (red). Among these there is barrier function, played through mucus secretion and by cell-cell adhesion through tight junctions to prevent microbial species invasion. Epithelial cells also can sense and bind PAMPs through dedicated receptors PRRs. Endometrial epithelial cells also showed the ability to present microbial derived antigens to T-cells via MHC type I and MHC type II interaction with the T-cell TCR. Lastly, epithelial cells of the FRT respond to bacterial infection by secreting AMPs, whose

action is microbicidal, and cytokines and chemokines to attract and activate immune cells involved in infection clearance. AMPs: antimicrobial peptides; MHC: major histocompatibility complex; PAMPs: pathogens associated molecular patterns; PRRs: pattern recognition receptors; TCR: T-cell receptor.

1.13 Epithelial cells: roles in defence and as mediators of microbiome and host interaction

In mucosal sites the epithelial cell compartment plays an important role in order to prevent and fight infections. Epithelial cells have been shown to be the first line of defence against microbial invasion by acting as a barrier which is not penetrable by pathogens. Alongside this “passive” function, epithelial cells are also shown to play active roles in fighting infections through sensing foreign and pathogenic microbes with pattern recognition receptors (PRRs) and by secreting antimicrobial peptides (AMPs), cytokines and chemokines (7) (Figure 1.8). The epithelial compartment in the FRT has

evolved even more specialised features in order to optimise the processes involved in fertilisation, implantation and placentation, while remaining active against pathogen infections.

1.13.1 Barrier function

The mucosal epithelial layer of cells must act as a barrier to prevent microbial species invasion and this has been reported to happen in the FRT, despite with some differences between the upper and lower tract (281). These differences are partially explained by the different organisation of the epithelial cells in the FRT, with a stratified squamous epithelium present in the lower FRT and a single-layered columnar epithelium in the endometrium. It has been reported that in the lower FRT tight junctions are only located in the basal cells, resulting in a lesser compact outer layer (281). In the endometrium, conversely, the epithelium is formed by polarised columnar cells which are closely linked with tight junctions (281). Under oestrogen influence, the junctions relax due to the increased expression of claudin and occludin, allowing the trophoblast for an easier invasion during implantation (282). Another protective function mediated by epithelial cells is the production of mucus, which is used to block pathogens and prevent their interaction with the epithelial layer (7). Sex hormones have been shown to modify the thickness and content of mucus in order to accommodate the changes needed for sustaining pregnancy and to prevent infection of the upper FRT with bacterial species derived from the lower FRT (283).

1.13.2 Pattern Recognition Receptor expression

All nucleated cells can recognise foreign molecules through pattern recognition receptors (PRRs) which are able to bind a broad spectrum of molecules displayed by pathogens known as pathogen-associated molecular patterns (PAMPs) (284). Cells in the FRT express Toll-like receptors (**TLRs**) and have been shown to be able to recognise a wide variety of bacterial, viral and fungal PAMPs (285, 286). Cells belonging to the lower FRT have been described to express TLR3, TLR1, TLR2 and TLR6, responsible for the recognition of double stranded DNA-viruses (TLR3) and lipopeptides expressed in bacterial and fungal cell walls (TLR1-TLR2 or TLR2-TLR6 complexes) (287). Cultured primary human epithelial cells from the endometrium have been shown to express TLRs

1-9 as well as MD-2, thus showing ability to recognise even bacterial lipopolysaccharide (bound by TLR4-MD2), flagellin (TLR5), viruses showing genome organised in single stranded RNA (TLR7 and TLR8) and pathogens whose DNA presents unmethylated CpG such as some bacteria and herpesviruses (TLR9) (288). However, when stimulated *in vitro* those cells were only shown to be responsive to TLR3 activation with poly(I:C), resulting in an increased expression and secretion of cytokines, IFN- β and chemokines (288). With regards to LPS stimulation, endometrial epithelial cells have been shown to be responsive to LPS only when the soluble co-receptor CD14 is added to the stimulation (289). Another family of PRRs show a peculiar nucleotide binding oligomerisation domain (NOD), thus are named NOD-like receptors (**NLRs**) and these receptors are able to recognise molecules deriving from the degradation of bacterial peptidoglycans and activate the inflammasome machinery. NOD1 and NOD2 have been identified in the endometrium and, despite NOD1 is constitutively expressed, NOD2 is increased during the late secretory phase (290). Stimulation of primary endometrial epithelial cells with a NOD2 ligand led to increased cytokine mRNA expression (290). Another class of NLRs includes molecules containing a Pyrin domain and are thus named NLRP (Nucleotide-binding oligomerization domain, Leucine rich Repeat and Pyrin domain containing). NLRP3 expression has been identified in the endometrium and its expression, as well as inflammasome activation, is increased during menstruation (291) but also during fertility complications (292, 293). Furthermore, NLRP3 expression has been shown to be under estradiol influence (293), leading to a switch from its expression mainly found in the epithelium in secretory phase towards expression in the stromal decidual compartment in late-secretory and menstruation (291). A third class of PRRs comprises molecules able to detect intracellular viruses by sensing intracellular RNAs and are named RIG-I (Retinoic acid-Inducible Gene I)-like receptors or **RLRs**. The two receptors belonging to this class, RIG-I and MDA5 (Melanoma differentiation associated gene 5), are expressed with low levels in endometrial epithelial cells (294) and in a bovine model of infection they have been shown to respond by increasing type-1 IFN transcription (295). For intracellular DNA instead another pathway is activated by binding of the DNA to the cyclic GMP-AMP synthase (**cGAS**) which leads to activation of **STING** (STimulator of INterferon Genes) and production of interferons. STING is poorly localised in the endometrial epithelial cell compartment, is mostly localised in the stromal

compartment and is greatly enhanced in endometriosis and adenomyosis patients (296). According to the human protein atlas, cGAS shows a medium staining score in FRT in both epithelial and stromal cell compartments, thus cells are ready to respond to foreign DNA found in the cytoplasm, even though functional studies are still missing.

1.13.3 Antigen presentation

Along with professional APCs, all nucleated cells in the body can present antigens to CD8⁺ T-cells using MHC class I molecules. Studies using animal models have highlighted how uterine epithelial cells can present antigens to T-cells and that oestradiol enhances antigen presentation concomitantly to the overall immunosuppressive environment found in late proliferative phase (285). Furthermore, it has been noted how endometrial epithelial cells express MHC class II and, like for professional APC, this can lead to direct CD4⁺ T-cell activation and is even more upregulated by IFN- γ treatment (297, 298). It was described that during oestradiol peak epithelial cells produce TGF- β in the basolateral layer, thus resulting in the inhibition of antigen presentation by professional APCs (11, 299).

1.13.4 Antimicrobial peptides (AMPs) secretion

Several classes of AMPs have been shown to be secreted by epithelial cells in both the upper and lower FRT: defensins, S100-family proteins, whey acid proteins, cathelicidins (145). These molecules are secreted in the mucus to scavenge any pathogen that might get trapped, but they can also be actively produced upon infection and are shown to be modulated by sex hormones as well, with different AMPs secreted at different stages of the menstrual cycle (145). AMPs are particularly upregulated in the endometrium during the secretory phase, which coincide with an overall decreased responsiveness of immune cells, thus is possible that in this phase the immunosurveillance is mainly played by AMPs (145). AMPs levels are tightly regulated also during pregnancy and labour, to protect both the foetal and the maternal tissues from infections (145). AMPs belong to many classes and each of them show many functions beyond just killing of microbes. They have been shown to modulate and enhance the immune response by recruiting and activating immune cells in the site of infection (300), as well as mediating bacterial phagocytosis through opsonisation (301). AMPs show also anti-inflammatory and

homeostatic functions. SLPI, whose expression peaks during the secretory phase and it is known to promote epithelial cell proliferation and protect them from the pro-inflammatory activity of immune-derived proteases (302).

1.13.5 Cytokine and chemokine secretion

Epithelial cells from the FRT have been shown to mediate microbicidal functions by secreting cytokines and chemokines to attract and activate immune cells (285). In endometrial epithelial cells has been identified the production of several chemokines (IL-8, MCP-1, MIP-1 β) and cytokines (TNF α , IL-6, GM-CSF) which are released in the uterine lumen (285). Oestrogen has an anti-inflammatory action on endometrial epithelial cells by dampening both the constitutive and the stimulated production of cytokines and chemokines (303). Studies using co-culture of endometrial epithelial and stromal cells have shown that epithelial cells cultured alone secrete TNF α towards the lumen and TGF β towards the basolateral layer and that in co-culture with stromal cells or in the presence of stromal cells conditioned media, TNF α release by epithelial cells is decreased (304). Human epithelial cells in the FRT have been shown to produce IFN- ϵ , which is not expressed in any other organs and it is shown to follow a cyclical variation under direct progesterone influence, thus suggesting that a potential important function might be played by this protein in the FRT (305). Endometrial epithelial cells have been found to produce increased levels of IFN- β upon viral stimulation and this is not influenced by oestrogen (306) thus, despite dampening of most cytokines and chemokines is observed in the proliferative phase, the surveillance to viral infection remains high throughout all the menstrual cycle phases. In the lower FRT has also been found secretion of immunomodulating molecules, however the concentration and the molecules identified vary according to the method for sample collection (303). Cervico-vaginal lavages (CVL) demonstrated the presence of IL-6 and IL-8 and MIP-1 β (303). Studies using primary vaginal cells showed that they are particularly responsive to viral stimulation, similarly to the endometrial counterparts (303). Using vaginal epithelial cell lines it was demonstrated that oestrogen dampens greatly the production of IL-1 α and TNF α , thus showing an overall anti-inflammatory environment which can tolerate sperm entry and facilitate its mobility for fertilisation (7). CCL20 is another chemokine which was recently shown to be secreted by uterine epithelial cells that creates a gradient of

attraction for chemotaxis of capacitated sperm in the endometrium, where fertilisation occurs (307).

1.14 Overall Rationale and Aims

It is now clear that the immune response is fundamental for female fertility processes, as well as the microbiome. However, the interaction between maternal immunity and pregnancy, especially during the implantation step, which is the most crucial for pregnancy establishment, is not completely understood yet. The same can be said regarding the local microbiome. It is not known yet the exact composition of a healthy endometrial microbiome and much less is known about its roles in modulating female fertility during the implantation steps. It is also clear that the endometrial epithelial cells, due to their barrier activity and location, are able to crosstalk with both the immune system and the microbiome, giving them the ability to orchestrate the inflammatory response which can also impact on female fertility. Not much is known about IL-17s role in fertility, despite the literature confirms a possible role for these cytokines in mediating embryo implantation processes. Our group has recently identified increased levels of IL-17A in women with unexplained infertility undergoing ART with unsuccessful outcome. We therefore hypothesized that IL-17A might cause an excessive pro-inflammatory activity which impacts in female fertility by preventing embryo implantation. Furthermore, since IL-17A is secreted in response to bacterial infections, we think that in the women displaying higher IL-17A protein there could be a different microbiome, which would explain the pro-inflammatory immune activation. Given the role of epithelial cells in mediating the interaction with both the immune system and the microbiome, this study aims at characterising the innate immune activity of epithelial cells to understand the role of IL-17s and the microbiome in female fertility. We will address this question by using multiple approaches:

- 1) Analyse the evolution of IL-17s in mammalian organisms to clarify their involvement in mammalian pregnancy.**

For answering this question, analysis on the genes codifying for IL-17s will be carried out in mammalian clades (prototherian, metatherian and eutherian) to assess whether they are conserved and syntenic. Furthermore, multiple sequence alignment will be performed on the proteins from mammalian IL-17s to infer evolution and analyse structural identity between the mammalian clades. Lastly, interrogation of publicly available datasets related to female fertility will uncover whether IL-17s expression is upregulated or downregulated.

2) Define whether endometrial epithelial cells can produce IL-17A and explore the mechanism of action of this cytokine in female fertility.

To understand the source for the IL-17A we observed in women undergoing ART with unsuccessful pregnancy, we will explore whether it can be produced by endometrial epithelial cells. Using two cell models, a tumoral cell line and primary human endometrial epithelial cells stimulated with bacterial and viral ligands, the expression of IL-17A, ROR γ t and its immune activator will be performed. The autocrine effect that IL-17A stimulation has on endometrial epithelial cells will be assessed by treating Ishikawa and human endometrial epithelial cells with rIL-17A.

3) Reveal whether women with unexplained infertility undergoing ART show a different microbiome correlating with IL-17A and the role that dysbiosis has on endometrial epithelial cells.

The possibility of a different microbiome causing IL-17A increase will be assessed through microbiome analysis using 16S sequencing on the endometrial biopsies from the cohort of women undergoing ART. The effect that a dysbiosis could have on endometrial epithelial cells will be explored by treating tumoral and primary human endometrial epithelial cells with microbial derived short chain fatty acids. The pathways and the possible epigenetic regulations leading to pro-inflammatory gene induction will also be analysed.

4) Understand the effect that IL-17A and butyrate have on the window of implantation.

Given the dysregulation observed for IL-17A and of a possible dysbiosis in impairing embryo implantation, we will use *in vitro* models for inducing the window of implantation in Ishikawa and human endometrial stromal cells with and without IL-17A and butyrate, respectively.

Chapter 2. Materials and Methods

2.1 Patient recruitment

This study was enabled thanks to the long-lasting collaboration with the National Maternity Hospital, Dublin, and the associated Merrion Fertility Clinic, Dublin. The National Maternity Hospital is the largest maternity hospital in Ireland, providing outstanding healthcare for maternity and gynaecological services. Merrion Fertility Clinic is the leading in vitro fertilisation (IVF) clinic in Ireland and carries out best practice reproductive medicine, which granted this centre to be accredited as an ESHRE training centre.

2.1.2. Subjects for primary epithelial and stromal cell isolation

Another model used in this study were primary human endometrial epithelial (hEEC) and stromal (hESC). Endometrial biopsies were obtained from laparoscopic surgeries performed on women of reproductive age who attended the National Maternity Hospital for gynaecological investigations. Ethical approval (see appendix II) was granted by the National Maternity Hospital for the collection of eutopic endometrial biopsies. Written informed consent (see appendix III) was received from participants prior to inclusion in the study.

These samples were obtained from February 2021 until February 2022, however due to SARS-CoV2 pandemic which resulted in several lockdowns, the number of patients undergoing fertility investigation and laparoscopic intervention was extremely reduced.

The endometrial biopsies were obtained using a pipelle de Cornier and placed in transport medium: Hanks' balanced salt solution (HBSS) supplemented with 100U/mL Penicillin-Streptomycin, 2.5µg/mL (corresponding to 5% vol/vol) Amphotericin B and 5% vol/vol charcoal-stripped Fetal Bovine Serum (FBS). The biopsies were then collected from the hospital and primary cells isolated.

Patient details		N=8	
Age (years)	42.1 (8.2)		
Body Mass Index (kg/m ²)	32.3 (6.7)		
Parity (number of live births)	2 (1.5)		
Menstrual cycle length (28 days)	Regular: 50% (n=4)	Irregular: 50% (n=4)	
Menstrual phase	Menstrual: 12.5% (n=1)	Proliferative: 25% (n=2)	Secretory: 37.5% (n=3)
Menstrual cycle complications	Amenorrhea: 12.5% (n=1)		Menorrhagia: 12.5% (n=1)
Diagnosis of infertility	Yes: 50% (n=4)		No: 50% (n=4)
Diagnosis of endometriosis	Yes: 12.5% (n=1)		No: 87.5% (n=7)

Table 2.1. General characteristics of the participants from which primary cells were obtained.

Values are reported as mean with standard deviation in parentheses, except for the menstrual cycle, Infertility and endometriosis, which are presented as the percentage of patients who presented each anamnesis and the number of participants in parentheses.

2.1.3. Subjects for the 16S-sequencing and immune cell abundance estimation

The samples were obtained by patients recruited in the study at Merrion Fertility Clinic, Dublin, Ireland between October 2016 and February 2018, as already reported (214). Ethical approval was obtained from the National Maternity Hospital in Dublin in 2016 and informed consent was obtained from all the study participant prior to sample collection.

The study included women with unexplained infertility (n=30) who underwent assisted reproductive technologies (ART) after receiving an endometrial scratch in the menstrual cycle before embryo was transferred (Table 2.2). The study participants were asked if the scratch samples could be used for research purposes. The samples were then retrospectively referred according to the ART outcome, allowing to divide the cohort in women who had a successful (n=12) and an unsuccessful (n=18) pregnancy. Inclusion

criteria for the study included women with age <38 years, regular menstrual cycles, normal semen analysis in the partner and BMI <30 Kg/m². Furthermore, women who have had previously pregnancies or miscarriages or have used steroid hormones within 3 months or have been diagnosed with endometriosis were excluded from the study.

The endometrial biopsy was obtained using a pipelle de Cornier at mid-luteal day corresponding to the 7th day after luteinizing hormone surge (LH+7), on the menstrual cycle before the cycle when the embryo would be transferred. Urinary LH levels were assessed twice daily from day 9 of the menstrual cycle. All the study participants received a good to top quality embryo transferred on day 5 of the following menstrual cycle. The samples were snap frozen and stored at -80°C.

Patient details	Successful (n=12)	Unsuccessful (n=18)	p-value
Age (years)	34.8 (1.6)	35.6 (1.5)	0.549
Body Mass Index (kg/m ²)	23.6 (3.4)	23.0 (2.2)	0.604
Menstrual cycle stage (day)	21.6 (3.9)	21.9 (2.3)	0.775
Serum β hCG positivity	100% (n=12)	27.7% (n=5)	N/A
Gestation length (weeks)	39.5 (1.9)	N/A	N/A
Miscarriage	8.3% (n=1)	5.5% (n=1)	N/A
Smoking	0% (n=0)	0% (n=0)	N/A

Table 2.2. General characteristics of the study cohort. Values are reported in mean with standard deviation in parentheses and the corresponding p-value were calculated using unpaired two-sample t-tests. The serum β hCG positivity, miscarriage and smoking data is displayed as the percentage of patient relative to the total number with the exact number in parentheses.

2.2 Computational Biology techniques

2.2.1 Databases

The resources used in this study to retrieve protein and nucleic acid sequences of IL-17/IL-17R family members were: GenBank and RefSeq databases at the National Centre

for Biotechnology Information (NCBI), Ensembl genome browser and the University of California Santa Cruz (UCSC) genome browser.

2.2.2 Identification of IL-17 proteins

2.2.2.a Search using Genome Browsers for IL-17 proteins

IL-17 family members protein sequences across several organisms were retrieved from the linked gene sequence and cross-referenced with the databases, to collect protein IDs in the chosen species (outlined in [Table 2.3](#)). A first step of similarity check was performed by aligning all proteins against the corresponding human IL-17 family member using ClustalW (<https://www.genome.jp/tools-bin/clustalw>). This allowed us to establish, in organisms with poorly annotated proteomes, that the protein in question was in fact the most similar to the human one. Sequences were considered for further analysis if they showed a percentage identity higher than 20%, which corresponds to the upper bound of the "Twilight zone" (308).

2.2.2.b Reciprocal Best Hits analysis

Given that the focus of the research was to highlight differences in IL-17s among mammalian clades (eutherian, metatherian and prototherian), Reciprocal Best Hits analysis was performed to define orthologous (309). Human IL-17 protein sequences were used as input for BLASTP (<https://blast.ncbi.nlm.nih.gov/Blast.cgi?PAGE=Proteins>) searches against non-redundant protein sequence databases from *Phascolarctos cinereus* (Koala), *Monodelphis domestica* (Gray short-tailed Opossum), *Vombatus ursinus* (common Wombat) and *Ornithorhynchus anatinus* (Platypus) proteomes. The highest ranked protein (Best Hit) found in those species were reciprocally used as input to repeat the BLASTP search using the same conditions but searching back against human proteome. In both cases, the percentage of identity (meaning how much the proteins were similar each other) and the statistical expected value showing goodness of alignment was annotated.

2.2.3 Protein analysis

2.2.3.a Multiple sequence alignment

To identify conserved residues and establish phylogenetic evolution among IL-17 isoforms, all IL-17s sequences from included species were used as input to generate a multiple sequence alignment (MSA) using Muscle algorithm within MEGA version X (310), using default parameters.

2.2.3.b Phylogenetic analysis

Evolution of IL-17 family members was inferred using the MSA and applying the Minimum Evolution Method and with the bootstrapping test set to 5000. Gaps in any sequence were completely removed the other aligned sequences and rates among sites were considered uniform. Evolution of mammalian species was also tested using a Minimum Evolution Method Phylogenetic tree on a concatenated MSA. Briefly, all IL-17s protein sequences were concatenated to generate a single all-IL17 protein sequence for each species that was used as input for the MSA and phylogenetic analysis. Furthermore, sequences from *M. domestica* and *O. anatinus* were compared with those of human to find which amino acid residues were different and their location in the protein domains. In the case of *B. taurus* IL-17C, *P. troglodytes* IL-17F and *O. anatinus* IL-17B, IL-17F, the deposited protein sequences were much longer than those from other species, with extra amino acids upstream of the beginning of the alignment consensus. Therefore, the sequences were shortened to start with the first methionine as close as possible to the start of the other IL-17s in the alignment. IL-17 proteins from *N. eugenii* were not included as the sequences showed poor quality in the deposited databases.

2.2.3.b Protein modelling

Homology modelling of IL-17A and IL-17F was performed using the plugin PyMOD 3.0.2 from the PyMOL visualisation system. The protein sequences from *M. domestica* and *O. anatinus* were aligned with the PDB entry 4HR9 and 3JVF, corresponding to the human

IL-17A and IL-17F crystal structure respectively. For the modelling, PDB entries were used as a template building the 3D structure using MODELLER, particularly using the template disulfide bonds forming the cystine-knot. Within PyMOD, MODELLER generates scores for the modelling session based on the Discrete Optimized Protein Energy (DOPE) score and the GA341 method. The GA341 score uses as parameter the percentage sequence identity between the template and the model and is a number between 0 and 1 (with a score closer to 1 being diagnostic of a good model).

	H. sapiens	P. troglodytes	M. musculus	B. taurus	M. domestica	V. ursinus	O. anatinus
IL17A	ENST00000648244.1	ENSPTRT00000033782.3	ENSMUST00000027061	ENSBTAT00000002786.4	ENSMODT00000023892.3	XP_027705508.1	ENSOANT000000004969.3
IL17B	ENST00000261796.4	ENSPTRT000000032186.3	ENSMUST000000025471	ENSBTAT000000013986.5	ENSMODT00000007343.3	ENSVURT000100000318.1	ENSOANT0000000021271.2
IL17C	ENST00000244241.5	ENSPTRT000000015582.4	ENSMUST000000050963	DAA20250.1	XP_007477360.1	ENSVURT000100031023.1	XP_028931927.1
IL17D	ENST00000304920.3	ENSPTRT000000060316.2	ENSMUST000000089494	ENSBTAT000000035680.5	ENSMODT00000010395.4	ENSVURT000100031863.1	ENSOANT0000000067368.1
IL25	ENST00000329715.2	ENSPTRT000000011316.4	ENSMUST000000037863	ENSBTAT000000008806.4	XP_001380065.1	XP_027698821.1	ENSOANT0000000060877.1
IL-17F	ENST00000336123.5	ENSPTRT000000033784.3	ENSMUST000000039046	ENSBTAT000000022393.6	XP_001370182.3	ENSVURT00010019629.1	XP_028907333.1

Table 2.3. NCBI or Ensembl IDs relative to IL-17 family members present in chosen organisms.

2.2.4 Genetic analysis of IL-17 genes between mammals

2.2.4.a Identification of IL-17 genes

To identify IL-17 family members across several organisms, we carried out extensive searches in the datasets mentioned above. Furthermore, in the case of genes which have not yet been annotated, their identity was confirmed by performing BLAT searches within the UCSC Genome Browser of gene sequences to identify sequences with 95% or greater similarity to the human IL-17 genes in the genomes of other species (311). Due to the lack of a completed genome sequencing, *Phascolarctos cinereus* (Koala) and *Vombatus ursinus* (common Wombat) were excluded from this analysis.

2.2.4.b Identification of gene conservation using synteny

To assess the conservation of IL-17 family genes and their neighbouring genes in metatherian and prototherian species compared to the human genome, synteny between chromosomes was assessed using the most recently released assemblies: *Monodelphis domestica* (Broad/monDom5 Oct. 2006), *Notamacropus eugenii* (Meug_1.0, INSDC Assembly GCA_000004035.1 Dec. 2008), *Sarcophilus harrisii* (WTSI Devil_ref v7.0/sarHar1 Feb. 2011) and *Ornithorhynchus anatinus* (ASM227v2/ornAna2 Feb.2007). The synteny tool from Ensembl (<https://m.ensembl.org/info/genome/compara/analyses.html>) was used to make pairwise whole genome alignments to identify and visualize where the IL-17 family genes were located in chromosomes belonging to both species. This allows consideration of the region in detail to identify the genes flanking the gene of interest, their orientation and function. To confirm these findings, UCSC genome browser was interrogated by searching the region of interest for each IL-17 in each species. Summary of IL-17s and neighbouring genes was plotted in BioRender.com.

2.2.5 Transcriptomic analysis and cell population abundance estimation

2.2.5.a Transcriptomic analysis

Microarray data or RNA-seq raw data were collected from previously published datasets. In particular, datasets were chosen if they were focusing on female fertility transcriptomic studies. Unfortunately, the lack of transcriptome studies from prototheria, resulted in the exclusion of this clade from fertility dataset analysis, which focused on Therian mammals only. The datasets analysed which showed IL-17s among the differentially expressed genes comprised human menstrual cycle transcriptome (312), human fertility complication transcriptome (unexplained infertility, endometriosis and recurrent implantation failure) (214, 313, 314), mouse pregnancy and placentation transcriptome studies (315, 316), as well as metatherian transcriptome throughout pregnancy (317-320). The full list of datasets analysed, including those not included in the results, can be found in [Table 2.4](#).

Microarray transcriptomic analysis was performed using the GEO2R option from NCBI database and normalisation of the data was applied when discrepancies between samples were identified. Limma was applied to compute differences between the control sample group (samples from non-pregnant or post-pregnant or healthy controls) and the test sample group (321). By default, Limma analysis was carried out using Benjamini-Hochberg correction for multiple comparisons and accounting for false discovery rate. The analysis resulted in a series of tables containing Differentially Expressed Genes (DEG) with their relative \log_2 fold change and \log_{10} adjusted p-value.

RNA-seq analysis for the *H. sapiens* unexplained infertility dataset GSE144895 was previously performed (214). Other RNA-seq datasets from *M. domestica* were analysed using the web-based workflow platform Galaxy. Raw reads were first subjected to quality inspection using FASTQC and trimming/filtering with TrimGalore for working with only high scored runs. Read mapping and annotation was carried out against the latest genome release Mon.dom5. Reads were mapped using Bowtie2 (322). Feature counts were used to annotate the coding genes and generate the normalised count matrix for *M. domestica* (323). *N. eugenii* RNA-seq normalised counts matrix was retrieved directly from GEO dataset. For the metatherian RNA-seq DEG analysis the

limma-voom method was applied, filtering out samples with the sum of counts for all samples less than 5 (321, 324). The outcome of the analysis was a list of DEG with fold change against the control sample, p-value and adjusted p-value.

The \log_2 fold changes obtained from *Mus musculus* (315) and *Notamacropus eugenii* (319) RNA-seq analysis were also plotted throughout pregnancy stages. Due to difficulty in obtaining the factor used to calculate the TPM of genes expressed throughout pregnancy in *Monodelphis domestica* (325), the data from (320) are presented as TPM.

2.2.5.a Immune cell abundance estimation from a bulk RNA-seq dataset

The above-mentioned bulk RNA-seq from the unexplained infertility dataset GSE144895 (214) was used to infer immune cell abundance using the web-based platform Cybersortx. First, the counts per million matrix from the RNA-seq was uploaded on the platform as a “mixture file”. Then, the LM22 signature matrix was selected, containing the gene signature from 22 different cell types based from circulating immune cells. The signature matrix was then overlapped with the mixture file and retrieved the relative abundance of each immune cell type for each sample. The results were used to build an heatmap using ComplexHeatmap package in R and further statistical analysis and visualisation was performed on GraphPad Prism v8.0.1.

Reference	Type of Dataset	Raw data source	Type of sequencing	Included/ Excluded	Reason for Inclusion/ exclusion
(312) *	Menstrual cycle	GSE4888	Microarray dataset	Included	IL-17s between DEG
(314)	Recurrent Implantation Failure (RIF)	GSE58144	Microarray dataset	Included	IL-17s between DEG
(214)	Unexplained infertility (UI)	GSE144895	RNA-seq dataset	Included	IL-17s between DEG
(313) *	Endometriosis	GSE141549	Microarray dataset	Included	IL-17s between DEG
(315) *	Mouse Implantation	GSE11224	Microarray dataset	Included	IL-17s between DEG
(316) *	Mouse pregnancy	GSE44451	Microarray dataset	Included	IL-17s between DEG
(317)	Opossum pregnancy	PRJNA543903	RNA-seq dataset	Included	IL-17s between DEG
(318) *	Opossum pregnancy	SRP111668	RNA-seq dataset	Included	IL-17s between DEG
(320)	Opossum pregnancy	TPM file in Supplementary data 7	RNA-seq dataset	Included	IL-17s between DEG
(319)	Wallaby Pregnancy	GSE90838	RNA-seq dataset	Included	IL-17s between DEG
(326)	Menstrual cycle	GSE126581	Microarray dataset	Excluded	No IL-17 probes in array
Sezerman U.O., Ulgen E. 2021 (unpublished)	UI/RIF	GSE165004	Microarray dataset	Excluded	No IL-17s in DEG
(327)	Pre-eclampsia	GSE190639	Microarray dataset	Excluded	No IL-17s in DEG
(328)	Rat late pregnancy	GSE12799	Microarray dataset	Excluded	No IL-17s in DEG

Table 2.4. Public datasets analysed in the study. For each dataset is listed the citation, the type of samples analysed, the source where raw data can be found, the type of transcriptomic technology applied and if the analysis was included in the results and the reason. *Datasets where the IL-17s had an adjusted p-value below 0.05

2.2.6 ChIP-seq analysis

The ChIP-seq dataset GSE77277, obtained from a previously published study (329), was used to identify butyrylation peaks located near the transcription starting sites (TSS) of genes of interest. The analysis was performed on the web-based workflow platform Galaxy. Quality control was performed on the raw reads using FASTQC and then mapped against the mouse genome (release GRCm38/mm10) using Bowtie2. Eventual duplicated reads were removed using the function RmDup. The background control obtained from the ChIP-seq performed on the input control was subtracted from the butyrylated samples and normalised using the function BamCompare, which retrieves the Reads Per Kilobase of transcript, per Million mapped reads (RPKM). The resulting bigwig files corresponding to the peaks of the butyrylated lysine 5 and lysine 8 on histone 4 were uploaded on the web-based Integrative Genomics Viewer (igv.org/app) to visualize and inspect peak location relative to coding genes.

2.2.7 Peak identification in the corresponding human sequence

The ChIP-seq analysis retrieved a peak located upstream TSS of IL-17A gene. Through IGV the location of the peak was obtained and the nucleotide sequence in the mouse genome was obtained through interrogating UCSC genome browser. Once obtained the mouse sequence corresponding to the peak, it was used to perform a BLAT search against the mouse genome in UCSC genome browser and conserved sequences in the human genome were identified through adding the track for chained alignment with the human genome. This highlighted two conserved regions that were named peak A and peak B and used to design primers to perform ChIP.

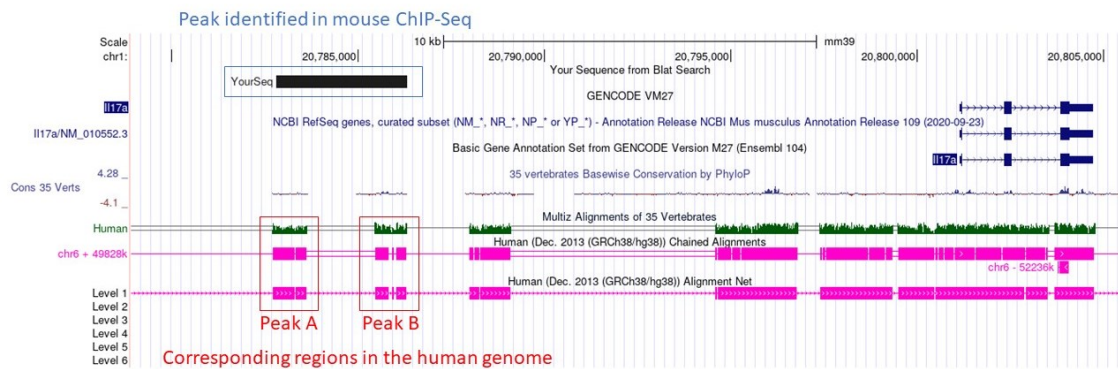


Figure 2.1. Conserved regions in the human genome corresponding to the peak identified in the ChIP-seq analysis. The sequence of the peak obtained from the ChIP-seq analysis in mouse (shown in the blue square) was used to identify conserved genomic regions in the human genome by adding the tracks for the Human Chained alignment and the Human aligned net. This identified two conserved regions in human chromosome 6, closely located near the human *IL-17A* gene, which were named peak A and peak B (in the red squares).

2.3 Wet laboratory techniques

2.3.1 Immortalised cell culture

The human endometrial adenocarcinoma cell line Ishikawa (catalogue number 99040201-1VL) was purchased from the European Collection of Authenticated Cell Cultures (ECACC) repository. Cells were grown in Minimum Essential Media (MEM) supplemented with 5% vol/vol Fetal Bovine Serum (FBS), Non-essential Amino Acids 1% vol/vol and Penicillin-Streptomycin 1% vol/vol (corresponding to 50U/mL). Cells were grown in T75 cm² flasks and split when reaching 95% confluency. Briefly, the old growth media was removed, and cells were washed with 5mL warm (37°C) PBS, then detached by replacing the PBS with 2.5mL warm (37°C) Trypsin and placed in the incubator at 37°C for 5 minutes to allow detaching. Once cells were in suspension, trypsin was inactivated by adding 3X volumes of fresh complete media (7.5mL) and centrifuged at 250g for 3 minutes at room temperature. Cells were then resuspended in 10mL complete media and counted by using Trypan-Blue to dilute them and check for viability and then plated

for the various stimulations. The seeding density used are summarised in [Table 2.5](#). The remaining cells were plated in a ratio 1:5. Cells were split three times per week and, once reaching passage numbers around 28-30 were replaced with freshly thawed cells.

Plate type	Number of cells	Media volume	Application
10 cm plate	4.05x10 ⁶ cell/plate	10mL	ChIP
12-well plate	0.25x10 ⁶ cell/well	0.5mL	ELISA
24-well plate	0.14x10 ⁶ cell/well	0.5mL	Various stimulations
96-well plate	0.25 x10 ⁵ cell/well	100µL	Viability assay

Table 2.5. Seeding densities used for the study.

2.3.2 Primary endometrial epithelial and stromal cell isolation

Endometrial biopsies were obtained using a cornier pipelle and placed into transport medium: Hanks' balanced salt solution (HBSS) supplemented with 100U/mL Penicillin-Streptomycin, 2.5µg/mL (corresponding to 5% vol/vol) Amphotericin B and 5% vol/vol charcoal-stripped Fetal Bovine Serum (FBS). A single cell suspension was generated by adapting previously described protocols (shown in [Figure 2.2](#)) (190, 292, 330). The endometrial biopsies were washed with fresh transport medium to remove excessive blood by centrifuging the tube at 400g for 10 minutes and replacing the old transport medium with 10mL of fresh one. The biopsies were then placed in a 10cm sterile petri dish for weighing and minced finely using opposing scalpels and then resuspended in 5mL digestion media, composed of RPMI 1640, 20mM HEPES, 1% vol/vol charcoal-stripped FBS, 1% vol/vol Bovine Serum Albumin (BSA), 0.5mg/mL Collagenase IV and 35 U/mL DNase I. Digestion was carried out for 25 minutes using a shaking incubator at 37°C at 150rpm. To separate the single cell suspension from bigger undigested debris, the digested mixture was passed through a 70µm cell strainer and 3X volumes of Digestion Inactivation Medium (composed by HBSS supplemented with 10% vol/vol charcoal-stripped FBS) were added. Then, hESCs and hEECs were separated using their size: hESCs are smaller and were separated using a 40µm cell strainer, which blocked the bigger hEECs. To obtain the hEECs, the cell strainer was turned upside down in a fresh tube and 20mL of Digestion Inactivation Medium were used to reverse wash the

cell strainer. Cells were then centrifuged at 400g for 10 minutes and resuspended in 1mL growing medium: Keratynocyte Serum Free Media (KSFM) supplemented with 0.5% vol/vol of Penicillin-Streptomycin and Amphotericin B, 5% charcoal-stripped FBS and growing supplements (recombinant Epidermal Growth Factor, rEGF, 0.2ng/mL and Bovine Pituitary Extract, BPE, 30µg/mL). Cells were then counted and plated in T25 cm² flasks for expansion.

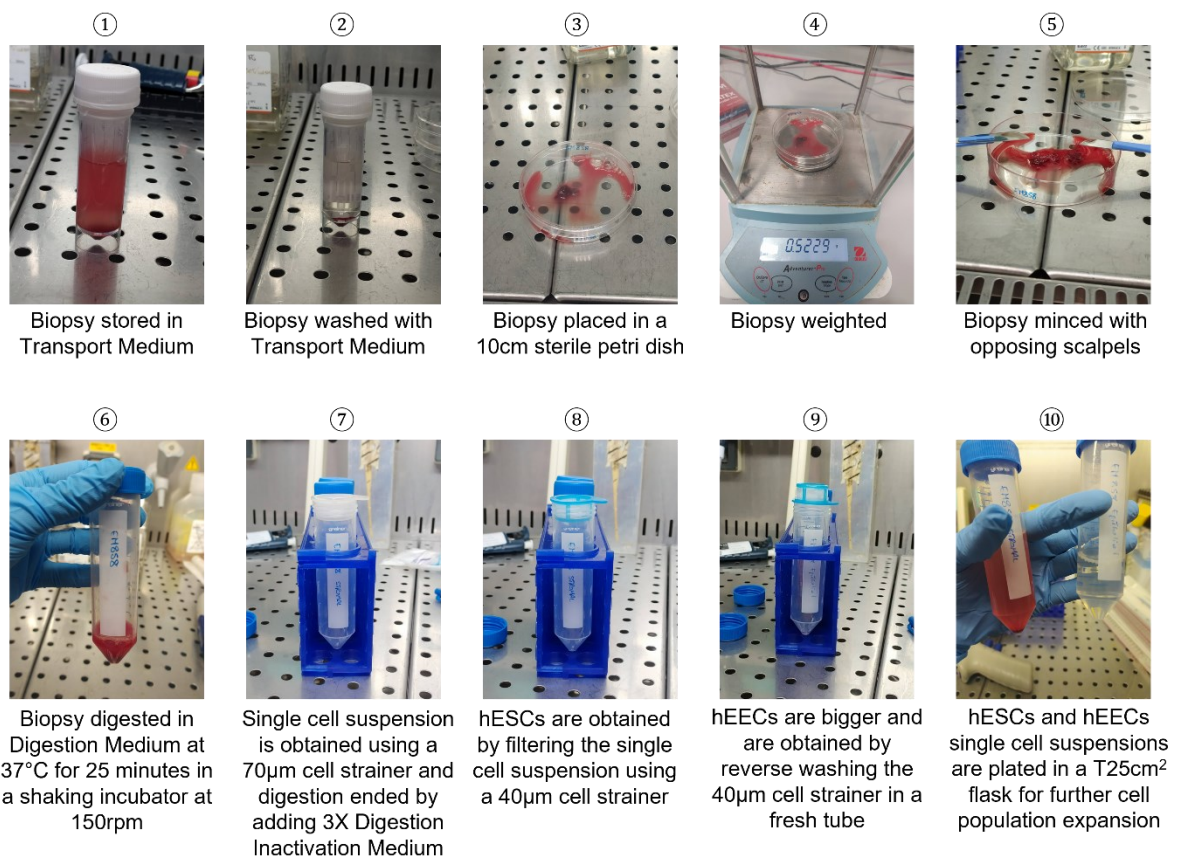


Figure 2.2. Procedure to obtain primary human endometrial epithelial and stromal cells. In the figure are shown the steps required to process endometrial biopsies to obtain single cell suspension of human endometrial epithelial cells (hEECs) and human endometrial stromal cells (hESCs).

2.3.3 Hormonal treatment to induce endometrial receptivity

2.3.3.a Decidualisation model in primary hESCs

Decidualization of primary hESCs was performed as previously reported (331). Briefly, hESCs were cultured in a T25 cm² flask until confluent in KSFM media, supplemented with 5% vol/vol charcoal-stripped FBS, 0.5% 0.5% vol/vol of Penicillin-Streptomycin and Amphotericin B and growth supplements rEGF and BPE at 0.2ng/mL and 30µg/mL, respectively. Cells were then plated in 24-well plates at a cell density of 140,000 cell/well and then treated with decidualisation media, composed by regular growing media to which were added 1µM Progesterone and 0.1 mg/mL 8-Br-cAMP. Some cells were supplemented with 2mM sodium butyrate or 10ng/mL rIL-17A. The control cells were grown with regular growing media alone and the vehicle control cells were treated with growing media with equivalent amount of DMSO. The treatment was carried out for 1, 2, 4 and 6 days, replacing the treatment media every 2 days. When the timepoint was reached, cell supernatants were removed, and the cells were lysed in TRIzol™ Reagent for performing RNA extractions.

2.3.3.b Receptivity model in Ishikawa cells

Ishikawa cells have been described as a good model to recapitulate the changes induced in the endometrium by sex hormones treatment (332, 333). Ishikawa cells were seeded in 24-well plates in regular MEM media, supplemented with 5% vol/vol FBS, 1% vol/vol Non-essential Amino Acids and 1% vol/vol Penicillin-Streptomycin. Before the treatment, the growing media was removed, and cells washed in PBS. The treatment was carried out in MEM media with the same formulation as the growing media, except for the supplementation with 5% vol/vol charcoal-stripped FBS, instead of regular FBS. Cells were treated with 1µM Progesterone and 0.01µM β-Estradiol to induce epithelial receptivity, in presence or absence of 2mM Butyrate or 10ng/mL rIL-17A. The control cells were grown with charcoal-stripped FBS supplemented MEM alone and the vehicle control cells were treated with equivalent amount of DMSO and ethanol. The treatment was carried out for 1, 2, 3 and 4 days, replacing the treatment media every 2 days. When

the timepoint was reached, cell supernatants were removed, and the cells lysed in TRIzol™ Reagent.

2.3.4 Viability assays

Viability assays were performed by seeding cells in triplicate on a 96-well plate and performing the treatments by adapting the treatment volumes for reaching the final volume of 100µL/well. A triplicate containing 100µL/well of media only, without cells, was also added, to be used as a background media control. Two hours before the timepoint was reached, 10% vol/vol Alamar blue cell viability reagent was added to each well and incubation was continued at 37°C. During these two hours, viable cells were able to reduce the resazurin to resorufin, which is highly fluorescent. The cell viability was assessed by measuring the absorbance of converted resorufin at 570 and 600nm and then the relative viability compared to the control was calculated. Briefly, the background measure (R0) obtained by the media was obtained by dividing the average absorbance obtained in the wells with media alone at 570nm (absorbance of the low wavelength or AbsLWL) by the mean absorbance of the same wells at 600nm (absorbance of the high wavelength or AbsHWL):

$$R0 = AbsLWL(media)/AbsHWL(media)$$

Then, the relative viability of the test samples against the control sample was calculated with the following formula:

$$\left(\frac{(AbsLWL - (AbsHWL * R0))_{test}}{(AbsLWL - (AbsHWL * R0))_{control}} \right) * 100$$

2.3.5 Gene silencing

To block the expression of IL-17 receptors and S100A9, specific siRNAs were designed (Table 2.6). The control scramble siRNA was purchased from Dharmacon, catalogue number D-001810-01-05.

siRNA name	Sequence sense (5' – 3')	Sequence antisense (5' – 3')
Scramble	UGG UUU ACA UGU CGA CUA A	N/A
IL-17RA #1	GGU UUG AGU UUC UGU CCA A	UUG GAC AGA AAC UCA AAC C
IL-17RA #2	GGA ACG AAU CUA CCC AUU A	UAA UGG GUA GAU UCG UUC C
IL-17RC #1	UCU CAA AGA CGA UGU GCU A	UAG CAC AUC GUC UUU GAG A
IL-17RC #2	GGU ACG AGA AGG AAC UCA A	UUG AGU UCC UUC UCG UAC C
S100A9 #1	UCA AAG AGC UGG UGC GAA A	UUU CGC ACC AGC UCU UUG A
S100A9 #2	UCA AGA AGG AGA AUA AGA A	UUC UUA UUC UCC UUC UUG A

Table 2.6. Sequence details of siRNAs used in the study.

The silencing was performed on Ishikawa cells using the lipofectamine RNAiMax, following manufacturer instructions. Briefly, 3 μ L/well of lipofectamine RNAiMax was mixed with 50 μ L/well Opti-MEM reduced serum medium. Concomitantly, another mix was made with 20nM/well siRNAs and 50 μ L/well Opti-MEM. Two different siRNAs were used for silencing of each target. The mix with the lipofectamine and with the siRNAs were combined in a 1:1 ratio and incubated for 10 minutes to allow siRNAs to be loaded into liposomes. During this incubation, the media was removed from the 24-well where cells were plated the day before and replaced with 400 μ L/well. At the end of the incubation, 104 μ L of the lipofectamine/siRNAs mix were added for each well, reaching 500 μ L final volume. After 36h from the knock-down, 8mM sodium butyrate or growing media was added to the cells, calculating a 6X concentrated stock in 100 μ L/well final volume. After 6h and 24h from adding sodium butyrate, the cell supernatants were removed, and cells lysed in 500 μ L/well TRIzol™ Reagent.

2.3.6 Chromatin Immuno-Precipitation (ChIP)

Ishikawa cells were seeded on 4x10cm petri dishes. The following day, 2x10cm petri dishes were treated with control growing medium or with growing medium containing 8mM sodium butyrate. After 6h, the medium was removed from the cells, which were washed three times with PBS. Histones were crosslinked by adding 1% Formaldehyde and incubating for 10 minutes at room temperature on a rocking incubator. Crosslinking was stopped by incubating with 125mM Glycine for 5 minutes at room temperature on

a rocking incubator. Cells were washed three times with ice cold PBS and then scraped on ice with 0.75ml/dish ice cold PBS with protease inhibitors (1µg/mL leupeptin, 1µg/mL aprotinin and 1mM phenylmethylsulfonyl fluoride, PMSF). The detached cells deriving from the two petri dishes treated with either control media or butyrate, were combined in one Bioruptor tube and spun down at 900g for 5 minutes at 10°C. The supernatant was discarded, and the cell pellet was lysed in 400µL/tube lysis buffer (50mM Tris-HCl pH8, 10mM EDTA, 1%SDS, supplemented before using with protease inhibitors: 1µg/mL leupeptin, 1µg/mL aprotinin and 1mM PMSF). The cells were pulse vortexed for 20 seconds and lysis was performed leaving the tubes on ice for 30 minutes. After the lysis, the DNA was fragmented by sonication in a Bioruptor Pico sonicator connected to a water cooler system to keep the temperature of the water at 4 degrees. The cells were sonicated for 6 cycles alternating 30 seconds sonication with 90 seconds intervals. The fragmented DNA was obtained by centrifuging the samples at 14.000g for 10 minutes at 10°C and collecting the supernatant in a fresh tube. 50µL of supernatant were used as “input” sample and used straight for reversing crosslinks and DNA purification. The remaining 300µL of supernatant were diluted 1:10 in IP Buffer (16.7mM Tris-HCl pH8, 1.1% Triton-x 100, 0.01% SDS, 1.2mM EDTA and 167mM NaCl, supplemented before using with protease inhibitors: 1µg/mL leupeptin, 1µg/mL aprotinin and 1mM PMSF). Then, each sample (control cells or butyrate treated cells) was split in three tubes:

-100µL sonicated DNA + 900µL IP Buffer

-100µL sonicated DNA + 900µL IP Buffer + 2.5µg Isotype Rabbit IgG

-100µL sonicated DNA + 900µL IP Buffer + 2.5µg Anti-butyryl-lysine rabbit IgG

The samples were left incubating overnight at 4°C on a rotor.

The following morning, Protein A Sepharose® Cl-4B beads, which have higher affinity for rabbit IgG, were prepared for immunoprecipitating the chromatin-antibody complexes, which derived from the overnight incubation. 40µL slurry beads/tube were washed three times with 1mL complete IP buffer by spinning them at 1000g for 3minutes on a benchtop centrifuge. The beads were then blocked by incubating for 40 minutes with 480µL complete IP buffer, with 20mg/mL BSA and 4.8µL Salmon sperm DNA. Beads were washed again three times with complete IP buffer and after the last was, 100µL fresh IP

buffer was added and 45µL beads were aliquoted in six tubes. The overnight samples of chromatin-antibody complexes were spun down at 13.000rpm for 10 minutes at 4°C and the supernatant from each tube (900µL approximately) was transferred to each tube containing the beads:

Control media treated sample	Butyrate treated sample
Beads + sonicated DNA	Beads + sonicated DNA
Beads + sonicated DNA + Isotype rabbit IgG	Beads + sonicated DNA + Isotype rabbit IgG
Beads + sonicated DNA + butyryl-lysine IgG	Beads + sonicated DNA + butyryl-lysine IgG

The samples were left incubating for 3h rotating at 4°C to form the complexes: beads-antibody-DNA. Once finished the incubation, the beads were washed three times with 1mL complete IP buffer and centrifuging at 3000g for 3 minutes at 4°C. Then, the antibody-DNA complexes were eluted from the beads by adding 250µL/tube Elution Buffer (1% SDS, 0.1M NaHCO₃, mixed before using them). Elution was carried at 65°C for 2 hours, then beads were spun down at 3000g for 3 minutes and supernatant transferred in a fresh tube. Elution was repeated twice more with 125µL/tube Elution Buffer left incubating for 30 minutes at 65°C, then all the three supernatants from the elution were combined. The crosslinks between proteins and DNA were reversed with 0.3M NaCl and left incubating at 65°C overnight. After this incubation, RNAs and proteins were degraded by using respectively RNase A (incubated for 1h at 37°C) and Proteinase K (incubated for 2h at 45°C). DNA was then purified using the Wizard® SV Gel and PCR Clean-Up System, following manufacturer instructions. DNA was eluted in 30µL and diluted 1:3 to perform qPCRs.

2.3.7 RNA-extraction and cDNA generation

RNA extraction was performed using TRIzol™ Reagent according to manufacturers instructions. Briefly, the cell culture media was removed from the cells and replaced with TRIzol™ Reagent (500µL for a 24-well plate well). Cells were detached by pipetting

and transferred to a fresh 1.5mL tube. 100µL Chloroform were added to each tube and mixed thoroughly to obtain a cloudy pink mixture. The samples were centrifuged at 12.000g for 15 minutes at 4°C. After this step, three layers are formed: an upper aqueous layer containing RNA, a white interphase containing DNA and a pink phenol-chloroform bottom layer, containing a mix of proteins and DNA. The upper aqueous layer was transferred to a fresh tube and RNA was precipitated by adding 250µL Isopropanol and incubating at -20°C for 30 minutes. The precipitated RNA was pelleted by centrifuging at 12.000g for 10 minutes at 4°C and supernatant was replaced with 75% ethanol, to wash the RNA. The sample was spun down at 8000g for 10 minutes at 4°C and the supernatant was completely removed and the pellet air dried for 20 minutes. The pellet was then resuspended in 20µL distilled, sterile, nuclease-free water and RNA concentration and purity was measured using a NanoDrop™ 2000 Spectrophotometer. RNA was also inspected using a 1.5% Agarose gel, to determine eventual DNA contamination or RNA degradation.

RNA was then used to synthesize cDNA. To do so, 500ng or 1000ng RNA, depending on the starting RNA concentration, were used for setting up the retro-transcription in 20µL final volume. For the reaction was used the High-Capacity cDNA Reverse Transcription Kit, according to manufacturers instructions. For each sample, the following mix was prepared:

Reagent	Quantity (per sample)
RNA	Amount corresponding to 500/1000ng
Distilled nuclease-free water	Up to 14.2µL (depending on RNA volume)
10X RT Buffer	2µL
10X RT Primers	2µL
25X dNTP Mix	0.8µL
Multiscribe Reverse Transcriptase (50U/µL)	1µL
Total volume: 20µL	

The reaction mix was prepared on ice and carried out in a Techne ³Prime Thermal cycler with the following cycling stages, using pre-heated lid:

Step 1 -	Step 2 –	Step 3 – Enzyme	Step 4 - Hold
Annealing	Retrotranscription	Inactivation	
10 minutes	120 minutes	5 minutes	Indefinite
25°C	37°C	85°C	4°C

After the cycle was completed, the cDNA was diluted to reach 100ng, therefore 1:5 for a starting 500ng RNA concentration and 1:10 for 1000ng RNA.

2.3.8 qPCR

cDNA obtained from the previous step was then used to perform quantitative PCR or qPCR. PowerUp™ SYBR™ Green Master Mix was used to perform the qPCR according to manufacturer's guidelines, loading the samples in triplicate on a MicroAmp™ Optical 384-Well Reaction Plate. The qPCR were performed on a QuantStudio5 qPCR machine.

2.3.8.a Primer design and optimisation

Firstly, primers were designed for the target genes of interest and housekeeping genes in order to target exon-exon junctions, where possible ([Table 2.7](#)). The primers were then tested for the optimal concentration to be used in the qPCR. To do so, the same primer set (composed by a mix of 5µM forward and reverse primer) was titrated, using it at 700nM, 500nM, 300nM and 100nM. The concentration that retrieved the lowest cycle threshold with the lowest standard deviation was the optimal concentration. By inspecting the melting curves, primers who displayed multiple peaks were excluded as were not specific for retrieving a singular amplicon. Once established the optimal concentration for each primer set, their efficiency in discriminating small amount of cDNA was tested by performing a relative standard curve using increasing cDNA dilution up to 1:1000. Only primers who showed efficiency higher than 85 and lower than 115, calculated using the slope of the trendline connecting the readouts of the Ct values of the cDNA dilutions, were considered for the study. The amplicon obtained from the primer sets chosen to satisfy the efficiency threshold, were purified using the Wizard® SV Gel and PCR Clean-Up System and sent for sequencing to confirm specificity in their target. Then, the optimal housekeeping gene was determined by running a qPCR with

control samples and samples subjected to the various treatment. The Ct values obtained from this qPCR were used to determine the optimal housekeeping primer, which shows the least variation induced by the treatment. This was calculated by uploading the Ct values on the website: <https://www.heartcure.com.au/reffinder/?type=reference>, which is a repository of multiple algorithms used to determine optimal housekeeping genes such as geNorm or bestKeeper. With this approach, RPLP0 primers were chosen as the most stable housekeeping for this project.

Target name	Forward primer (5'-3')	Reverse primer (5'-3')	Conc (nM)
RPLP0	ACTTGCTGAAAAGGTCAAGGC	CCAAATCCCATATCCTCGTCCG	700
IL-17A	ACTGCTACTGCTGCTGAG	GAGATTCCAAGGTGAGGTG	500
IL-17B	TACAGCATCAACCACGACCC	TTCACACAGCCCAGACACAG	500
IL-17C	TTGCCTGTAGCCCTGGTGTC	ATAGCGGTCCTCATCCGTGTC	300
IL-17D	GCCTACAGAATCTCCTACGACC	GACGGTGGGCATGTAGACAG	300
IL-25	TTGGCAATGGTCATGGGAAC	CTGTTGAGGGGTCCATCTTC	500
IL-17F	ATTACACTGTCACTTGGGACC	TCTCTTGCTGGATGGGAACG	700
IFNB1	AAACTCATGAGCAGTCTGCA	AGGAGATCT TCAGTT TCGGAGG	300
IL-23A	CTCAGGGACAACAGTCAGTTC	ACAGGGCTATCAGGGAGCA	700
IL-12B	GCGGAGCTGCTACTCTC	CCATGACCTCAATGGGCAGAC	700
RORC	GTGGGGACAAGTCGTCTGG	AGTGCTGGCATCGGTTTCG	700
HIF1 α	TTCCAGTTACGTTCTTCGATCA	GCTGGAATACTGTA ACTGTGCTTT G	700
SPP1	GAGGGCTTGGTTGTCAGC	CAATTCTCATGGTAGTGAGTTTTTC	700
MUC1	TGCCGCCGAAAGAACTACG	TGGGGTACTCGCTCATAGGAT	100
ITGAV	ATCTGTGAGGTCGAAACAGGA	TGGAGCATACTCAACAGTCTTTG	700
IGFBP1	TTTTACCTGCCAAACTGCAAC	CCCATTCCAAGGGTAGACGC	700
PRL	AAAGGATCGCCATGGAAAG	GCACAGGAGCAGGTTTGAC	700
LIF	CTGTTGGTTCTGCACTGGAA	GCCACATAGCTTGTCCAGGT	500
IL-15	AGAAGCCAACTGGGTGAATG	TACTTGCATCTCCGACTCA	300

S100A9	CTCCTCGGCTTTGACAGAGTG	TCTTTTCGCACCAGCTCTTTG	300
S100A8	AGCTGTCTTTCAGAAGACCTG	TCTGCACCCTTTTTCTGATATAC	300
PI3/ Elafin	TGTTGAATCCCCCTAACCGC	CTGTCACCTCCCACAACCTC	300
CXCL8 (IL-8)	CTCCAAACCTTTCCACCCCA	TCTCAGCCCTCTTCAAAACTTC	500
TNF α	TGGCCCAGGCAGTCAGATCA	GTAGGAGACGGCGATGCGGC	300
HMOX1 (HO1-)	AAGACTGCGTTCCTGCTCAAC	AAAGCCCTACAGCAACTGTCG	500
IL-17RA	CGGTGGCGTTTTACCTTCAG	TCTTGGACTGGTGGTTTGGG	300
IL-17RC	CCTCCAACTGCCAGACTTC	ACTTGCTCCGCTCTCTTTG	700
MME (CD10)	AGAAGAAACAGCGATGGACTC C	CATAGAGTGCGATCATTGTCACA	700
KRT8	TCCTCAGGCAGCTATATGAAGA G	GGTTGGCAATATCCTCGTACTGT	300
Vimentin	AGTCCACTGAGTACCGGAGAC	CATTTACGCATCTGGCGTTC	500
TLR4	CTCTGCCTTCACTACAGAGAC	TGGATGATGTTGGCAGCAATG	500
TLR3	TGCAAAAGATTCAAGGTACATC AT	TTCGCAAACAGAGTGCATGG	500
MCT1	GGGTTATAAGGCAGCCTCGCT	TCCAAGTCTGGTGGCATTTC	500
MCT4	GAGTTTGGGATCGGCTACAG	CGGTTCACGCACACTG	500

Table 2.7. Primers used in the study. Housekeeping reference gene is shown in bold and highlighted in red.

2.3.8.b qPCR

Once established the primers to be used in the study (**Table 2.7**), qPCR for determining the expression level of genes of interest were performed. For each primer set and each well was prepared a mix with the following composition:

PowerUp™ SYBR™ Green Master Mix (2x)	Primer (Forward+Reverse)	Distilled nuclease-free water
5µL	Depending on the optimal concentration	Up to a final volume of 8µL (depending on the primers volume)

Then, the amount of reagents for the total number of well to be covered was calculated, counting each sample to be loaded in triplicate and adding a well for the non-template control (NTC), containing water instead of cDNA. 8µL of each primer mix were aliquoted in the corresponding wells of a 384-well plate and followed by adding 2µL of water (for the NTC) or cDNA (previously diluted after retro-transcription). The plate was sealed and spun down at 3000g for 1minute and qPCR was performed in a QuantStudio5 PCR machine with the following cycle:

Hold stage	PCR stage		Melt Curve stage		
95°C	95°C	60°C	95°C	60°C	95°C
20 seconds	3 seconds	30 seconds	15 seconds	1 minute	15 seconds

After the cycle was completed, the value of the cycles where the fluorescent signal obtained for each well overcame the intensity threshold of detection was collected. This corresponds to the Cycle threshold, or Ct value. Due to the exponential increase of amplicon production during each cycle, is possible to determine the quantity of amplicons generated by using an intercalating agent, in our case was the SYBR green contained in the PowerUp™ SYBR™ Green Master Mix. As long as the cycling stage progresses, more amplicons are generated leading to increased amount of SYBR green intercalation and production of fluorescent intensity. qPCR machines are designed to register this variation in fluorescent intensity and to register when the fluorescent signal overcomes the threshold of fluorescence. With this value, is possible to calculate the relative fold change of a given target gene by using the $\Delta\Delta C_t$ method. First of all, the Ct value of the target gene for each sample is calibrated and normalised using the corresponding Ct value of an housekeeping reference gene, in our case RPLP0. This operation retrieves the first differential in the Ct values or ΔC_t :

$$\Delta Ct[\text{sample 1}(\text{gene } x)] \\ = Ct[\text{sample 1}(\text{gene } x)] - Ct[\text{sample 1}(\text{housekeeping gene})]$$

Then, it is possible to assess the differential expression of the target gene in the test sample against the internal experimental control. To do so, a second differential analysis is performed by subtracting the ΔCt of the control sample to the ΔCt of the test sample, retrieving the $\Delta\Delta Ct$ value:

$$\Delta\Delta Ct[\text{sample 1}(\text{gene } x)] = \Delta Ct[\text{sample 1}(\text{gene } x)] - \Delta Ct[\text{control}(\text{gene } x)]$$

This operation is performed for each sample, including the internal experimental control sample, which will give zero. Then, to obtain the fold change it is calculated the value deriving to the exponentiation of 2 to the power of the negative $\Delta\Delta Ct$:

$$\text{Fold change} = 2^{-(\Delta\Delta Ct[\text{sample}(\text{gene } x)])}$$

In this way, the internal experimental control sample would every time correspond to 1 (given that $2^{(-0)}=1$) and the test samples would show a fold change that is relative to the expression of the control.

2.3.8.c ChIP-qPCR

ChIP-qPCR were performed using the same protocol as for the regular qPCR using 2 μ L of DNA obtained by a 1:3 dilution of the purified DNA from ChIP. The primers used for ChIP-qPCR were designed by comparing the corresponding human genomic regions to the positive and negative controls, as well as for the IL-17A peaks identified in a mouse study (329). GAPDH primers have been described previously (334) ([Table 2.8](#)).

The fold enrichment over IgG in each DNA region was calculated as follows. The Cycle threshold, Ct, from the immunoprecipitated samples were normalised with the Ct obtained from the input sample, given that this sample has not been subjected to immunoprecipitation and contains all the DNA fragments obtained from the cell lysis and sonication stages. Since 50 μ L of Input sample were taken from a 400 μ L total volume, this corresponds to a 12.5 dilution which, considering the cycling from the qPCR

machine follows an exponential increase, corresponds to a dilution factor of $\log_2(12.5)$ = 3.64 cycles. Therefore, the Ct values of the IP samples were normalised as follows:

$$\Delta Ct[IP\ sample] = (Ct[IP\ sample] - (Ct[Input\ sample] * 3.64))$$

Then, the reading was adjusted by subtracting the ΔCt obtained for the isotype IgG sample to the ΔCt of the other IP samples from that stimulation (either control cells or butyrate treated cells). This calculation retrieves the differential enrichment, or $\Delta\Delta Ct$, of the binding of the IP sample in each given DNA region compared to the one obtained by the isotype IgG:

$$\Delta\Delta Ct[IP\ sample] = (\Delta Ct[IP\ sample] - \Delta Ct[Isotype\ IgG])$$

Lastly, to obtain the fold enrichment, the $(-\Delta\Delta Ct)$ value was used as exponent for the base number 2:

$$Fold\ enrichment = 2^{-(\Delta\Delta Ct[IP\ sample])}$$

Target name	Forward primer (5'-3')	Reverse primer (5'-3')	Conc. (nM)
MAPKAPK5	TGACGTCATTAGCGCAGC	CCTAAGACACGCCGCATAC	700
GAPDH	TACTAGCGGTTTTACGGGCG	TCGAACAGGAGGAGCAGAG AGCGA	125
Chr12	TCTTTCCTTACTCCAGGGCAG	GCCAATGCTCAATGATGACA G	700
IL-17A-Peak A-1	CAGAACACCAATGGGTCAGT	GCTCAGGTCCCCAGTAGAA	700
IL-17A-Peak A-2	AGCACTTCTTCAACCACTGA G	CTAAGCTCTCTTCACACTCGG	500
IL-17A-Peak A-3	GAGCATGGGAGCAAGATTG A	TATCCAGACAGCATGGGTGA	500
IL-17A-Peak B- 1	ATGGGTGGGGATGTTTGAT G	CCTGCCTTTATGCTTGTTGC	500

IL-17A-Peak B- 2	TGTGTCAAGTGGTCTGTCAA C	CTGAAAGTGAGAGATGGGG AG	500
IL-17A-Peak B- 3	TAAGAACCAGGCTCCCAAAC	CCATCAGGGAAGTGGTTGAC	300

Table 2.8. ChIP-qPCR primers used in the study.

2.3.8.d Determination of cell markers for primary hEEC and hESCs and Ishikawa cells

To determine the separation of the primary hEECs with the hESCs we assessed the expression of known markers of epithelial (KRT8) and stromal (membrane metalloendopeptidase MME gene, encoding for CD10) cells ([Figure 2.3A.](#)). Also, to control the ability of these cells to respond to the stimulations which they were subjected, the expression of TLRs (TLR3 and TLR4), butyrate transporters (MCT1 and MCT4) and IL-17A receptors (IL-17RA and IL-17RC) were assessed with qPCR ([Figure 2.3B-C.](#)).

The relative abundance of expression of each cell marker was obtained with the standard qPCR protocol. Once obtained the Ct values, the relative abundance was calculated using the expression values obtained for the housekeeping RPLP0 gene. Briefly, the ΔCt was calculated as in section 2.3.8.b for each well and then this value was used for the exponentiation of 2:

$$\text{Relative abundance} = 2^{-(\Delta Ct[\text{sample}])}$$

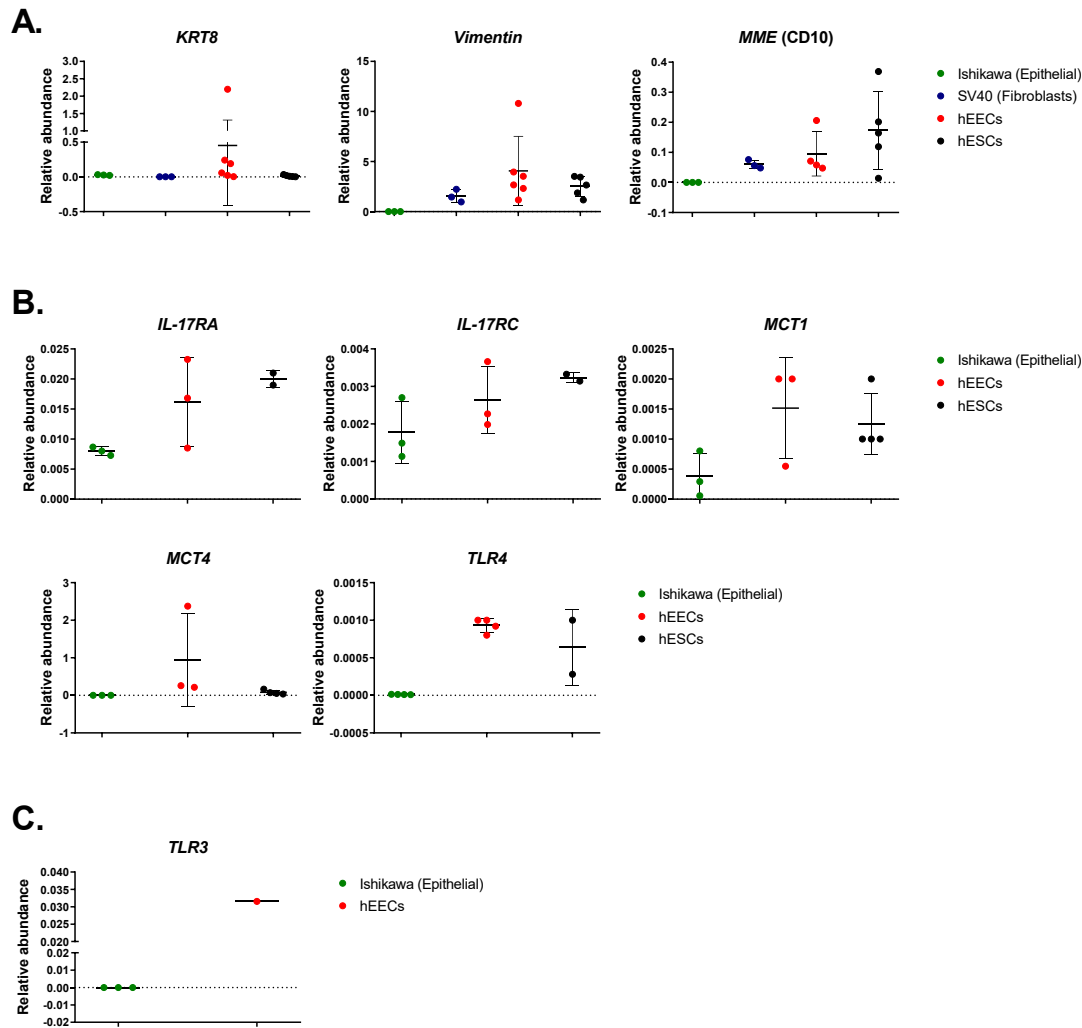


Figure 2.3. Expression of cell markers in the cell models used in the study. Expression was determined with qPCR using RPLP0 as reference gene. **A.** Cell markers expression of cytoskeleton proteins (keratin 8, KRT8 and Vimentin) and matrix metalloendopeptidase, MME (CD10) in epithelial cells (Ishikawa and hEECs) and stromal cells (SV40 fibroblasts and hESCs). KRT8 is a marker of epithelial cells, whereas in the FRT CD10 is used as a stromal cell marker (335), given that vimentin is expressed ubiquitously. **B.** Expression of receptors responsible for mediating the stimulations with IL-17A (IL-17RA and IL-17RC), sodium butyrate (MCT1 and MCT4) and bacterial lipopolysaccharide, LPS (TLR4) in Ishikawa cells, hEECs and hESCs. **C.** Expression of TLR3 in Ishikawa cells and hEECs, responsible for Poly(I:C) response. $N \geq 3$.

2.3.9 Immunocytochemistry staining for epithelial and stromal cell markers

To check separation of hEECs and hESCs, cells were also plated on Millicell EZ slides (Merck-millipore, catalogue number PEZGS0816) and once confluent stained for markers of epithelial (cytokeratin) and stromal cells (CD10) (Figure 2.4). Briefly, growing media was removed from the slides and cells were washed three times with PBS, followed by a fixation step with ice cold methanol, incubated for 10 minutes at room temperature. Cells were washed again three times with PBS and cell peroxidases were blocked with 3% hydrogen peroxide, incubated for 20 minutes at room temperature. Cells were washed once more and aspecific antigens were blocked with casein block (Vector Lab Supplies) for 1 hour at room temperature. The slides were washed once, and primary antibodies were incubated overnight at 4°C. Cells were stained for cytokeratin (Dako, M3515), CD10 (Abcam, ab126593) or isotype control. After three washes in PBS, the slides were incubated for 30 minutes with EnVision Detection Systems Peroxidase/DAB Kit (Dako, K5007). Cells were washed three times with PBS and then freshly prepared DAB was added to the cells and incubated until colorimetric change was observed. Cells were washed twice more and counterstained with haematoxylin. After a first wash with water, cells were washed once more with PBS and then air dried before mounting coverslips using Pertex Mounting medium (Pioneer Research Medicals, PRC/R/750). Pictures were obtained using an Olympus BX51 upright microscope.

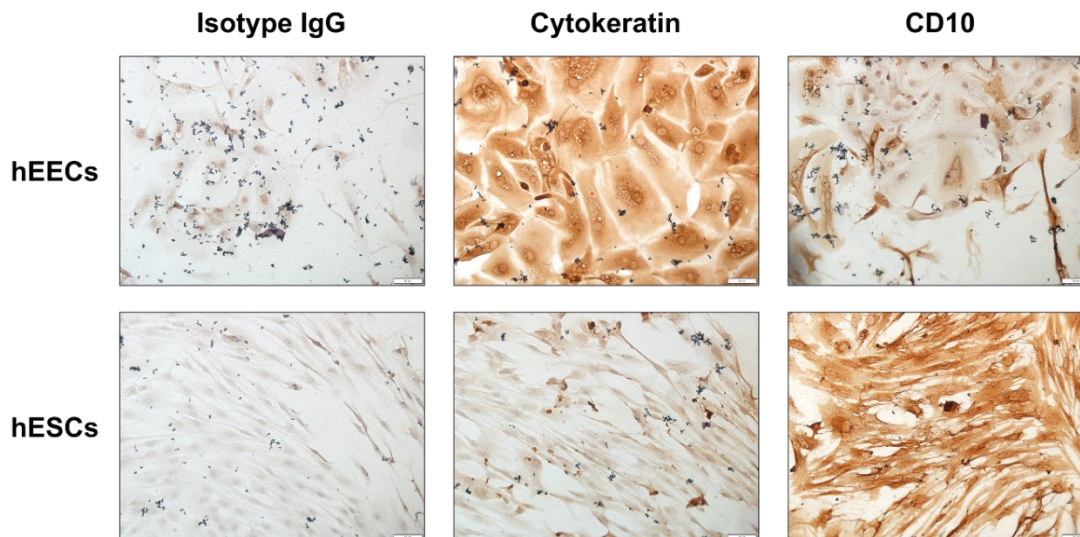


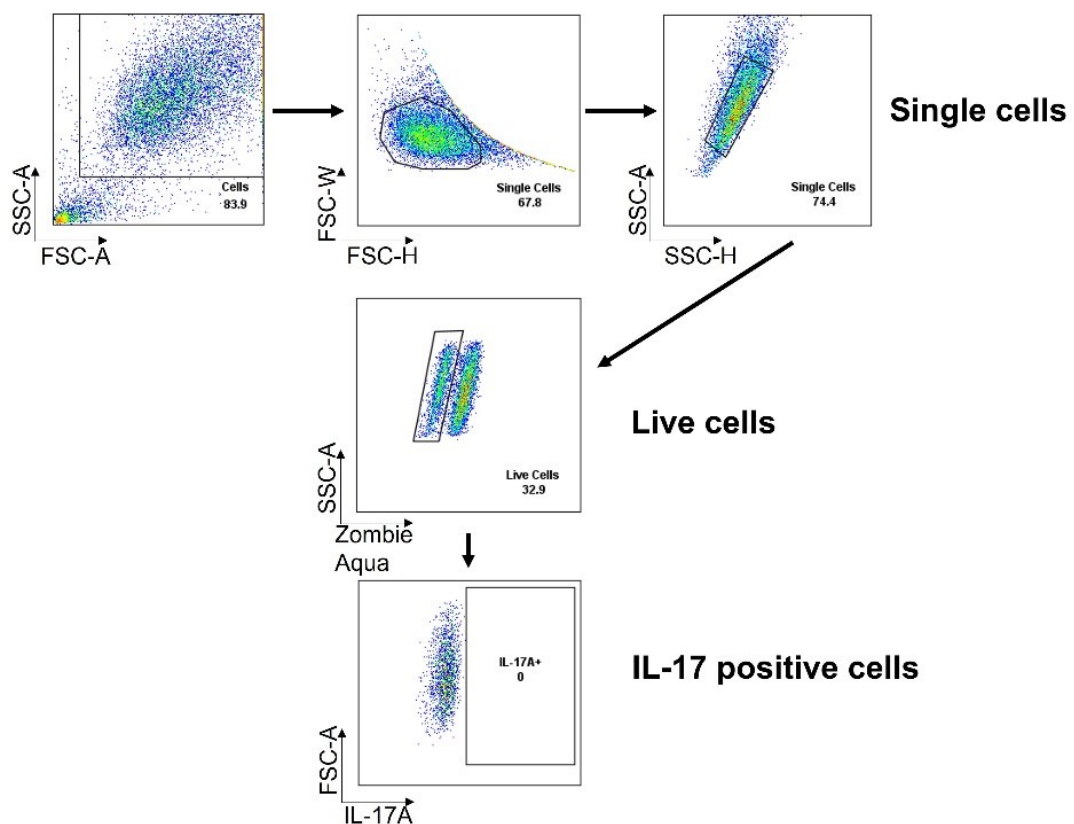
Figure 2.4. ICC staining for epithelial and stromal cell markers. hEECs and hESCs were seeded on Millicell EZ slides and then stained with isotype control antibody, anti cytokeratin antibody and anti CD10 antibody. It can be noticed a different morphology of the two cell type and that epithelial cells are positive for DAB staining with cytokeratin, whereas stromal cells are positive for CD10 staining.

2.3.10 Flow cytometry

Flow cytometry technology allows to investigate cell physical properties as well as intracellular and extracellular antigen presence by a cell using fluorophore-conjugated antibodies. The antibodies used for this technology are listed in appendix [Table I.3](#). The assay was performed on Ishikawa cells seeded on a 24-well plate the day before butyrate treatment. 4h before the 24h timepoint, brefeldin A was added to each well in order to prevent secretion of proteins in the supernatant. At the 24h timepoint, cells were washed with PBS and 10mM EDTA was added to each well and incubated at 37°C until all cells were detached. Cells were placed in polystyrene FACS tubes, washed with 1mL Flow Cytometry buffer (PBS supplemented with 10% vol/vol FBS) and centrifuged at 400g for 5 minutes. To check for cell death, cells were first stained with viability dye Zombie Aqua and incubated at room temperature in the dark for 15 minutes. Cells were then washed again with flow cytometry buffer and permeabilised using the eBioscience™ Foxp3 / Transcription Factor Staining Buffer Set, according to

manufacturer guidelines. After 30 minutes incubation with the permeabilization buffer, cells were washed with the buffer and provided in the buffer set and centrifuged again. After the centrifuge, the supernatant was discarded and cells resuspended in the remaining volume (approximately 100 μ L) and 1 μ L Fc block was added to each tube for 5 minutes, followed by incubation with the specific antibodies for 30 minutes in the dark. Cells were washed twice more with the buffer provided in the kit and, after the last centrifuge, cells were resuspended in 200 μ L Flow Cytometry buffer. A positive sample for the antibody staining was obtained by incubating equal volume of antibodies with the ABC total Antibody Compensation Bead Kit. Similarly, a negative control for each antibody was obtained using a Fluorescence Minus One, or FMO, sample, containing all the other fluorescent antibodies/dyes, except one.

The samples were run on a BD LSRFortessa cytometer from which the FSC files were exported, and subsequent analysis was carried out on FlowJo. For the analysis, gates were first designed on the FMO controls so to have a negative value for the antigen of



interest. The gating strategy is displayed in [Figure 2.5](#).

Figure 2.5. Gating strategy used in the study. The main cell population was gated to remove cell debris, then doublets were separated according to FSC and SSC properties. Live cells were gated using the staining obtained by the viability dye Zombie Aqua and then this population was analysed for the positive/negative staining for the antibody of interest, probing for IL-17A or ROR γ t. The FMO sample (shown in the figure) was used to set the gate in order to show no positivity for the specific antibody of interest. The same gating was then applied to the other stained samples.

2.3.11 Enzyme-linked immunosorbent assay (ELISA)

For the ELISA, Ishikawa cells were seeded on a 12-well plate, but the treatment was performed in half the volume (500 μ L) required by this plate format, in order to concentrate the supernatants. The kits used are listed in appendix [Table I.3](#) and were used according to manufacturer's guidelines. ELISA was performed on fresh supernatants, to prevent freezing-thawing procedures, loaded in triplicate alongside a standard curve and a "blank" sample, consisting of sample diluent only. The samples/standards and blanks were incubated overnight at 4°C, to increase sensitivity. The substrate used for the colorimetric reaction was TMB contained in the kit and stopped with 1M sulfuric acid. Absorbance was read using a spectrometer set at 450nm and plate correction was also measured at 570nm. For the analysis, the value obtained by the absorbance at 570nm were subtracted for each well to the value read at 450nm, then the value of the blank sample was subtracted to all the remaining well to perform background correction. Then, the standard curve was used to obtain the R² value (which was accepted if above 0.95) and the slope formula, which was used to infer the concentration of the unknown samples.

2.3.12 SDS-gel protein electrophoresis, western blotting and membrane staining

2.3.12.a SDS-gel protein electrophoresis

For assay cell protein content, Ishikawa cells were plated in 24-well plates with two technical replicates which were then combined. At the treatment timepoint, cells were

lysed on ice directly adding 50µL sample lysis buffer (1M Tris-HCl pH 6.8, glycerol, 10% SDS, 5% DTT, bromophenol blue) per well. The samples were then combined in a tube and boiled at 95°C for 5 minutes. 20µL of samples were loaded on an 8% Acrylamide gel alongside 5µL of the Spectra™ Multicolor Broad Range Protein Ladder and run in running buffer (2.5mM Tris, 19.2mM glycine, 0.01% SDS) using a Mini-PROTEAN® Tetra Cell gel electrophoresis cassette.

2.3.12.b Western blotting

When the run was finished, the proteins were transferred from the acrylamide gel to a PVDF membrane by western blotting. The membrane was activated by soaking in methanol for 5 minutes and then assembled together with the gel in a Mini Trans-Blot® Cell blotting cassette. The procedure was carried out in transfer buffer (0.025M Tris, 0.19M glycine, 3.5mM SDS), running at 40mA overnight.

2.3.12.c Immunostaining

After the proteins were transferred to the membrane, non-specific sites were first blocked by incubating the membrane with 5% dried milk resuspended in Tris-buffered saline-tween, TBS-T, (12.11g Tris, 87.6g NaCl, 10ml tween 20 in 1L) for 1 hour rotating at room temperature. Membranes were washed three times with TBS-T and then specific antibodies, listed in appendix [Table 1.3](#), were diluted according to manufacturer's guideline in 5% BSA in TBS-T and left incubating overnight rotating at 4°C. Membranes were washed three times with TBS-T and incubated for 1 hour with peroxidase-conjugated secondary antibodies Goat anti-rabbit or Goat anti-mouse, diluted 1:2000 in 5% milk in TBS-T. After three washes with TBS-T, the substrate for the peroxidase was added using WesternBright ECL Spray and chemiluminescent signal was acquired using ChemiDoc MP Imaging system.

2.3.13 16S-sequencing

2.3.13.a Bacterial DNA extraction

Biopsies were obtained using a pipelle de Cornier, which ensures sterility of the sample thanks to its outer catheter section passing through the vagina and the cervix and allowing collection of a biopsy from the endometrium using the inner pipelle section, which is then pulled back into the catheter section before removing the instrument. Approximately 100-200mg of tissue were used to extract bacterial DNA from endometrial biopsies using QIAmp UCP Pathogen Mini kit (QIAGEN, 50214) and with Pathogen Lysis tubes size S (QIAGEN, 19091), as already published (263). Bacterial DNA was quantified using a NanoDrop™ 2000 Spectrophotometer and 5ng/μL DNA was sent to ELDA biotech, Kildare, Ireland for library preparation and 16S-sequencing. Alongside samples, negative contamination controls such as theatre room air, gloves swabs and water samples were sent for sequencing, as well as a positive control consisting of a vaginal microbiome genome mix from ATCC.

2.3.13.b 16S sequencing and data analysis

The sequencing featured amplification of the variable regions V3-V4 of the 16S ribosomal RNA subunit gene. Primers were removed prior to filtering, denoising and read merging and Amplicon Sequence Variants (ASV) were generated using DADA 2 package in R. ASVs were assigned to genus level using a naive Bayesian classifier method against the SILVA database. This resulted in a matrix of normalised reads associated with each bacterial genus. From this, relative abundance was calculated using the number of reads for each genus against the total number of reads within the same sample. Heatmap was generated using ComplexHeatmap package in R and correlations were computed in GraphPad prism v8.0.1.

2.3.13 Statistical analysis

GraphPad Prism v8.0.1 was used for statistical analysis. Data were tested for normality to assess whether parametric tests could be applied or not. Then, different tests were

applied depending on the experimental design and if the samples were paired or unpaired.

Chi-square tests with and without Yates correction were applied to compute significance of the different amino acid identified in the mammalian IL-17s.

T-test was applied to the flow cytometry data and two-samples unpaired t-tests was applied to the 16S sample cohort characteristics.

Two-way ANOVA tests were applied to most of the wet-lab experimental procedure, with correction for multiple testing, such as Dunnett or Sidak. Mixed-effects model fitting test was applied where Two-way ANOVA could not be applied due to missing values. Again, Dunnett correction was applied for correcting for multiple testing.

Chapter 3: Evolution of IL-17 family of cytokines and possible roles in placentation

3.1 Introduction

3.1.1 Organization of mammalian groups

Mammals are vertebrates with peculiar characteristics such as the presence of mammary glands, three middle ear bones and a unique jaw joint. Can be found 4810 species of extant mammals which comprise the main fauna of all continents and, thanks to cetaceans, the major water reserves on earth (336).

Since Linnaeus classified mammals in 18th century, his classification has been updated and revised through the years. The most recent classification for mammalian species is based on molecular evidence of retrotransposon elements located in mammalian genomes (337). According to this study, mammals can be divided into two main groups: **Monotremata** (or Prototheria) and **Theria**, which is in turn divided in two subclasses, **Metatheria** (or Marsupials) and **Eutheria** (or Placental mammals). This classification also reflects the distinct reproductive features of this classes of mammals:

- Monotremata are represented by only one species of platypus and two species of echidna and are egg-laying mammals, or oviparous, although they still breast feed their offspring;
- Metatheria are represented by marsupials, which are viviparous and characterised by relatively short pregnancies, resulting in the birth of an extremely immature or altricial offspring, which continues its development in the maternal pouch;
- Eutheria mammals are viviparous and are also known as "placental" mammals. Their pregnancy is long enough to allow complete development of the foetus within gestational period.

In the next sections will be discussed in more detail the reproductive characteristics of these three main groups, referring to the involvement of maternal immune system for establishment and completion of pregnancy

3.1.2 Characteristics of mammalian pregnancy

Differences distinguish the reproductive biology of these mammalian subclasses, but there are also several similarities.

3.1.2.a Embryonic development in fertilised eggs

Like reptiles, all mammals have three egg-coat layers surrounding their female gametes, organised in the zona pellucida. In monotremata and marsupials, a further egg-coat is deposited after fertilisation when the egg reaches the upper portion of the uterus (338), while in eutherian mammal this does not happen. The most obvious difference between these three subclasses is that eutherian and marsupials are viviparous, but this property evolved from an heterochronic shift of the egg hatching when the foetus is still inside the maternal reproductive tract (Figure 1) (339). Thus, it is possible that the mammalian common ancestor was egg-laying and with similar characteristics to echidnas, where the external incubation of the egg occurs in a maternal skin pouch (340).

3.1.2.b Maternal recognition of pregnancy

The crosstalk between mother and foetus starts in the early stages of pregnancy, soon after fertilization. The first signal from trophoblast acts to interrupt estrous cycle and support progesterone production to sustain early embryonic development, implantation and placentation (341). This phenomenon is known as maternal recognition of pregnancy and, despite it is present in all eutherian mammals and some marsupials, it has been studied only in few species. The difficulties in the studies focusing on this matter are characterised by the fact that the method of trophoblast communication is highly variable and it can either be luteotrophic, to maintain luteal function, or anti-

luteolytic, to prevent luteolytic prostaglandin F_{2a} (PGF) to be released (341). In human and high primates this action is guaranteed by releasing of Chorionic Gonadotropin, a luteotrophic hormone (342), but this does not happen in strepsirrhines, lemurs and related species, which are part of primates clades as well. Both ruminants and pig use an anti-luteolytic approach by secretion of IFNT (343) and the hormone estrogen (344), respectively. In marsupials maternal recognition seems to not occur in the case of *Monodelphis domestica* (345), however in macropodids (kangaroos and wallabies) there is clear recognition of pregnancy since it is known that their placenta has ability to secrete hormones such as steroids, cortisol, prostaglandins and in gravid female there is upregulation of mesotocin receptors under feto-maternal regulation (346). Further studies are needed in order to collect data regarding maternal recognition of pregnancy in monotremata.

3.1.2.c Placentation

Despite eutheria are being regarded as "placental" mammal, all mammals are able form a placenta, even with differences in terms of invasiveness and embryonic cellular source. While eutherian mammals can form four different types of placenta, with greater or lesser contact between trophoblast cells and maternal circulation (347), monotremata can still form a simple allantoic vitelline placenta from vitellocytes, which are trophoblast-like cells (348). Marsupials, instead, generally form a non invasive epitheliochorial placenta which lasts only few days before parturition, although are present some differences between the species contained in this subgroup (347). Particularly, placental formation in marsupials follows the egg-coat hatching, allowing the growth of the embryo at a faster speed due to the nutrients transferred from maternal circulation (**Figure 3.1**) (349).

The length of pregnancy as well as the formation of the placenta allowing nutrient transport from the mother to the growing embryo, determine the rate of embryo development. This is well reflected in mammalian subgroups. In monotremata and marsupials it is clear that the mother provides nutrients to the embryo before the fourth egg-coat is added in the uterus and during the short placentation period. However, the

offspring from those subgroups are still altricial and need a postnatal development phase, which can last 15 months in the case of wallabies (350). Conversely, in eutherian mammals, despite differences according to placental typology and length of pregnancy, the exchange of nutrients through the placenta lasts for a longer period, allowing the foetus to reach a more complete development stage at parturition (350). A misleading idea might be to think that a more invasive placenta is more efficient in providing nutrients and therefore allowing a better development of the foetus. From an evolutionary point of view, placenta did not appear only in mammal. This strategy has evolved independently in other organisms in which occurs maternal provisioning of nutrients during embryonic development, such as some species of Cartilaginous fish (stingray and ground sharks), Teleosts (*Poecilopsis* and syngnathid fish), Amphibian (some types of frogs and marsupial frogs), and reptiles (*Trachylepis ivensi* and Mabuya lizard) (347). It is thought that the placenta of the last common mammalian ancestor was discoid and either hemochorial or epitheliochorial with labyrinth-type interdigitation (351).

3.1.2.d Partuition

Another similarity, especially between eutherian and metatherian mammals is the involvement of a pro-inflammatory response to allow parturition. In metatherian mammals indeed, this phase follows directly the inflammatory activation that leads to the short placentation period, and it is regulated and induced by prostaglandin F2 alpha ($PGF_{2\alpha}$) (350). This pro-inflammatory environment is present also in eutherian mammal parturition, where prostaglandin, cytokines and immune cells are involved to mediate this process (187).

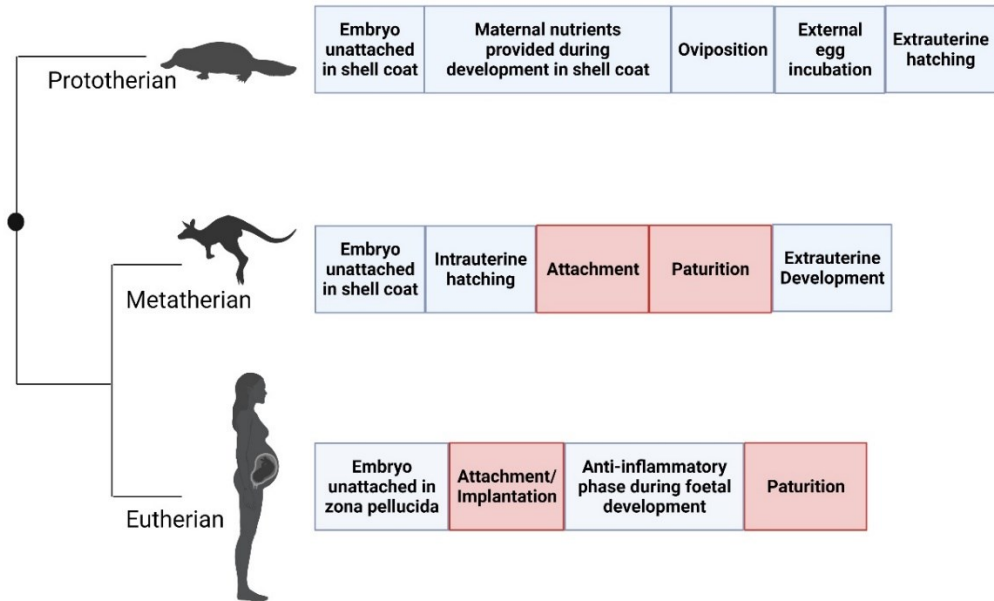


Figure 3.1. Phases of mammalian pregnancy. Phylogenetic tree highlighting the three main extant mammalian orders (monotremata, eutherian and metatherian) and their principal gestational phases. The pregnancy phases present in the mammalian Most Recent Common Ancestor (MRCA) are retained in monotremata, with development of the foetus within the shell coat, oviposition and an external egg incubation. In Therian MRCA the egg-coat hatching chronologically shifted to before parturition, allowing for the attachment of the embryo to maternal uterus and the evolution of viviparity. This phases are retained in Metatherian, where the attachment is only for short periods before parturition. Eutherian mammals have evolved their phases from the therian MRCA by preventing the fourth egg-coat addition and the attachment to the mother which lasts for a longer period than in metatherian, before parturition. The red boxes illustrates stages linked to a pro-inflammatory environment. Adapted from (339).

3.1.3 Involvement of immune response in mammalian pregnancy

The extensive involvement of the immune response in all the above mentioned gestational phases is a similarity shared by all mammalian subgroups

The Nobel Prize Peter Medawar was one of the first to describe the "paradox" of the semi-allogenic foetus not being rejected by the maternal immune system, while remaining capable of protecting the host against infections and malignancies (352). More than 60 years later, many studies helped to explain why and how immune

response is so pivotal for pregnancy success and how dysregulation in maternal immune system can severely impact on these mechanisms. It is indeed clear that inflammation is required for embryo implantation and parturition in eutherian and metatherian (**Figure 3.1**), where the link between inflammation and pregnancy is more studied than in monotremata (350). Since metatherian show a shorter pregnancy than eutherian mammals, the inflammatory reactions of the embryo implantation and parturition happen basically at the same time (350). Eutherian mammals, conversely, have a longer pregnancy and it is fundamental that the inflammatory response caused by embryo implantation must be inhibited once attachment has occurred, for a correct embryo development and growth. If the inflammation is sustained for longer periods or an inflammatory insult occurs during this non-inflammatory phase, there will be indeed deleterious consequences, such as preterm birth or miscarriage. At the end of eutherian pregnancy, the inflammatory response is reactivated to prepare for parturition (350).

3.1.4 Evolution of mammalian pregnancy

Pregnancy in the three clades evolved from a common process in which an early inflammatory reaction is critical for successful embryo implantation, after which the eutherian mammals 'added' a prolonged non-inflammatory phase required for foetal tolerance (**Figure 3.1**) (187, 350). Metatherian mammals have a shorter gestation period (only 15 days in the opossum) in which the foetus is retained in the egg coat until day 12.5, when it hatches inside the uterus, and is followed by a short superficial placentation step. This step involves a highly pro-inflammatory response, followed directly by parturition of an extremely under developed offspring (350). Involvement of inflammation in the reproduction of prototherian mammals, the most distant clade of the mammalian family, has not yet been explored. In these animals there is no implantation step due to the development of the embryo within the shell coat (**Figure 3.1**). However recent analysis confirmed that the mother provides additional nourishment to the eggs before oviposition, thus confirming that, even in such species, maternal-foetal communication occurs (353).

3.1.5 Involvement of IL-17s in inflammatory diseases

As already mentioned, dysregulated levels of IL-17 cytokines are associated with several inflammatory conditions, including psoriasis, psoriatic arthritis, and ankylosing spondylitis (146). These findings encouraged the development of monoclonal antibody therapies to neutralise IL-17A/F action (Ixekizumab and Secukinumab) or block the receptor (Brodalumab). These therapies help prevent the pro-inflammatory symptomatology linked to psoriasis (354), psoriatic arthritis (355) and multiple sclerosis (356).

3.1.7 Involvement of IL-17s in mammalian pregnancy and fertility

As well as involvement in inflammatory conditions, a role for IL-17s in female reproduction is likely, as controlled inflammation characterises each stage of successful pregnancy (185, 186). IL-17A and IL-25 are required to allow establishment of a successful pregnancy, given their involvement in trophoblast implantation and decidual cell proliferation (194, 195). Activation of the pro-inflammatory response has been shown to be critical during the window of receptivity in humans (357), confirming that inflammation is not only activated as a mechanism of defence and during pathologic conditions, but is also a key player needed for physiological processes to occur (350, 358).

It is not surprising therefore that female fertility complications derive from impaired or exaggerated local immune and inflammatory activity (190, 327, 359). IL-17s, and in particular IL-17A and IL-25, have been linked to other fertility complications such as endometriosis, preeclampsia or miscarriage (205, 219, 225, 229).

Activation of the IL-17A pathway and increased systemic and endometrial IL-17A protein levels during the process of implantation in human is associated with unexplained infertility and unsuccessful implantation (214), further emphasizing a role in unsuccessful pregnancy. Therapies targeting IL-17 have recently been shown to be effective in controlling pre-eclampsia (229), further emphasising a role for this cytokine in successful human reproduction.

3.2 Hypothesis and aims

In order to better define the roles of IL-17 cytokines in relation to female fertility, we performed evolutionary analysis in mammalian clades (eutherian, metatherian and prototherian), to understand if the members of the protein family are conserved and thus, share similar functions in distantly related mammals.

Study Outline:

- Identification of genes coding for the IL-17 cytokines in various organisms representing the three mammalian clades (prototherian, metatherian, eutherian) and analysis of their genomic location to infer synteny;
- Identification of mammalian IL-17s proteins and analysis of their sequence homology and phylogeny;
- Analysis of structural similarities between human and metatherian or human and prototherian IL-17s;
- Analysis of IL-17s expression in fertility-related datasets from various mammalian organisms.

3.3 Results

3.3.1 IL-17s genes are conserved and syntenic among mammals

The sequences and location of the six members of the IL-17 family genes were used to examine synteny. The latest genome releases of *Monodelphis domestica* (Short grey-tailed opossum, Broad/monDom5 Oct. 2006), *Notamacropus eugenii* (Wallaby, Meug_1.0, INSDC Assembly GCA_000004035.1 Dec. 2008), *Sarcophilus harrisii* (Tasmanian devil, WTSI Devil_ref v7.0/sarHar1 Feb. 2011) and *Ornithorhynchus anatinus* (Platypus, ASM227v2/ornAna2 Feb. 2007) deposited in the Genbank, Ensembl and UCSC genome databases were used for these analyses. Pairwise comparison with human genomic loci highlighted the presence of genes predicted to be homologous to the human genes deposited in RefSeq, Augustus and Ensembl. In cases where relevant regions were not yet annotated, UCSC prediction using the human chain-net and comparative genomic tools was applied to infer similarity in the region. The analysis identified the IL-17 genes and the surrounding genomic content in each species selected, confirming the presence of all IL-17 family members, ([Figure 3.2A.](#)). Moreover, the flanking genes are also conserved in all the species through evolution, particularly in IL-17D and IL-25 flanking regions ([Figure 3.2D.](#) and [3.2E.](#), respectively), with the same gene orientation, transcription direction and gene size. Therefore, all IL-17 family members can be defined as syntenic and as orthologous, since we see the same number of IL-17s in all mammalian clades, with same surrounding genes and orientation. IL-17s must also have been inherited vertically from one ancestral species to the other through

evolution, without involving gene duplications which would have instead generated paralogs.

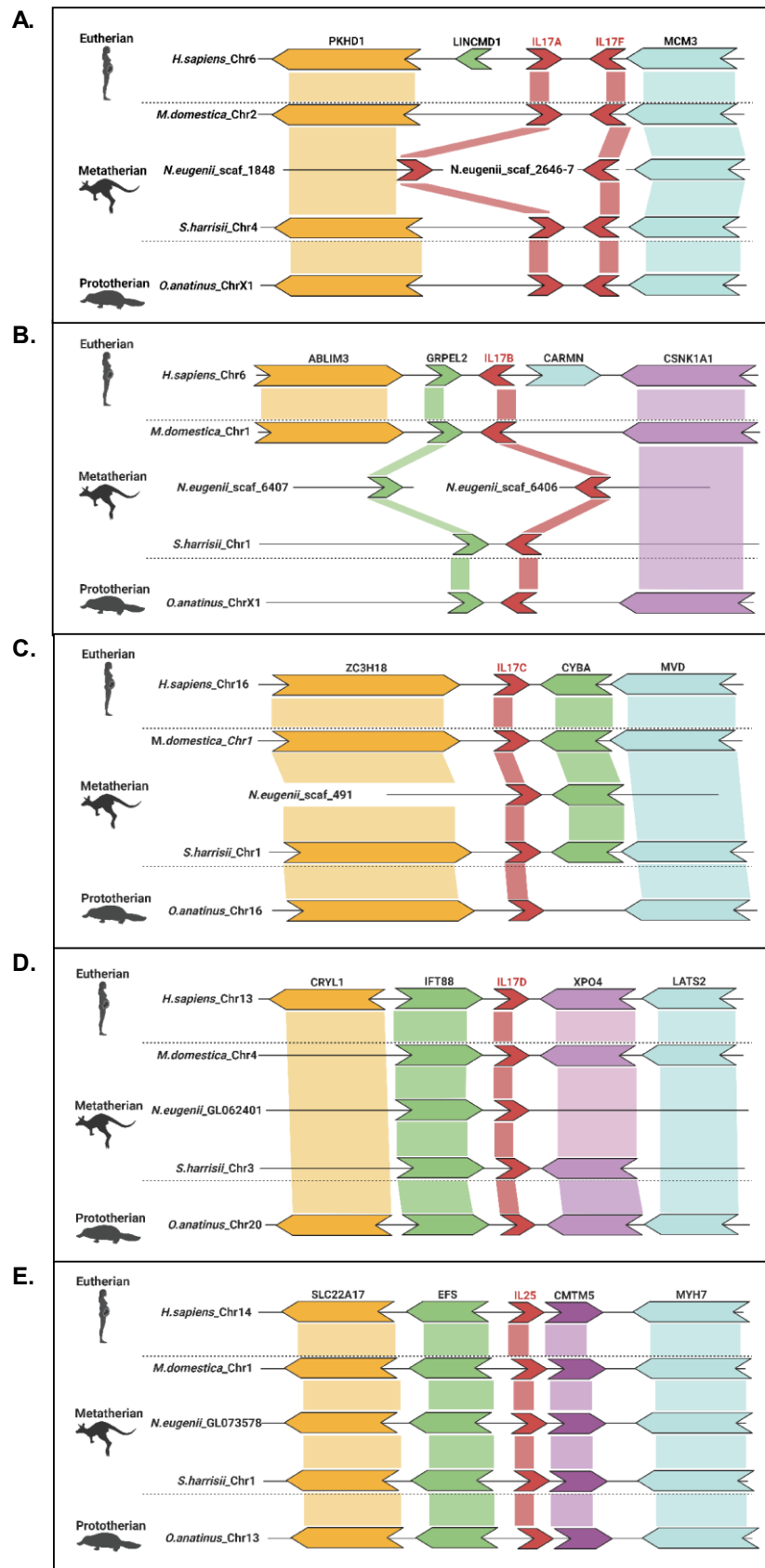


Figure 3.2. Synteny maps indicating IL-17 gene location in metatherian, prototherian and human genomes. Information regarding gene location and surrounding genomic content were retrieved from UCSC, NCBI Genbank and Ensembl; graphs were generated using BioRender. A. IL-17A and IL-17F synteny map; B. IL-17B synteny map; C. IL-17C synteny map; D. IL-17D synteny map; E. IL-25 synteny map.

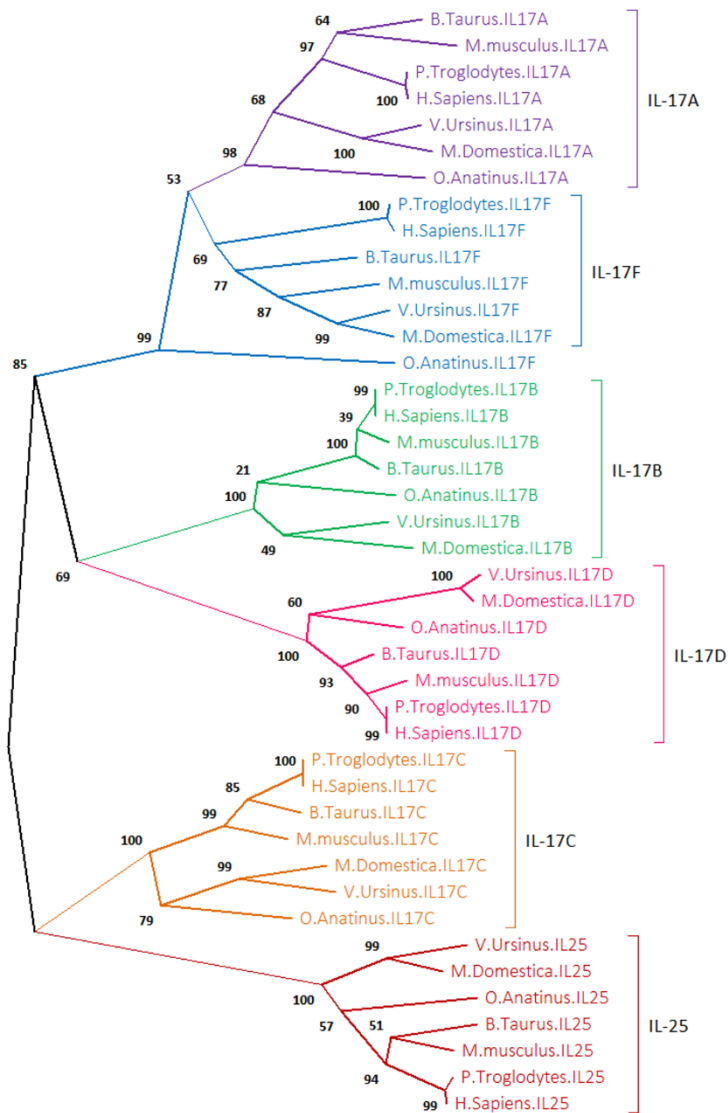
3.3.2 IL-17s protein are conserved in the three mammalian clades with high percentage identity.

IL-17s can also be confirmed as orthologous in mammals by analysis of their protein sequences. Protein sequences of IL-17s in the mammal species under investigation were collected and aligned using ClustalW to confirm they showed at least 20% identity with human IL-17s. Multiple sequence alignment (MSA) of mammalian IL-17s was performed, allowing for the construction of a phylogenetic tree using the Minimum Evolution method. This highlighted how each of IL-17s cluster with orthologues from different species (**Figure 3.3A.**). The branch length of the phylogenetic tree represents the evolutionary distance calculated using the number of amino acid substitutions per site. All the IL-17 family members had similar evolutionary rates among species and among family members. Closely related species show high bootstrapping values, which indicates confidence in the topology of the tree at those nodes.

IL-17 sequences are short and variable with insufficient informative sites to confidently infer evolutionary relationships among taxa. To investigate the pattern of evolution of mammalian clades, all IL-17 family members for each species were concatenated to generate a “metaprotein” which was used for MSA and phylogenetic analysis (360). This resulted in a phylogenetic tree that agrees with the suggested evolution of mammalian clades showing very high values for the bootstrapping test, meaning that these concatenated proteins were found in the same node in all the reiterations performed to retrieve the final tree (**Figure 3.3B.**). Thus, IL-17 proteins can be used to infer evolution of mammals, with prototherian as the most distantly related clade given that their divergence from the mammalian common ancestor happened approximately 200 million years ago (mya), whereas in metatherian mammals it has occurred only 90 mya.

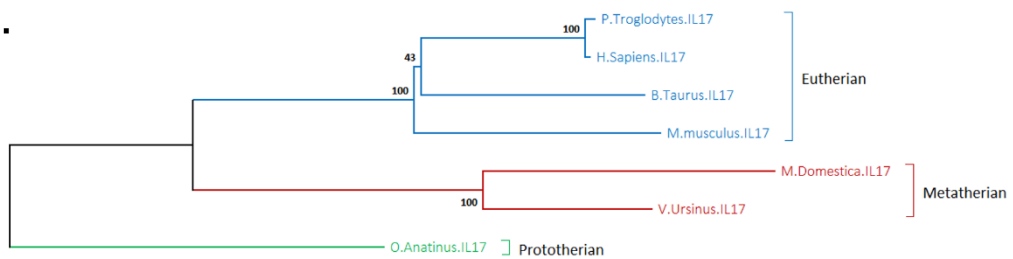
These findings indicate a vertical inheritance of IL-17s throughout evolution, confirming their status as orthologous.

A.



0.20

B.



0.050

Figure 3.3. The evolutionary history of IL17s in mammals. **A.** Phylogenetic tree analysis was conducted in MEGA X using the Minimum Evolution method on IL-17s sequences from several mammalian species. The results from the bootstrap test (5000) are shown at each node. Bootstrap analysis performs multiple resampling of the original MSA data and estimates the degree of confidence in the topology of phylogenetic trees. The tree is drawn to scale, with branch lengths in the same units as those of the evolutionary distances used to infer the phylogenetic tree. Different colours highlight the branch corresponding to each IL17. **B.** Evolutionary history of mammals was inferred by using the Minimum Evolution method by the concatenating the sequences of each species IL-17s and performing MSA and phylogenetic analysis by minimum evolution with bootstrap test of 5000 replicates.

Reciprocal best hits analysis was also used to characterise the relationship among members of the IL-17 family. Pairwise BLAST-P searches of all IL-17s were performed on proteomes from organisms of interest. The top hit results from the searches were examined for reciprocity. If the two proteins are retrieved as the reciprocal best hits, it confirms that they are orthologous and that they share enough percentage identity to be considered to have the same function. Reciprocal best hits analysis in metatherian and prototherian proteomes using human IL-17s as input allowed all IL-17s to be identified with at least 50% identity and very low e-values, demonstrating excellent alignment performed by BLAST. Similarly, BLAST-P searches using metatherian or prototherian IL-17s against the human proteome showed that the proteins are reciprocal hits, with similar % identity and e-values ([Table 3.1](#)).

Organism	Reciprocal hit	Measure	IL17A	IL17B	IL17C	IL17D	IL-25	IL17F
<i>Monodelphis domestica</i>	<i>H.sapiens</i> –	% Identity	59%	75%	51%	72%	52%	53%
	<i>M.domestica</i>	E-value	4e-52	2e-64	2e-62	8e-109	2e-54	23-46
	<i>M.domestica</i>	% Identity	59%	75%	51%	72%	52%	53%
	– <i>H.sapiens</i>	E-value	2e-51	3e-51	1e-61	3e-101	1e-53	4e-51
<i>Phascolartos cinereus</i>	<i>H.sapiens</i> –	% Identity	60%	66%	51%	72%	58%	53%
	<i>P.cinereus</i>	E-value	1e-52	8e-82	2e-64	5e-107	8e-59	1e-45
	<i>P.cinereus</i> –	% Identity	60%	66%	51%	71%	58%	51%
	<i>H.sapiens</i>	E-value	9e-52	1e-73	1e-63	1e-100	7e-58	2e-50
<i>Vombatus ursinus</i>	<i>H.Sapiens</i> –	% Identity	60%	67%	51%	72%	54%	53%
	<i>V.ursinus</i>	E-value	3e-53	3e-82	4e-65	5e-106	3e-58	1e-44
	<i>V.Ursinus</i> –	% Identity	60%	67%	51%	72%	54%	50%
	<i>H.sapiens</i>	E-value	3e-52	4e-74	3e-64	5e-101	3e-58	2e-49
<i>Ornithorhynchus anatinus</i>	<i>H.sapiens</i> –	% Identity	50%	57%	57%	51%	68%	60%
	<i>O.anatinus</i>	E-value	3e-47	4e-47	5e-72	4e-61	9e-81	1e-56
	<i>O.Anatinus</i> –	% Identity	57%	57%	58%	51%	68%	60%
	<i>H.sapiens</i>	E-value	4e-46	3e-46	2e-67	2e-60	1e-75	2e-56

Table 3.1. Reciprocal best hits analysis results. The table shows the percentage identity and e-value from reciprocal BLAST-P searches comparing metatherian and prototherian IL-17s against the reciprocal human orthologues.

3.3.3 IL-17F in prototherian is significantly different from the human ortholog in terms of amino acid composition in the important residues and 3D protein structure.

To look at the functional conservation of the IL-17s in mammals in greater detail, we analysed amino acid differences from the human IL-17s in *Monodelphis domestica* and *Ornithorhynchus anatinus*, as representatives of metatherian and prototherian, respectively. Human IL-17A and IL-17F protein sequences have been well characterised for the residues involved in the cystine-knot formation, dimerization, glycosylation and receptor interaction (361). Unfortunately, the other IL-17 sequences have not been entirely characterised yet, therefore only the signal peptide sequence, the cystine-knot cysteines and glycosylation residues are known. A smaller MSA was performed to

identify residues identical between human and *M. domestica* or human and *O. anatinus* (Figure 3.4A. and 3.4B. examples for IL-17A and IL-17F respectively). The non-identical residues were then analysed to identify where in the protein they are located and whether they involve a residue known to have a key function in human IL-17s (colour coded in the MSA and summarised in Tables 3.2 and 3.3). Overall, all IL-17s have a large number of non-identical residues in the N-terminus of the protein and in the signal peptide portion of the sequence. From the first cysteine involved in the knot, the sequences seem to have an increased number of identical residues in both metatherian and prototherian clades. Also, prototherian IL-17s show a higher number of non-identical residues, which agrees with the phylogenetic evolution of the proteins, with prototherian being more distantly related to the human than metatherian. Residues involved in a specific function, e.g. cysteine of the cysteine knot are conserved in all the IL-17s, apart from IL-17F in *O. anatinus* which has two arginine residues instead of the last two cysteine (Figure 3.4B.).

Once identical and non-identical residues were identified, the percentage identity was calculated for the whole protein and for the key amino acids by dividing the identical residues with the total amino acid residues. In most cases, for example *M. domestica* IL-17A, the percentage identity for the key residues is higher than the percentage identity for the whole protein. This can be explained by the fact that key residues are generally more conserved than scaffold residues. However, in other cases, such as for *O. anatinus* IL-17A, the percentage identity of the key residues is lower than for the whole protein. Chi-square testing, with or without Yates correction, was carried out to test the hypothesis that key residues were significantly different from the human in the chosen organisms (Tables 3.2 and 3.3, final rows). A p-value of 0.05 approves the hypothesis, whereas p-value higher than 0.05 rejects the null hypothesis that the residues are the same. From this analysis, only *O. anatinus* IL-17F and IL-25 were found to have significantly different key residues compared to the human, possibly suggesting that their function might be different from human IL-17.

A.

IL17A Alignment

	SIGNAL PEPTIDE				
	10	20	30	40	50
H. sapiens	<u>M</u> T <u>P</u> G <u>K</u> T <u>S</u> L <u>V</u> --S <u>L</u> L <u>L</u> L <u>L</u> L <u>S</u> L <u>E</u> A <u>I</u> V <u>K</u> A)G <u>I</u> T <u>I</u> P <u>R</u> N <u>P</u> ----- ----G <u>C</u> P <u>N</u> S <u>E</u>				
M. musculus	-M <u>S</u> P <u>G</u> R <u>A</u> S <u>S</u> V S <u>L</u> M <u>L</u> L <u>L</u> L <u>L</u> L <u>S</u> L A <u>A</u> T <u>V</u> K <u>A</u> A <u>A</u> I <u>I</u> P <u>Q</u> S <u>S</u> ----- ----A <u>C</u> P <u>N</u> T <u>E</u>				
O. anatinus	-M <u>S</u> P <u>L</u> V <u>Q</u> F <u>L</u> F P-T <u>L</u> V <u>L</u> M <u>A</u> T <u>L</u> Q <u>E</u> S <u>V</u> L <u>G</u> K <u>A</u> I <u>A</u> A <u>K</u> Q <u>P</u> Q <u>N</u> N <u>L</u> H <u>L</u> K <u>K</u> E <u>K</u> G <u>C</u> P <u>S</u> S <u>E</u>				
M. domestica	M <u>S</u> S <u>P</u> S <u>N</u> L <u>P</u> G <u>F</u> K-S <u>L</u> L <u>L</u> L <u>L</u> L <u>L</u> L A <u>V</u> M <u>M</u> K <u>M</u> G <u>V</u> S <u>M</u> P <u>K</u> R <u>S</u> ----- ----G <u>C</u> P <u>K</u> I <u>E</u>				
	60	70	80	90	100
H. sapiens	D <u>K</u> N <u>F</u> P <u>R</u> T <u>V</u> M <u>V</u> N <u>I</u> N <u>I</u> H <u>N</u> R- <u>N</u> T N <u>T</u> N <u>P</u> K <u>R</u> S <u>S</u> D <u>Y</u> Y <u>N</u> R <u>S</u> T <u>S</u> P <u>W</u> N <u>L</u> H <u>R</u> N <u>E</u> D <u>P</u> <u>R</u> <u>Y</u> P				
M. musculus	A <u>K</u> D <u>F</u> L <u>Q</u> N <u>V</u> K <u>V</u> N <u>L</u> K <u>V</u> F <u>N</u> S <u>L</u> G <u>A</u> K <u>V</u> S <u>S</u> R <u>R</u> P <u>S</u> D <u>Y</u> L <u>N</u> R <u>S</u> T <u>S</u> P <u>W</u> T <u>L</u> H <u>R</u> N <u>E</u> D <u>P</u> <u>D</u> <u>R</u> <u>Y</u> P				
O. anatinus	S <u>D</u> D <u>F</u> P <u>H</u> S <u>V</u> T <u>V</u> N <u>L</u> S <u>I</u> T <u>N</u> G--- N <u>G</u> T <u>S</u> K <u>K</u> F <u>P</u> S <u>V</u> N <u>K</u> R <u>S</u> T <u>S</u> P <u>W</u> E <u>Y</u> Y <u>L</u> N <u>E</u> D <u>P</u> <u>N</u> <u>R</u> F <u>P</u>				
M. domestica	G <u>N</u> D <u>S</u> L <u>Q</u> S <u>I</u> R <u>V</u> N <u>M</u> N <u>M</u> I <u>N</u> R--- N <u>Q</u> G <u>S</u> K <u>I</u> S <u>P</u> D <u>Y</u> K <u>N</u> R <u>S</u> T <u>S</u> P <u>W</u> D <u>L</u> V <u>Q</u> N <u>V</u> D <u>E</u> N <u>R</u> Q <u>P</u>				
	110	120	130	140	150
H. sapiens	S <u>V</u> I <u>W</u> E <u>A</u> K <u>C</u> R <u>H</u> <u>I</u> G <u>C</u> I <u>N</u> A <u>D</u> G <u>N</u> V D <u>Y</u> H <u>M</u> N <u>S</u> V <u>P</u> I <u>Q</u> Q <u>E</u> I <u>L</u> V <u>L</u> R <u>R</u> E <u>P</u> P <u>H</u> C <u>P</u> N <u>S</u> <u>F</u> R <u>L</u> E				
M. musculus	S <u>V</u> I <u>W</u> E <u>A</u> Q <u>C</u> R <u>H</u> Q <u>R</u> C <u>V</u> N <u>A</u> E <u>G</u> K <u>L</u> D <u>H</u> H <u>M</u> N <u>S</u> V <u>L</u> I <u>Q</u> Q <u>E</u> I <u>L</u> V <u>L</u> K <u>R</u> E <u>P</u> E <u>S</u> C <u>P</u> F <u>T</u> F <u>R</u> M <u>E</u>				
O. anatinus	S <u>K</u> I <u>L</u> E <u>A</u> K <u>C</u> S <u>T</u> T <u>G</u> C <u>L</u> D <u>A</u> Q <u>K</u> K <u>E</u> D <u>P</u> H <u>M</u> N <u>S</u> L <u>P</u> I <u>Q</u> Q <u>E</u> I <u>L</u> V <u>L</u> R <u>R</u> E <u>T</u> Q <u>S</u> C <u>P</u> T <u>S</u> F <u>R</u> M <u>E</u>				
M. domestica	R <u>V</u> I <u>W</u> E <u>A</u> R <u>C</u> R <u>Y</u> S <u>G</u> C <u>I</u> N <u>V</u> E <u>G</u> K <u>V</u> D <u>Y</u> H <u>R</u> N <u>S</u> V <u>P</u> I <u>Q</u> Q <u>E</u> I <u>M</u> V <u>L</u> R <u>R</u> E <u>S</u> P <u>N</u> C <u>S</u> T <u>S</u> F <u>R</u> L <u>E</u>				
	160				
H. sapiens	K <u>I</u> L <u>V</u> S <u>V</u> G <u>C</u> T <u>C</u> V <u>T</u> P <u>I</u> V <u>H</u> H <u>V</u> A				
M. musculus	K <u>M</u> L <u>V</u> G <u>V</u> G <u>C</u> T <u>C</u> V <u>A</u> S <u>I</u> V <u>R</u> Q <u>A</u> A				
O. anatinus	K <u>I</u> L <u>V</u> S <u>V</u> G <u>C</u> T <u>C</u> V <u>T</u> P <u>N</u> I <u>H</u> R <u>L</u> G				
M. domestica	K <u>I</u> L <u>V</u> T <u>V</u> G <u>C</u> T <u>C</u> V <u>I</u> P-R <u>T</u> V <u>P</u>				

C - Cystine knot cysteine residue

I - Dimerization residue

Interaction with Receptor: Site 1 - Site 2 - Site 3

B.

IL17F Alignment

	SIGNAL PEPTIDE				
	10	20	30	40	50
H. sapiens	<u>M</u> T <u>V</u> K <u>T</u> L <u>H</u> G <u>P</u> A <u>M</u> V <u>K</u> Y <u>L</u> L <u>L</u> S <u>I</u> L <u>G</u> L <u>A</u> F <u>L</u> S <u>E</u> A <u>A</u>)A R <u>K</u> I <u>P</u> K <u>V</u> G <u>H</u> T <u>F</u> F <u>Q</u> K <u>P</u> E <u>S</u> C <u>P</u> P <u>V</u>				
M. musculus	--M <u>K</u> C <u>T</u> R <u>E</u> T <u>A</u> M <u>V</u> K <u>S</u> L <u>L</u> L <u>L</u> M <u>L</u> G <u>L</u> A <u>I</u> L <u>R</u> E <u>V</u> A <u>A</u> R <u>K</u> N <u>P</u> K <u>A</u> G <u>V</u> P <u>A</u> L <u>Q</u> K <u>A</u> G <u>N</u> C <u>P</u> P <u>L</u>				
M. domestica	--M <u>F</u> F <u>K</u> R <u>G</u> T <u>R</u> M <u>F</u> E <u>L</u> L <u>L</u> L <u>V</u> M <u>L</u> G <u>L</u> I <u>F</u> L <u>G</u> N <u>V</u> G <u>A</u> L <u>K</u> I <u>T</u> K <u>R</u> G <u>A</u> S <u>S</u> - <u>Q</u> N <u>G</u> D <u>N</u> C <u>P</u> P <u>M</u>				
O. anatinus	----- M <u>L</u> K <u>S</u> L <u>L</u> S <u>L</u> S <u>G</u> L G <u>L</u> A <u>L</u> V <u>E</u> S <u>V</u> P <u>G</u> R <u>P</u> A <u>A</u> G <u>T</u> G--- -----C <u>P</u> A <u>V</u>				
	60	70	80	90	100
H. sapiens	P <u>G</u> <u>S</u> S <u>K</u> L <u>D</u> I <u>G</u> <u>I</u> N <u>E</u> N <u>Q</u> R <u>V</u> S <u>M</u> S <u>R</u> N <u>I</u> E <u>S</u> <u>F</u> S <u>T</u> S P <u>W</u> N <u>Y</u> T <u>V</u> T <u>N</u> D <u>E</u> <u>N</u> R <u>Y</u> P <u>S</u> E <u>V</u> V <u>Q</u> A				
M. musculus	E <u>D</u> N <u>T</u> V <u>R</u> V <u>D</u> I <u>R</u> I <u>F</u> N <u>Q</u> N <u>Q</u> G <u>I</u> S <u>V</u> P <u>R</u> E <u>F</u> Q <u>N</u> R <u>S</u> S <u>S</u> P <u>W</u> D <u>Y</u> N <u>I</u> T <u>R</u> D <u>P</u> H <u>R</u> F <u>P</u> S <u>E</u> I <u>A</u> E <u>A</u>				
M. domestica	E <u>N</u> N <u>S</u> V <u>K</u> V <u>D</u> I <u>R</u> Y <u>I</u> N <u>Q</u> H <u>K</u> V <u>I</u> H <u>S</u> A <u>R</u> A <u>F</u> Q <u>N</u> R <u>S</u> I <u>S</u> P <u>W</u> D <u>Y</u> N <u>I</u> T <u>K</u> D <u>P</u> D <u>R</u> F <u>P</u> S <u>E</u> I <u>A</u> E <u>A</u>				
O. anatinus	E <u>G</u> N <u>R</u> V <u>A</u> V <u>D</u> T <u>R</u> V <u>L</u> K <u>A</u> R <u>R</u> D <u>A</u> P <u>V</u> F <u>H</u> D <u>Y</u> R <u>N</u> R <u>S</u> V <u>S</u> P <u>R</u> D <u>Y</u> S <u>I</u> N <u>R</u> D <u>P</u> H <u>R</u> I <u>P</u> Q <u>E</u> L <u>A</u> E <u>A</u>				
	110	120	130	140	150
H. sapiens	Q <u>C</u> R <u>N</u> L <u>G</u> C <u>I</u> N <u>A</u> Q <u>G</u> K <u>E</u> D <u>I</u> S <u>M</u> N <u>S</u> V <u>P</u> I <u>Q</u> Q <u>E</u> I <u>L</u> V <u>L</u> R <u>R</u> E <u>P</u> -Q <u>C</u> S <u>N</u> S <u>F</u> R <u>L</u> E <u>K</u> V <u>L</u> V <u>T</u>				
M. musculus	Q <u>C</u> R <u>H</u> S <u>G</u> C <u>I</u> N <u>A</u> Q <u>G</u> Q <u>E</u> D <u>S</u> T <u>M</u> N <u>S</u> V <u>A</u> I <u>Q</u> Q <u>E</u> I <u>L</u> V <u>L</u> R <u>R</u> E <u>P</u> -Q <u>C</u> S <u>N</u> S <u>F</u> R <u>L</u> E <u>K</u> M <u>L</u> L <u>K</u>				
M. domestica	S <u>C</u> R <u>Y</u> S <u>T</u> C <u>I</u> N <u>A</u> E <u>G</u> Q <u>E</u> D <u>N</u> S <u>K</u> N <u>S</u> V <u>P</u> I <u>Q</u> Q <u>E</u> I <u>L</u> V <u>L</u> R <u>R</u> E <u>P</u> A <u>Q</u> S <u>C</u> S <u>H</u> S <u>F</u> R <u>L</u> E <u>K</u> I <u>L</u> V <u>T</u>				
O. anatinus	R <u>C</u> L <u>L</u> S <u>G</u> C <u>R</u> N <u>A</u> E <u>G</u> R <u>R</u> D <u>L</u> L <u>K</u> E <u>S</u> V <u>P</u> I <u>R</u> Q <u>E</u> V <u>L</u> V <u>L</u> R <u>R</u> D <u>P</u> -R <u>C</u> P <u>R</u> S <u>F</u> R <u>I</u> E <u>K</u> L <u>L</u> V <u>T</u>				
	160				
H. sapiens	V <u>G</u> C <u>T</u> C <u>V</u> T <u>P</u> V <u>I</u> H <u>H</u> V <u>Q</u>				
M. musculus	V <u>G</u> C <u>T</u> C <u>V</u> K <u>P</u> I <u>V</u> H <u>Q</u> A <u>A</u>				
M. domestica	V <u>G</u> C <u>T</u> C <u>V</u> T <u>P</u> M <u>T</u> R <u>S</u> M <u>A</u>				
O. anatinus	V <u>G</u> R <u>T</u> R <u>V</u> T <u>P</u> V <u>I</u> H <u>S</u> R <u>S</u>				

C - Cystine knot cysteine residue

I - Dimerization residue

Interaction with Receptor: Site 1 - Site 2 - Site 3

█ - Glycosylation residue

Figure 3.4. Multiple Sequence Alignments (MSA) of eutherian, metatherian and prototherian IL-17A and IL-17F. **A.** MSA of IL-17A in eutherian (*H. sapiens*, *M. musculus*), metatherian (*M. domestica*) and prototherian (*O. anatinus*), highlighting the key residues involved in receptor binding, cystine knot or dimerization. **B.** MSA of IL-17F in eutherian (*H. sapiens*, *M. musculus*), metatherian (*M. domestica*) and prototherian (*O. anatinus*) clades, highlighting the key residues involved in receptor binding, cystine knot or dimerization.

Table 2	IL17A		IL17F	
Non-identical residues	<i>M. domestica</i>	<i>O. anatinus</i>	<i>M. domestica</i>	<i>O. Anatinus</i>
Total non-identical residues	68 (153)	84 (164)	77 (161)	81 (144)
Insertion/Gaps	NA	7	3	19
Scaffold residues	37 (79)	44 (90)	35 (68)	35 (51)
Signal peptide	16 (23)	17 (23)	17 (29)	21 (29)
Receptor binding site 1	6 (10)	3 (10)	9 (15)	12 (15)
Receptor binding site 2	2 (12)	5 (12)	8 (17)	9 (17)
Receptor binding site 3	6 (15)	9 (15)	9 (19)	10 (19)
Dimerization core	6 (25)	6 (25)	12 (32)	20 (32)
Glycosylation site	NA	NA	1 (1)	1 (1)
Cystine knot	0 (5)	0 (5)	0 (5)	2 (5)
Overall % identity	55.5%	48.7%	52.1%	43.8%
Percentage identity in key residues	58.1%	47.2%	54.3%	50%
P-value (Chi-square test)	0.53	0.73	0.42	0.026
P-value (Yates correction)	0.20	0.85	0.40	0.04

Table 3.2. Non-identical residues in metatherian and prototherian IL-17A and F. Differences between human and either metatherian (*M. domestica*) or prototherian (*O. anatinus*) key IL-17A and IL-17F amino acid residues. The percentage identity was calculated as percentage of identical residues over the total number of residues either for the whole protein or for the key residues (shown in brackets).

Table 3	IL17B		IL17C		IL17D		IL-25	
Non-identical residues summary	<i>M. domestica</i>	<i>O. anatinus</i>	<i>M. domestica</i>	<i>O. anatinus</i>	<i>M. domestica</i>	<i>O. anatinus</i>	<i>M. domestica</i>	<i>O. anatinus</i>
Total different residues	74 (172)	87 (208)	146 (251)	99 (199)	63 (210)	116 (245)	82 (170)	108 (206)
Insertion/Gaps	20	23	61	8	17	44	19	33
Scaffold residues	62 (146)	74 (182)	135 (228)	86 (176)	54 (188)	105 (223)	62 (132)	83 (168)
Signal peptide	12 (20)	13 (20)	12 (18)	13 (18)	9 (16)	11 (16)	20 (32)	25 (32)
Glycosylation site	0 (1)	0 (1)	NA	NA	0 (1)	1 (1)	0 (1)	0 (1)
Cystine knot	0 (5)	0 (5)	0 (5)	0 (5)	0 (5)	0 (5)	0 (5)	0 (5)
Overall % identity	57%	58.1% %	41.8%	50.2%	70%	52.7%	51.7%	47.6%
Percentage identity in key residues	53.8%	50%	52.1%	43.5% %	59%	50%	47.3%	34.2%
P-value (Chi-square test)	0.72	0.37	0.30	0.50	0.24	0.80	0.54	0.067
P-value (Yates correction)	0.89	0.49	0.40	0.63	0.35	0.90	0.66	0.099

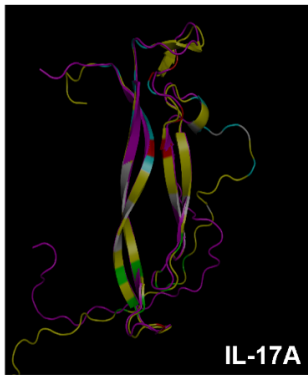
Table 3.3. Non-identical residues in metatherian and prototherian IL-17B to IL-25. The total number of residues for each animal and in each protein domain is presented within brackets. Chi-square tests with and without Yates correction were applied to the identical/non-identical

and important/non-important sum of residues to determine if they are significantly different and allow to infer a different function of the protein.

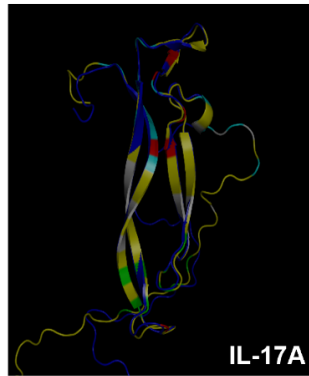
Structural modelling of metatherian and prototherian IL-17A and IL-17F protein was performed based on published models of human IL-17A and IL-17F crystalised structure deposited in PDB (**Figure 3.5A.** and **B.** respectively). For both IL-17A and IL-17F, the overall 3D structure is similar to human IL-17s and the key residues are colour coded according to **Figure 3.4.** Both *M. domestica* and *O. anatinus* IL-17A modelling has a GA341 score of around 0.9, which indicates a reliable modelling (**Figure 3.5D.**). The only exception is the model of IL-17F from *O. anatinus*, which has a GA341 score of 0.2012, supporting the previous protein analysis which indicated significant difference in residues compared to the human IL-17F, including the presence of two arginines instead of the cysteine residues involved in the knot. Indeed, if we modify the IL-17F sequence for *O. anatinus* to replace the arginines with cysteines and repeat the modelling with human IL-17F, the overall tertiary structure seemed similar to the original platypus IL-17F (**Figure 3.5C.**), but the GA341 score improves to 0.7776 (**Figure 3.5D.**), confirming that the differences in those two residues are critical for correct protein folding.

Taken together, these findings suggest that all mammalian IL-17s share a similar amino acid composition, which might suggest they also have a similar tridimensional structure and similar function. IL-17F in prototherians is significantly different from eutherian mammals in key residues, suggesting that the protein might have acquired different structure and functions through evolution.

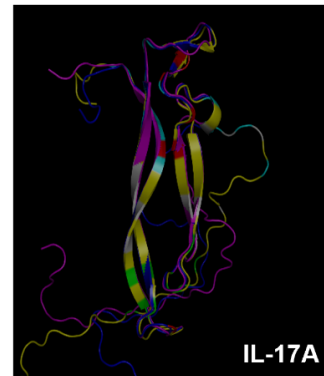
A.



H.Sapiens and *M.domestica*

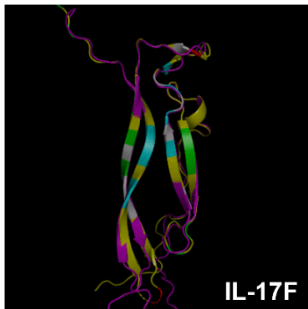


H.Sapiens and *O.anatinus*

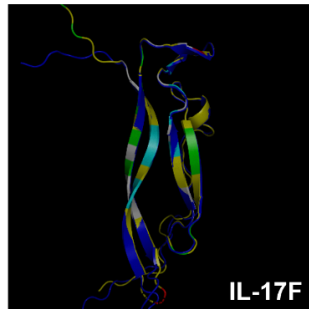


H.Sapiens, *M.domestica* and *O.anatinus*

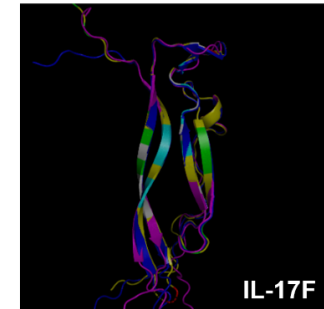
B.



H.Sapiens and *M.domestica*



H.Sapiens and *O.anatinus*

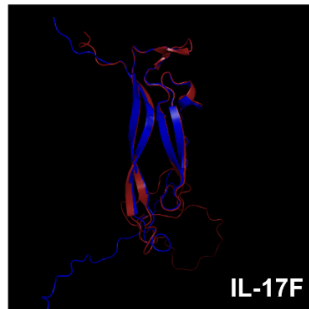


H.Sapiens, *M.domestica* and *O.anatinus*

C.



H.Sapiens and *O.anatinus* (R -> C)



O.anatinus (original) and *O.anatinus* (R -> C)

D.

Protein	GA341 score
IL-17A <i>M. domestica</i>	0.9641
IL-17A <i>O. anatinus</i>	0.9992
IL-17F <i>M. domestica</i>	0.9192
IL-17F <i>O. anatinus</i> (original)	0.2012
IL-17F <i>O. anatinus</i> (R -> C modification)	0.7776

Figure 3.5. IL-17A and F protein structures in mammals. **A.** Structure superimposition of IL-17A in *M. domestica* (magenta) or *O. anatinus* (blue) based on human (yellow) protein structure was performed using PyMOD plug-in within PyMOL. Matching colour for the key residues (highlighted as in **Figure 3.4.**) are kept in the 3D structure. **B.** Structure superimposition of IL-17F in *M. domestica* (magenta) or *O. anatinus* (blue) on the basis of the human (yellow) structure. **C.** Tridimensional structure of *O. anatinus* IL-17F modified sequence (maroon) to revert R133 and R135 to cystines compared to the human IL-17F (left) or to original unmodified protein (right) **D.** Table summarizing the GA341 score obtained from the modelling for each protein.

3.3.4 IL-17s are differentially expressed in female reproduction and fertility.

To generate functional insight into IL-17s in mammalian reproduction, IL-17 transcriptomes were analysed in datasets relating to female fertility. We aimed to determine whether there is a correlation between IL-17s expression and female fertility. Several transcriptomics datasets were collected and analysed to obtain the differential expression of IL-17s against the control samples and summarised in **Table 3.4** and **Figure 3.6** for therian placentation and pregnancy and in **Table 3.5** for human fertility.

With regards to the expression of IL-17s during pregnancy, expression of IL-17s is upregulated during implantation and placentation in both metatherian and eutherian mammals. IL-17A is higher during metatherian placentation but is not found in the differentially expressed gene (DEG) lists in eutherian datasets, where instead IL-17D shows to be upregulated during placentation (**Table 3.4**). The \log_2 fold change values for the IL-17s expression levels retrieved from the analysis of pregnancy stages datasets in mouse and metatherian studies were plotted (**Figure 3.6**). In particular, it seems that IL-17s reach their maximal expression when the placentation occurs in each organism.

Source	Type of study	Control sample	IL-17A	IL17B	IL17C	IL17D	IL25	IL17F
Knox, K., and Baker, G.C., 2008	<i>M.musculus</i> Transcriptome throughout pregnancy	Various pregnancy stages against post-natal	NA	NA	NA	↑*	NA	NA
Xiao, S., et al, 2014	<i>M.musculus</i> implantation transcriptome	Day 4.5 against day 3.5	↓*	↓*	↓*	↑*	↓*	↓*
Hansen, V.L., et al, 2016	<i>M. domestica</i> transcriptome throughout pregnancy	Late pregnancy stage (day 13.5-14.5) against non-pregnant	↑*	↑	↑	↓	NA	↓
Griffith, O.W., et al, 2017	<i>M. domestica</i> transcriptome before and during pregnancy	Late gestation (13.5 day) against mid gestation (7 day)	↑*	↑	NA	↑	NA	NA
Marinic M., et al, 2021	<i>M. domestica</i> transcriptome throughout pregnancy	Pregnancy stages against non-pregnant	↑*	↑	NA	↑	NA	NA
Guernsey, M.W., et al, 2017	<i>N. eugenii</i> transcriptome throughout pregnancy	Day 25 of pregnancy against day 21	↑	NA	↑	NA	↑	↑

Table 3.4. Involvement of IL-17 family members in pregnancy stages. Table summarising expression of IL-17s in either eutherian or metatherian pregnancy-related datasets. Differential expression of genes (DEG) was calculated applying the Limma-voom method to the counts retrieved from available datasets using either the non-pregnant, post-pregnant or early pregnancy stages samples as controls for the analysis. As result of the DEG analysis, log₂ fold

changes and adjusted *p*-values are generated for each gene. The relative expression changes of the IL-17s are summarised in the table with the arrow defining whether the fold change is increased (↑) or decreased (↓) compared to the control samples. NA corresponds to the absence of that IL-17s in the DEG table. The symbol * associated with the arrow means that the adjusted *p*-value for that IL-17 was below 0.05.

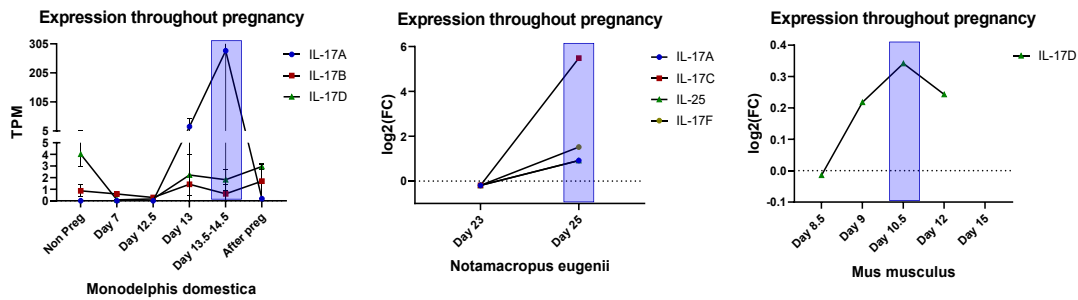


Figure 3.6. Involvement of IL-17 family members in pregnancy stages and placentation. Log₂ fold changes and TPM values obtained from DEG analysis of two metatherian datasets (*Monodelphis domestica* and *Notamacropus eugenii*) and eutherian mammals (*Mus musculus*) are plotted during pregnancy stages. The rectangle highlights when placentation process occurs in each animal.

To summarize the findings related to human fertility datasets, IL-17B and IL-17D are upregulated in most of the datasets suggesting a role in fertility complications (Table 3.5). IL-17D also seems to be significantly downregulated during the late stages of menstrual cycle if compared to the proliferative phase (Table 3.5).

Source	Type of study	Control sample	IL-17A	IL17B	IL17C	IL17D	IL25	IL17F
Talbi, S., et al, 2006	Human menstrual cycle transcriptome	Later phases of cycle against proliferative phase	NA	NA	NA	↓*	NA	NA
Koot, Y.E.M., et al. 2016	Human Recurrent Implantation Failure (RIF) transcriptome	RIF samples against healthy samples	↑	↑	↑	↓	↓	↑
Crosby, D., et al, 2020	Human transcriptome in WOI and correlation with pregnancy outcome	Unsuccessful against successful pregnancies	NA	↑	NA	↑	NA	NA
Gabriel M., et al, 2020	Human endometriosis transcriptome	Endometriosis against healthy samples	similar	↑*	similar	↑*	similar	similar

Table 3.5. Involvement of IL-17 family members in human female reproduction and fertility complications. Expression of IL-17s in fertility related datasets. Differential expression of genes (DEG) was calculated applying the Limma-voom method to the counts retrieved from available datasets using either the healthy controls or the early proliferative phase of the menstrual cycle as controls for the analysis. The relative expression changes of the IL-17s are summarised in the table with the arrow defining whether the fold change is increased (↑) or decreased (↓) compared to the control samples. NA corresponds to the absence of that IL-17s in the DEG table. The symbol * means that the adjusted p-value for that IL-17 was below 0.05 in the DEG list.

3.4 Discussion

These findings show conservation of IL-17 genes and proteins in mammalian clades. Among mammalian clades there is a certain level of genome conservation: around protein-coding regions, for example, eutherian mammals show an average percentage identity of approximately the 80%, whereas the percentage identity is lower in metatherian and prototherian, given that divergence happened at around 90 and 140 million years ago respectively (362). Previous studies have shown conservation of proteins in the three clades and a particular interest has been posed for immune-related genes and proteins, such as MHC-locus conservation and antimicrobial peptides in mammals (363, 364). In this study, we highlighted the evolutionary conservation of cytokines belonging to IL-17 family. The genes encoding these proteins can be found in all mammalian genomes which have been sequenced so far and they also show a similar organization of upstream and downstream neighbouring genes. This suggests that they are part of a syntenic block and that also the flanking non-coding regions should have been conserved through evolution, thus confirming that promoter regions and regulatory elements may act in the same way in all the species analysed (365). Also, the fact that we could observe the same number of family members in each species, points out that IL-17s are orthologous which have been vertically transmitted from one species to the other (366).

This finding is also confirmed by the reciprocal best-hits analysis and by the phylogeny of IL-17 proteins, which shows that all mammalian family members radiated from a common ancestor. Both IL-17A and F proteins share the same node and their genes both reside in the same chromosome in all mammals, suggesting that they have evolved from a recent gene duplication event. This finding has been previously described in other reports in which IL-17s were analysed in invertebrates and fishes, pointing out that gene duplication has happened before mammalian radiation (367, 368). Furthermore, the concatenated alignment of IL-17s allows us to retrieve a phylogenetic tree in agreement with the mammalian evolution (360), meaning that the overall amount of substitution per site in the protein sequence follows the expected evolutionary history, with prototherian being more distantly related to eutherian and metatherian IL-17s which

are more recently diverged sister taxa. Therefore, IL-17s in mammals are orthologous which have been inherited through evolution from the common mammalian ancestor of prototherian, metatherian and eutherian mammals. Through the evolution, these proteins were conserved with at least 50% identity, often more, confirming they must have retained the same function.

Also, by looking at differences in individual amino acids in either *Monodelphis domestica* or *Ornithorhynchus anatinus* IL-17s compared to those in human, confirms the latter as the more different sequences, due to their longer evolutive distance since radiation from the common mammalian ancestor. Overall, IL-17s in mammalian clades are not appreciably different from the human proteins, with the exception for *O. anatinus* IL-17F. In this protein certain key residues are different, especially the amino acids involved in a function. Among these residues, *O. anatinus* lacks the last two cysteines involved in the cystine-knot formation, which has a high impact in the secondary structure formation, as can be noticed by the low GA341 score obtained when modelling the protein on the basis of human IL-17F. When the two cysteines are introduced back in the sequence, indeed, it can be noticed an increase in the modelling score GA341, meaning that *O. anatinus* IL-17F has a different structure and, consequently, a different function if compared to the human one.

Given the striking difference in the reproductive strategies in the three mammalian clades, we analysed fertility-related transcriptomic datasets to identify any differences in IL-17s which might be linked to the evolution of pregnancy. Analysis of transcriptomic datasets highlights an upregulation of IL-17s in female fertility in both eutherian and metatherian mammals. In particular, IL-17D and IL-17B are upregulated in female fertility complication datasets. Intriguingly, IL-17A and IL-17F transcripts are generally not found (NA) or show similar levels of expression in the fertility complication datasets. This disagrees with other reports which suggest an active contribution of this cytokines in endometriosis (204, 205), suggesting that maybe this difference might be due to the timing of the sample collection for the transcriptomic analysis. Also, IL-17B and IL-17D are not known to be involved in fertility-related processes, mainly because other cytokines of IL-17 family are not well studied, so it would be helpful to obtain more insights on the expression and the function of these cytokines.

Looking at pregnancy and placentation datasets, a differential involvement of IL-17 family member in different species can be noticed. Specifically, IL-17A is upregulated in Metatherian pregnancy and placentation, whereas in mouse implantation and placentation we see an upregulation of IL-17D. The previous analysis showed no major differences in either IL-17A or IL-17D in terms of key residue differences or structure, therefore it could be possible that through evolution IL-17A has somehow lost its involvement in placentation or IL-17D has gained a novel function in placentation. A possible explanation for the lack of IL-17A expression in eutherian mammals can be found in the ability of Decidualised Stromal Cells (DSC) to decrease IL-17A production by local immune cells (T_H17 polarised T-cells) (369), despite other reports suggest an involvement in DSC in recruitment of T_H17 cells and thus production of IL-17A used as a gradient for trophoblast adhesion (194).

In both eutherian and metatherian mammals, involvement of the maternal immune response is pivotal to successful pregnancy. In particular, a pro-inflammatory environment is needed during embryo implantation and placentation; however the role for IL-17 in these mechanisms is still not well understood. Some reports suggest that IL-17A in eutherian pregnancy is needed for pregnancy establishment (187, 194), whereas a study performed by our group suggests that excessive IL-17A protein levels are detrimental for a successful pregnancy (214). This is in agreement with other publications in which elevated levels of IL-17A protein have been associated with excessive inflammation leading to fertility complications (205, 219, 225). Little is known about IL-17D, except for the fact that this cytokine seems to be more broadly expressed in the body but with a poor expression in lymphoid and myeloid cells (104). Similarly to the other IL-17s, IL-17D is able to induce a pro-inflammatory signature in endothelial cells and, in the presence of a viral infection or a tumour, it has been shown to mediate immunosurveillance (104, 106). However, in the case of a liver infection, IL-17D produced by hepatocytes was demonstrated to have anti-inflammatory roles as well. It is shown, indeed, to reduce cytotoxic T-cell response by suppressing dendritic cells activation (370). These reports demonstrate that IL-17D could exert different and more complex roles depending on the type of stressor or on the location where the process occurs.

Further studies are required to unravel the functions of the least characterised IL-17 family members, in order to reveal their roles in female fertility.

Chapter 4: IL-17A production by endometrial epithelial cells

4.1 Introduction

4.1.1 Dysregulation of IL-17A leads to unsuccessful pregnancy in women undergoing Assisted reproductive technologies Many fertility and pregnancy complications can be caused by dysregulation of the maternal immune response present in the female reproductive tract. Our group had previously performed a prospective study on a cohort of 20 women with UI who were undergoing assisted reproductive technologies. For our study, strict inclusion criteria were used, and the sample collection was rigorously performed at the mid-luteal LH+7 day on the cycle before the embryo was transferred. We first aimed to understand if there could be any dysregulation in their immune response that could explain their infertility. Furthermore, even though all the women were diagnosed with unexplained infertility, after ART 9 had a successful pregnancy, whereas 11 failed to become pregnant (**Figure 4.1**) (214). Thus, we focused to understand whether there were any differences in the immune response between the women who were able to become pregnant and those who failed to establish a successful pregnancy.

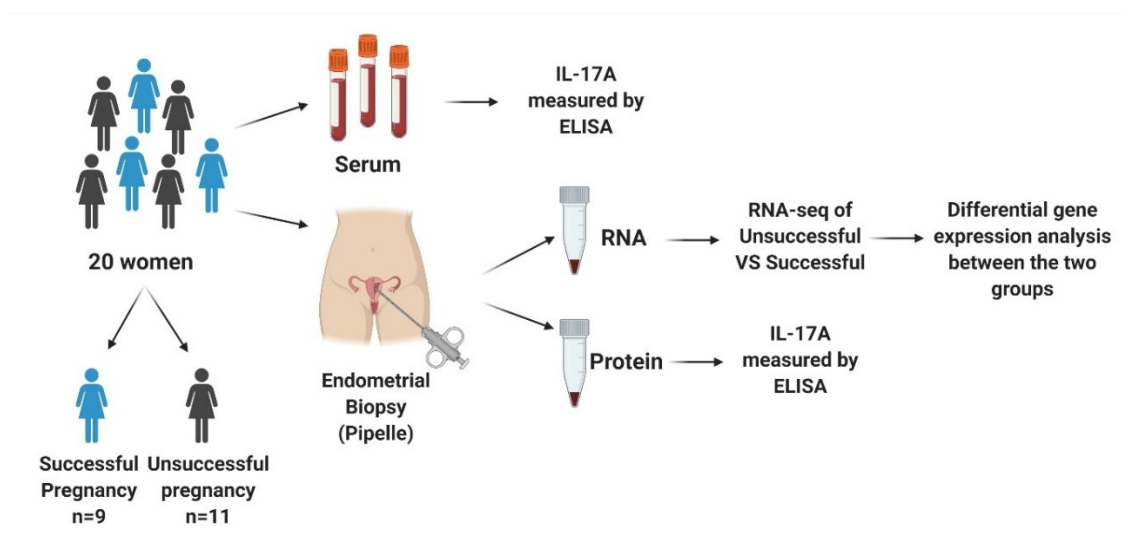


Figure 4.1. Overview of the sampling strategy and the technologies used in our study in the unexplained infertility cohort (214).

The sample recruitment was performed in 2016, when it was suggested to perform an endometrial scratch in the menstrual cycle before embryo was transferred. The rationale behind performing endometrial scratches during ART cycles was based on a number of publications suggesting how, stimulating a wound-healing response in the endometrium, contributed in recapitulating the processes of decidualisation and trophoblast implantation, which are characterised by immune responses activation and thus resulting in a more receptive endometrium when embryo would be transferred (214). Other publications in 2019 had confirmed that scratching of the endometrium did not improve embryo implantation (214), the participants for our study were enrolled before those publications were released, therefore an endometrial scratch was performed on the mid-luteal phase of the menstrual cycle before the embryo transfer.

Serum samples and endometrial biopsies were collected and were used to extract proteins and RNA from the biopsies. The RNA was used for RNA-seq analysis, and the data were correlated with pregnancy outcome ([Figure 4.1](#)) by retrieving the differentially expressed genes (DEG) of the unsuccessful pregnancies compared with the successful ones. In total, 204 DEG were identified in the unsuccessful group, which were used to perform pathway enrichment analysis ([Figure 4.2A.](#)). This retrieved several immune-related pathway, such as "regulation of inflammatory response" GO biological pathway, "cytokine binding" GO molecular pathway ([Figure 4.2B](#)) and among the KEGG enriched pathway were identified "IL-17 signalling pathway", "PI3K-Akt signalling pathway" and "cytokine–cytokine receptor interaction" ([Figure 4.2C](#)).

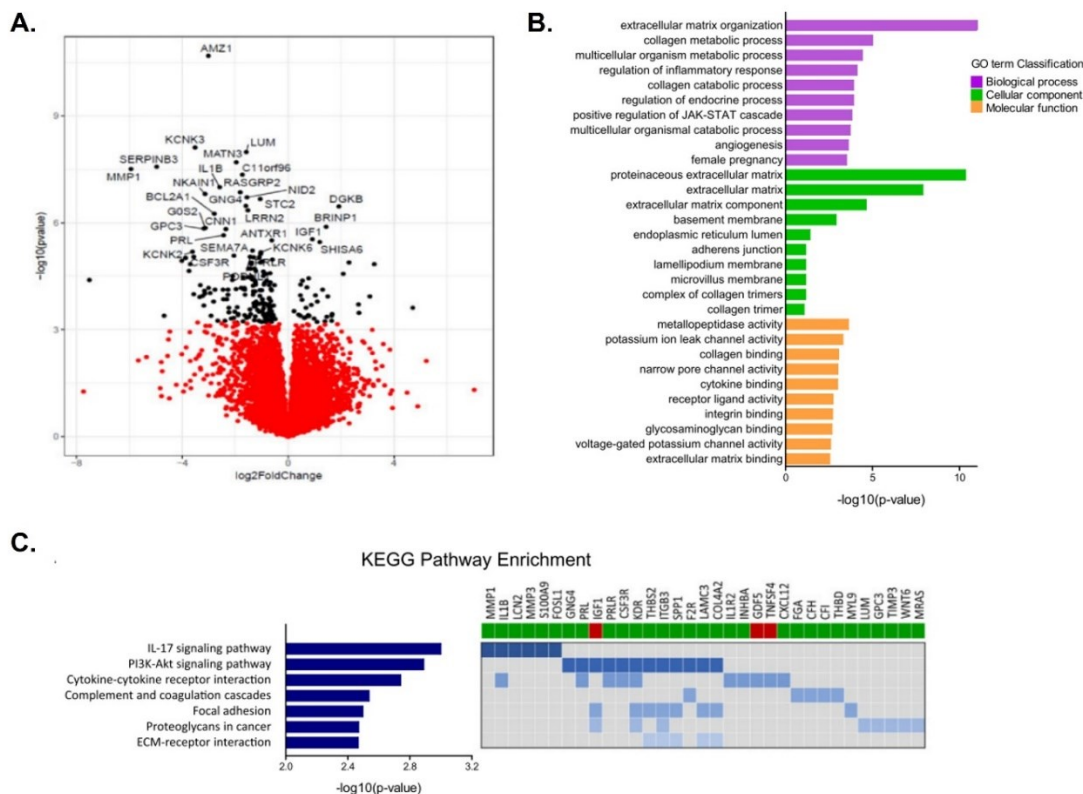


Figure 4.2. Overview of the RNA-seq results from our preliminary study (214). **A.** Volcano plot illustrating the 30 most DEGs between pregnant and not pregnant. Statistical analyses were performed using generalised linear model likelihood ratio test (EdgeR). **B.** ClusterProfiler functional annotation showing GO enrichment analysis of DEGs; groups reflect main categories of GO terms. Vertical and horizontal axes represent GO term and $-\log_{10}(\text{P-value})$ of the corresponding GO term, respectively. **C.** KEGG pathway enrichment analysis of DEGs between pregnant and not pregnant. Left panel: horizontal axis indicates $-\log_{10}(\text{P-value})$ of the corresponding KEGG classification (left). Right panel shows 33 genes involved in 7 KEGG pathways outlined on the left; bars below the gene names indicates whether a gene is up-regulated (green) or down-regulated (red) in the not pregnant group.

Given that “IL-17 signalling pathway” was shown to be the pathway with the higher $-\log(\text{P-value})$ and that IL-17A was shown to be increased in several diseases, including many fertility and pregnancy complications, it was then assessed if this cytokine showed different protein levels between the two groups. Circulating and local (endometrial) levels of IL-17A were increased in women who failed ART cycle and we showed that systemic IL-17A higher than 30pg/mL can be used as a predictor for failed pregnancy

with 94% sensitivity (214). We also found that in women with unsuccessful pregnancy there is significant upregulation of IL-17A pathway activation, thus suggesting that IL-17A might activate an excessive pro-inflammatory signature, which is preventing embryo implantation (214).

This study however did not address several important aspects. One of them is where this increased IL-17A was coming from. Unfortunately, at the time of sample collection, the serum samples and the biopsies were snap frozen and a very small sample was obtained from each donor, making it impossible to perform flow cytometry to assess whether the women with increased IL-17A had also increased immune cell infiltration in the endometrium or even in circulation.

The other aspect that this study could not expand was why IL-17A had caused implantation failure in the women who showed elevated levels of this protein. IL-17A shows a multifaceted role in female fertility, but several studies pointed out that an excessive activation of this cytokine is linked to unexplained infertility (212-214) and implantation failure (234). However, certain levels of IL-17A are required and considered normal for embryo implantation to occur. This is also confirmed by the fact that in our cohort the women with successful pregnancy displayed IL-17A protein levels which were approximately half of the amount identified in the unsuccessful women and yet they could carry on the pregnancy successfully. Therefore, it could be possible that IL-17A becomes problematic only when its levels are particularly increased.

A last question that is still unanswered is how increased levels of IL-17A lead to implantation failure. Since both the groups had received a good to top quality embryo transferred, it is likely that the pregnancy outcome was determined by the receptivity of the women, mediated by changes in their window of implantation. For example, it is not clear what is the effect that IL-17A stimulation has on endometrial epithelial cells and even less is known with regards to what effect this cytokine has if it is upregulated during the stages leading to the opening of the window of implantation.

4.2 Hypothesis and aims

We have identified an increase in local levels of IL-17A in the endometrium of women who failed to conceive after undergoing ART. Furthermore, in those patients there was significant activation of IL-17A pathway, with increased expression of some genes downstream of IL-17A such as MMP9, lipocalin-2, S100A9, IL-1 β . This led us to hypothesize that in those women there must have been an excessive pro-inflammatory activation which has resulted in the inability of the embryo to implant. We therefore wondered how in those women the IL-17A levels were so high both systemically and locally and what could be the role of IL-17A in modulating endometrial epithelial cells receptivity.

We hypothesized that in FRT non immune cells are responsible for IL-17A production; specifically, we wanted to explore the hypothesis that endometrial epithelial cells could induce IL-17A as a response to infections. We aimed to investigate the possibility of expression of IL-17A in epithelial cells from the FRT cells using tumour and primary cell lines, to better understand the role that this cytokine might have in infectious settings and the role it might have in reproduction complications. To address this hypothesis we used four approaches:

1. We first needed to identify whether there were differences in the immune repertoires in endometrial tissue from the two groups of women. This will be explored by analysing immune cell signature in the bulk endometrial RNA-seq and in the expression of known immune cell markers;
2. Analysis of the response of the endometrial adenocarcinoma Ishikawa cells to assess whether IL-17s can be stimulated by bacterial and viral ligands;
3. Analysis of primary human endometrial epithelial cells (hEECs) response upon bacterial and viral ligands stimulation to assess their ability to express IL-17s;
4. Exploration of the effect of IL-17A on Ishikawa and hEECs;

4.3 Results

4.3.1 Immune cell population estimation in bulk RNA-sequencing identifies similarities between the two groups

Given the difference in the levels of IL-17A in women with unexplained infertility who failed to carry on a successful pregnancy upon ART, we first wondered whether in their endometrial environment more immune cells, responsible for producing IL-17A, were present. In order to identify the cell composition in the endometrium, the normalised counts matrix obtained in the bulk RNA-seq was overlapped with immune cell-specific LM22 signature matrix, obtained from the profile of circulating immune cells (371). The overall immune-cell signature obtained between the successful and unsuccessful samples was similar (**Figure 4.3A**). Indeed, in **Figure 4.3B** is possible to see the signature for each cell type between the two sets of samples and it can be noticed that there are no statistically significant differences.

Furthermore, since with the gene signature it is not possible to dig deep into the cell types responsible for IL-17A production, the normalised counts per million from the RNA-seq counts matrix were also graphed for the genes coding for markers associated with certain immune subsets. **Figure 4.4A-F** shows the counts per million values for markers used for identifying T_H17 (CD4, RORC, AHR), ILC3 (RORC, AHR, NCR2, KIT) and NK cells (NCR2, NCAM1, KIT). **Figure 4.4G-I** shows the counts per million for markers used to identify T_{RM} cells such as CD69, CCR7, KLRB1, whereas **Figure 4.4J-L** shows the counts of the genes encoding for the chains of CD3 molecule, which is associated with the T-cell receptor in T_H17, T_{RM} and MAIT cells. It can be noted how, for all these genes, the counts per million are similar in the two sample sets, successful and unsuccessful. Thus, it does not seem that in the endometrial biopsies there was an enrichment in an immune cell type responsible for IL-17A production.

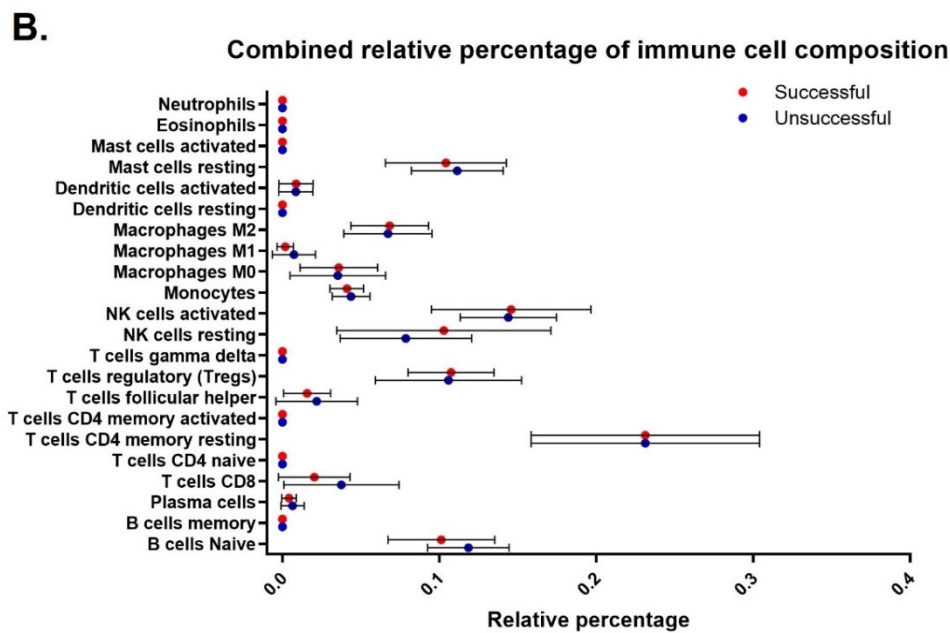
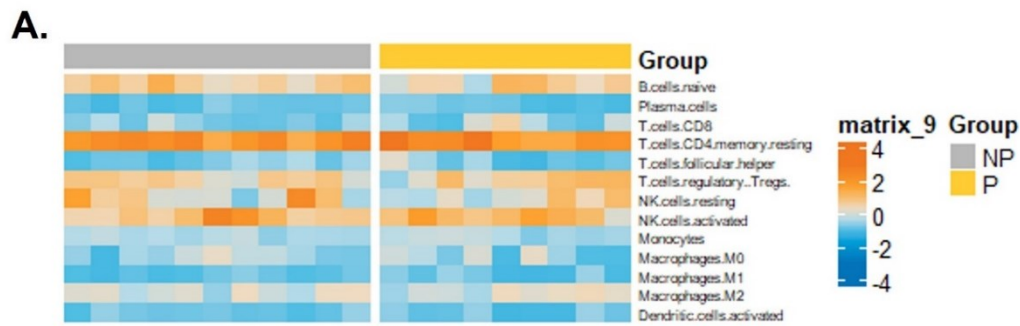


Figure 4.3. Immune cell composition of the endometrial samples from successful and unsuccessful pregnancies. The normalised counts per million matrix obtained from the RNA-seq was uploaded on the analytical tool Cibersortx (<https://cibersort.stanford.edu/>) along with the well validated immune-cell gene signature LM22. **A.** The resulting immune cells relative percentage matrix was used to build a heatmap for visualisation of the overall immune composition between the two sets of samples: P, pregnant (successful) and NP, non-pregnant (unsuccessful). **B.** The relative percentage values were averaged and graphed to show differences between the successful or unsuccessful pregnant group.

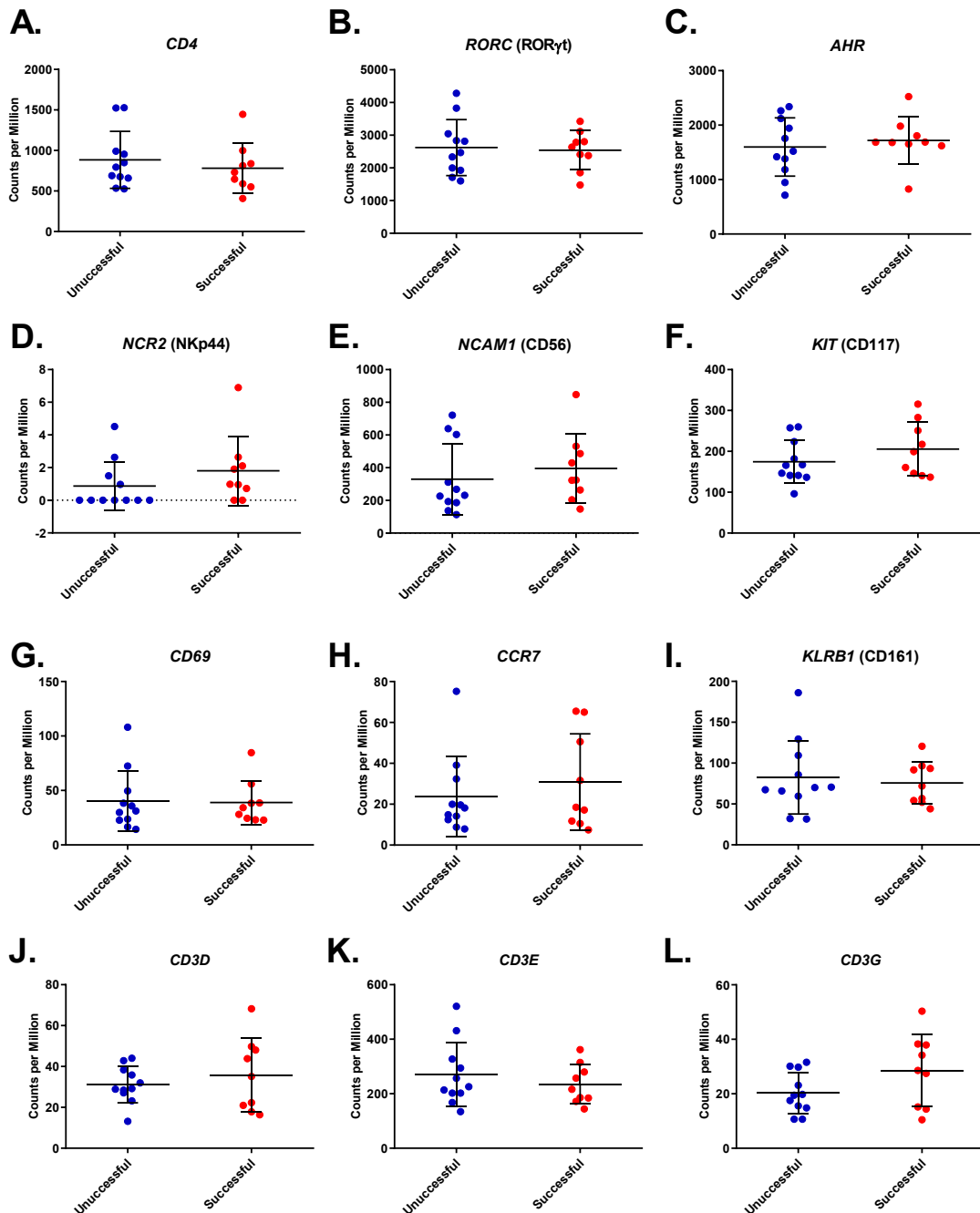


Figure 4.4. Immune cell markers in the RNA-seq result from the successful and unsuccessful pregnant endometrial biopsies. The counts per million values associated with each gene of interest were graphed by sample (successful pregnancy or unsuccessful). **A-F.** Graphs show markers of T_H17 (CD4, RORC, AHR), ILC3 (RORC, AHR, NCR2, KIT) and NK cells (NCR2; NCAM1; KIT); **G-I.** Markers associated with T_{RM} cells (CD69, CCR7 and KLRB1) and in **J-L.** are plotted the counts associated with the accessory CD3 molecule, expressed in T_H17 , T_{RM} and MAIT cells.

4.3.2 LPS has little effect on endometrial epithelial cells

Since we failed to identify any differences in the immune cell population present in the endometrial biopsies responsible for IL-17A production, we wondered if endometrial epithelial cells were able to express and produce IL-17A and the other IL-17s.

Given the role of IL-17A in activating immune response upon bacterial infection settings, we treated the endometrial epithelial adenocarcinoma cell line Ishikawa with different concentrations of bacterial lipopolysaccharide (LPS) for 6h and 24h. Ishikawa cells seemed to not be responsive to LPS challenge since no increase in *CXCL8*, which encodes for IL-8, production can be observed after the treatment (**Figure 4.5A.**). Surprisingly, *IL-17A* mRNA expression was increased after only 6h of treatment with 1µg/mL LPS, as shown in **Figure 4.5B**, even though there is some variability among the biological replicates and the overall fold change is very small. Similarly, also *IL-17B*, *IL-17D* and *IL-25* expression was increased after 6h from the stimulation (**Figure 4.5C.**, **4.5E.** and **4.5F.** respectively), whereas *IL-17C* expression increases after 24h from the stimulation (**Figure 4.5D.**). Interestingly, *IL-17F*, which encodes the IL-17F protein that often form heterodimers with IL-17A, did not show any modulation upon LPS treatment, suggesting that this cytokine is not involved in response to this PAMP (**Figure 4.5G.**).

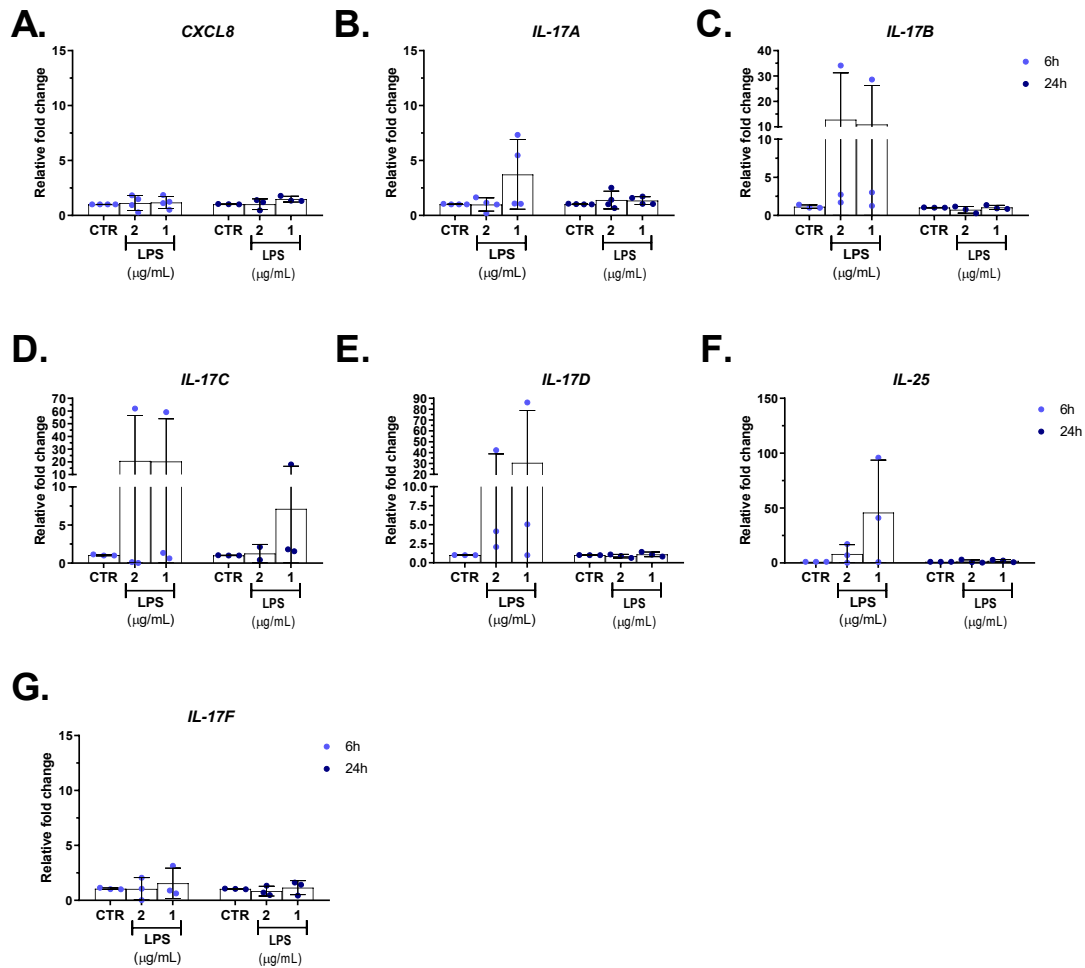


Figure 4.5: Expression of IL-17 in endometrial epithelial cells upon LPS stimulation. Ishikawa cells were treated with 1μg/mL and 2μg/mL LPS for 6h and 24h. mRNA was extracted and qPCR performed to assess changes in IL-17 gene expression induced by LPS treatment relative to the housekeeping gene RPLP0. CXCL8 (IL-8) expression was monitored as a positive control for LPS stimulation (A.). Expression of IL-17 isoforms (IL-17A-F) was assessed (B. through G.). N≥3. Statistical test applied: Two-Way ANOVA with Dunnett correction for multiple comparisons.

4.3.3 Endometrial epithelial cells produce IL-17A upon stimulation with viral ligands

We wondered if other stimulations could induce IL-17A expression in endometrial epithelial cells. Not much is known about IL-17A production upon viral infection, therefore we treated Ishikawa cells with the synthetic double strand RNA viral analogue soluble high molecular weight (HMW) poly(I:C), which stimulates the antiviral response

through TLR3. Ishikawa cells were stimulated with a titration of poly(I:C) for 3h, 6h and 24h. An earlier time point was added since antiviral responses in other epithelial cell models were shown to happen before 6h. Viral stimulation of Ishikawa cells significantly induced upregulation of *IL-17A* at 3h with 5µg/mL (**Figure 4.6A.**), even with a greater fold change than *IFNB1* (**Figure 4.6B.**), encoding for IFNβ, a canonically induced mediator for antiviral immunity. Both *IL-17A* and *IFNB1* show increased expression still at 6h, with a lower fold change, and then they drop at 24h. The other IL-17s were not particularly modulated by poly(I:C) treatment, *IL-17B* and *IL-17D* showed no fold change if compared to the control (**Figure 4.6C.** and **4.6E.**). *IL-17C* and *IL-25* showed an increased expression at 24h timepoint, although *IL-25* has quite a big variation between the samples, therefore only *IL-17C* is significantly increased by 5µg/mL poly(I:C) (**Figure 4.6D.** and **4.6F.**). *IL-17F* again seems to not be induced by the treatment, as it shows only an average fold change of 2.5 in cells treated for 3h with 5µg/mL poly(I:C) (**Figure 4.6G.**).

Our preliminary results suggest that both the bacterial and the viral ligands seem to induce an increase in IL-17A expression, thus suggesting that epithelial cells can be induced to express this cytokine to fight infections. In particular, Ishikawa cells demonstrated to be more responsive to poly(I:C) stimulation than to LPS.

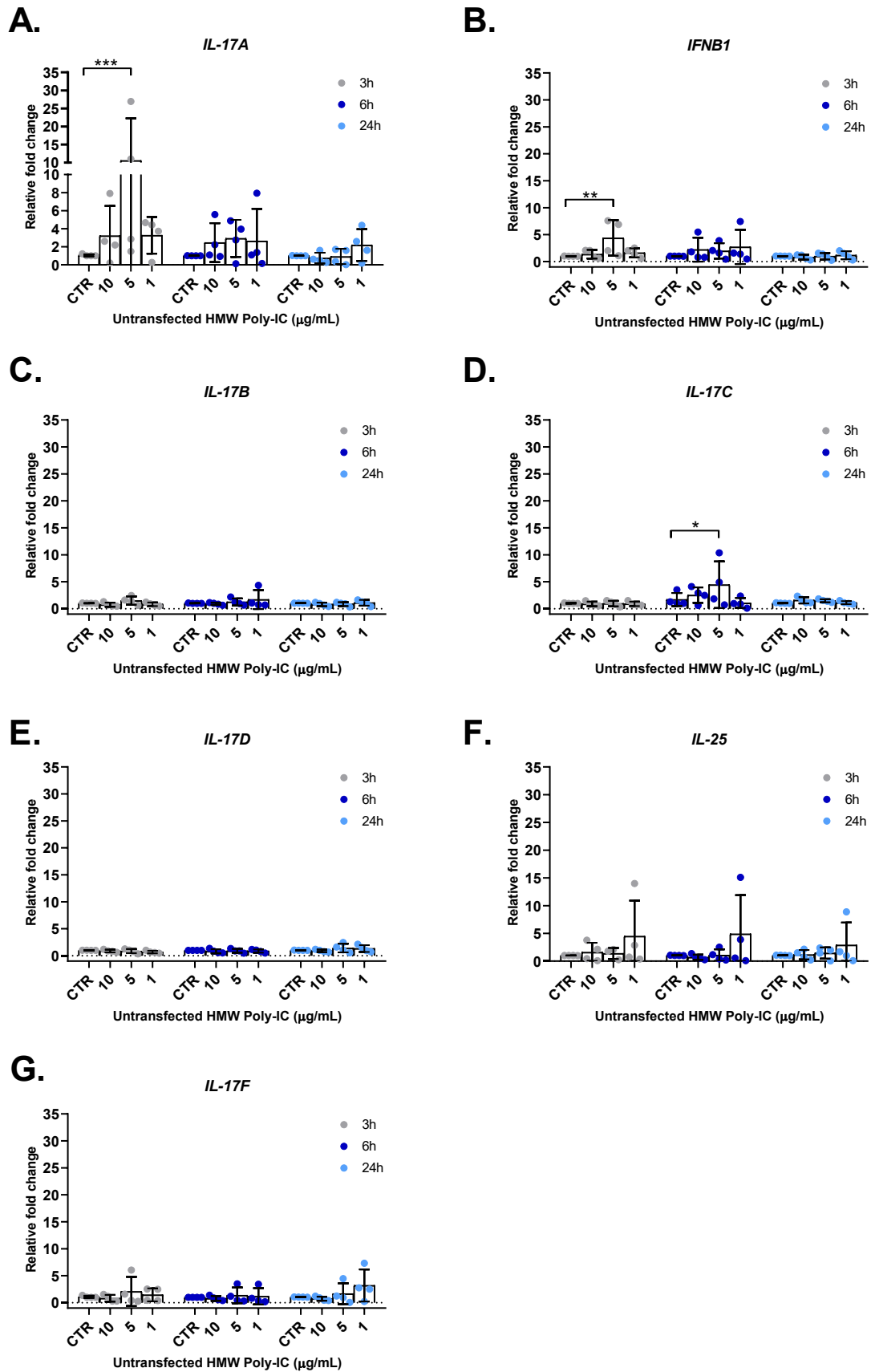


Figure 4.6. IL-17A expression is increased by simulated viral infection in Ishikawa cells. Ishikawa cells were treated with a titration of soluble High Molecular Weight (HMW) poly(I:C): 10, 5 and 1µg/mL for 3h, 6h and 24h. RNA was extracted from treated cells and expression of genes of interest (*IFNB1* and *IL-17A-F*) was measured by qPCR using *RPLP0* as a housekeeping reference. $N \geq 3$. Statistical test applied: Two-Way ANOVA with Dunnett correction for multiple comparisons. * $p < 0.05$; ** $p < 0.002$.

4.3.4 RORyt signalling is present in endometrial epithelial cells

RORyt is the master regulator of IL-17A expression in immune cells but, according to the Human Protein Atlas database, it is expressed by a wide variety of cell types and tissues. Another molecule that has been associated with IL-17A expression is HIF1 α . We wondered whether, in the bacterial or the viral stimulation, we could identify activation of RORyt or HIF1 α .

We started by analysing the fold change induced in *RORC*, the gene coding for RORyt upon LPS stimulation in Ishikawa cells. As it can be noticed in [figure 4.7A](#), Ishikawa cells express *RORC*, however the expression is not changed upon LPS stimulation, so as the expression of *HIF1 α* ([Figure 4.7B.](#)). *IL-23A* and *IL-12B* are the genes coding for IL-23 α and IL-12 β , the two subunits forming IL-23 which is responsible for RORyt activation and IL-17A production. It was noted that IL-12B expression is upregulated in cells treated for 6h with 1µg/mL LPS ([Figure 4.7C.](#)), which is the same concentration that induces IL-17A over-expression. *IL-23A* expression is not modified by LPS treatment instead ([Figure 4.7D.](#)).

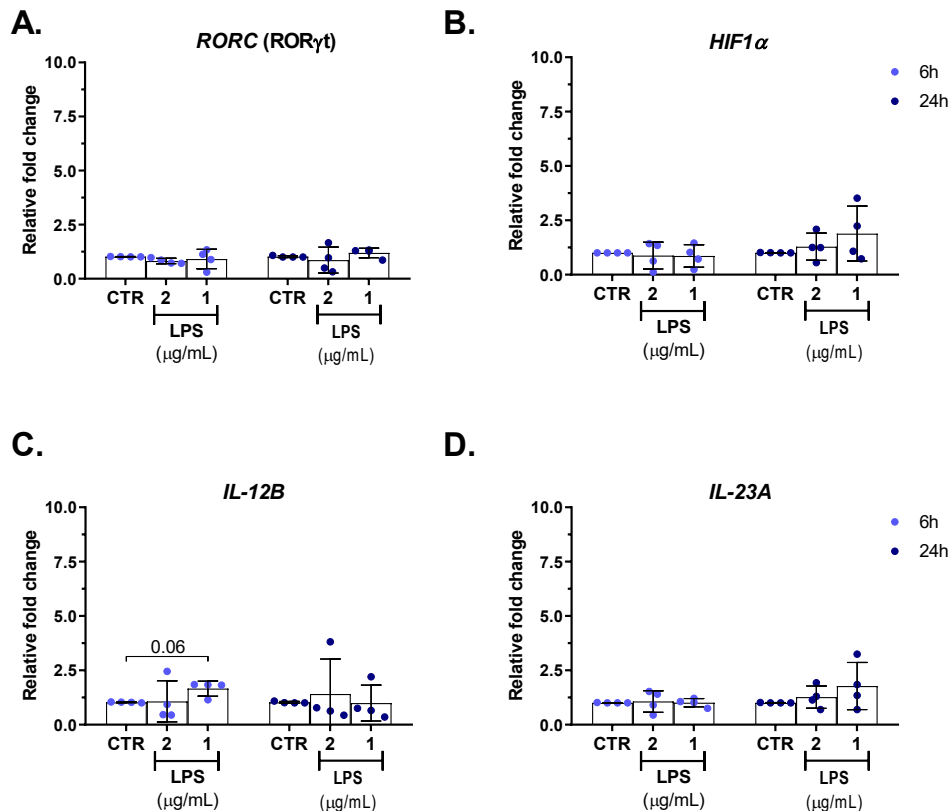


Figure 4.7. Influence of LPS on pathways upstream of IL-17A production. Ishikawa cells were treated with 2 and 1 μ g/mL LPS for 6h and 24h and RNA extracted. qPCR was performed to determine the impact of LPS treatment on epithelial expression of RORC (ROR γ t coding gene) (A.), HIF1 α (B.) and two subunits of IL-23: IL-12B (C.) and IL-23A (D.). Housekeeping reference gene used was RPLP0. $n=4$. Statistical test applied: Two-Way ANOVA with Dunnett correction for multiple comparisons.

The modulation of the molecules involved in IL-17A production was also monitored in Ishikawa cells treated with poly(I:C). As for LPS treatment, RORC, IL-23A and HIF1 α expression is not affected by the viral stimulation (Figure 4.8A, B. and D.), but IL-12B is significantly upregulated in cells treated with 5 μ g/mL poly(I:C) for 3h (Figure 4.8C.), which again is the same timepoint and concentration inducing IL-17A increased expression. Given that transcription factors, such as ROR γ t, are generally not transcribed *ex novo* whenever they get activated, the fact that we did not detect any change in RORC expression could be due to the fact that the protein is more affected by the stimulation. We therefore checked whether Ishikawa cells treated with 5 μ g/mL

poly(I:C) and for shorter timepoints show different protein levels if compared to the control via immunostaining for ROR γ t using flow cytometry. This confirmed that Ishikawa cells do have ROR γ t protein, however the protein levels are not affected by poly(I:C) treatment as it can be noticed no change in both the percentage positivity of live cells (Figure 4.9A.) or the Median Fluorescence Intensity (MFI) (Figure 4.9B.) signal between the control or the treated cells.

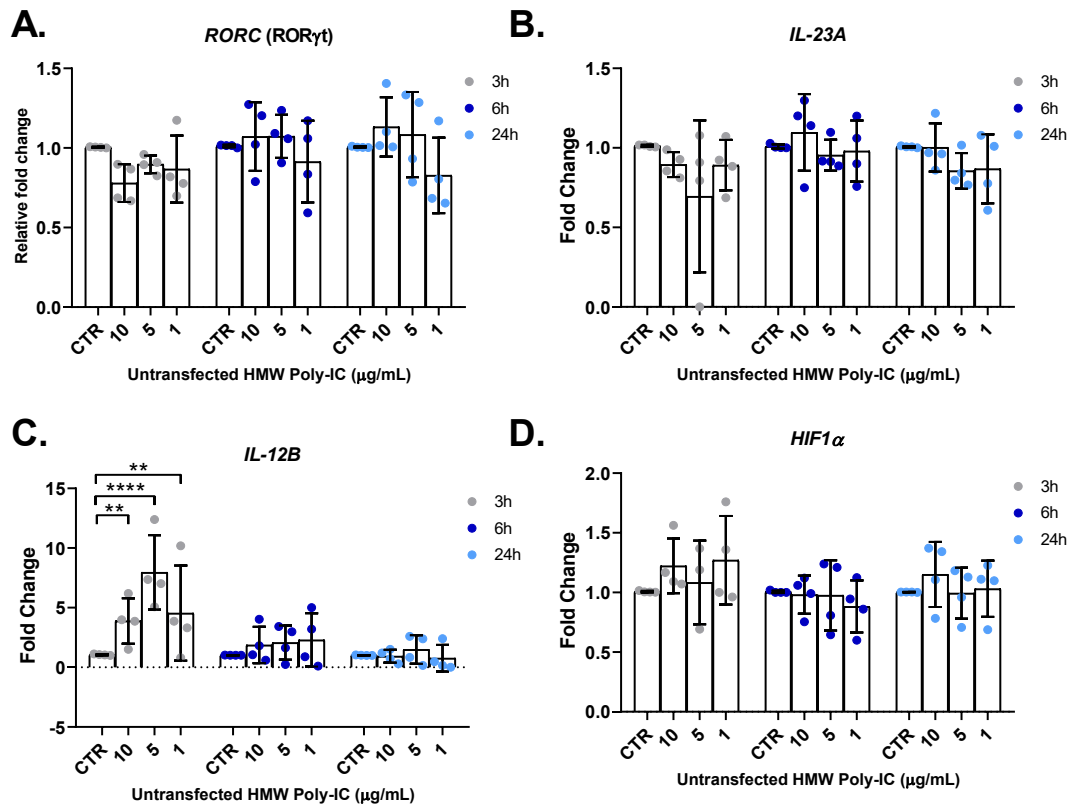


Figure 4.8. Activation of ROR γ t signalling in Ishikawa cells treated with poly(I:C). Ishikawa cells were treated with 10, 5 and 1 μ g/mL poly(I:C) for 3h, 6h and 24h. RNA was extracted, and qPCR was performed to determine modulation induced by the treatment on RORC (ROR γ t coding gene) (A.), HIF1 α (D.) and two cytokines, IL-12B (C.) and IL-23A (B.). $n=4$. Statistical test applied: Two-Way ANOVA with Dunnett correction for multiple comparisons. ** $p<0.002$; **** $p<0.0001$.

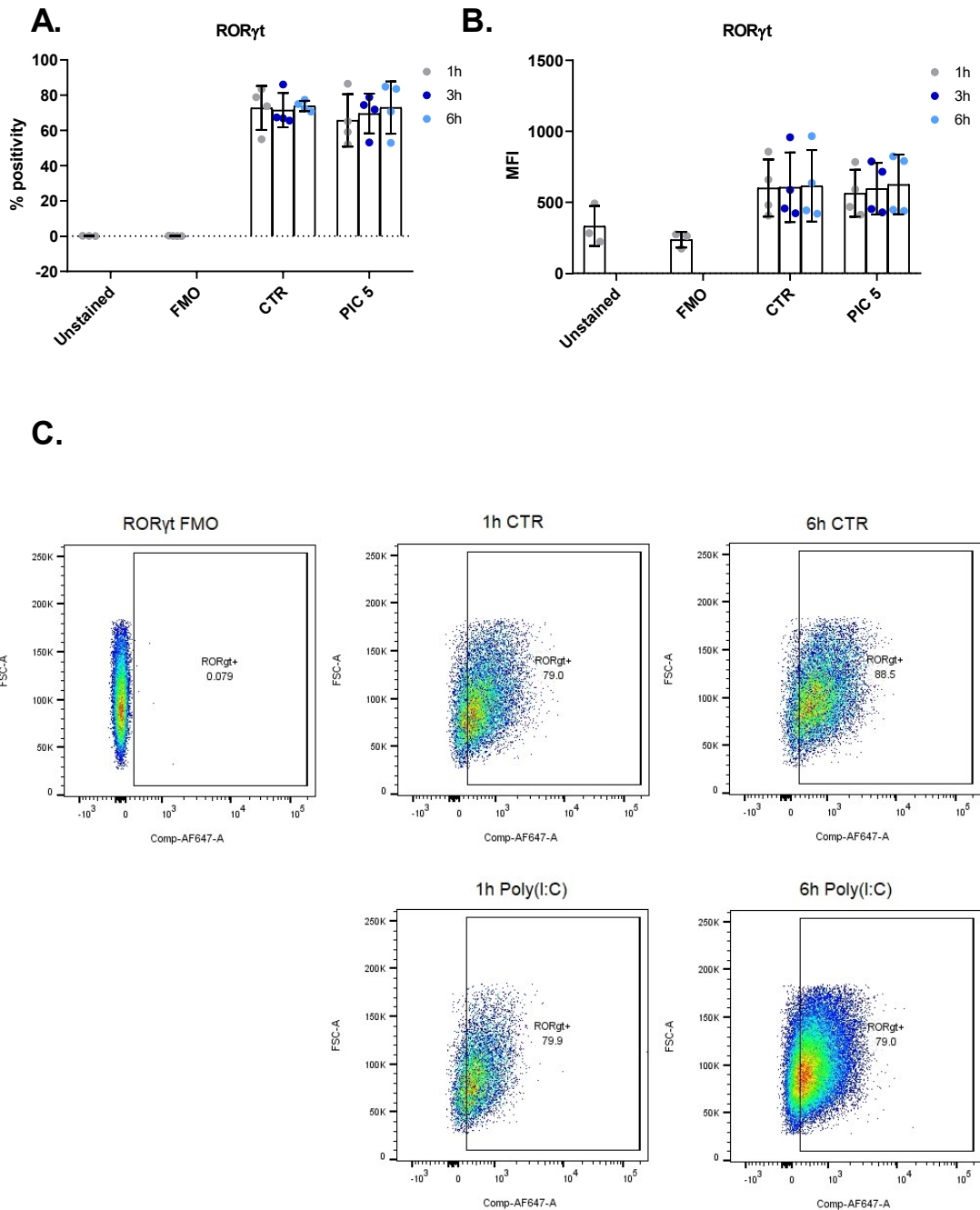


Figure 4.9. Ishikawa cells express ROR γ t protein. ROR γ t protein was detected in Ishikawa cells treated with 5 μ g/mL poly(I:C) for 1h, 3h and 6h; cells were stained for flow cytometry using a fluorophore-conjugated antibody specific for ROR γ t. Flow cytometry was also performed on unstained cells and on cells stained for a viability dye but not with ROR γ t antibody (FMO or Fluorescence Minus One). ROR γ t staining was calculated as percentage of positive cells compared to the live cells (A.) or by calculating the Median Fluorescence Intensity (MFI) (B.). The data obtained with flow cytometry was also graphed in C., with FSC-A on the Y-axis and the readout for the ROR γ t-conjugated antibody with Alexa-Fluor 647 on the X-axis. n=4.

These results confirmed that Ishikawa cells have both mRNA and protein expression of the transcription factor responsible for IL-17A transcription. Furthermore, the upstream activator of ROR γ t signalling, IL-12B, shows a significantly increased expression in the same treatments' concentrations and timepoint where it can be found IL-17A increased expression. No changes can be observed in ROR γ t protein between control and treated cells, however, is possible that the signalling activation leads to ROR γ t translocation in the nucleus, rather than in increased protein levels.

4.3.5 IL-17A induces a pro-inflammatory mucosal signature in endometrial epithelial cells

Once it was established that endometrial epithelial cells can produce IL-17A upon infection, we wondered what effect it would have in those cells. Therefore, Ishikawa and primary human endometrial epithelial cells (hEEC) were treated with a titration of recombinant IL-17A (rIL-17A) and expression of target genes known to be induced by rIL-17A stimulation was analysed. **Figure 4.10** shows that pro-inflammatory genes associated also to mucosal immunity are activated in response to IL-17A stimulation, these comprise chemokines (CXCL8, **Figure 4.10A.** and **4.10B.**) and AMPs belonging to two different classes, the whey acidic protein (WAP) family (PI3, also known as Elafin, **Figure 4.10C.** and **4.10D.**) and the S100As family (S100A9 and S100A8, **Figure 4.10E-H**). The expression relative to the treatment in Ishikawa cells is displayed on the left of the figure panel and on primary hEEC cells on the right. Both cell models responded to IL-17A stimulation, even though hEEC cells show a significantly greater response. In Ishikawa cells CXCL8 expression is enhanced at 24h timepoint for all the three doses (**Figure 4.10A.**), whereas in hEEC cells the chemokine expression is significantly increased already at 6h in a dose-dependent manner (**Figure 4.10B.**). For the AMPs PI3/Elafin and S100A9 both these cell models respond at the same timepoint, with increased expression of PI3/Elafin at 6h (**Figure 4.10C.** and **4.10D.**) and S100A9 reaching significantly higher expression levels at 24h in hEEC and Ishikawa (**Figure 4.10F.** and **E.**, respectively). On the other hand, it seems that Ishikawa cells do not modulate S100A8,

given that its expression is not affected by the treatment, whereas hEEC show a significant dose-dependent increase in S100A8 expression after 24h rIL-17A treatment.

Furthermore, treatment in both cell models with rIL-17A resulted in increased IL-17A expression, as a sort of positive feedback. Indeed, treatment with 100, 10 and 2ng/mL rIL-17A for 6h resulted in increased IL-17A expression in Ishikawa ([Figure 4.11A.](#)) and in hEEC cells treatment with 50ng/mL induced a significant increase of IL-17A at 6h, even though also other concentrations increased its expression but not significantly ([Figure 4.11B.](#)). At 24h the expression of IL-17A is then reduced in both models.

IL-17A treatment in hEEC, which are a better model for understanding what would happen *in vivo*, activates the mucosal response by inducing CXCL8 and some AMPs as early as 6h, and other AMPs such as S100A8 and S100A9, after 24h from the treatment. Also, we noticed that there might be in place a positive feedback loop since IL-17A treatment induces an early IL-17A expression in endometrial epithelial cells. IL-17A expression is then reduced at 24h, thus suggesting that these cells can potentiate the mucosal response in early timepoints of infection settings, but then they shut down IL-17A expression, possibly to avoid excessive pro-inflammatory signalling activation.

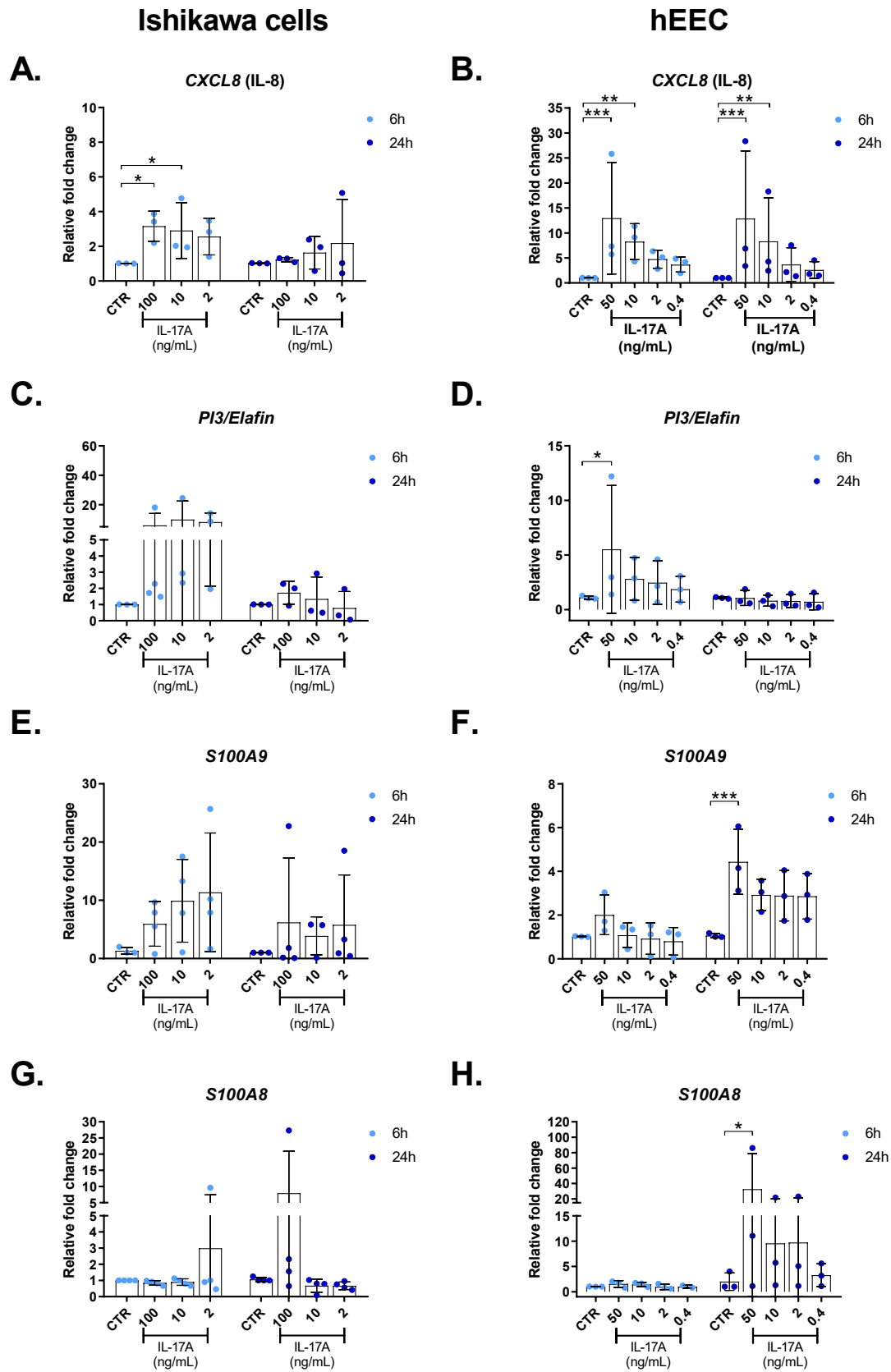


Figure 4.10. A response characteristic of mucosal inflammation is activated in endometrial epithelial cells by IL-17A. Ishikawa and hEEC cells were treated with recombinant IL-17A (rIL-

17A) at 100, 10 and 2ng/mL in Ishikawa cells and 50, 10, 2 and 0.4ng/mL in hEEC for 6h and 24h (100ng/mL was not used in hEEC due to a low response to this dose in Ishikawa cells). RNA was extracted and gene expression measured by qPCR. IL-17RA and IL-17RC expression was confirmed in both cell models (see method). Relative gene expression in Ishikawa cells is displayed on the left of the panel: CXCL8 (A.), PI3/Elafin (C.), S100A9 (E.) and S100A8 (G.). Gene expression in hEEC is displayed on the right of the panel: CXCL8 (B.), PI3/Elafin (D.), S100A9 (F.) and S100A8 (H.). $N \geq 3$. Statistical test applied: Two-Way ANOVA with Dunnett correction for multiple comparisons. * $p < 0.05$; ** $p < 0.002$; *** $p < 0.0002$.

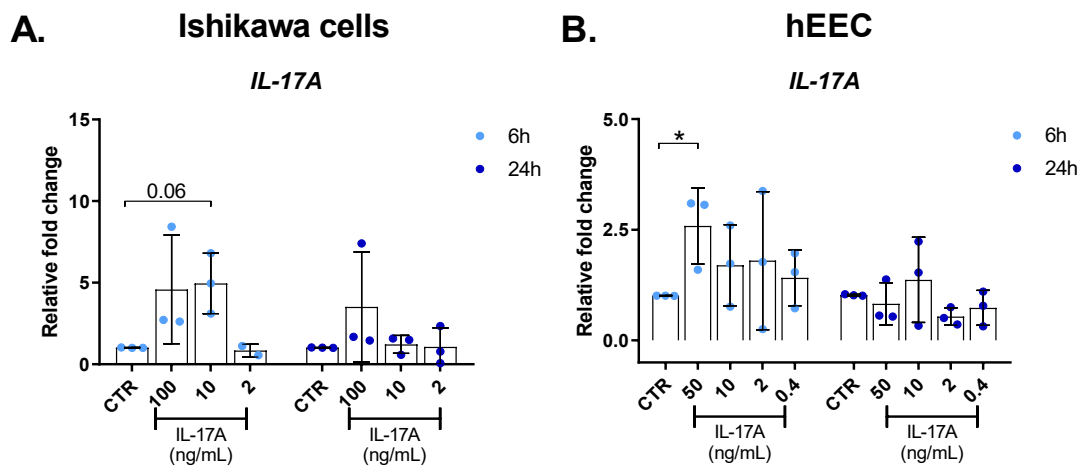


Figure 4.11. rIL-17A treatment increases IL-17A expression in endometrial epithelial cells. Ishikawa and hEEC cells were treated with a titration of rIL-17A: 100, 10 and 2ng/mL in Ishikawa cells and 50, 10, 2 and 0.4ng/mL in hEEC for 6h and 24h. RNA was extracted, and gene expression measured by qPCR. IL-17A expression was measured in Ishikawa (A.) and in hEEC (B.). $N=3$. Statistical test applied: Two-Way ANOVA with Dunnett correction for multiple comparisons. * $p < 0.05$.

4.4 Discussion

Given the observation of increased IL-17A protein and IL-17A activated pathway in women with unexplained infertility, we wondered if an increased percentage of immune cells in those samples might be responsible for the local IL-17A production. Although bulk RNA-seq was performed, and there was no remaining tissue suitable for immunohistochemistry, we decided to apply a tool that has recently been developed to identify the abundance of a specific cell population by using a gene signature showed by certain cell-types (371). Using the well validated immune-cells gene signature, we could not identify any differences in the percentage abundance between the two sample sets (Figure 4.3). It could be possible that the gene matrix chosen was not the best model since it is derived from genes expressed in circulating immune cells. In the female reproductive tract the resident immune cells show a very different phenotype compared to circulating ones (185), thus it could be possible that a matrix obtained from resident immune populations would be more powerful in estimating the abundance of immune cells between the two groups. Another indication that the gene matrix chosen was not the best model can be noticed in the overall proportion of immune cells present in the samples, which sees resting CD4⁺ memory T-cells as the most abundant immune population in the endometrium, followed by NK cells which only represent 10-15% of the immune population. However it is known that during the mid-luteal phase, when the biopsies were collected, the most abundant immune cell population are dNK cells which reach up to 40-60% of the total immune cells (20). It is still possible that the method chosen for sampling might have collected only the epithelial layer of the endometrium and not reach the decidua, where dNK cells are more abundant (20).

Looking at the normalised counts per million obtained in the result from the RNA-seq were also analysed. However even with this approach it was not possible to identify differences between the samples obtained from women who had a successful or unsuccessful pregnancy outcome (Figure 4.4). Of course, this approach is not enough to exclude differences between immune cell populations, given that other approaches, such as immunostaining or flow cytometry, are more reliable in picturing what the

immune milieu could have been, but were not feasible due to impossibility in performing them retrospectively.

Since we could not identify striking differences between the immune cells in the two sample sets and given that epithelial cells have important roles in local immune responses, beyond acting as a simple barrier for pathogen entry, we wondered whether these cells could produce IL-17A. Since IL-17A is released upon bacterial infection, we first assessed whether LPS treatment would modulate IL-17A expression using the endometrial epithelial adenocarcinoma cells Ishikawa. These cells derive from a 39 year old woman and it is widely used as an endometrial epithelial cell model, especially studies involving treatment with hormones since these cells can respond to hormonal stimulation (372). There is contrasting evidence regarding the expression of TLR4 in Ishikawa cells. According to some studies Ishikawa cells very weak expression of TLR4 (373), whereas other studies reported positivity for such TLR via immunohistochemistry and real time PCR (374) and in this study it was also reported very little reactivity against LPS. In our model it was confirmed that the relative abundance of TLR4 transcript in Ishikawa was much smaller if compared to primary human endometrial epithelial cells (**Figure 2.3B.**). This could explain why treatment with LPS did not induce increase in *CXCL8* expression in this cell model and why the fold changes observed were very small (**Figure 4.4**). IL-17A expression shows a tenuous increase by 6h LPS stimulation, with no fold increase for 2 out of 4 biological replicates (**Figure 4.5B.**). Furthermore, IL-17F, which is shown to be co-expressed with IL-17A to form heterodimers (109), is not significantly increased by this stimulation(**Figure 4.5G.**), suggesting that in some settings IL-17A homodimer could be forming, rather than the IL-17A/F dimer. The reduced expression of TLR4 and responsiveness to LPS could be explained by the fact that epithelial cells at mucosal sites are often found to interact with the local microbiome, thus they show less sensitivity to bacterial stimulation to avoid excessive immune response against commensals.

We next wondered whether viral stimulation could induce IL-17A release by endometrial epithelial cells. Ishikawa cells had been previously shown to express and present TLR3 although this was not enough to induce a response to the viral ligand analogue poly(I:C) (374). Once again, TLR3 relative abundance in Ishikawa was found to

be much smaller if compared to primary human endometrial epithelial cells (**Figure 2.3C.**). Furthermore, only IL-17D was shown to be involved in viral infection and clearance among the members of IL-17 cytokine family (104). Treatment of Ishikawa cells with the viral ligand analogue poly(I:C) resulted in the activation of the antiviral response through increase of *IFNB1* gene at early timepoint such as 3h (**Figure 4.6B.**). The treatment with this PAMP induced a significant increase in IL-17A expression after 3h from the treatment (**Figure 4.6A.**). Of note, IL-17A fold increase in Ishikawa cells is much higher than the one obtained for IFN β , a molecule known to be actively involved in viral response. IL-17F expression, is again not modulated in Ishikawa cells (**Figure 4.6G.**). It is interesting to note that IL-17A fold change returns comparable to the control after 24h from both stimulations, confirming that endometrial epithelial cells express this cytokine transiently, in order to prevent excessive pro-inflammatory activation.

IL-17A expression is modulated by the transcription factor ROR γ t and is induced by IL-23, which is formed by two subunits IL-23 α and IL-12 β (111, 147). We would expect to identify changes in either ROR γ t or IL-23 subunits expression in the cells treated with LPS and poly(I:C) showing increased IL-17A expression. *RORC* (encoding for ROR γ t) and *IL-23A* expression is not modulated by the treatments, similarly to *HIF1 α* expression, a transcription factor involved in transcription of *RORC* mRNA (**Figure 4.7** and **4.8**). *IL-12B*, on the other hand, is significantly increased in both LPS and poly(I:C) treated cells, in the same doses and timepoints showing IL-17A increased expression (**Figure 4.7C.** and **4.8C.**). We then wondered if the protein expression of ROR γ t would be upregulated by poly(I:C) treatment. Flow cytometry for ROR γ t positive cells, however, did not show differences between the control and treated samples (**Figure 4.9A.** and **4.9B.**), even adding earlier timepoints, when transcription factor activation would be likely to happen before mRNA transcription. Therefore, we identified *IL-12B* significantly increased by the stimulations, but no changes in either ROR γ t mRNA or protein levels (**Figure 4.7**, **Figure 4.8** and **4.9A.**). These results, however, do not exclude ROR γ t activation. When transcription factors are activated, they generally migrate from the cytoplasm to the nucleus for allowing a fast response. Other approaches, such as immunofluorescence or western blotting for cytosolic and nuclear ROR γ t, would be

more indicated for confirming if this transcription factor is activated or not by these stimulations.

We observed a significant increase of *IL-17A* expression by poly(I:C) stimulation as well as increase in the upstream cytokine *IL12B*, which was not observed for LPS. In both cases, there is quite variability between the biological replicates, with some replicates showing a very little fold change, thus it is still questionable whether the Ishikawa cell line can produce IL-17A. Ishikawa cells are an adenocarcinoma cell line, and it is known that immortalised cells show an altered glucose metabolism with preferential energy source being anaerobic glycolysis, a phenomenon known as Warburg Effect. For this reason, immortalised cell line might show a different physiology if compared to primary human cells, therefore repeating these experiments in hEEC cells would clarify if these results and the fold changes observed would be consistent. Furthermore, other models have been developed which can better resemble the complexity of the interaction found in the endometrium. In our model, a 2D culture of Ishikawa cells can be useful to see the response of epithelial cells per-se, however this model does not consider both the polarisation of the epithelial cells and the communication with the underlying stromal cells. Several studies use endometrial organoids consisting of a 3D culture of both epithelial and stromal endometrial cells which better recapitulate the polarisation of the epithelial layer as well as maintaining the interaction between the epithelium and the stromal cells (375, 376).

We then wondered what effect this cytokine would stimulate on those cells. As already mentioned above, IL-17A binds to its receptors, IL-17RA-IL-17RC, which are expressed by a wide variety of cells including epithelial cells (50). In mucosal sites, binding of IL-17A to its receptors activate the transcription of various molecules involved in the mucosal response, such as chemokines and AMPs (Figure 1.5). Treatment of Ishikawa and hEEC with recombinant IL-17A recapitulated these processes. Indeed, it induced *CXCL8*, *PI3* and *S100A9* expression in both Ishikawa and hEEC cells, even though some genes were upregulated at 6h and other at 24h (Figure 4.10) confirming that, within IL-17A pathway, there are some genes upregulated earlier than others. We also noticed that there is a potential positive feedback induced by IL-17A treatment, as we observed increased *IL-17A* expression after 6h from the treatment (Figure 4.11). As for the other

stimulations, *IL-17A* expression decreases after 24h of stimulation, thus confirming that in these cell models IL-17A pathway is turned off for preventing exacerbated inflammation.

Chapter 5: The uterine microbiome and the microbial metabolite butyrate stimulate pro-inflammatory responses in the human female reproductive tract

5.1 Introduction

5.1.1 Microbial-derived metabolites in the FRT

5.1.1.a Lactic acid

Lactic acid is the most abundant metabolic by-product produced by healthy vaginal microbiota, reaching a concentration of approximately 110mM (377). This is produced mainly by *Lactobacillus* spp. which use glycogen as carbon sources to produce this metabolite in either its D- or L- conformation (378). These isoforms are differently produced by different Lactobacilli strains, with *L. iners* being able to only produce the D-isoform (379), which is more associated with prevention of *Chlamydia* infection (380). Lactic acid plays important roles in protection of vaginal homeostasis through lowering the pH, which in healthy condition is around 3.5 but, in the case of dysbiosis such as in bacterial vaginosis, it reaches pH >4.5 (273). Conversely, in the endometrium the pH is higher (381), with a mean pH approximately around 7-7.5. The pH in the endometrium was shown to be highly variable during the menstrual cycle, reaching pH 6-6.5 during the secretory phase (382). Thus, it is possible that in the endometrium the lactic acid content is not as high as in the lower vaginal compartment. Two recent studies highlighted how elevated levels of lactic acid or lactate in the endometrium (>1ppm) correlate with endometriosis and unsuccessful embryo transfer in women with recurrent implantation failure (383, 384).

5.1.1.b Short chain fatty acids

In healthy vaginal fluid, small amounts of short chain fatty acids have been identified, such as acetate, propionate, butyrate, isobutyrate, and succinate (385, 386). These are

molecules constituted by less than six carbon atoms and are produced by anaerobic bacteria using polysaccharides such as glucose, galactose, fucose or pentoses (261). In bacterial vaginosis or in non-specific vaginitis, a significant increase in the SCFA content in the cervicovaginal mucus it has been observed, due to the decrease in *Lactobacillus* spp. and increase in Bacterial Vaginosis-associated bacteria (BVAB) (387). As a result, acetate becomes the most abundant metabolite, with a concentration around 120mM, followed by lactate (<20mM)(388), and propionate and butyrate with much lower concentrations <2-4mM (389). Given that there is no consensus on the endometrial microbiome which it has recently being investigated, there is no information yet regarding SCFAs content of this compartment. Given the lower microbial biomass present in the endometrium, is possible that the metabolite concentration might be lower than the one observed in the lower reproductive tract (250, 254).

5.1.2 Bacterial species producing SCFAs

Most studies regarding the production of SCFAs have been performed in the gut. Here, it seems that there are certain microbial species associated with the production of each SCFA (Table 5.1). It was also observed to happen cross feeding between different microbial species, where intermediate products for production of a given SCFAs can be used by another microbial specie to produce a different SCFAs (261). In the FRT, and specifically in the vaginal compartment, SCFAs are mainly produced during dysbiosis caused by expansion of BVAB: *Gardnerella*, *Atopobium*, *Prevotella*, *Mobiluncus*, *Megasphaera*, *Dialister*, *Sneathia*, *Leptotrichia*, *Streptococcus*, *Bacteroides*, *Mycoplasma*, *Clostridiales* BVAB 1, 2, 3 (273). Among those species, SCFAs production has been well characterised for some of them, such as *Gardnerella vaginalis* has been shown to produce acetate and species from *Peptococcus* spp. are able to produce both acetate and butyrate (386). Similarly, *Prevotella*, *Gardnerella* and *Mobiluncus* spp. are mainly able to produce succinate and acetate and lower amounts of butyrate, propionate and valerate (388). Interestingly, in a gut model of infection with *Prevotella* spp., it has been shown a significant decrease in acetate and increase in butyrate, even though this effects were not due to direct butyrate production by *Prevotella* (390).

SCFA	Bacterial phylum	Bacterial species	Reference	
Acetate	Actinomycetota	<i>Bifidobacterium</i> spp. ^A	(261)	
		<i>Gardnerella vaginalis</i> ^A	(386, 388)	
		<i>Mobiluncus</i> spp. ^A	(388)	
	Firmicutes	<i>Clostridium</i> spp. ^A	(261)	
	Bacillota	<i>Peptococcus</i> spp.	(386)	
	Bacteroidota	<i>Prevotella</i> spp. ^A	(388)	
Butyrate	Firmicutes	<i>F. prausnitzii</i> ^B	(261, 391)	
		<i>Roseburia</i> ^B	(261, 391)	
		<i>Anaerostipes</i> spp. ^B	(261)	
		<i>Eubacterium</i> spp. ^B	(261, 391)	
		<i>Ruminococcus</i> spp. ^A	(261, 391)	
	Bacteroidota	<i>Bacteroides</i> spp. ^A	(261)	
		<i>Prevotella</i> spp. ^A	(388)	
	Actinomycetota	<i>Bifidobacterium</i> spp. ^A	(261)	
		<i>Mobiluncus</i> spp. ^A	(388)	
		<i>Gardnerella</i> spp. ^A	(388)	
		Bacillota	<i>Peptococcus</i> spp.	(386)
		Verrucomicrobiota	<i>Akkermansia</i>	(391)
Propionate	Bacteroidota	<i>municiphilla</i> ^A	(261)	
		<i>Bacteroides</i> spp. ^A	(261, 388)	
	Actinomycetota	<i>Prevotella copri</i> ^A	(261)	
		<i>Bifidobacterium</i> spp. ^A	(388)	

Firmicutes	<i>Mobiluncus</i> spp. ^A	(388)
	<i>Gardnerella</i> spp. ^A	(261)
	<i>Veillonella</i> spp. ^A ,	(261)
	<i>Eubacterium halii</i> ^A	(261)
	<i>Anaerostipes</i> spp. ^A	(261)
	<i>Ruminococcus</i> spp. ^A	

Table 5.1. Bacterial species responsible for production of the more abundant SCFAs in the gut and FRT. ^ADirect production by the microbial specie; ^BProduction derived by cross feeding from an intermediate product.

5.1.3 Mechanisms of SCFAs modulation on immunity

Interestingly, SCFAs show different immunomodulatory abilities depending on the organ where they are produced. Indeed in the gut SCFAs are extremely important for maintaining healthy homeostasis of gut epithelial cells as well as inducing an anti-inflammatory environment and tolerance in immune cells (392, 393). Conversely, in the FRT these molecules are associated with a pro-inflammatory signature and activation of mucosal responses in epithelial cells (261, 273).

5.1.3.a Anti-inflammatory and protective actions in the gut

In the human gut SCFAs are produced mainly by Firmicutes converting the starch fibres into acetate, propionate and butyrate in a proportion of 60:20:20 (394). The concentrations are highly variable and depend on the ethnicity, the diet and the location where the SCFA are measured, but generally acetate shows an higher concentration in the colon, ranging from a mean value of 39 to 87mM and is followed by propionate and butyrate, which show a much lower concentration of approximately 12-20mM (392). In the gut, SCFAs can permeate intestinal epithelial cells and immune cells by using monocarboxylate transporters, MCT1 and MCT4, as well as engaging G-protein coupled receptors such as GPR41 and GPR43, leading to AMP- and phospholipase C-dependent pathways activation (392).

Involvement of SCFAs in gut epithelial cell homeostasis

The effect that SCFA have on epithelial cells are various and contribute heavily to maintain the healthy homeostasis, as confirmed by various models of germ-free mice showing impaired gut functions (**Figure 5.1**) (395, 396). SCFAs have been shown to induce epithelial cell proliferation and turnover (395), despite butyrate has been shown to inhibit intestinal stem cells proliferation, therefore this metabolite is generally metabolised by colonocytes before reaching the crypts, where the proliferating stem cells are located (397). Butyrate is indeed the main energy source for colonocytes leading to Acetyl-CoA production through the TCA cycle (398, 399). Furthermore SCFA, and particularly butyrate, help in maintaining the epithelial barrier by inducing tight junction protein expression and leading to increased transepithelial electrical resistance in several *in vitro* models (400, 401). Intracellular butyrate has been shown to consume oxygen and stabilise the transcription factor hypoxia-inducible factor (HIF)-1, which is also involved in mediating epithelial barrier integrity (396, 402). Butyrate also promotes barrier function in intestinal epithelial cells through enhancing the secretion of mucins (403).

Immunomodulatory effects of SCFAs in the gut

SCFAs in the gut are associated with anti-inflammatory responses induced in both the intestinal epithelial cells as well as in the immune cells (**Figure 5.1**). Butyrate was shown to inhibit lipopolysaccharide (LPS)-induced Nf- κ B activation in human and mouse colon models (404), whereas acetate shows a protective role in the epithelium by inducing NLRP3 inflammasome activation (405). In LPS-stimulated monocytes and PBMCs, SCFAs induce the release of prostaglandin E2 (PGE2) and of the anti-inflammatory IL-10 cytokine (406). The presence of butyrate during the differentiation from monocytes to macrophages was shown to imprint an antimicrobial activation program through HDAC3 inhibition (407). As a result, these macrophages upon infection have shown a faster response mediated by expression of AMPs, lysozyme, cytokines and chemokines without causing an exacerbated inflammatory response (407). Butyrate HDAC inhibitory action is also responsible in mediating the shift of CD4⁺ cells from a pro-inflammatory T_H1/T_H17 phenotype towards the anti-inflammatory T_{REG} phenotype, in the gut and in the thymus (408-410). Thus, HDAC inhibitors such as butyrate and propionate show

protective roles against inflammatory bowel diseases, as demonstrated by mice models of hyperacetylation and how these result in dampening the highly pro-inflammatory environment seen in colitis (409, 411). Recently have been identified butyrylation and beta-hydroxybutyrylation as two novel epigenetic modifications leading to activation of gene transcription, in contrast to acetylation with which have been demonstrated to compete for histone binding (329, 412).

5.1.3.b Pro-inflammatory actions in the vagina

Within the FRT, only vaginal SCFAs have been studied, even though not extensively as in the gut and, some of the studies mentioned in this section, would not have focused on highlighting the specific actions of SCFA, but rather mimicked the infection *in vitro*. Since SCFAs are the main metabolites produced upon infections, thus the processes described in this section are most likely related to SCFA stimulation. As mentioned earlier, in the FRT high amounts of SCFAs are produced upon infections/dysbiosis caused by decrease in lactic acid producing bacteria *Lactobacillus* spp. Once produced in the vagina, SCFAs contribute to sustain the dysbiosis by increasing the pH and by favouring polymicrobial growth through a mutualistic metabolite exchange that favours pathogenic species takeover (413) (Figure 5.1). This action is also obtained by impairing the antimicrobial response whilst causing a pro-inflammatory environment in both epithelial and immune cells.

Harmful effects of SCFAs on epithelial cells

Acetate, succinate, and butyrate stimulation of vaginal epithelial cells impairs the recruitment of neutrophils and monocytes by dampening the release of chemokines such as RANTES and CXCL10 (388, 414). Vaginal epithelial cell stimulation with BV-associated bacterial strains also induced pro-inflammatory cytokine release (IL-6, IL-8, IL-1 β , TNF α) as well as release of antimicrobial peptides such as defensins (415, 416). Also, upon BV a reduction in epithelial cells of the secretory leukocyte protease inhibitor (SLPI) has been noted. SLPI is a molecule involved in inactivating serine proteases used by immune cells, which has a protective role for epithelial cells in inflammatory settings (417) (Figure 5.1).

Pro-inflammatory activation of immune cells mediated by SCFAs

SCFAs also elicit pro-inflammatory responses in immune cells (Figure 5.1). *Megasphaera elsdenii* and *Prevotella timonensis*, two species associated with SCFA production (388, 418), have been shown to induce maturation of dendritic cells (DC), resulting in increased expression of cytokines and chemokines such as IL-1 β , IL-6, IL-8 and TNF α (419). Furthermore, DC matured in the presence of *P. timonensis* were able to polarize CD4⁺ T-cell maturation into the pro-inflammatory phenotype T_H1, thus suggesting that in infections there must be species-specific actions associated with every microbial invader (419). Acetate and butyrate stimulation of PBMCs using mucosal sites concentrations (20mM) led to increased release of pro-inflammatory mediators (IL-8, IL-6 and IL-1 β) (420). Despite lower concentrations (2mM) of acetate and butyrate stimulations alone did not elicit a significant response, they greatly enhanced PBMCs responsiveness when co-stimulated with TLR2 (Pam2CSK4) and TLR7 (imiquimod) ligands (420).

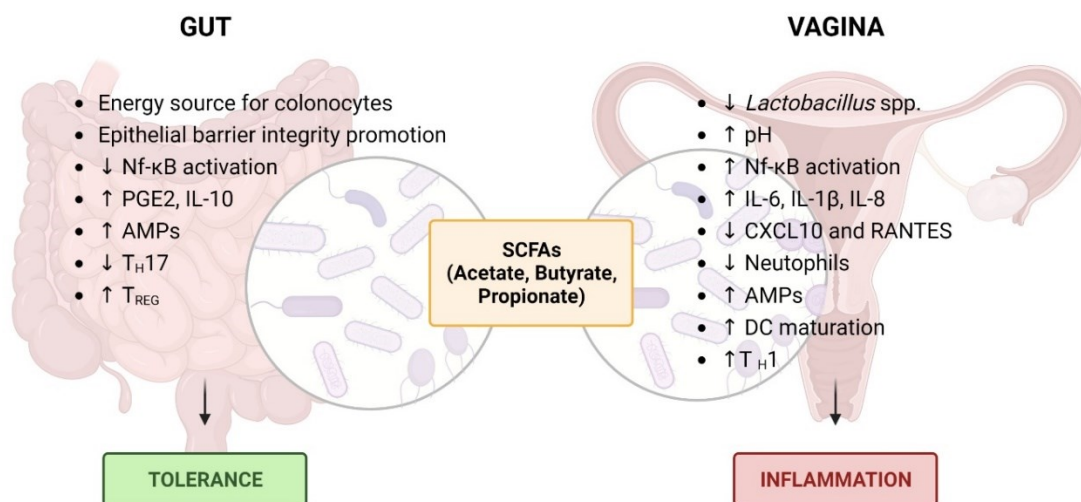


Figure 5.1. Immunomodulatory roles of short chain fatty acids (SCFAs) in the gut and vagina. Microbial-derived SCFAs (acetate, butyrate and propionate) promote homeostatic functions in the gut by promoting barrier integrity and suppressing pro-inflammatory activities, resulting in a tolerogenic environment. In the vagina, SCFAs promote dysbiosis with decrease of *Lactobacillus* spp and increase in the local pH. Furthermore, they also promote pro-inflammatory cytokine release and activation of immune cells driving inflammation such as T_H1 T-cells. PGE2,

prostaglandin E2; AMPs, antimicrobial peptides; T_H17, CD4⁺ T-cells with IL-17A-producing phenotype; T_{REG}, CD4⁺ T-cells with regulatory and anti-inflammatory phenotype; DC, dendritic cells; T_H1, CD4⁺ T-cells with pro-inflammatory phenotype. Adapted from (261).

5.1.4 Crosstalk between mucosal responses and the microbiome

It is now known that commensal bacteria and mucosal immunity are in continuous crosstalk each other, with bacteria educating the immune response and the immune cells being constantly surveillant over eventual infections. Very little is known about the crosstalk between the bacteria and the mucosal response in the FRT, but a clear picture is known for the gut (421). It has been already described above how microbial-derived SCFA show immunomodulatory effects in the gut, with a broad anti-inflammatory moiety, but even the bacteria themselves show direct immunomodulatory actions. Bacterial species localised at the mucosal interface are responsible for boosting the production of IgA which, in turn, can control pathogen overgrowth by coating them and limit their ability to penetrate the mucous layer (422). This interplay is crucial for the production of IgA which must be ready to fight any pathogen infection and also, studies performed on germ-free mice or in people with impaired IgA secretion, have shown an increased susceptibility to IBD and allergies (421). Furthermore, gut microbiota is the main driver of T_H17 maturation in the lamina propria. The interaction of microbial species with epithelial cells drives production of cytokine and other mediators such as serum amyloid A (SAA), which lead to differentiation of CD4⁺ T-cells towards the IL-17A producing cell phenotype (423). As mentioned earlier, T_H17 lymphocytes are involved in bacterial infection clearance through IL-17A secretion, thus controlling bacterial proliferation.

5.2 Hypothesis and aims

Since we identified different reproductive outcomes in the women undergoing ART in our cohort and given the importance of the microbiome in maintaining homeostasis, we wondered whether there might be a different microbiome characterising unsuccessful pregnancies. Furthermore, we reported an upregulation of IL-17A pathway and an overall increase in IL-17A cytokine in the biopsies from women who had unsuccessful pregnancy, thus we hypothesized that those women might present a different microbiome which had resulted in such pro-inflammatory activation. To assess if there are differences in the microbiome, bacterial DNA was extracted from the endometrial biopsies and subject to 16S sequencing to determine the species composing the local microbiome.

We also wondered what effect a possible dysbiosis might have on endometrial epithelial cells, thus primary and tumoral cell lines were treated with SCFA and in particular with Butyrate, which have been shown to be pathogenic in the lower FRT, but functional studies on endometrial epithelial cells are still missing.

Study Outline:

- Identification of the microbiome in the endometrium of women with infertility who undergo ART and correlation with the IL-17A levels observed in those patients;
- Identification of the effect that SCFA have on endometrial epithelial cells by treating endometrial adenocarcinoma cell line Ishikawa and hEECs;
- Analysis of the pathway activated by sodium butyrate treatment and the effect that selective inhibitor or gene silencing have on downstream gene activation;
- Analysis of the epigenetic effects that sodium butyrate has on its downstream gene activation and identification of a peak located upstream IL-17A transcription starting site;

5.3 Results

5.3.1 A different microbiome is present in the biopsies from unsuccessful pregnancy women

We first aimed to clarify which might be the endometrial microbiome and if there is a different microbial composition associated with negative reproductive outcomes. Thus, bacterial DNA was extracted from the endometrial biopsies of the women undergoing ART and the variable region of the 16S gene were sequenced to identify different bacterial species composing the microbial community in those samples. Alongside the samples, were also sent negative controls as well as a positive control consisting of a mock vaginal microbial community purchased from ATCC® MSA-1007. This vaginal genomix mix is composed by equal amounts of bacterial DNA from species often found in the vaginal microbiome and is suggested to be used as a standard to control that the sequencing retrieves the expected species with the right abundance proportion. As it can be noticed in figure 5.3, the real composition of the vaginal microbiome standard shows a variable amount of percentage of reads when subject to 16S sequencing by the supplier (**Figure 5.2A.**). It can be noticed that the bacterial composition observed in our sequencing harbours the same species as the ones expected by ATCC and that the species abundance is in between the expected values and the real composition of the sample (**Figure 5.2A.**). Once established that our sequencing is reliable in detecting the right species and in the right amounts, the counts obtained for each donor were used to build a PCA plot. **Figure 5.2B.** shows that the two groups successful (in yellow) and non-successful (grey) cluster together, meaning that the composition of the microbiome between these two groups might be quite similar as it cannot be observed a differential clustering in the PCA plot.

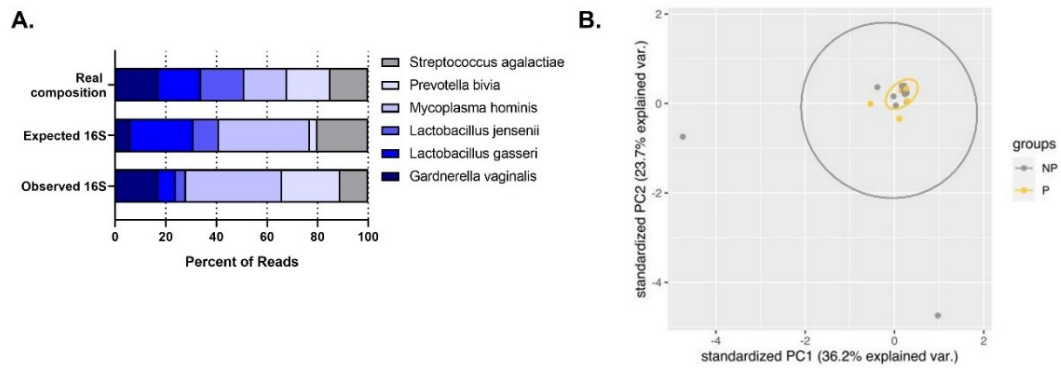


Figure 5.2. Controls for the 16S sequencing results. Bacterial DNA was extracted from the endometrial biopsies of the entire cohort ($n=30$), comprising women who had either a successful (pregnant, or P) or unsuccessful (not pregnant, or NP) ART cycle. The variable regions of 16S ribosomal RNA gene were sequenced and mapped to each corresponding bacterial species. **A.** A positive control consisting of vaginal microbiome community was also analysed, using the number of reads for each specie against the total reads in that sample to calculate the percent of reads. The composition of the sample is shown in the Real composition sample, however it has been shown by the supplier to present a different readout when performing 16S (Expected 16S), which we used as an expected readout to compare against our results (Observed 16S). **B.** The normalised counts corresponding to each donor were used to calculate the clustering between groups and generate a PCA plot to visualize difference between the successful (yellow) and unsuccessful group (grey). The values of the percent of reads for the real sample composition and the expected 16S readout were obtained from the ATCC microbiome standards brochure.

When looking at the bacterial composition at the genus level present in the microbiome of our cohort, we noticed that the bacteria displaying the higher relative abundance were *Lactobacillus* spp. in both the successful and non-successful group (Figure 5.3A.), thus explaining the overlap observed in the PCA plot. However, in the samples belonging to the non-successful group we could see an overall decreased relative abundance of *Lactobacillus* spp. and an increase in other bacterial species such as *Corynebacterium*, *Prevotella*, *Pseudomonas*, *Sphingobium* and *Atopobium*. This finding is also reflected when calculating the diversity indexes on the counts matrix, with a significantly increased diversity in the non-successful group when calculated with the Shannon method (Figure 5.3B.), as well as values close to significance with other diversity tests such as Simpson (Figure 5.3B.) and beta-diversity (Figure 5.3D.). Consequently, even the

heatmap resulting from the count matrix of the samples show a more variable composition of the microbial composition in the non-successful group samples, resulting from increased abundance of bacteria other than *Lactobacillus* (Figure 5.3C.). It can be observed quite an high variability in the bacterial composition of the non-successful group, however *Corynebacterium* and *Prevotella* showed statistically significant increase in their abundance compared to the successful group counterparts (Figure 5.3E.).

Thus we have demonstrated that in our cohort the predominant bacteria colonising the endometrium belong to the *Lactobacillus* genus and we identified a statistically significant difference in the microbiota of women who had a successful pregnancy compared to the women who failed to establish a successful pregnancy after ART. In those samples, it can be noticed an increased diversity in the bacterial species taking over the *Lactobacillus* dominance and particularly *Corynebacterium* and *Prevotella* abundance is shown to be significantly increased.

5.3.2 *Lactobacillus* spp. abundance correlates with serum level of IL-17A

Given the observed differences in the microbial composition in the endometrial biopsies and given the role that IL-17A has in controlling bacterial infections, we correlated the endometrial bacterial composition results with the circulating IL-17A protein levels measured in all the samples from the cohort. Linear regression analysis of bacterial diversity indices such as Shannon and Simpson compared with IL-17A protein did not show a statistically significant correlation, even though the regression line shows a weak positive trend (Figure 5.4A. and 5.4B). This means that IL-17A protein levels could increase with increase of bacterial diversity in the sample, even though this correlation was not significant. We then assessed whether certain bacterial genus correlated with IL-17A protein by calculating linear regression using either the relative % abundance or the normalised counts. We first performed this analysis with *Lactobacillus*, given the high abundance of this genus in the successful group. We identified a negative correlation of IL-17A protein concentration and *Lactobacillus* % abundance, with a p-value of 0.0474 (Figure 5.4C.). Conversely, the normalised counts did not show a

correlation of *Lactobacillus* with IL-17A protein levels (**Figure 5.4D.**). When performing the correlation with *Corynebacterium* and *Prevotella* we could not detect any significant correlation (**Figure 5.4E-H.**), mainly because very few samples from the non-successful biopsies had returned counts for these bacterial genus (8 samples for *Corynebacterium* and 5 samples for *Prevotella*). Thus, when calculating the % abundance of those bacterial strains many samples would show 0% and, even using the normalised counts for the few samples showing positivity for such bacteria, the number of individuals is too little for obtaining enough statistical power.

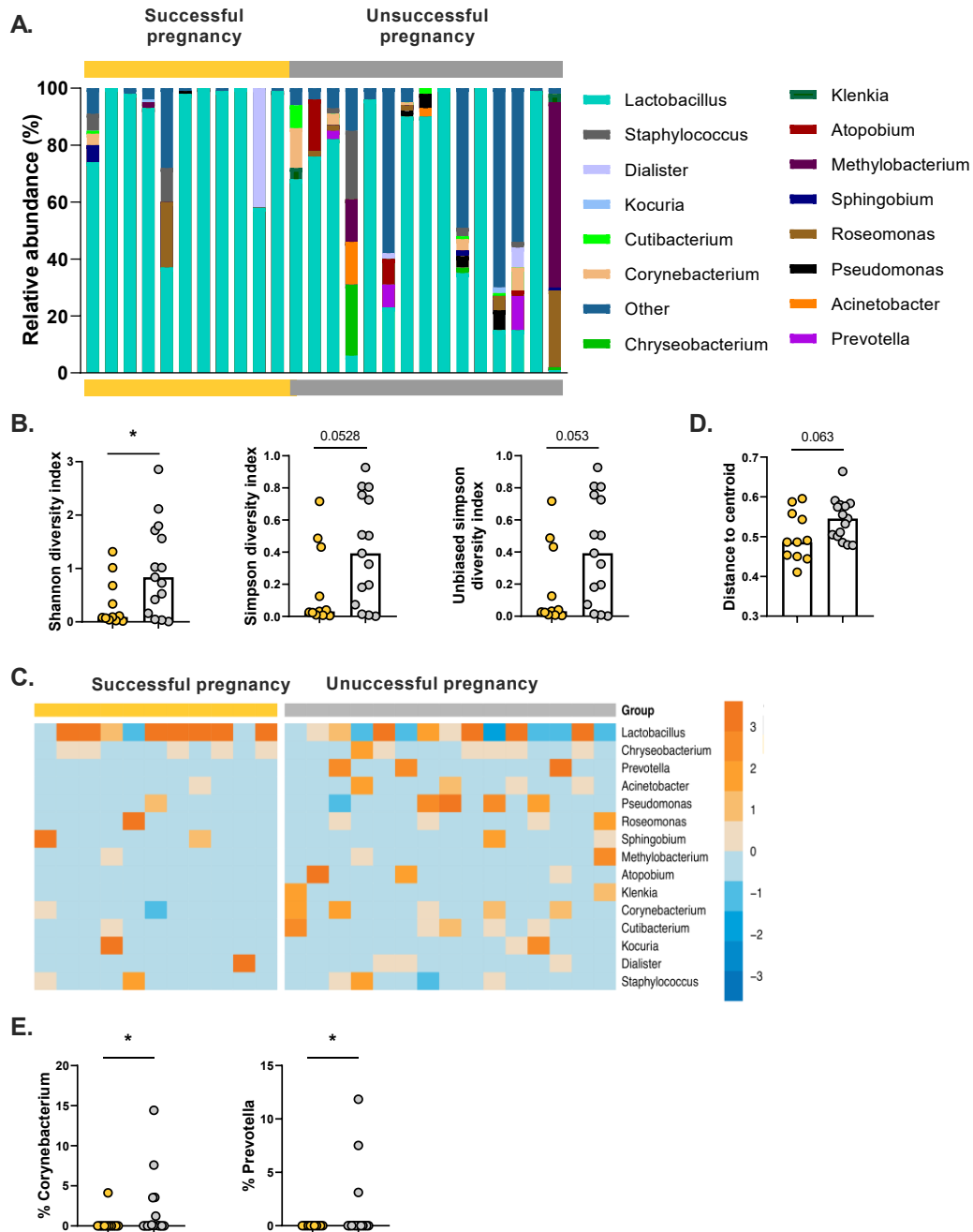


Figure 5.3. Women who failed to establish a successful pregnancy after ART show a different endometrial microbiome. The counts obtained from 16S sequencing of bacterial DNA derived from endometrial biopsies ($n=26$) of successful ($n=11$) and non-successful ($n=15$) were used to calculate the relative abundance of bacteria, expressed as percentage of abundance. The counts matrix was also used to calculate the diversity in microbiome composition and to generate the heatmap. **A.** Plot of the values of relative abundance for each bacterial genus in each sample. ART outcome is color-coded with yellow for successful (pregnant) and grey for unsuccessful (not pregnant). **B.** Shannon and Simpson diversity indices plotted by ART outcome. **C.** Heat map of

statistically different ($P < 0.05$) genus abundance between the two groups, with P values determined using a two-tailed Mann–Whitney test. **D.** Plots of the beta diversity between the two groups measured as the average steepness (z) of the species area curve in the Arrhenius model ($S = cXz$). **E.** The percentage abundance of *Corynebacterium* and *Prevotella* were plotted by pregnancy outcome. The statistical tests applied for the diversity indices were two-tailed parametric unpaired t -tests, with $*p < 0.05$; the statistical test applied for *Corynebacterium* and *Prevotella* % abundance was a non-parametric Mann-Whitney test, with $*p < 0.05$. In **C.** z -score scale is indicated, with upregulation shown in orange and downregulation shown in blue.

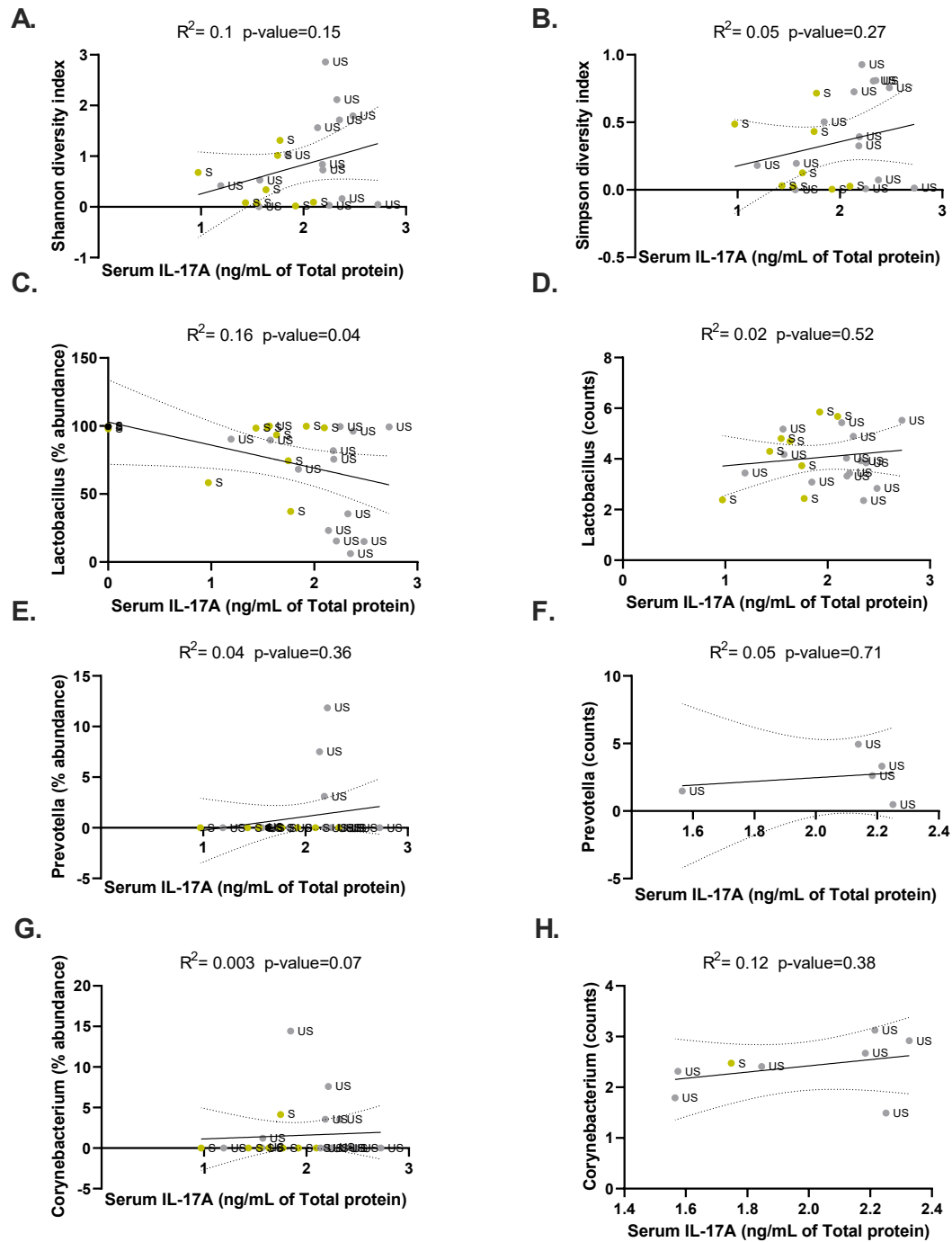


Figure 5.4. Correlation between endometrial bacterial composition and circulating IL-17A protein levels. The diversity indices, normalised counts and the relative % abundance obtained from 16S sequencing of successful (yellow points named “S” on the graphs, n=11) and non-successful (gray points named “US” on the graphs, n=15) endometrial biopsies were used for building correlations with IL-17A protein concentration in the serum. The protein concentration obtained from ELISA measures of IL-17A in the matching serum of women in the cohort was normalised based on the total protein amount detected in the sample and expressed as ng/mL

of total protein (214). **A.** Linear regression between IL-17A protein levels and the Shannon diversity index obtained for each sample. **B.** Correlation between IL-17A protein levels and the Simpson diversity index obtained for each sample. Linear regression between IL-17A protein levels and the % abundance (**C.**) or normalised counts (**D.**) of *Lactobacillus* genus in each sample. Correlation between IL-17A protein concentration and *Prevotella* % abundance (**E.**) or normalised counts (**F.**). Correlation between IL-17A protein concentration and *Corynebacterium* % abundance (**G.**) or normalised counts (**H.**). * $p < 0.05$ obtained by the linear regression analysis.

5.3.3 SCFAs induce a pro-inflammatory response in endometrial epithelial cells

A change in the microbial composition in the women who were unable to establish a successful pregnancy was identified, we then asked what impact that might have had on the local microenvironment. Decrease in *Lactobacillus* spp. in the context of BV is associated with decrease of lactate and increase in SCFAs content. Furthermore, among the species displaying an increased abundance in the non-successful cohort there are SCFA-producing bacteria, such as *Prevotella* spp. Therefore, we aimed to characterise the effect that SCFA and lactate treatment might have on endometrial epithelial cells. As it can be observed in **Figure 5.5A.**, treatment for 24h with SCFA (butyrate and acetate) or lactate did not induce cell death in Ishikawa cells, even though higher doses of butyrate and lactate induced an increase in cell death at 48h (data not shown). We then wondered whether the presence of bacterial-derived SCFAs would increase antimicrobial peptides (AMPs) expression. Butyrate was the most potent inducer of S100A family AMPs, as it can be observed a significant increase in *S100A8* and *S100A9* expression after 24h from the treatment (**Figure 5.5B.** and **C.**). *PI3/Elafin*, which belongs to the WAP family of AMPs, does not seem to be induced by butyrate but by 24h treatment with acetate or lactate (**Figure 5.5C.**).

The higher dose of butyrate (8mM) was also found to be the most potent inducer of a pro-inflammatory response with cytokines and chemokine increased release. It can be noticed indeed in **Figure 5.6** that treatment for 24h with the highest dose of butyrate, but not lactate or acetate, induce significantly increased expression *CXCL8* and *TNF α*

after 24h of treatment (**Figure 5.6A.** and **C.**). For both these immune mediators, increased protein secretion was also observed after 24h butyrate treatment through ELISA on cell supernatants (**Figure 5.6B.** and **D.**). Even if the treatment was performed in halved volume to concentrate supernatants, the levels of cytokine and chemokine observed were very low and close to the limit of detection of the assay (**Figure 5.6B.** and **D.**). *TNF α* expression was shown to be increased even at earlier timepoints, reaching statistically significant differences as early as 1h and 2h post butyrate stimulation at both 8mM and 2mM doses (**Figure 5.6E.**).

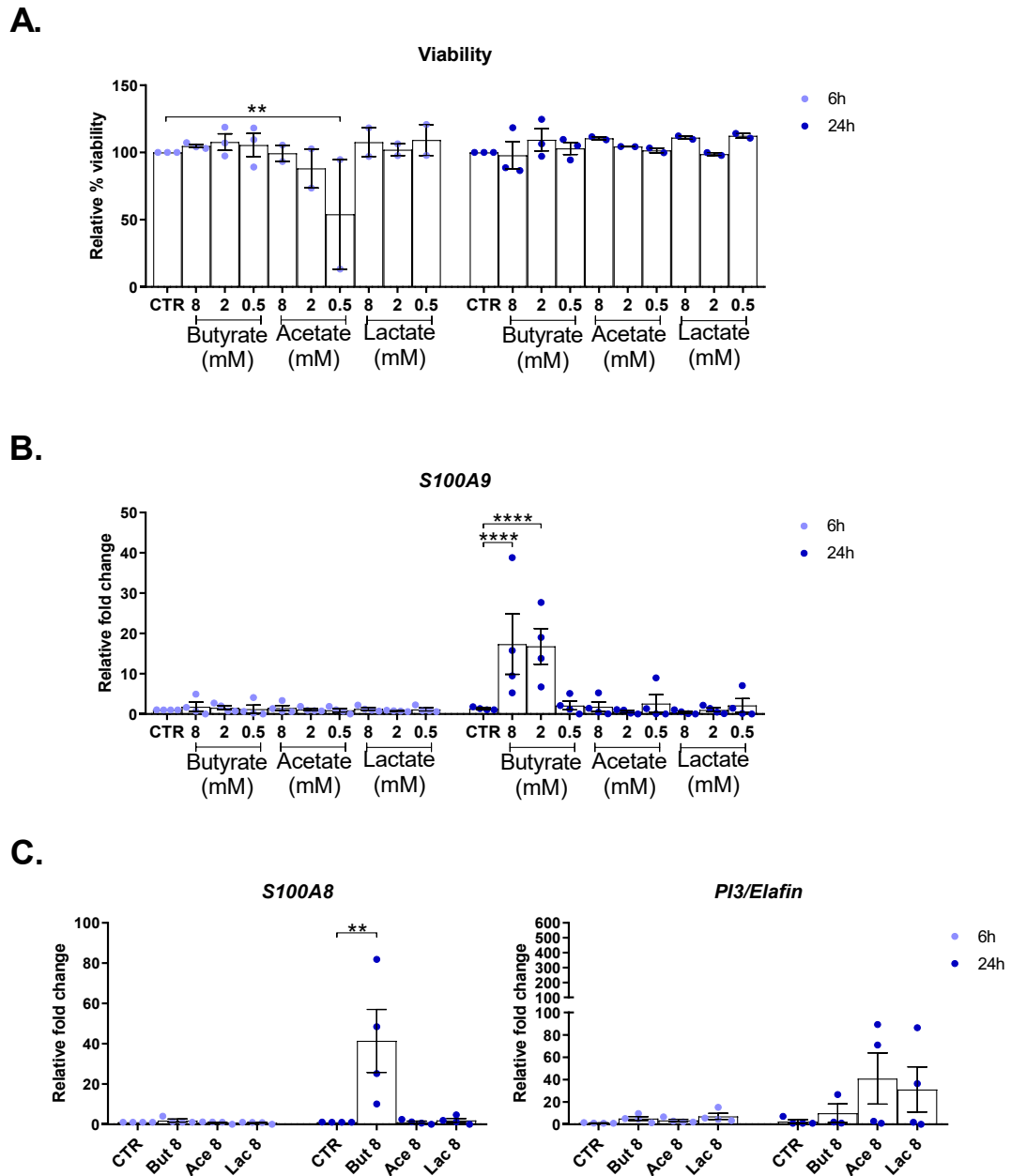


Figure 5.5 Treatment of Ishikawa cells with SCFA and lactate activates S100A AMPs. Ishikawa cells were treated with a titration of 8mM, 2mM and 0,5mM SCFAs (acetate and butyrate) and lactate for 6h and 24h. **A.** Cell viability was assessed by adding 10% vol/vol Alamar blue and reading the optical density of resazurin conversion. Calculation of cell viability was performed using the control cells as reference. **B.** RNA was extracted to assess modulation of S100A9. **C.** Ishikawa cells were treated with the highest dose (8mM) of butyrate, acetate and lactate for 6h and 24h. RNA was extracted, and qPCR performed for assessing the changes in expression of S100A8 (left) and PI3/Elafin (right). N=4. Statistical test applied: Two-way ANOVA with Dunnett correction. ** $p < 0.002$; **** $p < 0.0001$.

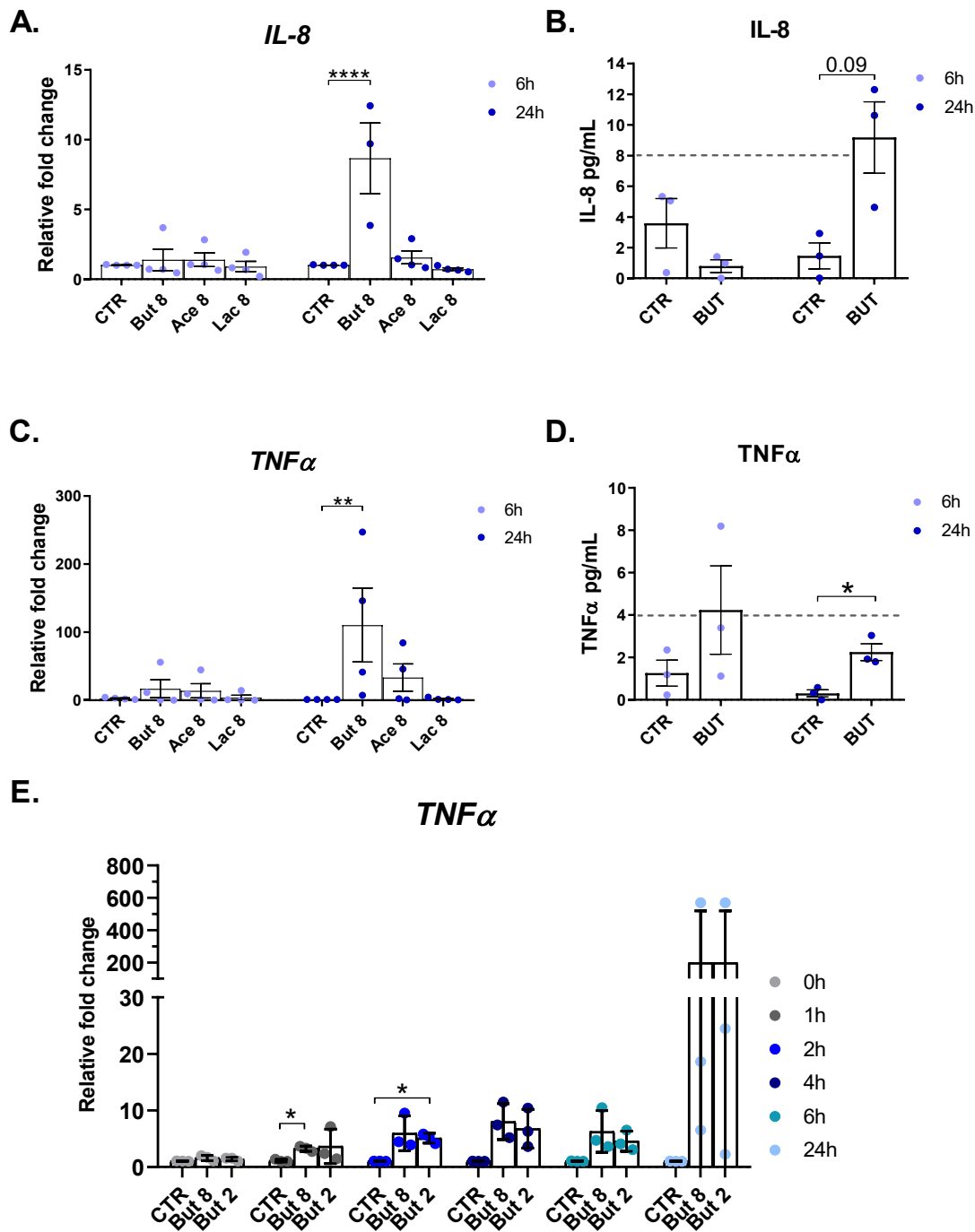


Figure 5.6. Butyrate induces a pro-inflammatory response in Ishikawa cells. Ishikawa cells were treated with the highest dose (8mM) of butyrate, acetate and lactate for 6h and 24h. RNA was extracted, and qPCR performed for assessing the changes in expression of CXCL8 (A.) and TNFα (C.). B-D. ELISA was performed on supernatants obtained from stimulation with Ishikawa cells with control media or media containing 8mM butyrate for IL-8 (B.) or TNFα (D.). The grey dotted line represents the limit of detection of the kit used to perform the ELISA. E. Ishikawa cells were treated with control media or with butyrate 2mM or 8mM for different timepoints (0h to 24h).

RNA was extracted and gene expression of TNF α was assessed. RPLP0 gene was used as housekeeping reference for qPCR analysis. $N \geq 3$. Statistical test applied: Two-way ANOVA with Dunnett correction. * $p < 0.05$; ** $p < 0.002$; **** $p < 0.0001$.

Due to its role in mediating mucosal immunity and given the observed induction of molecules also increased in mucosal responses, we wondered whether IL-17A expression could be modulated by butyrate. Treating Ishikawa cells with a butyrate timecourse using two doses, 8mM and 2mM, showed increased expression of IL-17A mRNA already at early timepoints such as 2h (Figure 5.7A.). We then performed ELISA after 24h butyrate treatment and we could observe increased IL-17A secretion in butyrate-treated cell supernatants (Figure 5.7B.). We wanted to confirm the production of IL-17A protein in Ishikawa cells using another method of detection. The treatment with butyrate was repeated, this time adding Brefeldin A 4h before the 24h timepoint in order to stop protein secretion. The treated cells were then stained for IL-17A and analysed through cytofluorimeter to see whether the percentage positivity for IL-17A staining would increase by the treatment. This approach confirmed that Ishikawa cells treated with butyrate produce IL-17A as they showed a consistent increased percentage positivity for IL-17A staining (Figure 5.7C.). Also looking at the staining plots, butyrate treated cells show a very distinct pattern if compared to the signalling observed with the sample without IL-17A staining (IL-17A FMO) or the control sample stained for IL-17A (Figure 5.7D.). This finding confirmed the suspect that also non-immune cells, such as endometrial epithelial cells, can also produce IL-17A, as mentioned in chapter 4.

To confirm whether the butyrate-induced pro-inflammatory response observed in Ishikawa cells would be activated even in a more physiological model, the treatment was repeated in human primary endometrial epithelial cells (hEEC). Again, this cell model recapitulates the same increase in expression of AMPs and CXCL8 observed in Ishikawa cells (Figure 5.8). Even though, as observed already in chapter 4, hEEC cells seem more responsive to treatments than Ishikawa cells, butyrate treatment did not induce a statistically significant increase in this model, due to the high interindividual variation. However, when treated with butyrate, it can be observed an increase in expression of AMPs and CXCL8 also with lower doses (2mM or 0.5mM) and already at

the 6h timepoint (Figure 5.8). Particularly, *S100A9* and *S100A8* expression increases already at 6h and it increases even more at 24h (Figure 5.8A-B.), whereas PI3/Elafin seems increased at 6h only, even though it can be observed a high variability among samples (Figure 5.8C). Similarly, also *CXCL8* shows increased expression at 6h and its levels decrease at the 24h timepoint (Figure 5.8D.). Regarding *IL-17A* and *IL-17F*, there seem to be a very high variability of response among sample, thus it is not possible to establish a clear signature (Figure 5.8E. and F.).

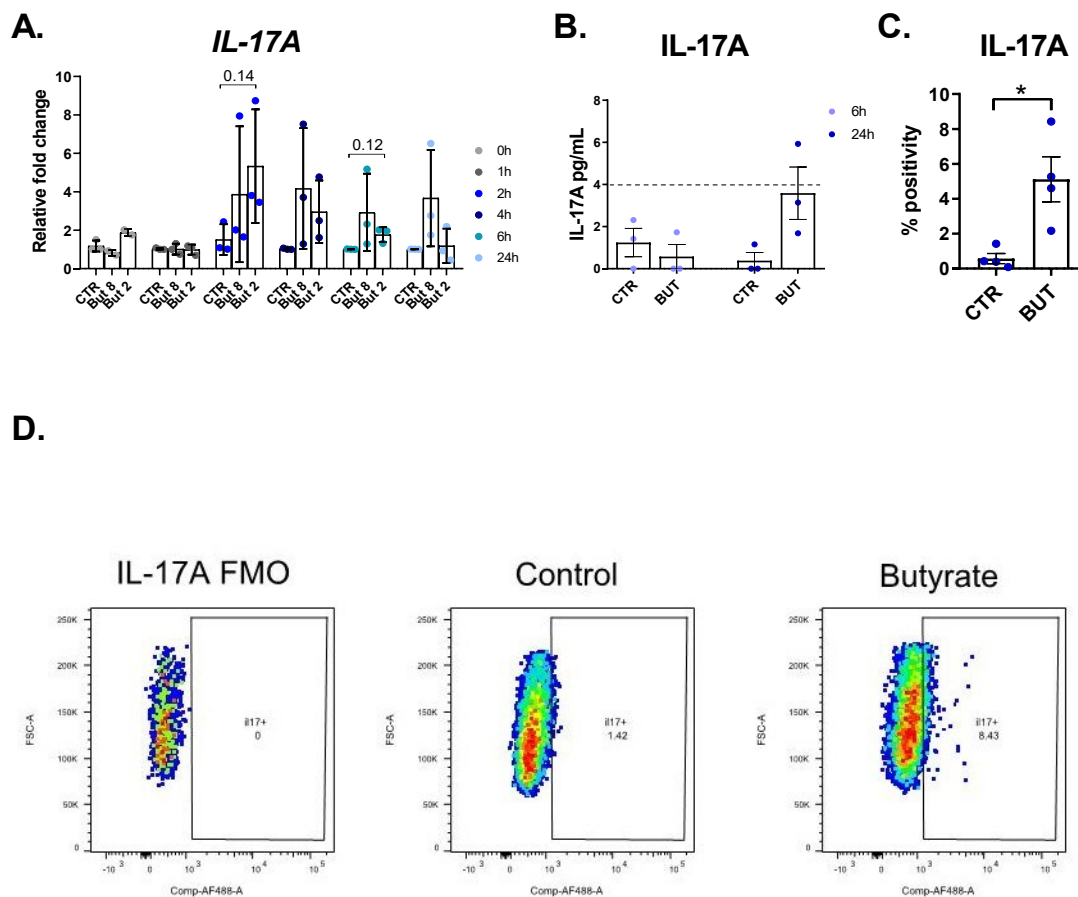


Figure 5.7. Butyrate induces IL-17A production in Ishikawa cells. **A.** Ishikawa cells were treated with control media or with 2mM or 8mM butyrate at different timepoints (0h to 24h). RNA was extracted and gene expression of *IL-17A* was assessed using *RPLP0* gene as housekeeping reference. **B.** Ishikawa cells were stimulated with control media or media containing 8mM butyrate and ELISA was performed on cell supernatants. The grey dotted line represents the limit of detection of the kit used to perform the ELISA. **C-D.** Ishikawa cells were treated for 20h with 8mM Butyrate or control media and then Brefeldin A was added for further 4h. Cells were isolated in suspension and flow cytometry immunostaining for *IL-17A* was performed to retrieve

the % positivity of cells for IL-17A positive staining. $N=3$. Statistical test applied: Two-way ANOVA with Dunnett correction. $*p<0.05$.

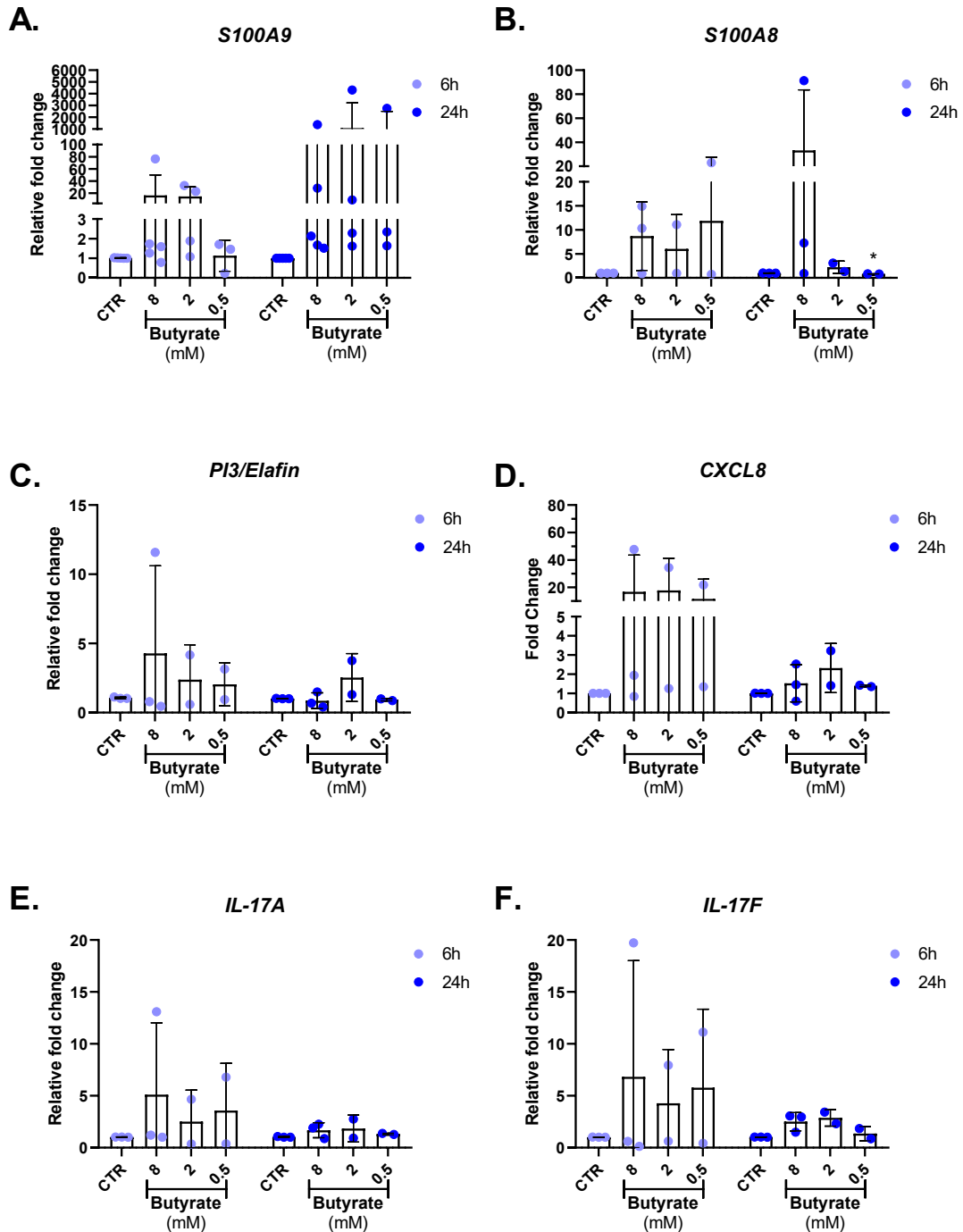


Figure 5.8. Butyrate and pro-inflammatory mucosal response in hEEC cells. hEEC cells were isolated from endometrial biopsies and treated with a titration of butyrate (8, 2 and 0.5mM) for 6h and 24h. RNA was extracted, and qPCR performed for assessing the changes in expression of AMPs (A. S100A9, B. S100A8, C. PI3/Elafin), chemokines (D. CXCL8) and cytokines (E. IL-17A, F.

IL-17F). *RPLP0* gene was used as housekeeping reference for qPCR analysis. $N \geq 3$. Statistical test applied: Mixed-effects model with Sidak correction.

5.3.4 Effect of butyrate stimulation on Nf- κ B pathway in Ishikawa cells

Once established that butyrate activates a pro-inflammatory response in both Ishikawa and hEEC cells, we then wondered which pathway might contribute to this phenomenon. Using the cell model of Ishikawa cells, we observed genes expression at different timepoints. For instance, *TNF α* and *IL-17A* expression is increased at early timepoints, whereas *S100A9* and *CXCL8* seem to be significantly increased only after 24h from the stimulation.

To discriminate which pathway might be activated by butyrate, cell lysates obtained by a time-course treatment were separated through SDS-page and then probed for phospho-p65. Given the observation of increased expression of various cytokines and chemokines upon butyrate treatment, the phosphorylation of p65, which is one of the subunits forming Nf- κ B transcription factor, was used as a readout for Nf- κ B activation. Phosphorylation of p65 can be observed some of the biological replicates for early timepoints, from 0h to 4h for the 8mM butyrate dose (**Figure 5.9A.** and **5.9B.**) and from 0h to 2h for the 2mM dose, however this approach did not led to consistent and conclusive results between the biological replicates (**Figure 5.9C.** and **5.9D.**).

To further assess the role of Nf- κ B in the induction of the molecules observed to be increased upon butyrate stimulation, Ishikawa cells were pre-treated, for 2h with BAY-11-7082, which is a known irreversible inhibitor of I κ B α phosphorylation, which is crucial for Nf- κ B activation. The treatment with 10 μ M BAY-11-7082 alone seemed to induce some stress in Ishikawa cells, as it can be observed a slight increase in *S100A9*, *TNF α* , *CXCL8* and *IL-17A*, especially in the early timepoint (**Figure 5.9E-H.**). Furthermore, treatment with 2h pre incubation of BAY-11-7082 followed by 6h butyrate treatment, increases the expression of all the markers studied, reaching higher levels than the matching cells treated with butyrate only (**Figure 5.9E-H.**). However, in the longer timepoint, corresponding to pre-incubation with BAY-11-7082 followed by 24h butyrate treatment, it can be noticed a slight decrease in the expression levels observed for

S100A9 (Figure 5.9E.), *IL-17A* (Figure 5.9H.), but not for *TNF α* (Figure 5.9F.) or *CXCL8* (Figure 5.9G.) if compared to those observed in the cells treated with butyrate only.

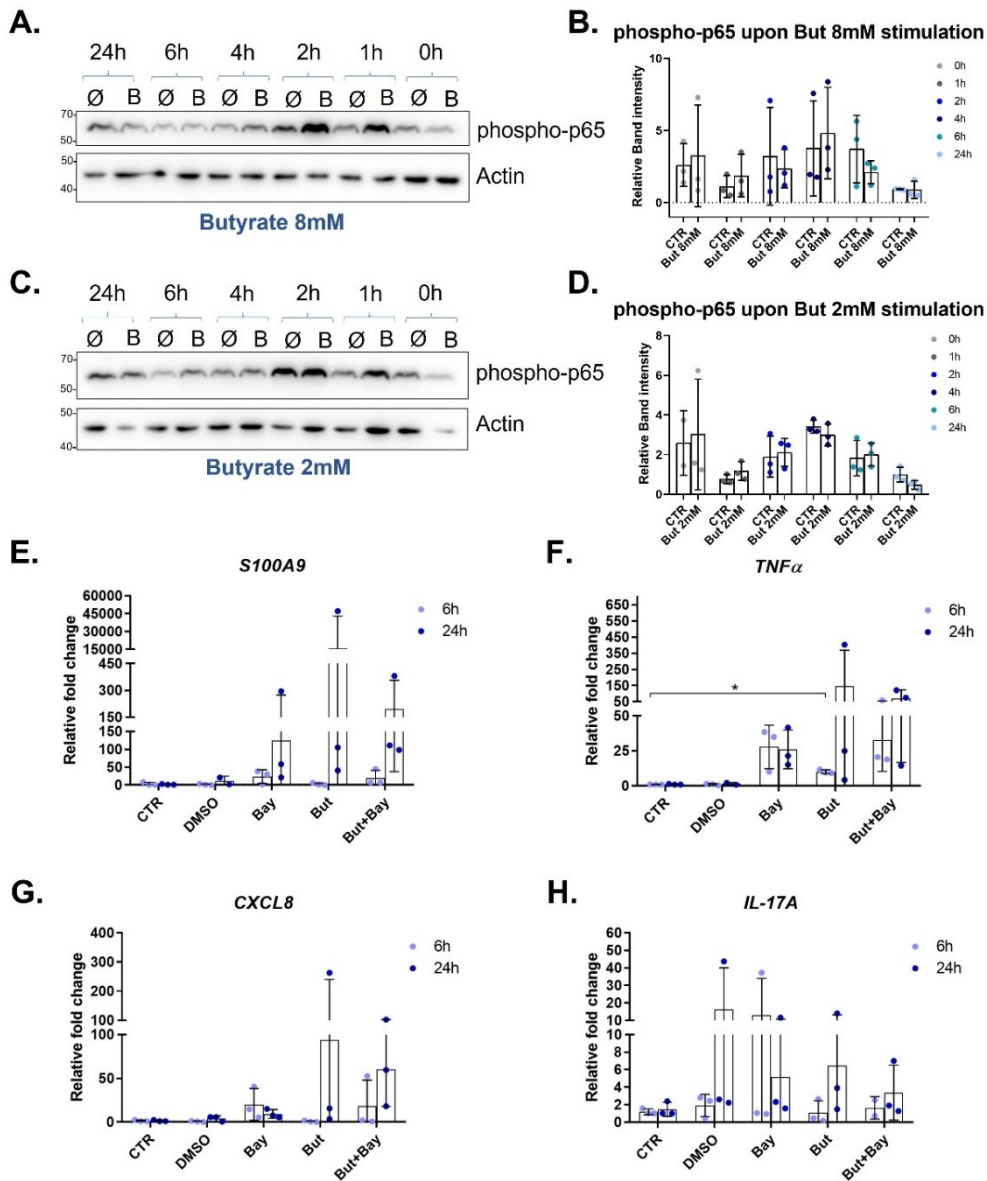


Figure 5.9. Influence of butyrate on Nf- κ B activation and inhibition of Nf- κ B pathway. A-D. Ishikawa cells were treated with 2mM and 8mM butyrate for various timepoints (ranging from 0h to 24h). Cell lysates were collected and separated through SDS-page and probed with specific antibody for phosphorylated p65. Relative band intensities were calculated in reference to the intensity of the housekeeping actin signal. Phosphorylation of p65 was assessed for 8mM (A. and B.) and 2mM (C. and D.) butyrate treatment. E.-H. Ishikawa cells were pre-incubated for 2h with 10 μ M BAY-11-7082, followed by a further incubation with butyrate 8mM for 6h and 24h. Cells were also treated with matching volumes of DMSO as a vehicle control, since BAY-11-7082 has

been resuspended in DMSO. RNA was extracted and qPCR were performed using RPLP0 as housekeeping gene reference. Expression levels of S100A9 (E.), TNF α (F.), CXCL8 (G.) and IL-17A (H.) were assessed. N=3. Statistical test applied: Two-way ANOVA with Tukey correction. * $p < 0.05$.

5.3.5 Assessment of HIF1 α pathway activation during butyrate stimulation

Another pathway whose activation was explored after butyrate treatment was HIF1 α . It has been already mentioned a link between butyrate and HIF1 α induction in the gut homeostasis (396, 402), but little is known in the FRT. To observe at what timepoint HIF1 α induction could be observed, Ishikawa were treated at different timepoints with two butyrate concentrations 8mM and 2mM. Cell lysates were probed by western blotting for HIF1 α stabilisation. Once again, this approach did not lead to conclusive results, as in certain replicates only it could be observed HIF1 α stabilisation at early timepoints such as 0h and 1h for both the doses (Figure 5.10A-D.).

To test whether HIF1 α was involved in the signalling pathways activated by butyrate, we asked whether its inhibition would modulate the expression of genes induced by butyrate treatment. Acriflavine is a compound known to inhibit HIF1 α dimerization and transcriptional activity. Ishikawa cells were then pre-incubated with 2h with acriflavine and then butyrate was added for further 6h or 24h treatment. Contrarily to BAY-11-7082, acriflavine treatment alone had very little effect on Ishikawa cells at both 6h and 24h (Figure 5.10E-I.). To control for HIF1 α transcriptional activation, the expression of HMOX1 was assessed. HMOX1 encodes for the protein heme oxygenase-1 (HO-1), a known transcriptional target of HIF1 α (424) and it shows a slight increased expression in cells treated with butyrate for 6h and even more at 24h, suggesting a possible activation of this pathway mediated by butyrate (Figure 5.10E.). However, the pre-treatment with acriflavine before 24h treatment with butyrate did not decrease the expression levels of HMOX1 if compared to cells treated with butyrate only (Figure 5.10E.). Acriflavine plus 24h butyrate treatment decreased the expression of S100A9 and CXCL8 (Figure 5.10F. and G., respectively). On the other hand, IL-17A and TNF α levels seemed to not be influenced by HIF1 α inhibition (Figure 5.10H. and I., respectively).

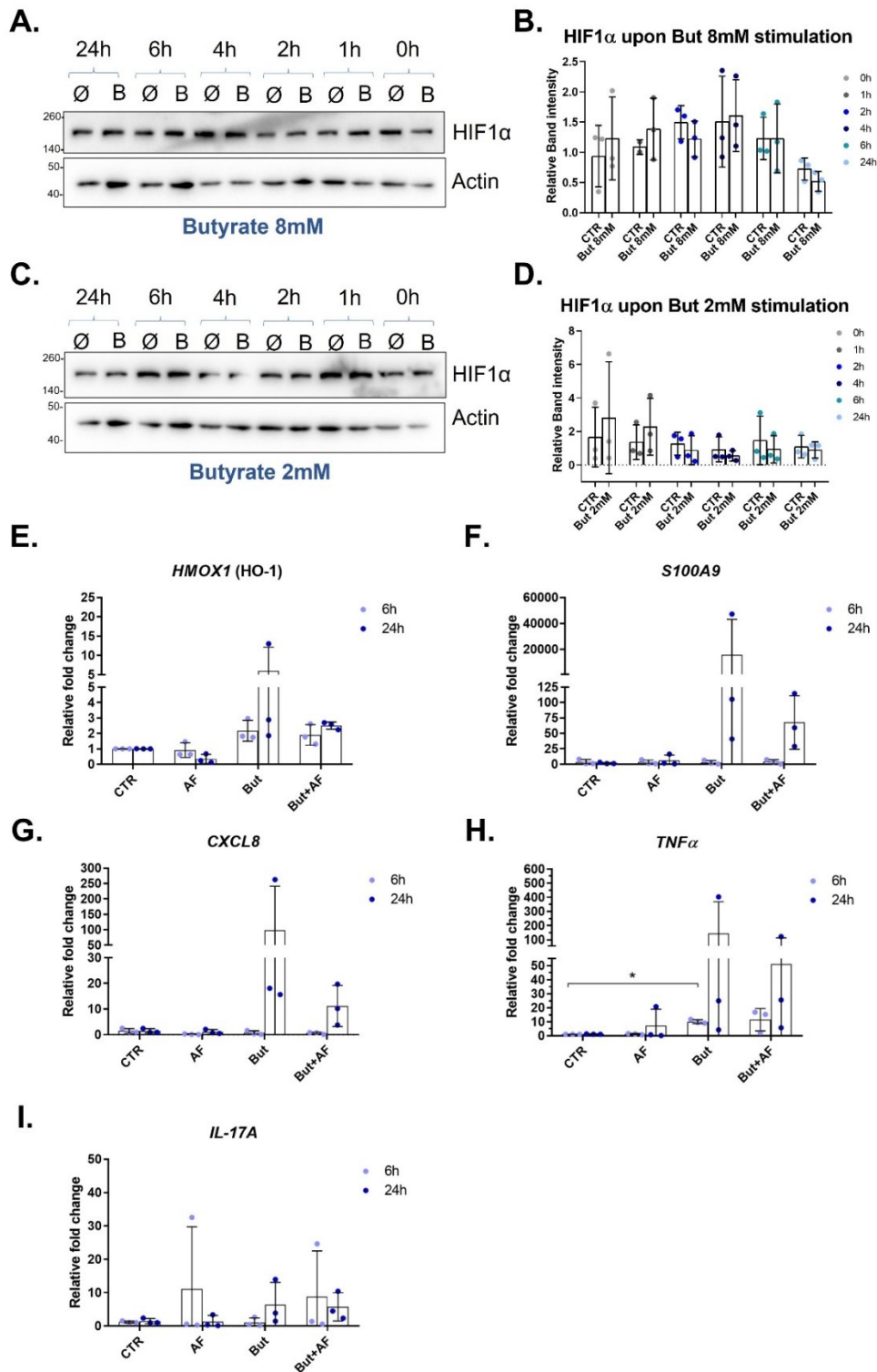


Figure 5.10. Impact of Butyrate on HIF1α pathway and S100A9 and IL-8 expression. A-D. Ishikawa cells were treated with 2mM (C. and D.) and 8mM (A. and B.) butyrate for various timepoints (ranging from 0h to 24h). Cell lysates were collected and separated through SDS-page and probed with specific antibody for stabilised HIF1α. Relative band intensities were calculated in reference to the intensity of the housekeeping actin signal. E-I. 0.3μM acriflavine was pre-

incubated in Ishikawa cells for 2h followed by 6h and 24h treatment with 8mM butyrate. RNA was extracted and the expression of genes of interest was assessed using RPLP0 as housekeeping control. Expression levels of HMOX1 (E.), S100A9 (F.), CXCL8 (G.), TNF α (H.) and IL-17A (I.) were assessed. N=3. Statistical test applied: Two-way ANOVA with Tukey correction. * p <0.05.

5.3.6 Assessment of epigenetic control induced by butyrate in endometrial epithelial cells

It has been already mentioned that butyrate has recently been shown to modify histones leading to activation of gene transcription (412). We therefore wondered whether some of the genes whose expression is increased by butyrate treatment would be regulated epigenetically. To do so the ChIP-seq dataset GSE77277 (329) was used to analyse possible butyrylation sites associated with lysine residues located nearby the transcription starting site (TSS) of the genes under investigation. This dataset comprises butyrylation of histone 4 on lysine 5 (H4K4Bu) and lysine 8 (H4K8Bu) obtained from a study carried out in mice round spermatides. The analysis confirmed a butyrylation peak of 3000pb located approximately 15kb from *il-17a* TSS (Figure 5.11.), but no peaks could be identified for the other genes of interest such as *S100A9*, *S100A8* or *TNF α* . Mice lack the expression of *CXCL8*, thus the butyrylation of the gene surrounding this gene was not possible.

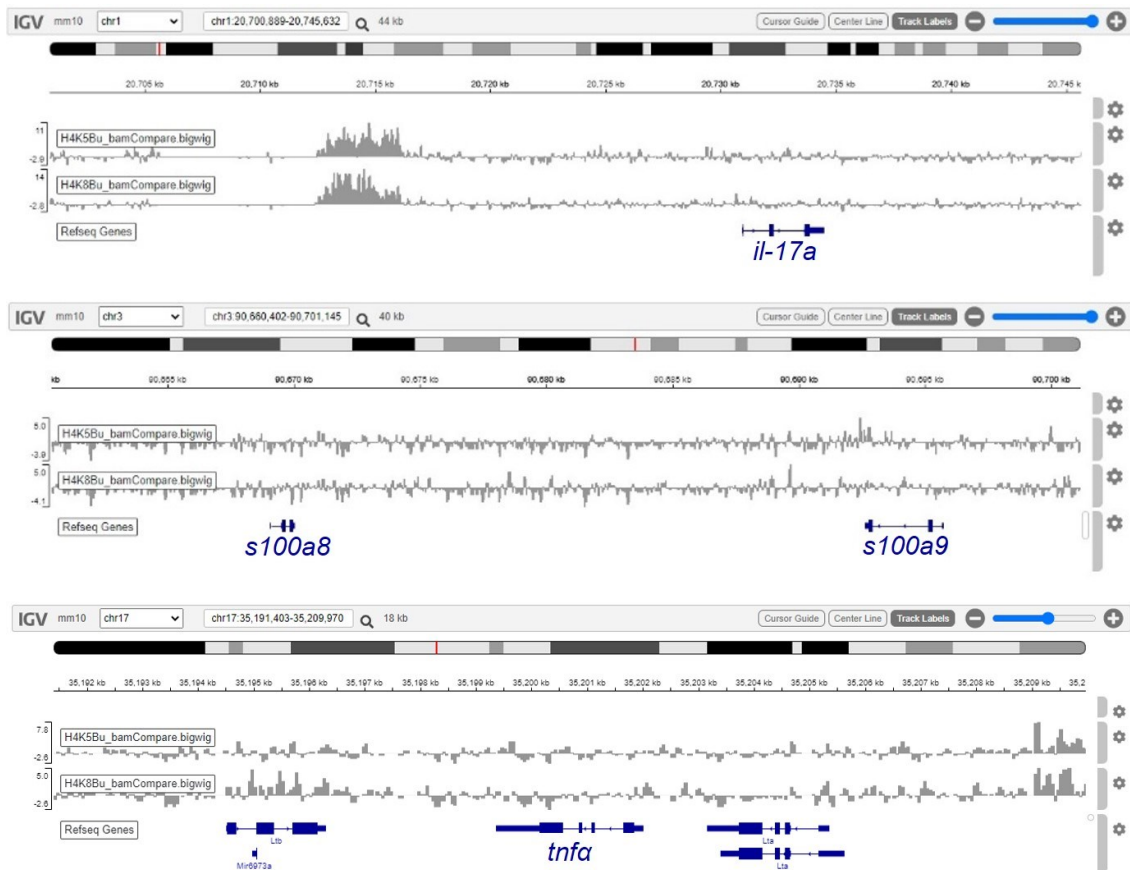


Figure 5.11. A region 15kb upstream *IL-17A* TSS is butyrylated in mouse round spermatids. Analysis of a publicly available ChIP-seq dataset (GSE77277) was performed to identify peaks located upstream TSS of genes induced by butyrate treatment. A peak was identified upstream of the *il-17a* TSS (upper panel) but not for other genes such as *s100a9* or *s100a8* (central panel) or *tnfa* (bottom panel).

IL-17A gene is located in a syntenic block conserved between human and mouse chromosome (Figure 5.12A.), meaning in both these species the same chromosome region shows a similar organisation and location of genes and regulatory elements. Therefore, we isolated the sequence corresponding to the butyrylation peak upstream *IL-17A* identified in the mouse model and we aligned it with the portion of human chromosome 6 containing *IL-17A* gene to identify which portion was conserved by chain-block alignment. This alignment retrieved two conserved regions of the mouse peak in the human genome, which we named “peak A” and “peak B” and where we investigated butyrylation by performing ChIP after butyrate treatment. We designed primer sets in order to recognise different regions of both the peaks identified (Figure

5.12B.), with which we performed qPCR of the butyrylated DNA regions after immunoprecipitation with a specific antibody against butyryl-lysine. Primers for GAPDH and MAPKAPK5 promoter region were used as positive controls of butyrylation (329), and they showed a consistent increase of fold enrichment over the use of non-specific isotype IgG antibody in the cells treated with butyrate (Figure 5.12C.). A region in chromosome 12 known to not be butyrylated (329) was used as a negative control and indeed it shows no difference between control cells or butyrate treated cells in the fold enrichment. Regarding the region upstream *IL-17A*, a big variation was observed in the biological replicates of the experiment and all the primer sets showed the same fold enrichment as the negative control region in butyrate treated cells (Figure 5.12C.). These results suggest that butyrylation of this region cannot be confirmed with the primer set chosen for the analysis.

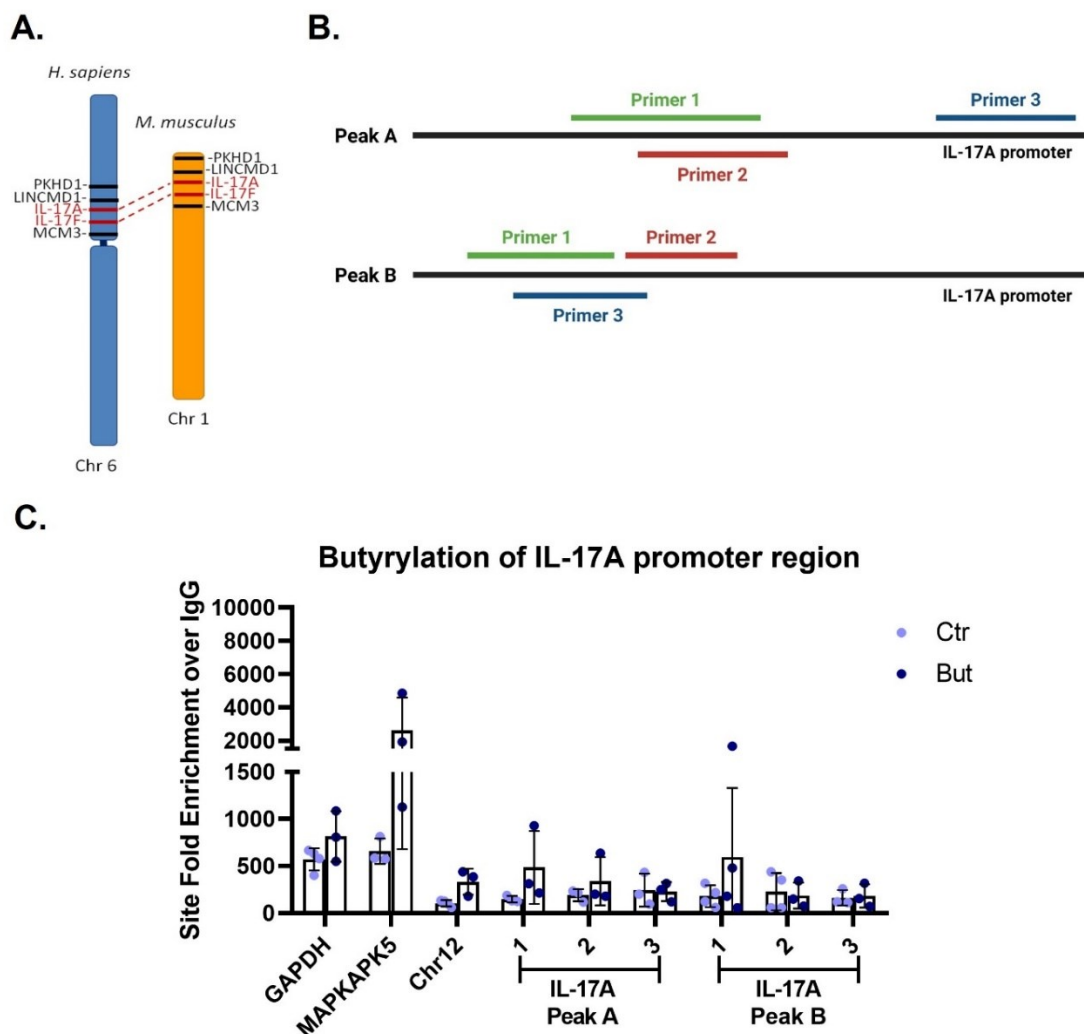


Figure 5.12. ChIP performed on Ishikawa cells cannot clarify the butyrylation site 15kb upstream IL-17A TSS. **A.** The chromosome surrounding genes of IL-17A in human and mouse were compared to identify similarities in the region, confirming synteny and obtaining the human region corresponding to the mouse butyrylation peak. **B.** In the human region corresponding to the mouse peak upstream IL-17A, can be identified two highly similar regions, which we named “peak A” and “peak B” and we designed primers to bind in different sites peak. **C.** Ishikawa cells were treated for 6h with control media or with 8mM butyrate. ChIP was performed using a specific butyryl-lysine antibody or an isotype IgG antibody. qPCR was performed on the immunoprecipitated DNA using an input DNA (not subjected to IP) to normalise the readouts and then the fold enrichment over the signal obtained with isotype IgG was calculated. N=3. Statistical test applied: Two-way ANOVA with Sidak correction.

5.3.7 Butyrate does not activate S100A9 through IL-17A signalling pathway

Given the observed differential time in activation and modulation of the various molecules induced by butyrate, it is clear that multiple pathways are activated by this SCFA. In chapter 4 the signalling pathway activated by IL-17A through binding to its receptors IL-17RA and IL-17RC, led to release of AMPs such as S100A9. We saw increased S100A9 expression after 24h butyrate treatment, whereas IL-17A increase is observed at 6h. Thus, we wondered whether the expression of S100A9 would be secondary to the activation of IL-17A pathway induced by butyrate, rather than by butyrate induction directly.

To do so, transient silencing of the IL-17 receptors was performed in Ishikawa cells followed by butyrate treatment for 6h and 24h. As can be observed in [Figure 5.13A.](#) and [5.13B.](#), the cells subjected to IL-17Rs silencing with IL-17RA and IL-17RC siRNAs show similar levels of S100A9 expression of the other butyrate treated controls, such as the untransfected cells, cells transfected with lipofectamine only or cells treated with a non-specific scramble siRNA. Interestingly, in the untreated cells the silencing of IL-17Rs seems to induce an increase in S100A9 expression ([Figure 5.13A.](#) and [5.13B.](#)). When using a siRNA targeting S100A9, it can be observed a significant decrease in S100A9 expression both at baseline and after butyrate treatment. We also observed an early induction of S100A9 expression already after 6h butyrate treatment ([Figure 5.13A.](#)), however we speculate that this action might be due to an overall stress status of the

cells subjected to siRNAs or that could be due to the lipofectamine present in the media which might help delivering butyrate inside the cell.

To control that the IL-17R were silenced, their expression in the treatment was also assessed. Both the siRNAs significantly decreased the expression of both the receptors at baseline or in the presence of butyrate (**Figure 5.13C-F**). The expression of IL-17Rs is not changed by the butyrate treatment, with exception for IL-17RC, which showed a consistently decreased expression after 24h butyrate treatment (**Figure 5.13F**).

Given the observation already mentioned in Chapter 4 of a possible positive feedback induced by IL-17A signalling in increasing IL-17A expression (**Figure 4.13**), we also measured IL-17A expression after IL-17R silencing and Butyrate treatment. We observed that the knock-down (KD) itself induced increased expression of IL-17A already in the untreated cells, in some cases with even higher level than the ones induced by Butyrate treatment (**Figure 5.13G-H**). Silencing of IL-17Rs did not change IL-17A expression levels, thus this suggests that it might not be in place a positive IL-17A feedback upon butyrate treatment.

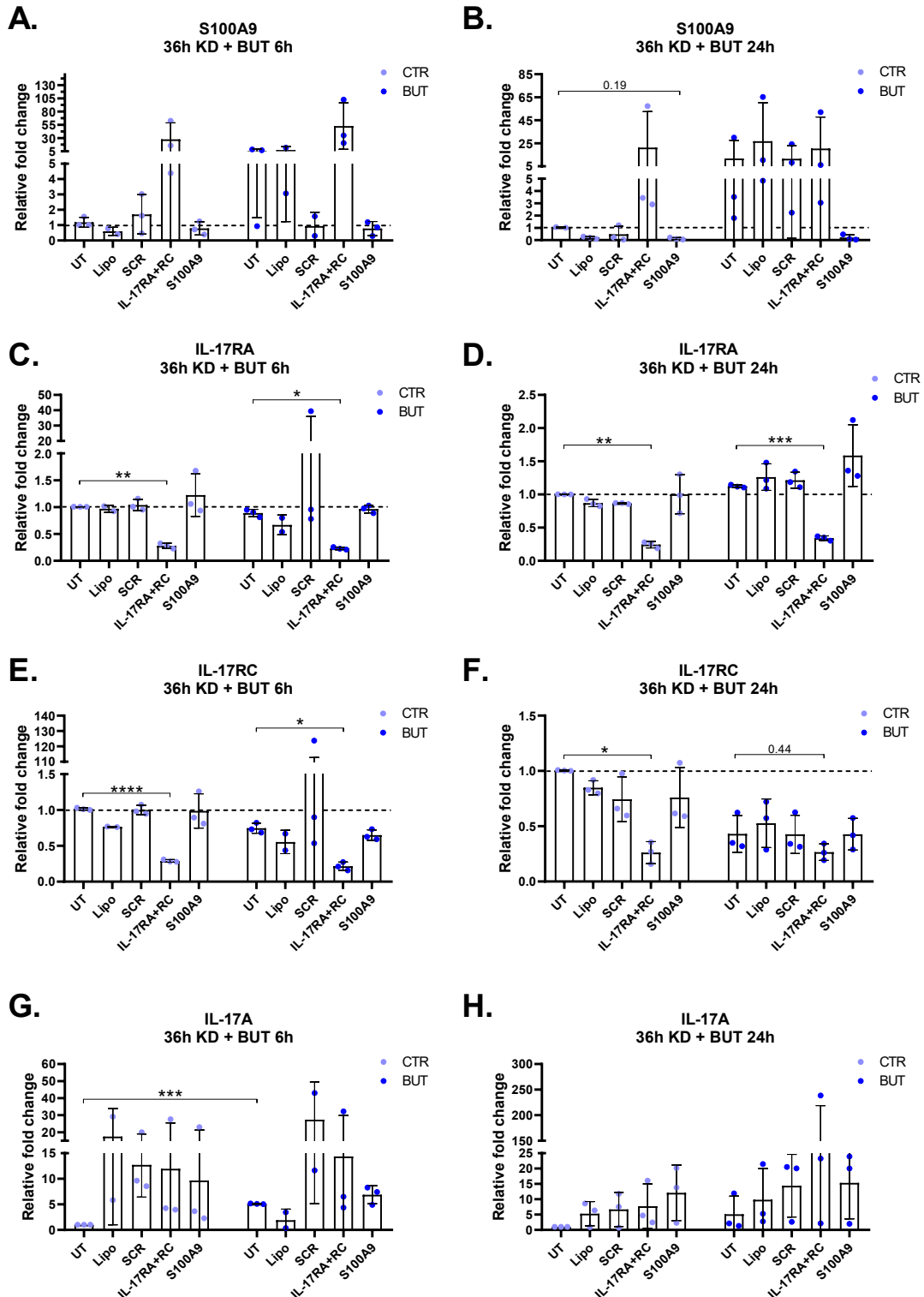


Figure 5.13. Silencing of IL-17 receptors does not prevent butyrate-induced increase in S100A9 expression . Ishikawa cells were seeded and then transfected with 20nM scramble siRNA or 20nM siRNAs targeting IL-17RA, IL-17RC and S100A9. The siRNAs were incubated for 36h, after which butyrate was added to the cells for further 6h and 24h. RNA was extracted and expression

of S100A9 (A-B.), IL-17RA (C-D.), IL-17RC (E-F.), and IL-17A (G-H.) was assessed for both timepoints (6h on the left and 24h on the right). Housekeeping control used for qPCR normalisation was RPLP0. UT: untransfected cells; Lipo: cells transfected with lipofectamine only; SCR: cells transfected with scramble siRNA; N=3. Statistical test applied: Two-way ANOVA with Tukey correction. * $p < 0.05$; ** $p < 0.002$; *** $p < 0.0002$.

5.4 Discussion

We identified a different microbiome in women undergoing ART who were unable to sustain a successful pregnancy when compared with women who become pregnant (Figure 5.3). In our study, women with a successful pregnancy outcome show a *Lactobacillus* dominated microbiome (Figure 5.3A.), which has also been suggested to be the normal endometrial microbiota in some studies (254-256). Some other studies, who had performed the sampling during caesarean sections, where absolute sterility is warranted, reported lack of an identifiable microbiome in the maternal side of the placenta (262, 263). The sampling performed by our study, and by many studies reporting a microbiome in the endometrium, have been carried out on cohorts of women undergoing for gynaecological investigation through laparoscopy or by vaginal route. In these instances, although attention was put in place to avoid vaginal contamination, it cannot be excluded that the microbiome observed in the endometrial samples could derive from a vaginal contamination. In our study the endometrial biopsy was obtained by transvaginal pipelle thus, performing a matched vaginal sampling could have highlighted whether the same species and composition could be identified, therefore confirming if the microbiome observed in the endometrium derived from a contamination during sampling.

Another aspect that needs to be considered is whether the presence of *Lactobacillus* spp. in the endometrium is possible. In the vagina these bacteria represent almost the entire proportion of the microbiome and it is known that they produce lactic acid which contributes in lowering the pH. In the endometrium it has been reported a much higher pH if compared to the vagina (425), and in the case of bacterial vaginosis the reduction of *Lactobacillus* spp results in an increase of the pH (426). Specifically, the low pH in the vagina is required to maintain the optimal pH for growing *Lactobacillus* spp. and prevents the growth of pathogenic bacteria (273). Therefore, it is questionable whether it is reliable to consider *Lactobacillus* spp. as a normal commensal for the endometrium. Very little is known about the endometrial pH in women with unexplained infertility,

therefore adding a pH measurement during our sampling might have helped determine whether the *Lactobacillus* abundance observed was plausible.

We should also bear in mind that the control group used in our study should not be referred as an “healthy” control, since those women were undergoing ART after being diagnosed with unexplained infertility (214). Unfortunately, due to the invasive nature of sample collection in a sterile way to prevent contaminants, studies on a real healthy microbiome are still very few, thus limiting the consensus on what the endometrial microbiota could be, if present at all. It has also been suggested that the endometrial microbiota changes during the menstrual cycle under the influence of sex hormones (4, 250, 258). These changes see increase of certain species such as *Propionibacterium*, *Sphingobium* and *Pseudomonas* during the secretory phase. Our samples were obtained during the luteal phase, specifically at day 7 after luteinizing hormone surge, which coincides with the secretory phase in the endometrial cycle. A very little diversity is observed in the successful pregnancy samples, however in the non-successful samples we could identify a greater variety of bacteria (Figure 5.3B-D.), confirming the presence of *Sphingobium* and *Pseudomonas*, in agreement with the literature, as well as other species such as *Atopobium*, *Prevotella* and *Corynebacterium*. *Prevotella* and *Corynebacterium* abundance is significantly increased in the non-successful group (Figure 5.3E.), confirming that in those samples there is a different microbial composition in the endometrial biopsies.

Given that in those women the levels of serum IL-17A were also increased, we wondered whether there was a correlation with the different microbiome observed. IL-17A is indeed released in the context of bacterial infections, thus a dysbiosis such as the one observed in the non-successful group, might have driven the increase of IL-17A. Surprisingly, IL-17A protein levels did not show a significant correlation with any microbial diversity index or with the abundance of what we identified as dysbiotic species: *Prevotella* and *Corynebacterium* (Figure 5.4A-B. and 5.4E-H.). As already mentioned in the results, only a few samples on the non-successful group retrieved counts for *Prevotella* and *Corynebacterium*, thus the linear regression calculation for these species is skewed by the low amounts of samples showing any counts or a value of percentage abundance different from the zero. On the other hand, we observed a

negative correlation between IL-17A levels and *Lactobacillus* abundance in the samples (Figure 5.4C.). This confirms that when *Lactobacillus* abundance is high there is less IL-17A, whereas when the number of *Lactobacillus* decrease IL-17A levels increase, possibly in response to a dysbiosis that activated mucosal immune responses.

In the women with unsuccessful pregnancy outcome, we observed decreased abundance of *Lactobacillus* spp and increase in other bacterial populations. When this phenomenon happens in the vagina it leads to bacterial vaginosis (BV), where there is a shift from lactic acid production towards the production of SCFAs (387). We thus wondered what effect SCFAs would have on endometrial epithelial cells, given that very few studies analysed the role of these molecules in the upper FRT. Overall it seems that, similarly to what happens in the lower FRT in the context of BV (415, 416), SCFAs treatment, particularly butyrate, on endometrial epithelial cells triggered a pro-inflammatory response. It is still not defined yet the concentration of butyrate in the endometrium, however some studies have suggested that in mucosal sites this molecule can reach up to 20mM concentration (261, 420). In our experiments we used 8mM and 2mM doses, which was already enough to elicit a response in our cell models. Butyrate was the most potent inducer of cytokines (IL-17A, IL-6, TNF α), chemokines (CXCL8) and AMPs (S100A8, S100A9, PI3/Elafin), in both Ishikawa cells and hEEC cells (Figure 5.5, 5.6, 5.7 and 5.8). Alongside the increase in gene expression, butyrate treatment resulted also in increased protein production and secretion in Ishikawa cells (Figure 5.6 and 5.7.). Most importantly, for the first time we were able to show increased production of IL-17A after 24h butyrate treatment in a non-immune cell line. We obtained this result by using two different approaches, thus confirming that endometrial epithelial cells are able to produce IL-17A.

We also noticed that the expression of these genes happened at different timepoints, with some being expressed at early timepoints (IL-17A and TNF α , Figure 5.6, 5.7), while other genes are upregulated after 24h from the treatment (Figure 5.5, 5.6). Again, we could observe some differences in the primary cells, where certain genes are upregulated already at the 6h timepoint such as S100A9, S100A8, IL-8 and PI3/Elafin (Figure 5.8), confirming again that primary cells might be more responsive to treatments. The observation of this different timing led us hypothesize that butyrate

might induce different pathways. Butyrate in the gut is shown to inhibit Nf- κ B activation (404), however we observed increased expression and secretion of cytokines and chemokines. Also, once again in the gut, butyrate was shown to promote epithelial integrity and prevent cell stresses by activating HIF1 α (396). We then wondered whether the stress induced by butyrate in our cell models might lead to activation of Nf- κ B and HIF1 α pathways. When using the western blot approach to probe for the active form of these two transcription factors, we could not observe a consistent Nf- κ B and HIF1 α activation in Ishikawa cells (**Figure 5.9A-D.** and **Figure 5.10A-D.**). Therefore, we assessed whether inhibition of Nf- κ B before adding butyrate to the cells would clarify the involvement of the transcription factor in the signalling activated. Two hours pre-treatment of Ishikawa cells with an Nf- κ B inhibitor resulted in a less potent gene induction for *IL-17A* and *S100A9*, but not for TNF α or CXCL8 expression (**Figure 5.9E-H.**). This might suggest that butyrate possess context-specific actions, with inhibition of Nf- κ B in the gut, but activation of this pathway in the FRT.

We assessed the involvement of HIF1 α in butyrate-induced gene activation by pre-treating the cells with 2h with an inhibitor before adding butyrate (**Figure 5.10**). We observed a slight increase in the expression of a known target gene for HIF1 α , *HMOX-1*, after 24h butyrate stimulation, but using this selective inhibitor of HIF1 α aggregation, acriflavine, we could not observe a significant decrease in the expression of any of the targets of interest, including *HMOX-1* (**Figure 5.10E-I.**).

Butyrate is also involved in mediating immune signalling by showing epigenetic functions. It was long known to be an HDAC inhibitor and recently have been discovered butyrylation and beta-hydroxybutyrylation modification of histones (412). A study performed in mice showed how butyrate can compete for the same sites with acetylation, so when they are butyrylated the transcription is active, whereas acetylation leads to transcription inactivation (329). We then hypothesized that the activation of some of the genes induced by butyrate might be mediated through butyrylation of sites located near their promoter region. The above-mentioned study provided a ChIP-Seq database which we analysed to identify butyrylation peaks close to the promoters of our genes of interest. We were able to identify a peak located approximately 15Kb from the *IL-17A* transcription starting site in the ChIP-seq database,

which we aimed to confirm with CHIP in Ishikawa treated with butyrate for 6h (**Figure 5.11 and 5.12C.**). The CHIP performed in Ishikawa confirmed that the positive controls were amplified with a greater fold enrichment, meaning that the immunoprecipitation of the butyrylated sites was successful. However, using primer sets designed for the region identified upstream IL-17A transcription starting site failed to show a greater fold enrichment in butyrate-treated cells, meaning that possibly those sites are not subject to butyrylation or that maybe the butyrylation in the human genes might happen in a different location, despite the high conservation of that genomic block between human and mouse. Furthermore, the location of this binding site in the mouse is far from the promoter region or the transcription starting site of IL-17A, therefore it could act as a regulatory element such as an enhancer. Recent studies have started uncovering the epigenetic regulation of IL-17A and they highlighted some regulatory elements responsible for STAT3 and STAT5 binding also at distal sites from IL-17A promoter (427). Most of the gene observed increased upon butyrate stimulation are also activated during IL-17A signalling pathway activation (see chapter 4). We then wondered whether blocking IL-17A receptors by using siRNAs would prevent the expression of S100A9, which is a known target of IL-17A activation. This approach however confirmed that S100A9 increased expression is independent from IL-17 signalling (**Figure 5.13A-B.**). We also noticed increased expression of IL-17A in cells treated with only lipofectamine or lipofectamine and siRNAs, suggesting that endometrial epithelial cells might produce this cytokine when stressed in general.

Chapter 6: Defining the impact of IL-17A and butyrate during the window of implantation

6.1 Introduction

6.1.1 Changes induced in the endometrium during the window of implantation

All the changes induced during the menstrual cycle take place to allow fertilisation and pregnancy establishment. For a successful pregnancy two things are required: a viable embryo and a receptive endometrium. Indeed, only if the embryo finds a suitable environment it can implant and start developing. However, the endometrium is receptive only for a short period of time, which is called window of receptivity or window of implantation (WOI) (428). This stage often occurs between day 19 and 21 of the menstrual cycle and is regulated by progesterone in humans (359, 428). When embryo reaches the receptive endometrium, it is at the blastocyst stage. It first gets oriented correctly towards the epithelium (apposition) and then it interacts with the epithelial cells which show pinopods and cell adhesion molecules (adhesion) (429). Then, the blastocyst penetrates through the epithelial layer and embeds completely with the uterine stroma (invasion) (430). This process requires a synchronised crosstalk between the endometrial epithelial and stromal cells and the blastocyst, which show peculiar characteristics in order to prepare for the interaction ([Figure 6.1](#)).

6.1.1.a Epithelial cell receptivity

Epithelial cell receptivity is reached by displaying on the luminal epithelium certain molecules that allow interaction with the blastocyst. Among these molecules are **pinopods**, cellular protrusions which have been shown to be progesterone-dependent in humans and are regulated by the homeobox gene HOXA-10, which is an important player for epithelial receptivity (429). It is still uncertain the role of pinopods, however they are thought to be involved in the regulation of endometrial fluid, as well as in the

binding with the blastocyst through expression of adhesion molecules in their structure (429).

Adhesion molecules are widely expressed throughout the menstrual cycle in epithelial cells, however certain show to be expressed only during the window of implantation, which led to the hypothesis that they are needed for interacting with the embryo, such as the integrins $\alpha1\beta1$, $\alpha4\beta1$, $\alphaV\beta3$ (429). Additionally, the negative cell-cell adhesion molecule MUC1 show decreased expression in non-ciliated cells and pinopods during the window of implantation, making easier for the blastocyst and the epithelial cells to interact. Furthermore, epithelial cells show positivity for the ligands of adhesion molecules: SPP1 (Secreted Phosphoprotein 1 or Osteopontin), which is ligand for $\alphaV\beta3$ integrin (which is also expressed by the blastocyst), the ligands for the L-selectin (known to be displayed in the blastocyst) MECA-79 or HECA-452. Furthermore, progesterone has been shown to induce calcitonin, which increases epithelial cytoplasmic calcium content and leads to suppression of E-cadherin expression from the lateral contact sites, making easier for the embryo to pass through the epithelial layer (429).

Cytokines also play important roles for endometrial receptivity. This highlights how inflammation is crucial for embryo implantation (see section 1.4). Among these, LIF is shown to be increased by epithelial cells during the WOI, whereas stromal cells can secrete it but do not change expression throughout the cycle. This cytokine belongs to the IL-6 family of cytokine and promotes proliferation and cell survival in both the epithelial cells and the blastocyst (359). Also IL-6 shows to be increased during the WOI and its receptor is present on the blastocyst, however knockout models have shown that disruption of IL-6-IL-6R interaction did not impair embryo attachment (429). IL-1 cytokines are also important for the WOI. Indeed IL-1 β induces integrin $\beta3$ expression and the receptor antagonist for IL-1, IL-1RA, is downregulated during the receptivity window (429). Also IL-15 is known to be a marker for endometrial receptivity and stromal decidualisation in the window of implantation, and it seems to have a role in controlling the proliferation of uterine natural killer cells (uNK) (431).

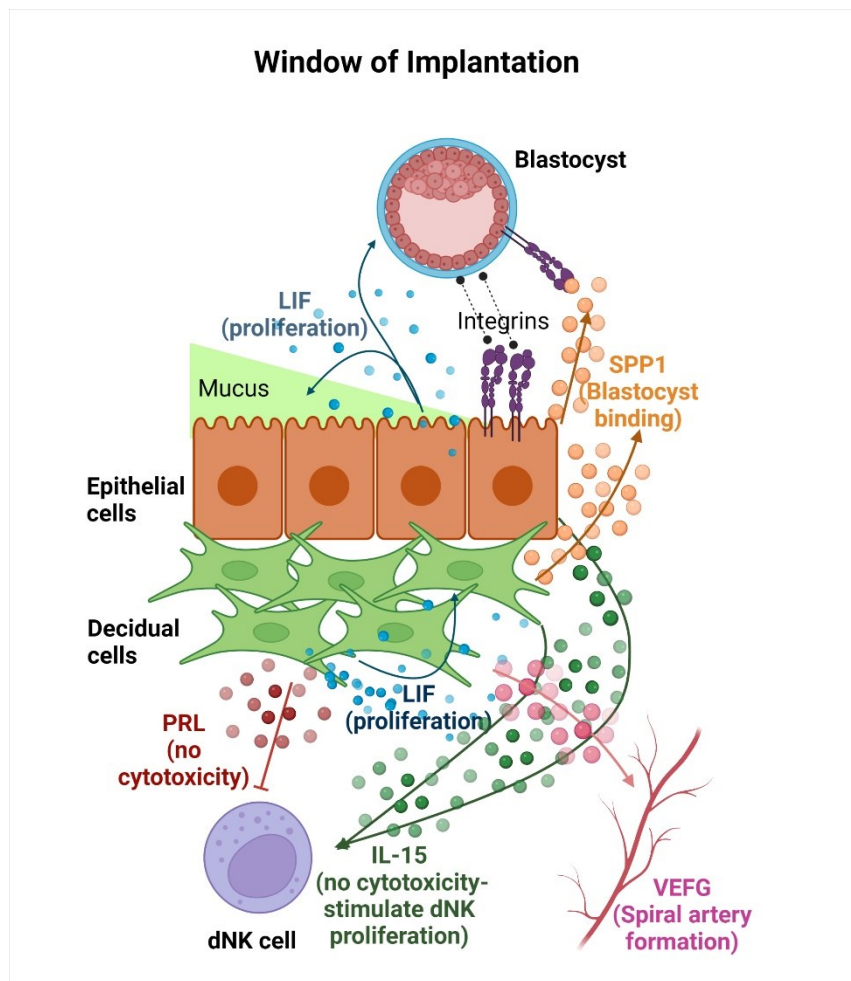


Figure 6.1: Molecules and processes associated to the window of implantation. During the uterine cycle, sex hormones stimulate endometrial epithelial and stromal cells to produce molecules in preparation for the window of implantation opening, which occurs during the luteal phase of the ovarian cycle. The endometrial epithelial cells produce less mucus and express adhesion molecules (such as integrins) which will be needed to interact with the blastocyst. Osteopontin (also called Secreted Phosphoprotein 1 or SPP1) is released by both epithelial and stromal decidual cells, enabling to bind to integrins expressed on the blastocyst surface. Leukaemia inhibitory factor (LIF) is also secreted by endometrial epithelial cells during the window of implantation to sustain proliferation of both the foetal and the epithelial cells. In the stromal cell compartment sex hormones induce decidualization, a process where stromal cells change their shape and produce molecules needed to allow implantation. Among these, cytokines, such as LIF, are secreted to stimulate autocrine proliferation. IL-15, another cytokine, is released by both decidual and epithelial cells to stimulate the proliferation of decidual NK (dNK) cells and to inhibit their cytotoxicity against the invading blastocyst. Decidual cells can further inhibit dNK cells cytotoxic activation by releasing prolactin (PRL), which can bind the

prolactin receptor located on the dNK cell membrane. Lastly, decidual cells are also able to secrete vascular endothelial growth factor (VEGF), which stimulates spiral artery formation, which is crucial for correct placentation.

6.1.1.b Stromal cell decidualisation

The stromal cell layer undergoes changes during the menstrual cycle. In particular during the luteal phase the stromal cell start a decidualization reaction which is driven *in vivo* by progesterone and Prostaglandin E₂ (PGE₂) (188). During this process, the stromal cells change their shape and display changes in the surface and secreted molecules to help embryo implantation. The decidualization starts around the blood vessels and then spreads throughout the endometrial stroma and, if pregnancy establishes, is continued throughout pregnancy (188). Given that the stromal cell compartment is enriched with immune cells, several molecules produced by decidual cells are needed to interact with those immune mediators. For example prolactin (PRL) is secreted in high quantity by decidualized stromal cells (DSC) and is required to reduce the cytotoxicity of uNK cells, which display the prolactin receptor on their cell surface (188). Another marker for decidualization is insulin growth factor binding protein-1 (IGFBP-1). The role for this molecule in implantation is still uncertain, however it is upregulated in amniotic fluid and its expression is controlled by progesterone. It was speculated that its main role is to modulate the growth induced by the oestrogen-stimulated Insulin-like Growth Factor 1 (IGF-1) (188). Decidual cells are located close to the spiral arteries, thus they also secrete Tissue Factor, a membrane-bound molecule which is able to inhibit bleeding and also possess angiogenic functions (188). Recent finding have also highlighted increased SPP1 (osteopontin) expression in decidualized stromal cells (432).

Decidual cells display **adhesion molecules**, needed to interact with the invading embryo and anchoring it. For example, laminin and fibronectin are expressed only by decidual cells and not by the underlying myometrium, allowing to direct trophoblast invasion and limit it only within the endometrium.

Decidual cells also secrete **cytokines** which are involved both in implantation as well as maintaining decidualisation. DSC can secrete LIF and IL-6, already discussed in the epithelial cell section, and also IL-11. IL-11 has been shown to mediate decidualisation using neutralisation models (188). IL-1 cytokines show an inhibitory function on decidualisation, since IL-1 β is shown to decrease PRL and IGFBP-1 if added to *in vitro* decidualisation models, however some levels of IL-1 are needed in the epithelial layer to allow correct implantation, as mentioned above. IL-15 also can be produced by decidualized stromal cells, again reinforcing their crosstalk with the immune cell by stimulating uNK cells to reduce their cytotoxicity and increase their proliferation (188). Stromal decidual cells also secrete VEGF as well as matrix-metalloproteinases, thus contributing to the extracellular matrix remodeling and blood vessel formation needed for trophoblast invasion and placentation (188).

6.1.2 In vitro models of the window of implantation

Due to the limited amount of time in which the endometrium is receptive and due to the limited success rates deriving from implantation outside the implantation window, consistent research has been carried out to study the processes leading to endometrial receptivity and stromal decidualization.

To assess endometrial receptivity, primary human endometrial epithelial cells (hEECs) as well as certain tumoral cell lines can be stimulated *in vitro* with progesterone for up to 4 days (332, 333, 372, 433). Some cell models, such as the Ishikawa cell line, have been shown to decrease the membrane display of progesterone receptor upon stimulation with progesterone, since this molecule has been shown to induce cell death in tumoral cells (434). To prevent such phenomenon, 17- β -Estradiol can be added to the stimulation, because it has been shown to maintain progesterone receptor expression on the cell membrane (332). After these stimulations, integrin expression or localisation, and other markers of endometrial receptivity, already mentioned above, can be assessed.

Similarly, primary human endometrial stromal cells (hESCs) can be treated with progesterone for up to 8 days to induce decidualisation *in vitro* (331, 432, 435).

However, *in vitro* treatment with progesterone alone does not fully induce decidualization. To allow decidualization, intracellular cAMP is shown to be critical *in vitro*, thus 8-bromo-cAMP must be added to the decidualization media (188). Decidualization markers, such as PRL and IGFBP1, can be measured to assess the effect of this stimulation.

6.2 Hypothesis and aims

Due to the observed failure of our cohort of women undergoing ART in establishing a successful pregnancy, we imagine that the implantation step is the one which failed in those women. All the women in our cohort, indeed, received an embryo transfer of good to high quality, therefore we think that the failure in the implantation step was caused by an altered maternal receptivity. We wondered whether the elevated levels of IL-17A or the different bacterial composition and, the consequent different bacterial-derived metabolome in the uterine microenvironment, might have had an impact on the window of implantation, making then impossible for the embryo being transferred to encounter an optimal ground to implant.

Study outline:

- Identify the impact that elevated IL-17A has on epithelial endometrial receptivity by using *in vitro* models of the window of implantation by treating Ishikawa cells with Progesterone and beta-Estradiol;
- Understand whether IL-17A impacts on stromal cells decidualization by performing *in vitro* decidualization models in presence or absence of IL-17A;
- Analyse the role that butyrate has during epithelial receptivity maturation by performing *in vitro* models with and without butyrate stimulation;
- Identify the effect that butyrate has on stromal cell decidualization using *in vitro* models.

6.3 Results

6.3.1 IL-17A does not impact on endometrial epithelial receptivity

We first wondered what effect IL-17A might have on endometrial epithelial cell receptivity for embryo implantation. The window of implantation (WOI) corresponds to the mid-luteal phase, where the high levels of progesterone induce in endometrial epithelial and stromal cells changes to allow embryo implantation. Ishikawa cells have been used as model of endometrial receptivity by treating with Progesterone (P4) and Oestradiol (E2) for up to four days in the presence or absence of rIL-17A. E2 is added to this model since it was shown that Ishikawa cells decrease progesterone receptors when treated with progesterone, whereas addition of oestradiol allows to keep progesterone receptors expression (332). Progesterone is also used as treatment for endometrial tumours, since it is shown to induce cell death in tumoral cells (434), therefore cell death was assessed for the treatments. The viability in cells treated with Progesterone and Oestradiol or Progesterone and Oestradiol plus IL-17A remained around 100% (**Figure 6.2A.**), thus the reagents did not show cytotoxicity in the doses and timepoints chosen. Then, the effect of the stimulation on the receptivity markers for mucin-1 (MUC1), integrin subunit α V (ITGAV) and osteopontin (SPP1) was assessed. When endometrial epithelial cells reach receptivity, during the window of implantation, they secrete less mucins and increase expression of integrins for allowing the interaction with the embryo. As expected, P4+E2 treatment results in decrease of MUC1 expression in cells treated for 1 and 2 days (**Figure 6.2B.**) and in significant increase in expression of ITGAV at day 3 and 4 (**Figure 6.2C.**). rIL-17A treatment alone did not show to modulate MUC1, whereas it showed contrasting effects on ITGAV expression by inducing a significant increase at day 3 and a decrease at day 4. The addition of IL-17A in combination with P4+E2 did not show to affect the expression of MUC1 and ITGAV. Another molecule which is shown to be expressed by endometrial epithelial cells during the window of implantation is osteopontin, a molecule that is involved in mediating embryo adhesion and implantation. P4+E2 treatment induces a significant increase in SPP1 expression after 4 days of stimulation, whereas IL-17A treatment did not change it (**Figure 6.2D.**).

Furthermore, addition of IL-17A to P4 and E2 did not show to modify the expression of SPP1, which is still significantly increased if compared to the control.

LIF and IL-15 are two other mediators often used as markers for the window of implantation. In our model, P4+E2 did not increase their expression over time and adding IL-17A to this stimulation does not seem to impact on their expression (Figure 6.2E-F.).

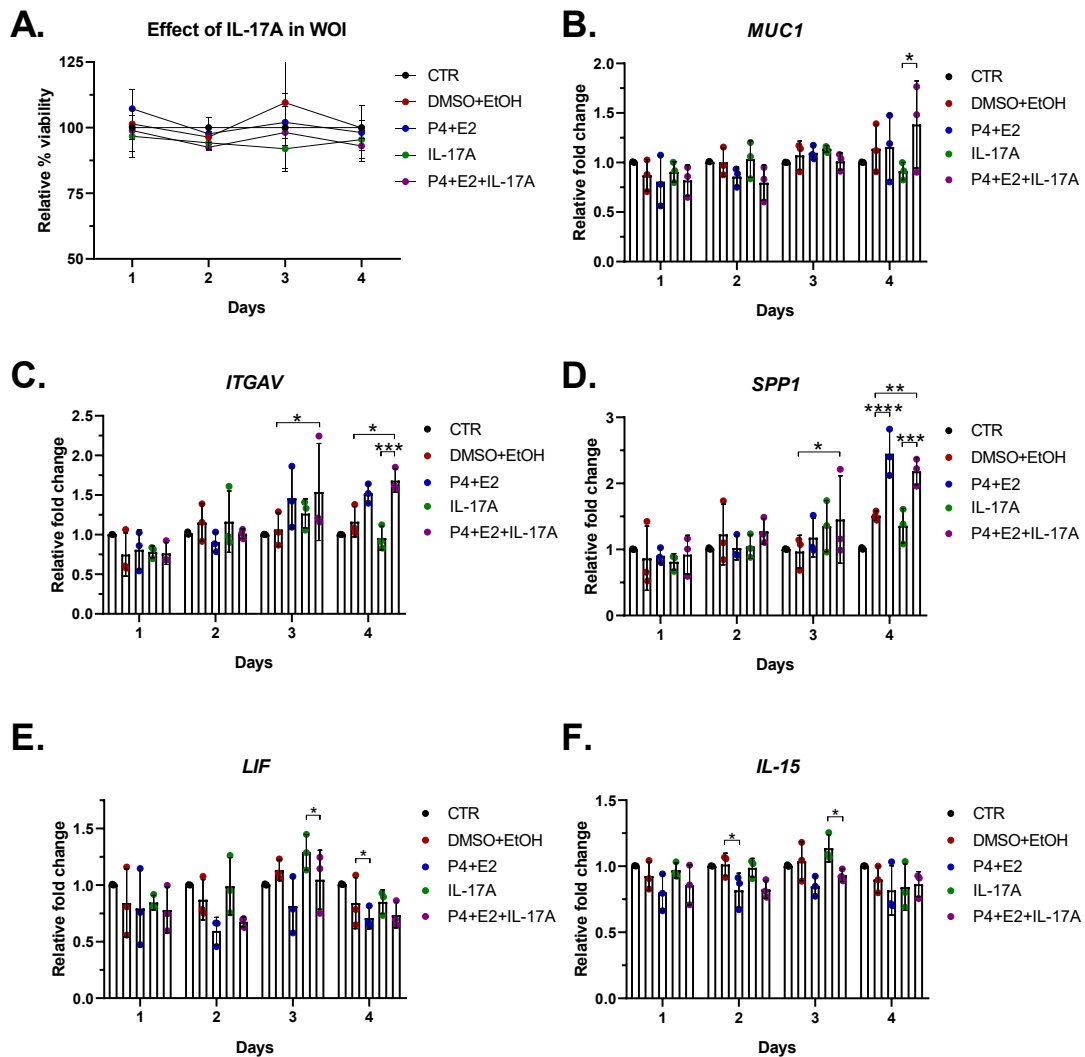


Figure 6.2. IL-17A does not affect endometrial epithelial receptivity markers. Ishikawa cells were treated for up to four days with P4 (1 μ M) and E2 (10nM) or with equal amounts of dissolving medium controls (DMSO or Ethanol, respectively), in the presence or absence of IL-17A (10ng/mL). Treatment media was refreshed every 2 days. **A.** Treatment was also performed in 96-wells to which cell viability was assessed by adding 10% vol/vol of Alamar Blue and absorbance reading were collected. Relative cell viability was calculated using the reading of

media only as background control and the reading from the control as reference. **B-F.** Every day up to 4 days cells were harvested for extracting RNA and performing qPCR for receptivity markers: Mucin 1 (*MUC1*, **B.**), Integrin αV (*ITGAV*, **C.**), Osteopontin (Secreted Phosphoprotein 1, *SPP1*, **D.**), Leukemia inhibitory factor (*LIF*, **E.**) and IL-15 (**F.**). $n=3$. Statistical test applied: Two-way ANOVA with Tukey correction. * $p<0.05$; ** $p<0.002$; *** $p<0.0002$; **** $p<0.0001$. .

6.3.2 Effect of IL-17A on endometrial stromal cell decidualisation

Another process that occurs during the window of implantation is stromal cell decidualisation. During this process, endometrial stromal cells change their shape and express genes coding for molecules involved in embryo implantation and dNK cell stimulation. Markers of stromal cell decidualisation are prolactin (PRL) and Insulin-like growth factor binding protein-1 (IGFBP1), whereas osteopontin (SPP1) is also increased by decidual cells as marker of endometrial receptivity. To see whether IL-17A has an impact in stromal cell decidualisation, primary human endometrial stromal cells were obtained from endometrial biopsies and decidualisation was induced in presence or absence of IL-17A. Endometrial stromal cell decidualisation can be induced *in vitro* by treating cells with progesterone (P4) in the presence of 8-Br-cAMP for up to 6 days. As expected, decidualisation of hESC induces increased expression of all these three markers (**Figure 6.3**). Decidualisation media increases SPP1 expression at day 4 and 6, whereas IL-17A treatment shows a decrease of SPP1 expression at day 6 (**Figure 6.3A.**). However, it can be noticed that in the cells treated with decidualisation media+IL-17A increased expression is maintained if compared to the control, except for a decrease showed at day 4, which is restored at day 6 (**Figure 6.3A.**). PRL and IGFBP1 show a time-dependent increase in their expression, which starts already after one day of decidualisation media treatment and reaches very high fold changes at day 4 and 6 (**Figure 6.3B.** and **C.**). It can be noticed that again IL-17A treatment, either alone or in combination with decidualisation media, shows no effects in modulating expression of these markers, even though it can be noticed a very slight decrease in PRL and IL-15 expression induced at day 4 (**Figure 6.3B.** and **D.**). Furthermore, IL-17A alone or added to the stromal decidualisation media induced a greater fold change in LIF expression if compared to decidualisation media alone (**Figure 6.3E.**). Cell viability was also

monitored, and it was noticed that IL-17A treatment did not affect stromal cell viability during the decidualisation treatment, so as for the decidualisation media alone (Figure 6.3F.).

Thus, IL-17A does not seem to have a sustained significant impact on stromal cells decidualisation. the decrease observed at day 4 upon IL-17A treatment alongside decidualisation media did not reach statistical significance, but probably having an increased number of biological replicates could give a better idea whether this is consistent and might suggest a role for IL-17A in impacting on embryo implantation through repression of stromal cell decidualisation markers at an early phase.

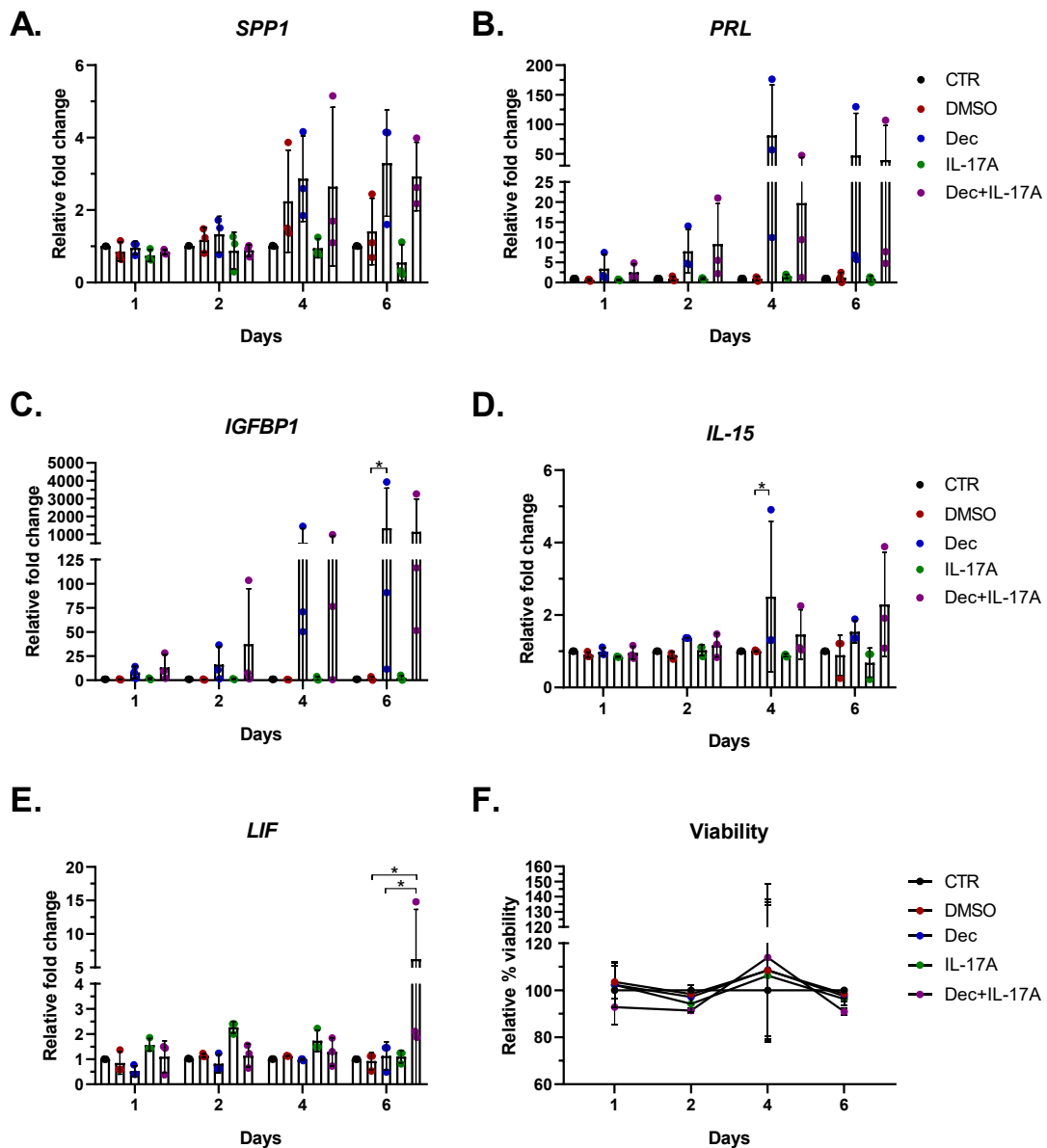


Figure 6.3. IL-17A treatment affects stromal cells decidualisation. Primary human endometrial stromal cells were obtained from endometrial biopsies. Cells were treated for up to six days with decidualisation media (P4, 1 μ M, and 8-Br-cAMP, 0.1mg/mL) or with equal amounts of dissolving medium controls (DMSO), in the presence or absence of IL-17A (10ng/mL). Treatment media was refreshed every 2 days. At timepoints 1, 2, 4 and 6 days RNA was extracted from cells and qPCR performed using RPLP0 as housekeeping reference gene. Genes of interest are endometrial receptivity marker SPP1 (A.), decidualisation markers Prolactin, PRL (B.) and Insulin-like growth factor binding protein-1,IGFBP1 (C.) and markers for the window of implantation IL-15 (D.) and LIF (E.). F. Viability was assessed by performing the same stimulation in a dedicated 96-well to which 10% vol/vol Alamar Blue was added and viability calculated as percentage compared to those observed for the control samples. n=3. Statistical test applied: Two-way ANOVA with Tukey correction. *p<0.05; **p<0.002; ***p<0.0002; ****p<0.0001.

6.3.3 Butyrate enhances endometrial epithelial receptivity and stromal decidualisation

Once established the pro-inflammatory roles of butyrate in endometrial epithelial cells, we then wondered what the functional consequences would be in fertility outcomes. Specifically, we aimed to understand the effect that butyrate has on the endometrium during the window of implantation (WOI), which is the most critical step for pregnancy establishment. To do so, we repeated the epithelial receptivity and stromal decidualisation models in the presence or absence of butyrate.

Given that we observed increased cell death in cells treated with 8mM butyrate for 48h and since the 2mM dose displayed to induce a similar response, the lower dose of butyrate was used to perform the endometrial receptivity assay since it requires 4 days of treatment. The treatment of Ishikawa cells with 2mM butyrate alone or in conjunction with Progesterone (P4) and Oestradiol (E2) showed to significantly decrease the relative viability of cells to approximately 60% if compared to the control cells (Figure 6.4A.). Treatment of Ishikawa cells with P4 and E2 decreases MUC1 expression and increases the expression of ITGAV and SPP1, recapitulating the changes happening during the WOI (Figure 6.4B-D.). The treatment of Ishikawa cells with butyrate alone or in conjunction with P4 and E2 significantly decreased MUC1 expression after 1 day, even

more than what it is observed with P4 and E2 treatment alone, however it then slightly increases over time in the other time points (Figure 6.4B.). ITGAV and SPP1 expression is greatly increased by butyrate, much more than the cells treated with only P4 and E2 and show an increase in a time-dependent manner (Figure 6.4C-D.). Furthermore, the treatment with butyrate in conjunction with P4 and E2 shows similar levels of induction of ITGAV and SPP1 to the ones observed in the cells treated with butyrate alone, meaning that the butyrate treatment is predominantly driving this response. Other two well-known markers of endometrial receptivity, Leukemia Inhibitory Factor (LIF) and IL-15, are substantially increased by butyrate treatment, showing significantly higher levels than in the cells treated with sex hormones alone (Figure 6.4E-F.).

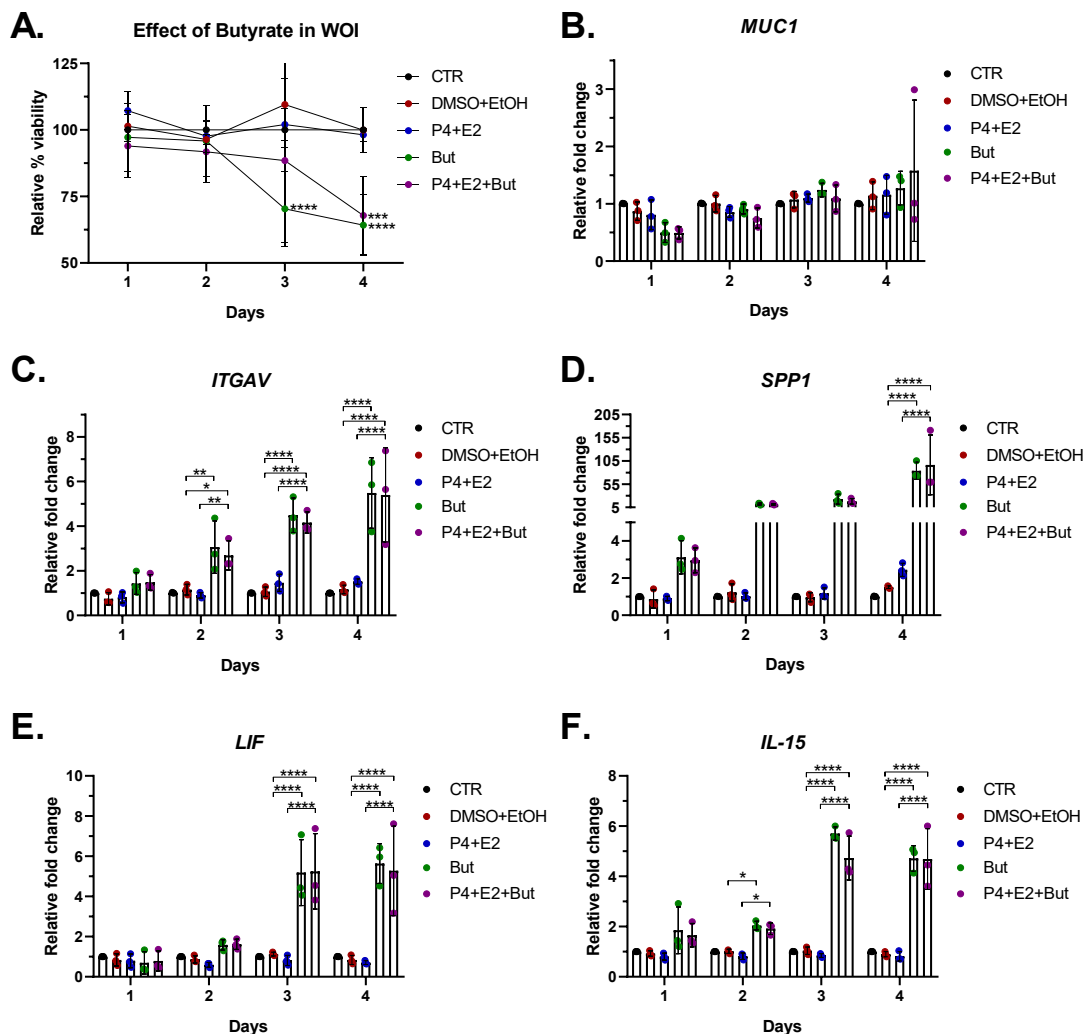


Figure 6.4. Butyrate enhances the epithelial expression of markers associated with endometrial receptivity. Ishikawa cells were treated for up to 4 days with P4 (1 μ M) and E2

(10nM) or with equal amounts of dissolving medium controls (DMSO or Ethanol, respectively), with or without 2mM butyrate. The treatment media was replaced every 2 days. **A.** Cell viability was assessed by adding to the growing media 10% vol/vol Alamar Blue and reading conversion of resazurin in live cells. Calculation of cell viability was performed using the control cells as reference. **B-F.** RNA was extracted and expression of MUC1 (**B.**), ITGAV (**C.**), SPP1 (**D.**), LIF (**E.**) and IL-15 (**F.**) was assessed with qPCR using RPLP0 as reference gene. N=3. Statistical test applied: Two-way ANOVA with Tukey correction. * $p < 0.05$; ** $p < 0.002$; *** $p < 0.0002$; **** $p < 0.0001$.

When the same dose of butyrate was used in the stromal decidualisation model we observed a similar trend (**Figure 6.5**). We observed that treatment of hESC with decidualisation media resulted in a time dependent increase of SPP1 (**Figure 6.5A.**), PRL (**Figure 6.5B.**) and IGFBP1 (**Figure 6.5C.**). Butyrate treatment alone induced increase of all these three markers, although the increase observed for SPP1 was greater than the one observed in the decidualisation media. Whereas PRL and IGFBP1 levels after butyrate treatment alone were in general lower than the ones observed in the decidualisation treated cells. SPP1 levels in cells treated with decidualisation media plus butyrate were much higher than the levels observed in cells treated with decidualisation media alone, but with a similar fold change as the butyrate alone treatment, suggesting that butyrate is a potent inducer of SPP1 expression (**Figure 6.5A.**). In the case of PRL and IGFBP1 the expression observed after treatment with decidualisation media in the presence of butyrate is higher than the one observed in the decidualisation media alone treatment, but it is much increased than the one observed in butyrate only treated cells (**Figure 6.5B-C.**). This finding suggest that butyrate might have an additive effect in driving the increase in expression of PRL and IGFBP1. Also, after 1 day of treatment it seems that butyrate inhibits IGFBP1 increase, as it can be observed a lower expression in cells treated with decidualisation media plus butyrate if compared to cells treated with decidualisation media only (**Figure 6.5C.**). Intriguingly, when butyrate is added to the decidualisation media, the expression of LIF and IL-15 is significantly reduced if compared to the decidualised cells (**Figure 6.5D-E.**). This result is in contrast with the earlier finding of increased IL-15 and LIF expression in epithelial cells. Another contrasting result compared to those observed for the epithelial cells is the effect of

butyrate on stromal cell viability. Contrarily to the decrease in cell viability observed during the epithelial receptivity assay, no changes can be observed in the percentage viability of butyrate treated cells, with or without the stromal decidualisation media, (Figure 6.5F.).

Butyrate seems to impact in the WOI by increasing the markers associated with endometrial receptivity and also those linked to stromal decidualisation. Butyrate treatment alone was shown to drive an increase in endometrial receptivity markers, more substantial than that observed after sex steroid hormone (P4 and E2) treatment. However, it seems that butyrate influences stromal decidualisation by potentiating the decidualisation signalling induced by sex-hormones.

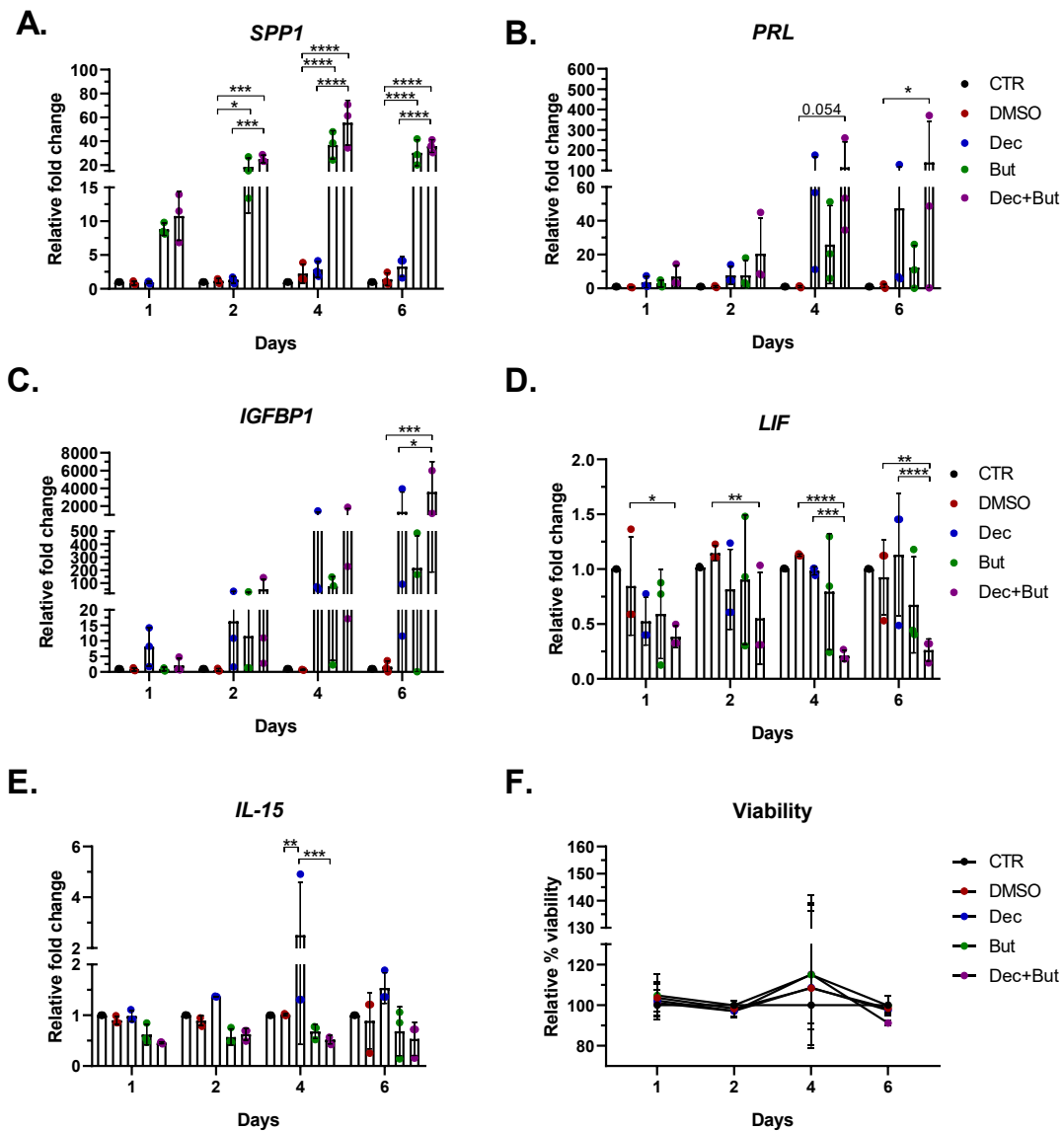


Figure 6.5. Butyrate enhances stromal decidualisation markers but decreases LIF and IL-15.

Human endometrial stromal cells were isolated from endometrial biopsies. Cells were treated for up to six days with decidualisation media (P4, 1 μ M, and 8-Br-cAMP, 0.1mg/mL) or with equal amounts of dissolving medium controls (DMSO), in the presence or absence of 2mM Butyrate. Treatment media was refreshed every 2 days. RNA was extracted and qPCR was performed using RPLP0 as housekeeping reference gene. Shown is relative gene expression of **A.** SPP1, **B.** PRL, **C.** IGFBP1, **D.** LIF, **E.** IL-15. **F.** Cell viability was assessed by adding 10%vol/vol Alamar Blue and recording resazurin conversion at each timepoint and then calculate the relative % viability compared with control cells. N=3. Statistical test applied: Two-way ANOVA with Tukey correction. * $p < 0.05$; ** $p < 0.002$; *** $p < 0.0002$; **** $p < 0.0001$.

6.4 Discussion

We aimed to establish a role that IL-17A and butyrate could have in modulating fertility. In particular, we were interested in understanding whether IL-17A could modulate epithelial and stromal cell receptivity for embryo implantation, which was the step which failed in the women who were unable to get pregnant through ART in our study (214). Several studies have now been performed to recapitulate *in vitro* the changes observed during the window of implantation (331, 332).

To establish *in vitro* models for the window of implantation we used Ishikawa cells for recapitulating endometrial receptivity and primary human endometrial stromal cells (hESC) to induce decidualisation. Ishikawa cells have already been reported in literature as a suitable model for inducing endometrial epithelial receptivity (332, 333) and, similarly, have been optimised doses and timepoints to induce decidualisation in hESCs (331, 432, 435). We have noticed that in both cases the expression of epithelial and decidual cell markers are increased by treatment with progesterone, however the decidualisation treatment induced the highest fold change. Despite hESCs would be collected from women undergoing surgery at various stages in their endometrial cycle (Table 2.1), maintaining stromal cells for few days in the stromal cell media completely deprived of hormones was enough to reset their maturation stage and, when hormones were added again in the stimulation, induce a greater response. On the other hand, Ishikawa cells were maintained in media supplemented with foetal bovine serum and then replaced with hormonal-deprived charcoal stripped media only the day before the stimulation. This might have dampened the response of this cell line to the hormonal treatment, causing the smaller fold change observed if compared to the hESCs.

Endometrial epithelial receptivity model performed in Ishikawa cells resulted in receptivity markers being upregulated (SPP1 and ITGAV) or downregulated (MUC1) as expected (Figure 6.2). However, IL-17A had no effect in the stimulation, meaning that would not likely impact directly on epithelial cells interaction with the embryo. In the model performed using primary human endometrial stromal cells, the decidualisation media induced increases decidualisation markers (PRL and IGFBP1) and in endometrial

receptivity (SPP1) (Figure 6.3). Also in this model, IL-17A did not change decidualisation markers, except for a slight decrease in PRL and SPP1 expression at the timepoint 4 days, which is restored at 6 days (Figure 6.3B.). The decrease is not statistically significant, however could point out for a possible role of IL-17A in impairing stromal cell decidualisation.

It is then possible that IL-17A, in conditions of infection, can be secreted by endometrial epithelial cells as well as from immune cells. This leads to increased levels of this cytokine which could impact on fertility by delaying decidualisation, a process fundamental for the early stages of pregnancy (Figure 6.6). Decidual cells are indeed needed for correct embryo implantation, as well as being involved in secretion of growth factors and angiogenic factors needed for embryo growth and for correct spiral artery formation during placentation (436). Another clue for IL-17A being harmful for decidualisation resides on the fact that decidual stromal cells have been found to downregulate IL-17A by impairing T_H17 maturation (369). However, other reports have suggested that the decidua is enriched in T_H17 cells, which do not have a negative impact on pregnancy outcomes if maintain IL-4 secretion (199, 200). However, these two publications are studying cohort of women which had already established a pregnancy and the IL-17A was shown to be protective against unexplained recurrent abortion, therefore it could still be possible that IL-17A is detrimental for early pregnancy steps such as implantation and placentation and show a protective role during later stages. This highlights again how IL-17A shows a dichotomous nature of being essential for certain processes, but on the other hand if dysregulated and present in a higher amount, it can turn out to have a negative impact. Further studies would be needed to better clarify the role that this cytokine might have in the early stages of pregnancy.

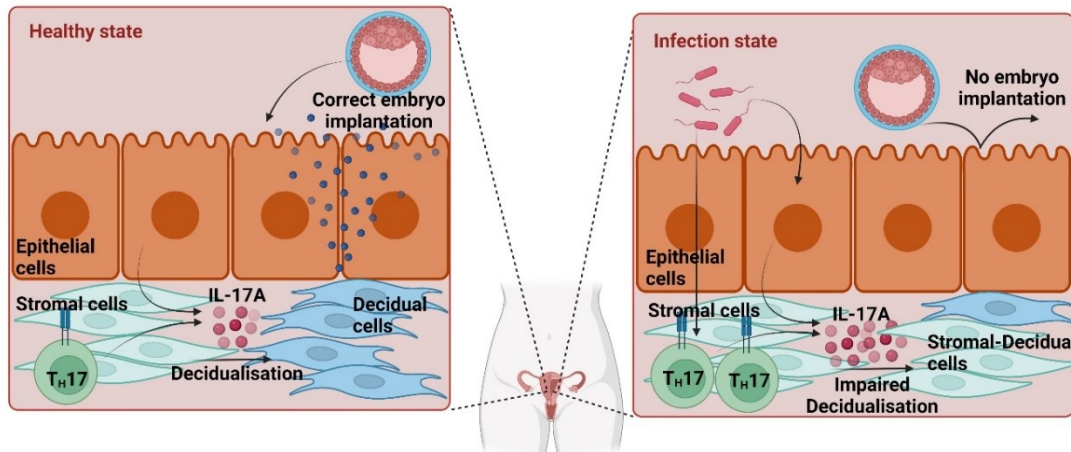


Figure 6.6. IL-17A impairs embryo implantation by decreasing decidualisation. The model proposed sees IL-17A produced by epithelial cells alongside TH17 cells. Under healthy conditions, some levels of IL-17A are produced but they are not impairing decidualisation. In this way, decidual cells can mature correctly and contribute to embryo implantation. In infection settings, on the other hand, there are higher levels of IL-17A produced by both epithelial and immune cells. This leads to a decreased ability of stromal cells to mature into decidual cells, thus leading to failed embryo implantation because of the lack of the signals from the decidua.

Once established that butyrate induces a pro-inflammatory signalling activation in endometrial epithelial cells, we then asked which are the functional consequences on female fertility. The most critical step for pregnancy establishment is the correct implantation, for which changes are put in place in the endometrium during the window of implantation. We wondered what effect butyrate does have when is added to cell models mimicking the window of implantation.

First of all, we had to use a lower dose of butyrate (2mM), because it would induce consistent cell death if kept on epithelial cells for longer periods. Unfortunately, the concentration of butyrate in the endometrium is still unknown, however it is suggested that at mucosal sites the concentration of acetate could reach up to 20mM and, at least in the gut, acetate would be more abundant than butyrate and propionate in a 60:20:20 ratio, which means that butyrate and propionate could be around 6mM (261). Of course, this reinforces the question whether this concentration of butyrate is physiologically present in the healthy endometrium or derived from a possible

dysbiosis/infection. In our case, we noticed that 2mM butyrate dose is already enough to significantly decrease epithelial cell viability after 3 days (**Figure 6.4A.**), suggesting that this concentration would not be tolerated if we hypothesize this as the butyrate concentration present in the healthy endometrium. On the other hand, 2mM butyrate has no effect on stromal cell viability, which again highlights the substantial differences between epithelial and stromal cells (**Figure 6.5F.**). The high decrease in cell viability induced by butyrate in epithelial cells also raises the question whether the effects observed are truly dependent on butyrate or maybe induced by activation of other cell death/stress pathways.

The treatment of Ishikawa cells with progesterone and oestradiol lead to increased expression of ITGAV and SPP1 and decreased expression of MUC1 (**Figure 6.4**). Adding butyrate to the epithelial maturation media, drastically enhanced this pattern, by reducing MUC1 expression and increasing the expression of ITGAV and SPP1, as well as driving the over expression of other two markers associated with the WOI: IL-15 and LIF (**Figure 6.4**). In a similar way, butyrate added to decidualisation media induced SPP1 and it also resulted in enhanced stromal decidualisation markers, which reach higher expression at earlier timepoint (**Figure 6.5**). The changes associated with the window of implantation must be tightly controlled in terms of timing for allowing the correct crosstalk between the embryo, the epithelial cells, and the stromal compartment. We see butyrate greatly enhancing endometrial receptivity markers and stromal decidualisation, thus it might create an unbalanced environment which could be not ideal for a correct implantation, potentially anticipating the opening of the window of implantation (**Figure 6.7**).

With regards of LIF and IL-15, we observe two opposite effects of butyrate, which increases their expression in epithelial cells and reduces them in the stromal cells. LIF is involved in inducing proliferation in both the maternal epithelial and stromal cells and in the invading trophoblast. IL-15 instead is involved in the communication of both epithelial and stromal cells with the decidual NK cells, inducing their proliferation and suppressing their cytotoxicity to favour beneficial effects such as spiral artery formation. Having an unbalanced IL-15 or LIF production, which is what seems to be present in both

the cases when there are too high levels of IL-17A and butyrate, might have an impact on fertility-related processes through dNK cells ([Figure 6.7](#)).

We identified a different microbiome in women who were not able to carry a successful pregnancy, and this might have caused an increase in SCFAs content. We showed that butyrate induces an inflammatory signature activation in endometrial epithelial cells and that, if present during the WOI, it leads to enhanced receptivity and decidualisation. We could not access SCFAs levels in the women from the cohort, but further studies in determining the role of SCFAs in the FRT might shed light on the role that these compounds have on female fertility.

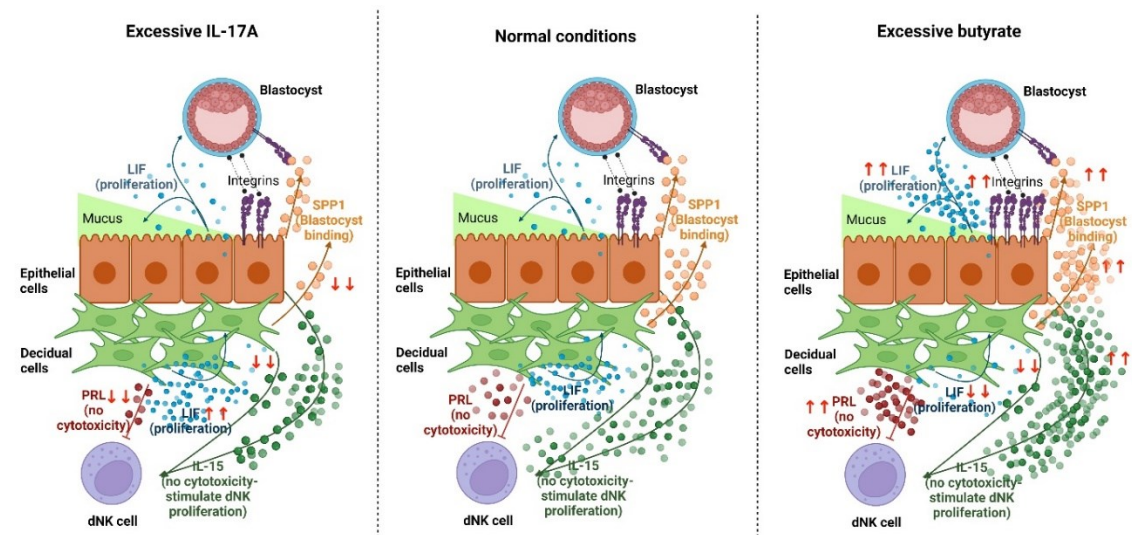


Figure 6.7. Effects of excessive IL-17A and butyrate during the window of implantation. Under healthy conditions, the mediators released during the window of implantation are produced by both the receptive epithelium and the decidual stromal cells. When there is excessive IL-17A or butyrate, these molecules are secreted in a different amount, leading to failure in the right timing and right communication between the blastocyst, the dNK and the crosstalk between epithelial and stromal cells.

Chapter 7: General discussion and future perspectives

7.1 General discussion

The immunological processes involved in female fertility and pregnancy establishment are complex and require the participation of the maternal specialised tissues, such as endometrial epithelial and stromal cells, the local maternal immune system, the microbiota, and foetal-derived cells. This complicated balance is the reason why, even when couples undergo ART, where fertilisation occurs optimally and a high-quality embryo is established, the successful pregnancy rates are still below 50% (437). Thus, it is necessary to understand the involvement of each of the above-mentioned player in pregnancy, especially during the window of implantation, which is the most crucial step for pregnancy establishment.

It was formerly believed that the maternal immune system was suppressed during pregnancy to allow foetal tolerance. However, it is now known that the maternal immune response is fundamental for pregnancy establishment and that this feature is maintained within the mammalian clade (318). As an example, dNK cells are shown to mediate spiral artery remodelling and help embryo implantation and placentation (31). Furthermore, during embryo implantation a pro-inflammatory signature is present and this process is shown to be mediated by two cytokines, LIF and IL-15 (187). Among the cytokines involved in pregnancy establishment, some studies also reported IL-17A. This pro-inflammatory cytokine shows a dichotomous nature since it is secreted in response to bacterial and fungal infections and is also linked to autoimmune diseases (56). In female fertility is not known the exact role of IL-17A, since it has been shown to mediate trophoblast chemotaxis (194) but it has also been linked to several fertility complications. Our group reported increased protein levels and pathway activation of IL-17A in women with unexplained infertility undergoing ART with unsuccessful outcomes (214). This points out that in those women there might have been an excessive pro-inflammatory activation, leading to implantation failure.

Also, the local microbiome plays an active part in female fertility. Unfortunately, the theory of the FRT being a sterile compartment has delayed the research, therefore is still missing a canonical consensus on what the healthy uterine microbiome is, provided that a microbiome will be confirmed to be present at all in this compartment. It must also be noted that the sampling for investigating the endometrial microbiome has been performed only in women undergoing surgical or laparoscopic procedures due to diagnosis or treatment for fertility complications, therefore they cannot be referred as healthy controls *per se* (438). A few studies reported that certain species are associated with fertility complications such as endometriosis (250, 256) or implantation failure and decreased pregnancy rates (255, 257). Furthermore, is not clear yet the impact that microbial-derived metabolites have on endometrial cells. For example, microbial-derived SCFAs have been shown to have a pro-inflammatory role in the lower FRT, thus making it possible for the microbiome to modulate the immune response, similarly to what happens in the gut (438).

The interaction between the immune system and the microbiome can be direct, however most of the times there is an epithelial layer acting as a barrier in dividing these two players. However the epithelial cells are now starting to be regarded not only as a mere physical barrier, but as active players in modulating innate immune responses (439). The endometrial epithelial cells can easily recognise several classes of pathogen associated molecular patterns (PAMPs) through expression of pattern recognition receptors (PRRs) (438), leading to cytokine and chemokine release to attract and activate immune cells (7). Furthermore, epithelial cells can directly mediate microbial killing by secreting AMPs (145).

In this study we aimed to further characterise the interaction between immune cells, the epithelial cells, and the microbiome in the FRT.

We were first interested in defining the effect that IL-17A and its related cytokines have on mammalian female fertility. Given that the pro-inflammatory signature observed during embryo implantation is also observed in marsupials (318, 350), we wondered whether the family of IL-17 cytokine might have evolved in mammalian clades to retain fertility-related functions. In these regards we were inspired by the work from Günter

P. Wagner group which, in the last years, have accumulated several publications to understand how mammalian pregnancy has evolved through comparative and evolutionary studies using eutherian and metatherian models (318, 440, 441). Modern mammals have evolved from the most recent common ancestor into three main clades: prototherian (also known as monotremes), metatherian (also known as marsupials) and eutherian mammals (also named placentals). It is likely that the mammalian MRCA displayed a similar gestation as the one observed in prototherian, thus they were egg laying mammals and performed an extrauterine incubation. Metatherian and eutherian mammals are viviparous, since they derive from the common most recent therian ancestor in which was present a shift in the egg hatching while the egg was still in the female womb (339). This process is still retained in metatherian and, despite the confusion generated by the nomenclature who defines eutherian as “placental mammals”, both metatherian and eutherian clades display maternal-foetal interactions through a placentation process which is accompanied by a pro-inflammatory environment (339). With this work we showed that IL-17 family of cytokines are present in all mammalian clades sharing the same genomic location, protein sequence and structure. Furthermore, IL-17s expression is elevated around placentation in both eutherian and metatherian datasets, confirming that this cytokine family might have role in this process. In particular, we saw upregulation of IL-17A in the marsupials *M. domestica* and *N. eugenii*, whereas in eutherian mammal we observed upregulation of IL-17D around placentation. This might be explained by the fact that stromal decidual cells, which are present only in eutherian mammals, are showed to inhibit IL-17A production (369), making thus possible for another family member, IL-17D, to take over.

Another question still open is the characterisation of the functions of the IL-17 cytokine family and why there are six members of this cytokine family. To date, IL-17A, IL-17F, and IL-25 are the most studied due to their involvement in several pathologies. These cytokines share a very high percentage identity and they all use similar signalling pathways to trigger downstream gene activation which, except for IL-25 and IL-17D, which has not been fully characterised yet, is very similar (50). Therefore, one could question why there are so many IL-17s. It seems that these cytokines evolved long time ago, since their homologous counterparts can also be identified in invertebrates (368).

If we look at the human IL-17s we could see that IL-17A and IL-17F are the most closely related, then IL-17B and IL-17D are the more similar each other and lastly IL-17C and IL-25, which are the most distantly related (442). The fact that we identified IL-17A and IL-17F genes located in a syntenic block suggests a gene duplication event. These two cytokines are also known to form heterodimers, however the heterodimers made by the other IL-17s are not yet been identified and their location is found in different chromosomes. It seems that, through evolution, these cytokines might have adapted their signalling pathway activation to respond to different infections. The role of IL-17A and IL-17F in activating mucosal immune responses against bacteria and fungi infection, happening in all mucosal sites throughout the body, has been already mentioned. IL-17B and IL-17C are expressed in certain mucosal sites such as lungs and gut and are heavily involved in antibacterial responses (45). IL-25 is instead associated with Th2 immunity activation, and it has been found to be fundamental against helminth parasitic infection (443). The function of IL-17D has not been completely understood yet, however it mediates NK cell recruitment leading to tumoral or viral-infected cell lysis (106). Alongside these functions, IL-17s are also associated with several pathologies, mainly driven by excessive autoimmune inflammation (444).

For what concerns female fertility, it seems that excessive IL-17 cytokine activation is linked to several complications, such as endometriosis (204), pre-eclampsia (225) and unexplained infertility (237). Our group has observed increased levels of IL-17A in women with unexplained infertility undergoing ART with unsuccessful outcome (214). Since the women with unsuccessful pregnancy received a good/top quality embryo but failed to display signs of clinical pregnancy such as a positive ultrasound scan and positive serum β hCG, we hypothesize that the embryo implantation step failed in those donors (214). Therefore, we used recombinant IL-17A to mimic the high levels observed in the donors to perform *in vitro* models of endometrial receptivity and stromal decidualization. This approach led to inconclusive results as no changes can be observed in cells who received rIL-17A together with progesterone, with only a slight decrease of certain stromal cell decidualisation markers at day 4 from progesterone administration. Given that the opening of the window of implantation is a tight timed process, this

decrease might delay the decidual cell signals, required to allow correct embryo implantation, but further analysis would be needed to confirm this hypothesis.

Regarding the cell types responsible for the production of these cytokines, IL-17A is the one whose production is known to be restricted to immune cells only (136). All the other IL-17s can be produced by non-immune cells, such as epithelial cells in the case of IL-17B, IL-17C and IL-25 (45). Since we observed increased IL-17A in the women with unexplained infertility undergoing ART, we first wondered whether an increased immune cell infiltration was causing such pro-inflammatory release. However, we saw that the immune cell population infiltration present in the biopsy was similar between the successful and unsuccessful group. We obtained this result using the bulk RNA-seq counts matrix and applying a gene signature characteristic of immune cells using Cybersortx. This is a retrospective approach to obtain single-cell data from bulk RNA-seq, through the Cybersortx tool which is now well established and used in the literature (445). The matrix used for the gene signature was derived from circulating blood, therefore the fact that no differences can be observed between the two groups might be an artifact due to the different phenotype of resident immune cells in the FRT showing a different gene signature. However, looking at the normalised expression of immune cell markers in the RNA-seq showed similar levels between the two groups, therefore we hypothesized that the production of IL-17A was mediated by non-immune cells.

Endometrial epithelial cells are known to be able to produce cytokines and chemokines (7), thus we hypothesized that this cytokine might be produced in the epithelial cells. We saw increased mRNA levels of IL-17A transcript in both tumoral cell line and in primary human endometrial epithelial cells (hEEC) in response to bacterial ligands, LPS and sodium butyrate, and viral RNA analogue poly(I:C). Intriguingly, sodium butyrate stimulation was the only one who resulted in increased IL-17A protein synthesis, which was not observed in LPS or poly(I:C) stimulation, despite the mRNA increase happened approximately at the same time and with similar fold change. It is possible that during poly(I:C) or LPS stimulation the regulation of IL-17A expression involves other pathways, since we observed no effect on IL-17A expression when Nf- κ B inhibitors are added during sodium butyrate stimulation. It is possible that the regulation of IL-17A mediated

by sodium butyrate involves epigenetic mechanisms, as we have observed a peak located 15kb upstream the transcription starting site. Butyrylation of histones has been linked to gene transcription activation (329), thus we think that the region involved in the butyrylation peak might be an enhancer for IL-17A expression.

It must also be noted that, even with sodium butyrate stimulation, the protein levels of IL-17A were still very low, for example the ELISA readout was very close to the assay limit of detection and the flow cytometry increased from 1% to approximately 5% positivity. Despite very low levels of IL-17A were found in epithelial cells, this data was not surprising. For example T_H17 cell stimulated for 5h with PMA and Ionomycin, a well-known stimulation for IL-17A production, reach a percentage positivity of about 6.6% (111) and IL-17A producing T_{RM} cells challenged for 56 days display 45% percentage positivity (115). In psoriasis, the most representative IL-17A-driven pathology in which extremely high level of this cytokine are observed, the concentration is around 80pg/mL in psoriatic lesions and 10pg/mL in adjacent non psoriatic skin (154). This gives us an idea of the intensity of the pro-inflammatory activation deriving from IL-17A, given that this cytokine is required in very low amounts to contribute to a very strong inflammatory signature.

Once established that also non-immune cells can produce IL-17A, we sought to investigate why there were such high levels of this cytokine in the women with unexplained infertility undergoing ART with unsuccessful pregnancies. Since IL-17A is released upon bacterial infection, we wondered whether a different microbiome might have characterised those women. We observed a different microbiome in the two groups, with a more diverse microbiome and a lower abundance of *Lactobacillus* spp. in women with unsuccessful pregnancy outcome. It must be pointed out that at sample collection those women did not display any symptoms related to bacterial infection, thus it is possible that the changes observed can be attributed to a silent dysbiosis. A study performed on fertile and infertile women with sample collected during pre-receptive and receptive phase showed a similar finding, with some donors displaying a *Lactobacillus*-dominated microbiota and some other with non-*Lactobacillus*-dominated microbiota, containing *Atopodium*, *Prevotella* and *Gardnerella* genera, similar to the ones identified by our study (255). The same study also highlighted how women with a

Lactobacillus-dominated microbiome showed higher successful implantation rates and live birth rates, which is also what we have observed in our group. Another question regards whether the dysbiosis observed is due to the upregulation of IL-17A pathway, which for some reason could have depleted more the *Lactobacillus* species leading to increased proliferation of the minor species, or if the IL-17A was secreted in response to the dysbiosis to restore homeostasis and return to the *Lactobacillus*-dominated microbiome. It could also be possible that some microbial species drive IL-17A production, as it happens in the gut. There, commensal segmented filamentous bacteria stimulate IL-17-producing cell expansion, leading to AMP release that can modify the intestinal microbiota (446). Thus, it could be possible that the interplay between IL-17A and microbiome involves a two-way communication.

What is also not known yet is the composition of microbial metabolites in the endometrium. Due to the difficulty in obtaining samples because of the invasive methods of collection, studying the endometrial microbial metabolome represents a challenge and what is known is obtained from women undergoing gynaecological investigation, who cannot be really considered as healthy controls. However, with this study we highlighted how the microbial derived SCFA sodium butyrate can induce pro-inflammatory mucosal activation *in vitro*, similarly to what happens when this metabolite accumulates in the vagina during bacterial vaginosis (273). It is intriguing how the same molecule can stimulate two opposite effects depending on the location. Indeed butyrate shows anti-inflammatory actions in the gut and lack of this metabolite results in higher risk of inflammatory bowel diseases, IBD (261). This is even more intriguing as HIF1 α pathway seems to be activated in cells treated with butyrate, which is one of the pathways also activated in the gut to promote barrier integrity (396).

Since both IL-17A and butyrate induce an inflammatory signature in the FRT, which we have shown to be detrimental for a positive outcome for pregnancy, we could speculate whether modulating these molecules could be beneficial. Some anti-inflammatory and immunosuppressive therapies are now used to ameliorate certain fertility complications such as pre-eclampsia (186). Therapies targeting IL-17A pathway are now used as a gold standard for auto-inflammatory diseases, however they are also associated with increased risk of bacterial and fungal infections, since the control over infections

mediated by this cytokine is also inhibited (146). In the context of gut inflammation, administration of enemas containing butyrate or prebiotics involved in SCFA production is showing encouraging effects in reducing the inflammation observed in IBDs, Crohn disease and ulcerative colitis (392). These therapies cannot be used yet for fertility complications, because more research would be needed to optimise them for safety and efficacy.

Therefore, another approach that could be put in place is to monitor when the levels observed of these molecules are optimal. Over the years, several studies have highlighted the markers associated with endometrial receptivity and stromal decidualisation during the window of implantation (188, 359, 428, 429). It is known that, since the window of implantation only lasts a couple of days, it is fundamental that embryo reaches the endometrium within those days, otherwise there will be implantation failure. Thus, the use of these markers is now becoming a popular strategy, for women undergoing ART, to determine when the window of implantation is open and proceed to embryo transfer (314, 447). Despite the opening of the WOI depends on progesterone, a study from Enciso *et al.* showed that 34.2% of the women enrolled in the study had a displaced WOI, ranging from women who were receptive as early as 2.5 days after progesterone intake, and women who become receptive after 8 days (447). The explanation for this broad range in variation might be the involvement of immune or microbial-derived mediators (Figure 7.1). We showed, indeed, that both IL-17A and sodium butyrate can impact on endometrial receptivity and decidualization markers by using *in vitro* models. IL-17A does not seem to impact on the markers for epithelial receptivity, however it causes a slight decrease in certain stromal decidualization markers at day 4 from the starting of decidualization treatment. Sodium butyrate has an even greater impact on both endometrial receptivity and stromal decidualization by increasing these markers by several folds. These findings confirm that both the immune system and the microbiome can impact directly on fertility, thus, when studying the WOI, we should look at the entire composition of the endometrium and not only focus on the specialised cells, such as the epithelial and decidual cell markers.

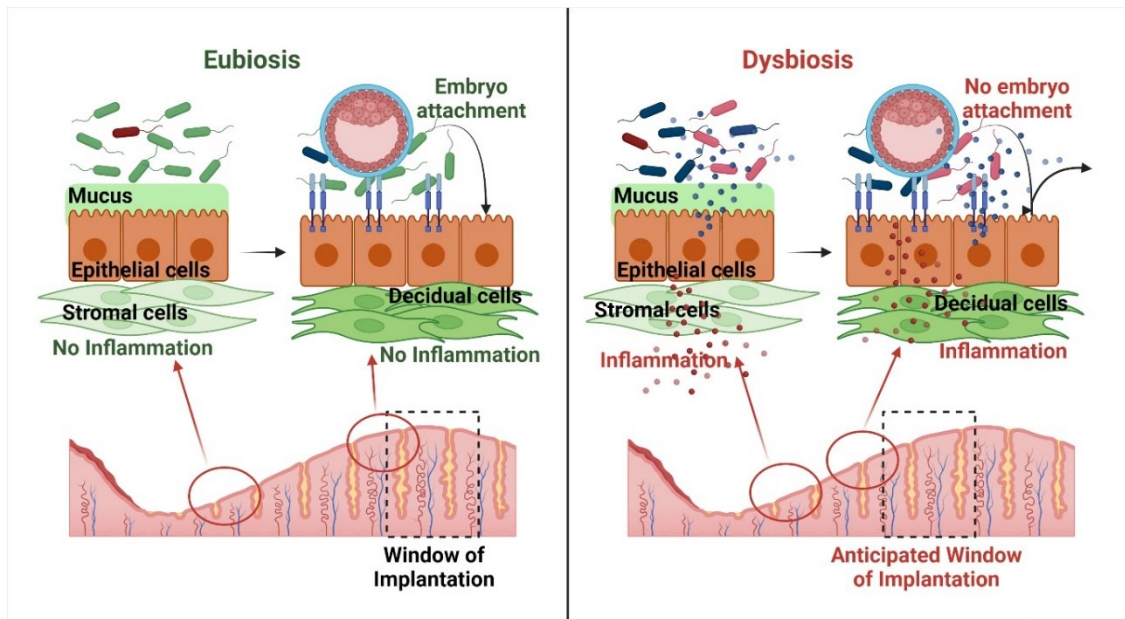


Figure 7.1. Proposed model associated with dysbiosis and inflammation in the FRT. In normal eubiosis condition (left) the endometrial epithelium and stromal cells are in the presence of commensal microbiota, resulting in no inflammatory activation. This leads to optimal epithelial receptivity maturation and stromal cell decidualisation culminating in correct embryo attachment. In infection settings (right), pathogens colonise the FRT thus causing inflammation and promoting the release of microbial-derived SCFAs such as butyrate (blue spheres). The presence of butyrate highly increases epithelial receptivity and stromal cell decidualisation markers, possibly leading to anticipation of the window of implantation and resulting in implantation failure.

7.2 Future perspectives

The work presented has generated several interesting findings opening new avenues for further research in the context of mucosal immunology and female fertility.

In particular we found, when analysing the structure of the IL-17 cytokines using bioinformatic approaches, that the cystine-knot motif they are characterised by is also shared by several other molecules such as hormones and growth factors, including β hCG, VEGF and placental growth factor (P1GF) (46, 448). Indeed, a lot of attention is given in literature to these molecules, often referred as if they are the only ones presenting the cystine-knot motif (46, 448). Interestingly, many molecules showing the cystine-knot motif have reproduction-related functions, such as β hCG, LH, FSH and TSH (449). The activation of IL-17A signalling pathway was also observed through synergistic activation with other growth factors, for example through simultaneous activation with FGF2 signalling through Act1 (70). The analysis of possible interactions of IL-17s with pregnancy-related hormones and growth factors was beyond the scope of this project. However, future studies might examine whether the action of IL-17s in pregnancy could also involve their ability to cooperate or hinder other molecules displaying a similar structure, such as the cystine-knot motif proteins. For example, it could be possible an heterodimerisation of proteins showing a cystine-knot motif or heterologous binding of a cystine-knot protein with the receptor for another protein, leading to different modulation of downstream signalling pathway.

Another open question regards which cells are responsible for IL-17A production in the endometrium. We could not obtain more samples or information from the donors of our study. However, obtaining more samples from another cohort of women with unexplained infertility could be useful to perform immune cell and non-immune cell phenotyping alongside IL-17A staining, to see which cell type is responsible for the production of this cytokine. It is known that stromal cells possess the IL-17RA/RC, making them able to respond to IL-17A stimulation, but whether this cytokine is actively produced by this cell type has not been investigated yet. Preliminary work performing immunohistochemistry on endometrial biopsies has showed that IL-17A positive staining is mainly localised within the stromal cells compartment ([Figure 7.2](#)). Further

work would be needed to identify whether stromal cells can produce IL-17A or if the cells identified in the stromal cell component are immune cells.

Also, it is possible that the high IL-17A protein observed was because those samples were taken during the window of implantation, in which a pro-inflammatory activation might be observed. Therefore, analysing whether this cytokine is subject to hormonal regulation and changes its levels during menstrual cycle could be useful to better understand the role of IL-17A in fertility.

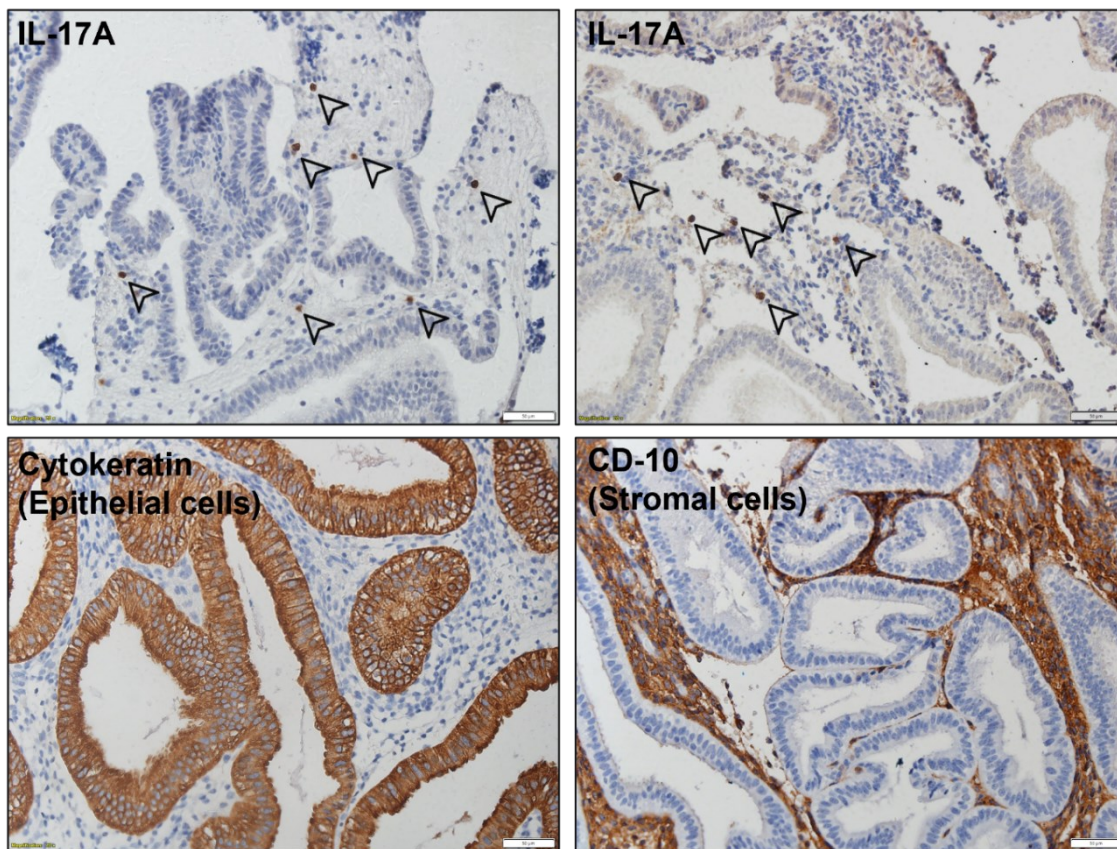


Figure 7.2. IL-17A staining is mainly localised within stromal cells in endometrial biopsies. Endometrial biopsies were obtained from women undergoing endometriosis assessment and then formalin-fixed and paraffin embedded. Sections of 0.5 μ m thickness were cut with a microtome and mounted on a glass slide. Immunohistochemistry was performed for IL-17A (upper panel) and markers for epithelial cells (cytokeratin) or stromal cells (CD10). Scale bar is shown in the bottom right corner (50 μ m). N=8.

Through using in vitro models of endometrial receptivity and stromal decidualisation we showed that inflammation and microbial-derived metabolites might impact the window of implantation. However, we believe this is just the tip of a much bigger iceberg.

Further studies would be required to characterise how these molecules impact on the window of implantation, possibly using *in vivo* mouse models or co-culture models of epithelial and stromal cells to give a complete vision of the epithelial-decidual cells interaction when there is a disturbing stimulus in play.

In this project, we describe a different microbiome in women undergoing ART with negative pregnancy outcome. Unfortunately, our cohort included only 30 women, thus repeating this finding in a validation cohort would be important to see whether this finding is confirmed or not.

Also, our samples were collected in the mid-luteal phase of the cycle before the embryo was transferred, thus we cannot be sure that the microbiome observed was the same as the one present when embryo was transferred in the following cycle. Microbiome communities are generally very dynamic and it is known that there is a gut-genital tract microbiota crosstalk that can contribute to change the uterine microbiota, alongside the changes induced by sex hormones (261). Using *in vivo* mouse models, it is possible to study whether the microbiome changes throughout individual menstrual cycle and whether is constant between cycles and what is the impact that gut microbiota and food has on genital microbiome. This would enhance the knowledge regarding the uterine microbiota and would also pose the bases for a possible therapeutic approach to obtain an optimal “fertile and receptive” microbiome.

We have identified that the SCFA butyrate induces inflammation in *in vitro* models of endometrial epithelial cells. However, it is not known precisely which components of the endometrial microbiome are responsible for butyrate secretion, nor the presence of butyrate or the exact concentration in the uterus. We hope that further studies will clarify the composition of the microbial metabolome in the uterus and possibly correlate with pregnancy outcome. It is generally believed that the cervix acts as a barrier to inhibit the exchange of bacterial species and metabolites between the endometrium and the vagina. However, some studies are showing that there is a continuity between the endometrium and the vagina. Thus, it might be possible accessing vaginal samples to observe what is also located in the endometrium. This would provide an easier way to access samples useful to determine the optimal microbiome/metabolome for a successful pregnancy establishment.

Identification of the butyrylation peak upstream of the IL-17A transcription starting site using an available ChIP-seq database represents an interesting modulation induced by this SCFA. Further studies would be required to characterise whether butyrylation is needed to allow IL-17A transcription, for example using the peak region of IL-17A cloned upstream the firefly luciferase reporter gene and looking at the effect that butyrylation of this region has on gene transcription. Another approach could be to use butyrylation inhibitors and see whether IL-17A transcription is abolished. In an adipogenesis model, a role for the p300 acetyltransferase in mediating lysine butyrylation was identified by using a selective inhibitor LTK-14A (450). Characterisation of the epigenetic regulatory effect that butyrate has on IL-17A could also be a conserved mechanism for other immune genes. Therefore, a ChIP-seq on human samples, for example immune and non-immune cells, could be useful to determine whether differential regulation characterises those different cell types.

Another interesting question would be whether butyrate is responsible for a higher and faster inflammatory response when a second infection would happen. Since butyrate stimulates pro-inflammatory mucosal activation in our cell models, adding a second stimulus mimicking a second bacterial or viral infection would be interesting to see whether the response to the second stimulus is faster and with higher potency, making butyrate a molecule responsible for epithelial cell training.

Obtaining more information with any of these approaches could lead to new therapies for the treatment of infertility. The maternal immune system plays a central role during pregnancy establishment and throughout all pregnancy stages, not only by allowing pregnancy-related processes, but also protecting the mother, and consequently the foetus, from infections. Therefore, a careful approach must be put in place when trying to stop excessive immune reactions, to maintain this delicate balance. Although therapies targeting IL-17A pathway show high efficacy in the treatment of psoriasis, in other contexts such as for IBD and Crohn's disease they show worsening clinical inflammation (146). Also, it has been noted an increase opportunistic infection of *Candida albicans* in patients under anti-IL-17A therapies, due to the reduced control of this molecule against this pathogen (184). Therefore, if we increase our understanding of the link between microbiome and immune system in the FRT, we could speculate that

modulating the microbiome could then modulate the immune system in a more physiological manner, avoiding side effects that might put at risk both the mother and the foetus.

Chapter 8: References

1. Chumduri C, Turco MY. Organoids of the female reproductive tract. *J Mol Med (Berl)*. 2021;99(4):531-53.
2. Thiyagarajan DK BH, Jeanmonod R. . Physiology, Menstrual Cycle. StatPearls [Internet]. 2021.
3. Nott JP, Bonney EA, Pickering JD, Simpson NAB. The structure and function of the cervix during pregnancy. *Translational Research in Anatomy*. 2016;2:1-7.
4. Agostinis C, Mangogna A, Bossi F, Ricci G, Kishore U, Bulla R. Uterine Immunity and Microbiota: A Shifting Paradigm. *Front Immunol*. 2019;10:2387.
5. Belkaid Y, Harrison OJ. Homeostatic Immunity and the Microbiota. *Immunity*. 2017;46(4):562-76.
6. Zhou JZ, Way SS, Chen K. Immunology of the Uterine and Vaginal Mucosae. *Trends Immunol*. 2018;39(4):302-14.
7. Wira CR, Rodriguez-Garcia M, Patel MV. The role of sex hormones in immune protection of the female reproductive tract. *Nat Rev Immunol*. 2015;15(4):217-30.
8. 7 - ANTIGEN PRESENTATION. In: Cruse JM, Lewis RE, Wang H, editors. *Immunology Guidebook*. San Diego: Academic Press; 2004. p. 267-76.
9. Duluc D, Gannevat J, Anguiano E, Zurawski S, Carley M, Boreham M, et al. Functional diversity of human vaginal APC subsets in directing T-cell responses. *Mucosal Immunology*. 2013;6(3):626-38.
10. Duluc D, Banchereau R, Gannevat J, Thompson-Snipes L, Blanck JP, Zurawski S, et al. Transcriptional fingerprints of antigen-presenting cell subsets in the human vaginal mucosa and skin reflect tissue-specific immune microenvironments. *Genome Med*. 2014;6(11):98.
11. Zhao X, Deak E, Soderberg K, Linehan M, Spezzano D, Zhu J, et al. Vaginal submucosal dendritic cells, but not Langerhans cells, induce protective Th1 responses to herpes simplex virus-2. *J Exp Med*. 2003;197(2):153-62.
12. Yeaman GR, Guyre PM, Fanger MW, Collins JE, White HD, Rathbun W, et al. Unique CD8+ T cell-rich lymphoid aggregates in human uterine endometrium. *J Leukoc Biol*. 1997;61(4):427-35.
13. Jensen AL, Collins J, Shipman EP, Wira CR, Guyre PM, Pioli PA. A subset of human uterine endometrial macrophages is alternatively activated. *Am J Reprod Immunol*. 2012;68(5):374-86.
14. Eidukaite A, Tamosiunas V. Endometrial and peritoneal macrophages: expression of activation and adhesion molecules. *Am J Reprod Immunol*. 2004;52(2):113-7.
15. Vacca P, Cantoni C, Vitale M, Prato C, Canegallo F, Fenoglio D, et al. Crosstalk between decidual NK and CD14+ myelomonocytic cells results in induction of Tregs and immunosuppression. *Proc Natl Acad Sci U S A*. 2010;107(26):11918-23.
16. Houser BL, Tilburgs T, Hill J, Nicotra ML, Strominger JL. Two unique human decidual macrophage populations. *Journal of immunology (Baltimore, Md : 1950)*. 2011;186(4):2633-42.
17. Kim SY, Romero R, Tarca AL, Bhatti G, Kim CJ, Lee J, et al. Methylome of fetal and maternal monocytes and macrophages at the feto-maternal interface. *Am J Reprod Immunol*. 2012;68(1):8-27.
18. Huang B, Faucette AN, Pawlitz MD, Pei B, Goyert JW, Zhou JZ, et al. Interleukin-33-induced expression of PIBF1 by decidual B cells protects against preterm labor. *Nat Med*. 2017;23(1):128-35.
19. Mantovani A, Cassatella MA, Costantini C, Jaillon S. Neutrophils in the activation and regulation of innate and adaptive immunity. *Nat Rev Immunol*. 2011;11(8):519-31.
20. Lee SK, Kim CJ, Kim DJ, Kang JH. Immune cells in the female reproductive tract. *Immune Netw*. 2015;15(1):16-26.

21. Salamonsen LA, Zhang J, Brasted M. Leukocyte networks and human endometrial remodelling. *J Reprod Immunol.* 2002;57(1-2):95-108.
22. Hahn S, Hasler P, Vokalova L, van Breda SV, Lapaire O, Than NG, et al. The role of neutrophil activation in determining the outcome of pregnancy and modulation by hormones and/or cytokines. *Clin Exp Immunol.* 2019;198(1):24-36.
23. Giaglis S, Stoikou M, Grimolizzi F, Subramanian BY, van Breda SV, Hoesli I, et al. Neutrophil migration into the placenta: Good, bad or deadly? *Cell Adh Migr.* 2016;10(1-2):208-25.
24. Vivier E, Artis D, Colonna M, Diefenbach A, Di Santo JP, Eberl G, et al. Innate Lymphoid Cells: 10 Years On. *Cell.* 2018;174(5):1054-66.
25. Doisne JM, Balmas E, Boulenouar S, Gaynor LM, Kieckbusch J, Gardner L, et al. Composition, Development, and Function of Uterine Innate Lymphoid Cells. *J Immunol.* 2015;195(8):3937-45.
26. Cording S, Medvedovic J, Cherrier M, Eberl G. Development and regulation of ROR γ t(+) innate lymphoid cells. *FEBS Lett.* 2014;588(22):4176-81.
27. Male V, Hughes T, McClory S, Colucci F, Caligiuri MA, Moffett A. Immature NK cells, capable of producing IL-22, are present in human uterine mucosa. *J Immunol.* 2010;185(7):3913-8.
28. Moffett-King A. Natural killer cells and pregnancy. *Nature Reviews Immunology.* 2002;2(9):656-63.
29. Geiselhart A, Dietl J, Marzusch K, Ruck P, Ruck M, Horny HP, et al. Comparative analysis of the immunophenotypes of decidual and peripheral blood large granular lymphocytes and T cells during early human pregnancy. *Am J Reprod Immunol.* 1995;33(4):315-22.
30. Vacca P, Moretta L, Moretta A, Mingari MC. Origin, phenotype and function of human natural killer cells in pregnancy. *Trends Immunol.* 2011;32(11):517-23.
31. Moffett A, Colucci F. Uterine NK cells: active regulators at the maternal-fetal interface. *J Clin Invest.* 2014;124(5):1872-9.
32. Thiruchelvam U, Wingfield M, O'Farrelly C. Natural Killer Cells: Key Players in Endometriosis. *Am J Reprod Immunol.* 2015;74(4):291-301.
33. Glover LE, Crosby D, Thiruchelvam U, Harmon C, Chorcora CN, Wingfield MB, et al. Uterine natural killer cell progenitor populations predict successful implantation in women with endometriosis-associated infertility. *Am J Reprod Immunol.* 2018;79(3).
34. Wang F, Qualls AE, Marques-Fernandez L, Colucci F. Biology and pathology of the uterine microenvironment and its natural killer cells. *Cellular & Molecular Immunology.* 2021;18(9):2101-13.
35. Southcombe JH, Mounce G, McGee K, Elghajji A, Brosens J, Quenby S, et al. An altered endometrial CD8 tissue resident memory T cell population in recurrent miscarriage. *Sci Rep.* 2017;7:41335.
36. Huang X, Liu L, Xu C, Peng X, Li D, Wang L, et al. Tissue-resident CD8(+) T memory cells with unique properties are present in human decidua during early pregnancy. *Am J Reprod Immunol.* 2020;84(1):e13254.
37. Lepore M, Kalinichenko A, Colone A, Paleja B, Singhal A, Tschumi A, et al. Parallel T-cell cloning and deep sequencing of human MAIT cells reveal stable oligoclonal TCR β repertoire. *Nat Commun.* 2014;5:3866.
38. Gibbs A, Leeansyah E, Introini A, Paquin-Proulx D, Hasselrot K, Andersson E, et al. MAIT cells reside in the female genital mucosa and are biased towards IL-17 and IL-22 production in response to bacterial stimulation. *Mucosal Immunol.* 2017;10(1):35-45.
39. Raffetseder J, Lindau R, van der Veen S, Berg G, Larsson M, Ernerudh J. MAIT Cells Balance the Requirements for Immune Tolerance and Anti-Microbial Defense During Pregnancy. *Front Immunol.* 2021;12:718168.

40. White HD, Crassi KM, Givan AL, Stern JE, Gonzalez JL, Memoli VA, et al. CD3+ CD8+ CTL activity within the human female reproductive tract: influence of stage of the menstrual cycle and menopause. *J Immunol.* 1997;158(6):3017-27.
41. Kahn DA, Baltimore D. Pregnancy induces a fetal antigen-specific maternal T regulatory cell response that contributes to tolerance. *Proc Natl Acad Sci U S A.* 2010;107(20):9299-304.
42. Rowe JH, Ertelt JM, Xin L, Way SS. Pregnancy imprints regulatory memory that sustains anergy to fetal antigen. *Nature.* 2012;490(7418):102-6.
43. Vargas-Rojas MI, Solleiro-Villavicencio H, Soto-Vega E. Th1, Th2, Th17 and Treg levels in umbilical cord blood in preeclampsia. *J Matern Fetal Neonatal Med.* 2016;29(10):1642-5.
44. Rouvier E, Luciani MF, Mattéi MG, Denizot F, Golstein P. CTLA-8, cloned from an activated T cell, bearing AU-rich messenger RNA instability sequences, and homologous to a herpesvirus saimiri gene. *The Journal of Immunology.* 1993;150(12):5445.
45. Brevi A, Cogrossi LL, Grazia G, Masciovecchio D, Impellizzieri D, Lacanfora L, et al. Much More Than IL-17A: Cytokines of the IL-17 Family Between Microbiota and Cancer. *Front Immunol.* 2020;11:565470.
46. Hymowitz SG, Filvaroff EH, Yin JP, Lee J, Cai L, Risser P, et al. IL-17s adopt a cystine knot fold: structure and activity of a novel cytokine, IL-17F, and implications for receptor binding. *Embo j.* 2001;20(19):5332-41.
47. Wright JF, Guo Y, Quazi A, Luxenberg DP, Bennett F, Ross JF, et al. Identification of an interleukin 17F/17A heterodimer in activated human CD4+ T cells. *J Biol Chem.* 2007;282(18):13447-55.
48. Yao Z, Fanslow WC, Seldin MF, Rousseau AM, Painter SL, Comeau MR, et al. Herpesvirus Saimiri encodes a new cytokine, IL-17, which binds to a novel cytokine receptor. *Immunity.* 1995;3(6):811-21.
49. Toy D, Kugler D, Wolfson M, Vanden Bos T, Gurgel J, Derry J, et al. Cutting edge: interleukin 17 signals through a heteromeric receptor complex. *J Immunol.* 2006;177(1):36-9.
50. Gaffen SL. Structure and signalling in the IL-17 receptor family. *Nature Reviews Immunology.* 2009;9(8):556-67.
51. Wright JF, Bennett F, Li B, Brooks J, Luxenberg DP, Whitters MJ, et al. The human IL-17F/IL-17A heterodimeric cytokine signals through the IL-17RA/IL-17RC receptor complex. *J Immunol.* 2008;181(4):2799-805.
52. Ely LK, Fischer S, Garcia KC. Structural basis of receptor sharing by interleukin 17 cytokines. *Nat Immunol.* 2009;10(12):1245-51.
53. Lee J, Ho WH, Maruoka M, Corpuz RT, Baldwin DT, Foster JS, et al. IL-17E, a Novel Proinflammatory Ligand for the IL-17 Receptor Homolog IL-17Rh1. 2001;276(2):1660-4.
54. Li TS, Li XN, Chang ZJ, Fu XY, Liu L. Identification and functional characterization of a novel interleukin 17 receptor: a possible mitogenic activation through ras/mitogen-activated protein kinase signaling pathway. *Cell Signal.* 2006;18(8):1287-98.
55. Pancer Z, Mayer WE, Klein J, Cooper MD. Prototypic T cell receptor and CD4-like coreceptor are expressed by lymphocytes in the agnathan sea lamprey. *Proc Natl Acad Sci U S A.* 2004;101(36):13273-8.
56. Amatya N, Garg AV, Gaffen SL. IL-17 Signaling: The Yin and the Yang. *Trends Immunol.* 2017;38(5):310-22.
57. Novatchkova M, Leibbrandt A, Werzowa J, Neubüser A, Eisenhaber F. The STIR-domain superfamily in signal transduction, development and immunity. *Trends Biochem Sci.* 2003;28(5):226-9.
58. Maitra A, Shen F, Hanel W, Mossman K, Tocker J, Swart D, et al. Distinct functional motifs within the IL-17 receptor regulate signal transduction and target gene expression. *Proceedings of the National Academy of Sciences.* 2007;104(18):7506.
59. Maezawa Y, Nakajima H, Suzuki K, Tamachi T, Ikeda K, Inoue J, et al. Involvement of TNF receptor-associated factor 6 in IL-25 receptor signaling. *J Immunol.* 2006;176(2):1013-8.

60. Goepfert A, Lehmann S, Blank J, Kolbinger F, Rondeau JM. Structural Analysis Reveals that the Cytokine IL-17F Forms a Homodimeric Complex with Receptor IL-17RC to Drive IL-17RA-Independent Signaling. *Immunity*. 2020;52(3):499-512.e5.
61. Benderdour M, Tardif G, Pelletier JP, Di Battista JA, Reboul P, Ranger P, et al. Interleukin 17 (IL-17) induces collagenase-3 production in human osteoarthritic chondrocytes via AP-1 dependent activation: differential activation of AP-1 members by IL-17 and IL-1beta. *J Rheumatol*. 2002;29(6):1262-72.
62. Hartupée J, Liu C, Novotny M, Sun D, Li X, Hamilton TA. IL-17 signaling for mRNA stabilization does not require TNF receptor-associated factor 6. *J Immunol*. 2009;182(3):1660-6.
63. Hartupée J, Liu C, Novotny M, Li X, Hamilton T. IL-17 enhances chemokine gene expression through mRNA stabilization. *J Immunol*. 2007;179(6):4135-41.
64. Datta S, Novotny M, Pavicic PG, Jr., Zhao C, Herjan T, Hartupée J, et al. IL-17 regulates CXCL1 mRNA stability via an AUUUA/tristetraprolin-independent sequence. *J Immunol*. 2010;184(3):1484-91.
65. Henness S, van Thoor E, Ge Q, Armour CL, Hughes JM, Ammit AJ. IL-17A acts via p38 MAPK to increase stability of TNF-alpha-induced IL-8 mRNA in human ASM. *Am J Physiol Lung Cell Mol Physiol*. 2006;290(6):L1283-90.
66. Henness S, Johnson CK, Ge Q, Armour CL, Hughes JM, Ammit AJ. IL-17A augments TNF-alpha-induced IL-6 expression in airway smooth muscle by enhancing mRNA stability. *J Allergy Clin Immunol*. 2004;114(4):958-64.
67. Andoh A, Hata K, Araki Y, Fujiyama Y, Bamba T. Interleukin (IL)-4 and IL-17 synergistically stimulate IL-6 secretion in human colonic myofibroblasts. *Int J Mol Med*. 2002;10(5):631-4.
68. Ruddy MJ, Wong GC, Liu XK, Yamamoto H, Kasayama S, Kirkwood KL, et al. Functional cooperation between interleukin-17 and tumor necrosis factor-alpha is mediated by CCAAT/enhancer-binding protein family members. *J Biol Chem*. 2004;279(4):2559-67.
69. Verma AH, Richardson JP, Zhou C, Coleman BM, Moyes DL, Ho J, et al. Oral epithelial cells orchestrate innate type 17 responses to *Candida albicans* through the virulence factor candidalysin. *Sci Immunol*. 2017;2(17).
70. Song X, Dai D, He X, Zhu S, Yao Y, Gao H, et al. Growth Factor FGF2 Cooperates with Interleukin-17 to Repair Intestinal Epithelial Damage. *Immunity*. 2015;43(3):488-501.
71. Wu L, Chen X, Zhao J, Martin B, Zepp JA, Ko JS, et al. A novel IL-17 signaling pathway controlling keratinocyte proliferation and tumorigenesis via the TRAF4-ERK5 axis. *J Exp Med*. 2015;212(10):1571-87.
72. Shi Y, Ullrich SJ, Zhang J, Connolly K, Grzegorzewski KJ, Barber MC, et al. A Novel Cytokine Receptor-Ligand Pair. *Journal of Biological Chemistry*. 2000;275(25):19167-76.
73. Rickel EA, Siegel LA, Yoon B-RP, Rottman JB, Kugler DG, Swart DA, et al. Identification of Functional Roles for Both IL-17RB and IL-17RA in Mediating IL-25-Induced Activities. *The Journal of Immunology*. 2008;181(6):4299-310.
74. Claudio E, Sønder SU, Saret S, Carvalho G, Ramalingam TR, Wynn TA, et al. The adaptor protein CIKS/Act1 is essential for IL-25-mediated allergic airway inflammation. *J Immunol*. 2009;182(3):1617-30.
75. Swaidani S, Bulek K, Kang Z, Liu C, Lu Y, Yin W, et al. The critical role of epithelial-derived Act1 in IL-17- and IL-25-mediated pulmonary inflammation. *J Immunol*. 2009;182(3):1631-40.
76. Angkasekwinai P, Park H, Wang YH, Wang YH, Chang SH, Corry DB, et al. Interleukin 25 promotes the initiation of proallergic type 2 responses. *J Exp Med*. 2007;204(7):1509-17.
77. Kuestner RE, Taft DW, Haran A, Brandt CS, Brender T, Lum K, et al. Identification of the IL-17 receptor related molecule IL-17RC as the receptor for IL-17F. *J Immunol*. 2007;179(8):5462-73.
78. Rong Z, Wang A, Li Z, Ren Y, Cheng L, Li Y, et al. IL-17RD (Sef or IL-17RLM) interacts with IL-17 receptor and mediates IL-17 signaling. *Cell Res*. 2009;19(2):208-15.

79. Tsang M, Friesel R, Kudoh T, Dawid IB. Identification of Sef, a novel modulator of FGF signalling. *Nat Cell Biol.* 2002;4(2):165-9.
80. Xiong S, Zhao Q, Rong Z, Huang G, Huang Y, Chen P, et al. hSef inhibits PC-12 cell differentiation by interfering with Ras-mitogen-activated protein kinase MAPK signaling. *J Biol Chem.* 2003;278(50):50273-82.
81. Yang RB, Ng CK, Wasserman SM, Kömüves LG, Gerritsen ME, Topper JN. A novel interleukin-17 receptor-like protein identified in human umbilical vein endothelial cells antagonizes basic fibroblast growth factor-induced signaling. *J Biol Chem.* 2003;278(35):33232-8.
82. Fossiez F, Djossou O, Chomarat P, Flores-Romo L, Ait-Yahia S, Maat C, et al. T cell interleukin-17 induces stromal cells to produce proinflammatory and hematopoietic cytokines. *J Exp Med.* 1996;183(6):2593-603.
83. Awane M, Andres PG, Li DJ, Reinecker HC. NF-kappa B-inducing kinase is a common mediator of IL-17-, TNF-alpha-, and IL-1 beta-induced chemokine promoter activation in intestinal epithelial cells. *J Immunol.* 1999;162(9):5337-44.
84. Parsonage G, Filer A, Bik M, Hardie D, Lax S, Howlett K, et al. Prolonged, granulocyte-macrophage colony-stimulating factor-dependent, neutrophil survival following rheumatoid synovial fibroblast activation by IL-17 and TNFalpha. *Arthritis Res Ther.* 2008;10(2):R47.
85. Tollin M, Bergman P, Svenberg T, Jörnvall H, Gudmundsson GH, Agerberth B. Antimicrobial peptides in the first line defence of human colon mucosa. *Peptides.* 2003;24(4):523-30.
86. Liang SC, Tan XY, Luxenberg DP, Karim R, Dunussi-Joannopoulos K, Collins M, et al. Interleukin (IL)-22 and IL-17 are coexpressed by Th17 cells and cooperatively enhance expression of antimicrobial peptides. *J Exp Med.* 2006;203(10):2271-9.
87. Chabaud M, Garnero P, Dayer JM, Guerne PA, Fossiez F, Miossec P. Contribution of interleukin 17 to synovium matrix destruction in rheumatoid arthritis. *Cytokine.* 2000;12(7):1092-9.
88. Lee JS, Tato CM, Joyce-Shaikh B, Gulen MF, Cayatte C, Chen Y, et al. Interleukin-23-Independent IL-17 Production Regulates Intestinal Epithelial Permeability. *Immunity.* 2015;43(4):727-38.
89. Chen Y, Thai P, Zhao YH, Ho YS, DeSouza MM, Wu R. Stimulation of airway mucin gene expression by interleukin (IL)-17 through IL-6 paracrine/autocrine loop. *J Biol Chem.* 2003;278(19):17036-43.
90. Ramani K, Garg AV, Jawale CV, Conti HR, Whibley N, Jackson EK, et al. The Kallikrein-Kinin System: A Novel Mediator of IL-17-Driven Anti-Candida Immunity in the Kidney. *PLoS Pathog.* 2016;12(11):e1005952.
91. Conti HR, Baker O, Freeman AF, Jang WS, Holland SM, Li RA, et al. New mechanism of oral immunity to mucosal candidiasis in hyper-IgE syndrome. *Mucosal Immunol.* 2011;4(4):448-55.
92. Patel DN, King CA, Bailey SR, Holt JW, Venkatachalam K, Agrawal A, et al. Interleukin-17 stimulates C-reactive protein expression in hepatocytes and smooth muscle cells via p38 MAPK and ERK1/2-dependent NF-kappaB and C/EBPbeta activation. *J Biol Chem.* 2007;282(37):27229-38.
93. Li H, Chen J, Huang A, Stinson J, Heldens S, Foster J, et al. Cloning and characterization of IL-17B and IL-17C, two new members of the IL-17 cytokine family. *Proc Natl Acad Sci U S A.* 2000;97(2):773-8.
94. Kouri VP, Olkkonen J, Ainola M, Li TF, Björkman L, Konttinen YT, et al. Neutrophils produce interleukin-17B in rheumatoid synovial tissue. *Rheumatology (Oxford).* 2014;53(1):39-47.

95. Zhou J, Ren L, Chen D, Lin X, Huang S, Yin Y, et al. IL-17B is elevated in patients with pneumonia and mediates IL-8 production in bronchial epithelial cells. *Clin Immunol.* 2017;175:91-8.
96. Shi Y, Ullrich SJ, Zhang J, Connolly K, Grzegorzewski KJ, Barber MC, et al. A novel cytokine receptor-ligand pair. Identification, molecular characterization, and in vivo immunomodulatory activity. *J Biol Chem.* 2000;275(25):19167-76.
97. Yamaguchi Y, Fujio K, Shoda H, Okamoto A, Tsuno NH, Takahashi K, et al. IL-17B and IL-17C are associated with TNF-alpha production and contribute to the exacerbation of inflammatory arthritis. *J Immunol.* 2007;179(10):7128-36.
98. Song X, Zhu S, Shi P, Liu Y, Shi Y, Levin SD, et al. IL-17RE is the functional receptor for IL-17C and mediates mucosal immunity to infection with intestinal pathogens. *Nature Immunology.* 2011;12(12):1151-8.
99. Ramirez-Carrozzi V, Sambandam A, Luis E, Lin Z, Jeet S, Lesch J, et al. IL-17C regulates the innate immune function of epithelial cells in an autocrine manner. *Nat Immunol.* 2011;12(12):1159-66.
100. Reynolds JM, Martinez GJ, Nallaparaju KC, Chang SH, Wang YH, Dong C. Cutting edge: regulation of intestinal inflammation and barrier function by IL-17C. *J Immunol.* 2012;189(9):4226-30.
101. Wolf L, Sapich S, Honecker A, Jungnickel C, Seiler F, Bischoff M, et al. IL-17A-mediated expression of epithelial IL-17C promotes inflammation during acute *Pseudomonas aeruginosa* pneumonia. *Am J Physiol Lung Cell Mol Physiol.* 2016;311(5):L1015-122.
102. Chang SH, Reynolds JM, Pappu BP, Chen G, Martinez GJ, Dong C. Interleukin-17C promotes Th17 cell responses and autoimmune disease via interleukin-17 receptor E. *Immunity.* 2011;35(4):611-21.
103. Han Q, Das S, Hirano M, Holland SJ, McCurley N, Guo P, et al. Characterization of Lamprey IL-17 Family Members and Their Receptors. *J Immunol.* 2015;195(11):5440-51.
104. Starnes T, Broxmeyer HE, Robertson MJ, Hromas R. Cutting edge: IL-17D, a novel member of the IL-17 family, stimulates cytokine production and inhibits hemopoiesis. *J Immunol.* 2002;169(2):642-6.
105. Seelige R, Washington A, Jr., Bui JD. The ancient cytokine IL-17D is regulated by Nrf2 and mediates tumor and virus surveillance. *Cytokine.* 2017;91:10-2.
106. Saddawi-Konefka R, Seelige R, Gross ET, Levy E, Searles SC, Washington A, Jr., et al. Nrf2 Induces IL-17D to Mediate Tumor and Virus Surveillance. *Cell Rep.* 2016;16(9):2348-58.
107. von Moltke J, Ji M, Liang HE, Locksley RM. Tuft-cell-derived IL-25 regulates an intestinal ILC2-epithelial response circuit. *Nature.* 2016;529(7585):221-5.
108. Fort MM, Cheung J, Yen D, Li J, Zurawski SM, Lo S, et al. IL-25 induces IL-4, IL-5, and IL-13 and Th2-associated pathologies in vivo. *Immunity.* 2001;15(6):985-95.
109. Akimzhanov AM, Yang XO, Dong C. Chromatin remodeling of interleukin-17 (IL-17)-IL-17F cytokine gene locus during inflammatory helper T cell differentiation. *J Biol Chem.* 2007;282(9):5969-72.
110. Chang SH, Dong C. A novel heterodimeric cytokine consisting of IL-17 and IL-17F regulates inflammatory responses. *Cell Res.* 2007;17(5):435-40.
111. Harrington LE, Hatton RD, Mangan PR, Turner H, Murphy TL, Murphy KM, et al. Interleukin 17-producing CD4+ effector T cells develop via a lineage distinct from the T helper type 1 and 2 lineages. *Nat Immunol.* 2005;6(11):1123-32.
112. Veldhoen M, Hocking RJ, Atkins CJ, Locksley RM, Stockinger B. TGFbeta in the context of an inflammatory cytokine milieu supports de novo differentiation of IL-17-producing T cells. *Immunity.* 2006;24(2):179-89.
113. Ghoreschi K, Laurence A, Yang XP, Tato CM, McGeachy MJ, Konkel JE, et al. Generation of pathogenic T(H)17 cells in the absence of TGF-beta signalling. *Nature.* 2010;467(7318):967-71.

114. Conti HR, Peterson AC, Brane L, Huppler AR, Hernández-Santos N, Whibley N, et al. Oral-resident natural Th17 cells and $\gamma\delta$ T cells control opportunistic *Candida albicans* infections. *J Exp Med*. 2014;211(10):2075-84.
115. Borkner L, Curham LM, Wilk MM, Moran B, Mills KHG. IL-17 mediates protective immunity against nasal infection with *Bordetella pertussis* by mobilizing neutrophils, especially Siglec-F(+) neutrophils. *Mucosal immunology*. 2021;14(5):1183-202.
116. Hamada H, Garcia-Hernandez MdLL, Reome JB, Misra SK, Strutt TM, McKinstry KK, et al. Tc17, a unique subset of CD8 T cells that can protect against lethal influenza challenge. *Journal of immunology (Baltimore, Md : 1950)*. 2009;182(6):3469-81.
117. Michel ML, Keller AC, Paget C, Fujio M, Trottein F, Savage PB, et al. Identification of an IL-17-producing NK1.1(neg) iNKT cell population involved in airway neutrophilia. *J Exp Med*. 2007;204(5):995-1001.
118. Passos ST, Silver JS, O'Hara AC, Sehy D, Stumhofer JS, Hunter CA. IL-6 promotes NK cell production of IL-17 during toxoplasmosis. *J Immunol*. 2010;184(4):1776-83.
119. Takahashi N, Vanlaere I, de Rycke R, Cauwels A, Joosten LA, Lubberts E, et al. IL-17 produced by Paneth cells drives TNF-induced shock. *J Exp Med*. 2008;205(8):1755-61.
120. Li L, Huang L, Vergis AL, Ye H, Bajwa A, Narayan V, et al. IL-17 produced by neutrophils regulates IFN-gamma-mediated neutrophil migration in mouse kidney ischemia-reperfusion injury. *J Clin Invest*. 2010;120(1):331-42.
121. Stockinger B, Omenetti S. The dichotomous nature of T helper 17 cells. *Nat Rev Immunol*. 2017;17(9):535-44.
122. Pappu R, Ramirez-Carrozzi V, Sambandam A. The interleukin-17 cytokine family: critical players in host defence and inflammatory diseases. *Immunology*. 2011;134(1):8-16.
123. Owyang AM, Zaph C, Wilson EH, Guild KJ, McClanahan T, Miller HR, et al. Interleukin 25 regulates type 2 cytokine-dependent immunity and limits chronic inflammation in the gastrointestinal tract. *J Exp Med*. 2006;203(4):843-9.
124. Hvid M, Vestergaard C, Kemp K, Christensen GB, Deleuran B, Deleuran M. IL-25 in atopic dermatitis: a possible link between inflammation and skin barrier dysfunction? *J Invest Dermatol*. 2011;131(1):150-7.
125. Rosani U, Varotto L, Gerdol M, Pallavicini A, Venier P. IL-17 signaling components in bivalves: Comparative sequence analysis and involvement in the immune responses. *Dev Comp Immunol*. 2015;52(2):255-68.
126. Du L, Feng S, Yin L, Wang X, Zhang A, Yang K, et al. Identification and functional characterization of grass carp IL-17A/F1: An evaluation of the immunoregulatory role of teleost IL-17A/F1. *Dev Comp Immunol*. 2015;51(1):202-11.
127. Kokubu T, Haudenschild DR, Moseley TA, Rose L, Reddi AH. Immunolocalization of IL-17A, IL-17B, and their receptors in chondrocytes during fracture healing. *J Histochem Cytochem*. 2008;56(2):89-95.
128. Moore EE, Presnell S, Garrigues U, Guilbot A, LeGuern E, Smith D, et al. Expression of IL-17B in neurons and evaluation of its possible role in the chromosome 5q-linked form of Charcot-Marie-Tooth disease. *Neuromuscul Disord*. 2002;12(2):141-50.
129. Huang J, Meng S, Hong S, Lin X, Jin W, Dong C. IL-17C is required for lethal inflammation during systemic fungal infection. *Cell Mol Immunol*. 2016;13(4):474-83.
130. Schneider C, O'Leary CE, von Moltke J, Liang HE, Ang QY, Turnbaugh PJ, et al. A Metabolite-Triggered Tuft Cell-ILC2 Circuit Drives Small Intestinal Remodeling. *Cell*. 2018;174(2):271-84.e14.
131. Senra L, Stalder R, Alvarez Martinez D, Chizzolini C, Boehncke WH, Brembilla NC. Keratinocyte-Derived IL-17E Contributes to Inflammation in Psoriasis. *J Invest Dermatol*. 2016;136(10):1970-80.

132. Sonobe Y, Takeuchi H, Kataoka K, Li H, Jin S, Mimuro M, et al. Interleukin-25 expressed by brain capillary endothelial cells maintains blood-brain barrier function in a protein kinase C ϵ -dependent manner. *J Biol Chem*. 2016;291(24):12573.
133. Chen Y, Chen Y, Cao P, Su W, Zhan N, Dong W. *Fusobacterium nucleatum* facilitates ulcerative colitis through activating IL-17F signaling to NF- κ B via the upregulation of CARD3 expression. *J Pathol*. 2020;250(2):170-82.
134. Costa MM, Pereiro P, Wang T, Secombes CJ, Figueras A, Novoa B. Characterization and gene expression analysis of the two main Th17 cytokines (IL-17A/F and IL-22) in turbot, *Scophthalmus maximus*. *Dev Comp Immunol*. 2012;38(4):505-16.
135. Cao Y, Yang S, Feng C, Zhan W, Zheng Z, Wang Q, et al. Evolution and function analysis of interleukin-17 gene from *Pinctada fucata martensii*. *Fish Shellfish Immunol*. 2019;88:102-10.
136. Veldhoen M. Interleukin 17 is a chief orchestrator of immunity. *Nat Immunol*. 2017;18(6):612-21.
137. Castro G, Liu X, Ngo K, De Leon-Tabaldo A, Zhao S, Luna-Roman R, et al. ROR γ t and ROR α signature genes in human Th17 cells. *PLoS One*. 2017;12(8):e0181868.
138. Solt LA, Kumar N, Nuhant P, Wang Y, Lauer JL, Liu J, et al. Suppression of TH17 differentiation and autoimmunity by a synthetic ROR ligand. *Nature*. 2011;472(7344):491-4.
139. Withers DR, Hepworth MR, Wang X, Mackley EC, Halford EE, Dutton EE, et al. Transient inhibition of ROR- γ t therapeutically limits intestinal inflammation by reducing TH17 cells and preserving group 3 innate lymphoid cells. *Nat Med*. 2016;22(3):319-23.
140. Khan D, Ansar Ahmed S. Regulation of IL-17 in autoimmune diseases by transcriptional factors and microRNAs. *Front Genet*. 2015;6:236-.
141. Liu HP, Cao AT, Feng T, Li Q, Zhang W, Yao S, et al. TGF- β converts Th1 cells into Th17 cells through stimulation of Runx1 expression. *Eur J Immunol*. 2015;45(4):1010-8.
142. Dang EV, Barbi J, Yang HY, Jinasena D, Yu H, Zheng Y, et al. Control of T(H)17/T(reg) balance by hypoxia-inducible factor 1. *Cell*. 2011;146(5):772-84.
143. Ye P, Garvey PB, Zhang P, Nelson S, Bagby G, Summer WR, et al. Interleukin-17 and lung host defense against *Klebsiella pneumoniae* infection. *Am J Respir Cell Mol Biol*. 2001;25(3):335-40.
144. Li J, Vinh DC, Casanova J-L, Puel A. Inborn errors of immunity underlying fungal diseases in otherwise healthy individuals. *Current Opinion in Microbiology*. 2017;40:46-57.
145. Yarbrough VL, Winkle S, Herbst-Kralovetz MM. Antimicrobial peptides in the female reproductive tract: a critical component of the mucosal immune barrier with physiological and clinical implications. *Hum Reprod Update*. 2015;21(3):353-77.
146. McGeachy MJ, Cua DJ, Gaffen SL. The IL-17 Family of Cytokines in Health and Disease. *Immunity*. 2019;50(4):892-906.
147. Liu T, Li S, Ying S, Tang S, Ding Y, Li Y, et al. The IL-23/IL-17 Pathway in Inflammatory Skin Diseases: From Bench to Bedside. *Frontiers in Immunology*. 2020;11.
148. Harbour SN, Maynard CL, Zindl CL, Schoeb TR, Weaver CT. Th17 cells give rise to Th1 cells that are required for the pathogenesis of colitis. *Proc Natl Acad Sci U S A*. 2015;112(22):7061-6.
149. Reynolds JM, Lee YH, Shi Y, Wang X, Angkasekwinai P, Nallaparaju KC, et al. Interleukin-17B Antagonizes Interleukin-25-Mediated Mucosal Inflammation. *Immunity*. 2015;42(4):692-703.
150. Su J, Chen T, Ji XY, Liu C, Yadav PK, Wu R, et al. IL-25 downregulates Th1/Th17 immune response in an IL-10-dependent manner in inflammatory bowel disease. *Inflamm Bowel Dis*. 2013;19(4):720-8.
151. Zrioual S, Ecochard R, Tournadre A, Lenief V, Cazalis MA, Miossec P. Genome-wide comparison between IL-17A- and IL-17F-induced effects in human rheumatoid arthritis synoviocytes. *J Immunol*. 2009;182(5):3112-20.

152. Marinoni B, Ceribelli A, Massarotti MS, Selmi C. The Th17 axis in psoriatic disease: pathogenetic and therapeutic implications. *Autoimmunity Highlights*. 2014;5(1):9-19.
153. Kenna TJ, Davidson SI, Duan R, Bradbury LA, McFarlane J, Smith M, et al. Enrichment of circulating interleukin-17-secreting interleukin-23 receptor-positive γ/δ T cells in patients with active ankylosing spondylitis. *Arthritis Rheum*. 2012;64(5):1420-9.
154. Johansen C, Usher PA, Kjellerup RB, Lundsgaard D, Iversen L, Kragballe K. Characterization of the interleukin-17 isoforms and receptors in lesional psoriatic skin. *Br J Dermatol*. 2009;160(2):319-24.
155. Fujino S, Andoh A, Bamba S, Ogawa A, Hata K, Araki Y, et al. Increased expression of interleukin 17 in inflammatory bowel disease. *Gut*. 2003;52(1):65-70.
156. Kleinschek MA, Boniface K, Sadekova S, Grein J, Murphy EE, Turner SP, et al. Circulating and gut-resident human Th17 cells express CD161 and promote intestinal inflammation. *J Exp Med*. 2009;206(3):525-34.
157. Lock C, Hermans G, Pedotti R, Brendolan A, Schadt E, Garren H, et al. Gene-microarray analysis of multiple sclerosis lesions yields new targets validated in autoimmune encephalomyelitis. *Nat Med*. 2002;8(5):500-8.
158. Benakis C, Brea D, Caballero S, Faraco G, Moore J, Murphy M, et al. Commensal microbiota affects ischemic stroke outcome by regulating intestinal $\gamma\delta$ T cells. *Nature Medicine*. 2016;22(5):516-23.
159. Xu D, Robinson AP, Ishii T, Duncan DAS, Alden TD, Goings GE, et al. Peripherally derived T regulatory and $\gamma\delta$ T cells have opposing roles in the pathogenesis of intractable pediatric epilepsy. *Journal of Experimental Medicine*. 2018;215(4):1169-86.
160. Ahmed M, Gaffen SL. IL-17 inhibits adipogenesis in part via C/EBP α , PPAR γ and Krüppel-like factors. *Cytokine*. 2013;61(3):898-905.
161. Zúñiga LA, Shen WJ, Joyce-Shaikh B, Pyatnova EA, Richards AG, Thom C, et al. IL-17 regulates adipogenesis, glucose homeostasis, and obesity. *J Immunol*. 2010;185(11):6947-59.
162. Chen S, Shimada K, Zhang W, Huang G, Crother TR, Ardit M. IL-17A is proatherogenic in high-fat diet-induced and *Chlamydia pneumoniae* infection-accelerated atherosclerosis in mice. *J Immunol*. 2010;185(9):5619-27.
163. Chen X, Cai G, Liu C, Zhao J, Gu C, Wu L, et al. IL-17R–EGFR axis links wound healing to tumorigenesis in Lrig1+ stem cells. *Journal of Experimental Medicine*. 2018;216(1):195-214.
164. Langowski JL, Zhang X, Wu L, Mattson JD, Chen T, Smith K, et al. IL-23 promotes tumour incidence and growth. *Nature*. 2006;442(7101):461-5.
165. Calcinotto A, Brevi A, Chesi M, Ferrarese R, Garcia Perez L, Grioni M, et al. Microbiota-driven interleukin-17-producing cells and eosinophils synergize to accelerate multiple myeloma progression. *Nat Commun*. 2018;9(1):4832.
166. Choi GB, Yim YS, Wong H, Kim S, Kim H, Kim SV, et al. The maternal interleukin-17a pathway in mice promotes autism-like phenotypes in offspring. *Science*. 2016;351(6276):933-9.
167. Ryan AW, Thornton JM, Brophy K, Daly JS, McLoughlin RM, O'Morain C, et al. Chromosome 5q candidate genes in coeliac disease: genetic variation at IL4, IL5, IL9, IL13, IL17B and NR3C1. *Tissue Antigens*. 2005;65(2):150-5.
168. Robak E, Kulczycka-Siennicka L, Gerlicz Z, Kierstan M, Korycka-Wolowiec A, Sysa-Jedrzejowska A. Correlations between concentrations of interleukin (IL)-17A, IL-17B and IL-17F, and endothelial cells and proangiogenic cytokines in systemic lupus erythematosus patients. *Eur Cytokine Netw*. 2013;24(1):60-8.
169. Bie Q, Jin C, Zhang B, Dong H. IL-17B: A new area of study in the IL-17 family. *Mol Immunol*. 2017;90:50-6.
170. Bie Q, Sun C, Gong A, Li C, Su Z, Zheng D, et al. Non-tumor tissue derived interleukin-17B activates IL-17RB/AKT/ β -catenin pathway to enhance the stemness of gastric cancer. *Sci Rep*. 2016;6:25447.

171. Butcher MJ, Waseem TC, Galkina EV. Smooth Muscle Cell-Derived Interleukin-17C Plays an Atherogenic Role via the Recruitment of Proinflammatory Interleukin-17A+ T Cells to the Aorta. *Arterioscler Thromb Vasc Biol.* 2016;36(8):1496-506.
172. Krohn S, Nies JF, Kapffer S, Schmidt T, Riedel JH, Kaffke A, et al. IL-17C/IL-17 Receptor E Signaling in CD4(+) T Cells Promotes T(H)17 Cell-Driven Glomerular Inflammation. *J Am Soc Nephrol.* 2018;29(4):1210-22.
173. Song X, Gao H, Lin Y, Yao Y, Zhu S, Wang J, et al. Alterations in the microbiota drive interleukin-17C production from intestinal epithelial cells to promote tumorigenesis. *Immunity.* 2014;40(1):140-52.
174. Jungnickel C, Schmidt LH, Bittigkoffer L, Wolf L, Wolf A, Ritzmann F, et al. IL-17C mediates the recruitment of tumor-associated neutrophils and lung tumor growth. *Oncogene.* 2017;36(29):4182-90.
175. Stamp LK, Easson A, Lehnigk U, Highton J, Hessian PA. Different T cell subsets in the nodule and synovial membrane: absence of interleukin-17A in rheumatoid nodules. *Arthritis Rheum.* 2008;58(6):1601-8.
176. Wang YH, Angkasekwinai P, Lu N, Voo KS, Arima K, Hanabuchi S, et al. IL-25 augments type 2 immune responses by enhancing the expansion and functions of TSLP-DC-activated Th2 memory cells. *J Exp Med.* 2007;204(8):1837-47.
177. Li Q, Ma L, Shen S, Guo Y, Cao Q, Cai X, et al. Intestinal dysbacteriosis-induced IL-25 promotes development of HCC via alternative activation of macrophages in tumor microenvironment. *J Exp Clin Cancer Res.* 2019;38(1):303.
178. Ishigame H, Kakuta S, Nagai T, Kadoki M, Nambu A, Komiyama Y, et al. Differential roles of interleukin-17A and -17F in host defense against mucoc epithelial bacterial infection and allergic responses. *Immunity.* 2009;30(1):108-19.
179. Chung AS, Wu X, Zhuang G, Ngu H, Kasman I, Zhang J, et al. An interleukin-17-mediated paracrine network promotes tumor resistance to anti-angiogenic therapy. *Nat Med.* 2013;19(9):1114-23.
180. Benatar T, Cao MY, Lee Y, Lightfoot J, Feng N, Gu X, et al. IL-17E, a proinflammatory cytokine, has antitumor efficacy against several tumor types in vivo. *Cancer Immunol Immunother.* 2010;59(6):805-17.
181. Furuta S, Jeng YM, Zhou L, Huang L, Kuhn I, Bissell MJ, et al. IL-25 causes apoptosis of IL-25R-expressing breast cancer cells without toxicity to nonmalignant cells. *Sci Transl Med.* 2011;3(78):78ra31.
182. Hueber W, Sands BE, Lewitzky S, Vandemeulebroecke M, Reinisch W, Higgins PD, et al. Secukinumab, a human anti-IL-17A monoclonal antibody, for moderate to severe Crohn's disease: unexpected results of a randomised, double-blind placebo-controlled trial. *Gut.* 2012;61(12):1693-700.
183. Targan SR, Feagan B, Vermeire S, Panaccione R, Melmed GY, Landers C, et al. A Randomized, Double-Blind, Placebo-Controlled Phase 2 Study of Brodalumab in Patients With Moderate-to-Severe Crohn's Disease. *Am J Gastroenterol.* 2016;111(11):1599-607.
184. Davidson L, van den Reek J, Bruno M, van Hunsel F, Herings RMC, Matzaraki V, et al. Risk of candidiasis associated with interleukin-17 inhibitors: A real-world observational study of multiple independent sources. *Lancet Reg Health Eur.* 2022;13:100266.
185. Ander SE, Diamond MS, Coyne CB. Immune responses at the maternal-fetal interface. *Sci Immunol.* 2019;4(31).
186. Colucci F. The immunological code of pregnancy. *Science.* 2019;365(6456):862-3.
187. Förger F, Villiger PM. Immunological adaptations in pregnancy that modulate rheumatoid arthritis disease activity. *Nat Rev Rheumatol.* 2020;16(2):113-22.
188. Dunn CL, Kelly RW, Critchley HO. Decidualization of the human endometrial stromal cell: an enigmatic transformation. *Reprod Biomed Online.* 2003;7(2):151-61.

189. Leimert KB, Xu W, Princ MM, Chemtob S, Olson DM. Inflammatory Amplification: A Central Tenet of Uterine Transition for Labor. *Front Cell Infect Microbiol.* 2021;11:660983.
190. Thiruchelvam U, Wingfield M, O'Farrelly C. Increased uNK Progenitor Cells in Women With Endometriosis and Infertility are Associated With Low Levels of Endometrial Stem Cell Factor. *Am J Reprod Immunol.* 2016;75(4):493-502.
191. Megli CJ, Coyne CB. Infections at the maternal–fetal interface: an overview of pathogenesis and defence. *Nature Reviews Microbiology.* 2022;20(2):67-82.
192. Jiang J, Karimi O, Ouburg S, Champion CI, Khurana A, Liu G, et al. Interruption of CXCL13-CXCR5 axis increases upper genital tract pathology and activation of NKT cells following chlamydial genital infection. *PLoS One.* 2012;7(11):e47487.
193. Conti HR, Gaffen SL. IL-17-Mediated Immunity to the Opportunistic Fungal Pathogen *Candida albicans*. *J Immunol.* 2015;195(3):780-8.
194. Wu HX, Jin LP, Xu B, Liang SS, Li DJ. Decidual stromal cells recruit Th17 cells into decidua to promote proliferation and invasion of human trophoblast cells by secreting IL-17. *Cell Mol Immunol.* 2014;11(3):253-62.
195. Wang Y, Zhang Y, Li MQ, Fan DX, Wang XH, Li DJ, et al. Interleukin-25 induced by human chorionic gonadotropin promotes the proliferation of decidual stromal cells by activation of JNK and AKT signal pathways. *Fertil Steril.* 2014;102(1):257-63.
196. Pongcharoen S, Supalap K. Interleukin-17 increased progesterone secretion by JEG-3 human choriocarcinoma cells. *Am J Reprod Immunol.* 2009;61(4):261-4.
197. Martínez-García EA, Chávez-Robles B, Sánchez-Hernández PE, Núñez-Atahualpa L, Martín-Máquez BT, Muñoz-Gómez A, et al. IL-17 increased in the third trimester in healthy women with term labor. *Am J Reprod Immunol.* 2011;65(2):99-103.
198. Kaminski VL, Ellwanger JH, Matte MCC, Savaris RF, Vianna P, Chies JAB. IL-17 blood levels increase in healthy pregnancy but not in spontaneous abortion. *Mol Biol Rep.* 2018;45(5):1565-8.
199. Lombardelli L, Logiodice F, Aguerre-Girr M, Kullolli O, Haller H, Casart Y, et al. Interleukin-17-producing decidual CD4+ T cells are not deleterious for human pregnancy when they also produce interleukin-4. *Clin Mol Allergy.* 2016;14:1.
200. Logiodice F, Lombardelli L, Kullolli O, Haller H, Maggi E, Rukavina D, et al. Decidual Interleukin-22-Producing CD4+ T Cells (Th17/Th0/IL-22+ and Th17/Th2/IL-22+, Th2/IL-22+, Th0/IL-22+), Which Also Produce IL-4, Are Involved in the Success of Pregnancy. *Int J Mol Sci.* 2019;20(2).
201. Bulun SE, Yilmaz BD, Sison C, Miyazaki K, Bernardi L, Liu S, et al. Endometriosis. *Endocr Rev.* 2019;40(4):1048-79.
202. Sourial S, Tempest N, Hapangama DK. Theories on the pathogenesis of endometriosis. *Int J Reprod Med.* 2014;2014:179515.
203. Hirata T, Osuga Y, Hamasaki K, Yoshino O, Ito M, Hasegawa A, et al. Interleukin (IL)-17A stimulates IL-8 secretion, cyclooxygenase-2 expression, and cell proliferation of endometriotic stromal cells. *Endocrinology.* 2008;149(3):1260-7.
204. Ahn SH, Edwards AK, Singh SS, Young SL, Lessey BA, Tayade C. IL-17A Contributes to the Pathogenesis of Endometriosis by Triggering Proinflammatory Cytokines and Angiogenic Growth Factors. *J Immunol.* 2015;195(6):2591-600.
205. Hirata T, Osuga Y, Takamura M, Saito A, Hasegawa A, Koga K, et al. Interleukin-17F increases the secretion of interleukin-8 and the expression of cyclooxygenase 2 in endometriosis. *Fertil Steril.* 2011;96(1):113-7.
206. Bungum HF, Nygaard U, Vestergaard C, Martensen PM, Knudsen UB. Increased IL-25 levels in the peritoneal fluid of patients with endometriosis. *J Reprod Immunol.* 2016;114:6-9.
207. Azziz R. Polycystic Ovary Syndrome. *Obstet Gynecol.* 2018;132(2):321-36.

208. Kuang H, Duan Y, Li D, Xu Y, Ai W, Li W, et al. The role of serum inflammatory cytokines and berberine in the insulin signaling pathway among women with polycystic ovary syndrome. *PLoS One*. 2020;15(8):e0235404.
209. Özçaka Ö, Buduneli N, Ceyhan BO, Akcali A, Hannah V, Nile C, et al. Is interleukin-17 involved in the interaction between polycystic ovary syndrome and gingival inflammation? *J Periodontol*. 2013;84(12):1827-37.
210. Hesampour F, Namavar Jahromi B, Tahmasebi F, Gharesi-Fard B. Association between Interleukin-32 and Interleukin-17A Single Nucleotide Polymorphisms and Serum Levels with Polycystic Ovary Syndrome. *Iran J Allergy Asthma Immunol*. 2019;18(1):91-9.
211. Gelbaya TA, Potdar N, Jeve YB, Nardo LG. Definition and epidemiology of unexplained infertility. *Obstet Gynecol Surv*. 2014;69(2):109-15.
212. Ozkan ZS, Deveci D, Kumbak B, Simsek M, Ilhan F, Sekercioglu S, et al. What is the impact of Th1/Th2 ratio, SOCS3, IL17, and IL35 levels in unexplained infertility? *J Reprod Immunol*. 2014;103:53-8.
213. Yang H, Gao C, Wang X, Qiu F, Wei M, Xia F. Associations between vaginal flora, MIP-1 α , IL-17A, and clinical pregnancy rate in AIH. *Am J Reprod Immunol*. 2022:e13543.
214. Crosby DA, Glover LE, Brennan EP, Kelly P, Cormican P, Moran B, et al. Dysregulation of the interleukin-17A pathway in endometrial tissue from women with unexplained infertility affects pregnancy outcome following assisted reproductive treatment. *Hum Reprod*. 2020.
215. Griebel CP, Halvorsen J, Golemon TB, Day AA. Management of spontaneous abortion. *Am Fam Physician*. 2005;72(7):1243-50.
216. Wang WJ, Hao CF, Qu QL, Wang X, Qiu LH, Lin QD. The deregulation of regulatory T cells on interleukin-17-producing T helper cells in patients with unexplained early recurrent miscarriage. *Hum Reprod*. 2010;25(10):2591-6.
217. Wang WJ, Hao CF, Yi L, Yin GJ, Bao SH, Qiu LH, et al. Increased prevalence of T helper 17 (Th17) cells in peripheral blood and decidua in unexplained recurrent spontaneous abortion patients. *J Reprod Immunol*. 2010;84(2):164-70.
218. Lee SK, Kim JY, Hur SE, Kim CJ, Na BJ, Lee M, et al. An imbalance in interleukin-17-producing T and Foxp3⁺ regulatory T cells in women with idiopathic recurrent pregnancy loss. *Hum Reprod*. 2011;26(11):2964-71.
219. Nakashima A, Ito M, Shima T, Bac ND, Hidaka T, Saito S. Accumulation of IL-17-positive cells in decidua of inevitable abortion cases. *Am J Reprod Immunol*. 2010;64(1):4-11.
220. Najafi S, Hadinedoushan H, Eslami G, Aflatoonian A. Association of IL-17A and IL-17 F gene polymorphisms with recurrent pregnancy loss in Iranian women. *J Assist Reprod Genet*. 2014;31(11):1491-6.
221. Zidan HE, Rezk NA, Alnemr AA, Moniem MI. Interleukin-17 and leptin genes polymorphisms and their levels in relation to recurrent pregnancy loss in Egyptian females. *Immunogenetics*. 2015;67(11-12):665-73.
222. Giannubilo SR, Landi B, Pozzi V, Sartini D, Cecati M, Stortoni P, et al. The involvement of inflammatory cytokines in the pathogenesis of recurrent miscarriage. *Cytokine*. 2012;58(1):50-6.
223. Li N, Saghafi N, Ghaneifar Z, Rezaee SA, Rafatpanah H, Abdollahi E. Evaluation of the Effects of 1,25VitD3 on Inflammatory Responses and IL-25 Expression. *Front Genet*. 2021;12:779494.
224. Phipps EA, Thadhani R, Benzing T, Karumanchi SA. Pre-eclampsia: pathogenesis, novel diagnostics and therapies. *Nat Rev Nephrol*. 2019;15(5):275-89.
225. Molvarec A, Czegle I, Szijártó J, Rigó J, Jr. Increased circulating interleukin-17 levels in preeclampsia. *J Reprod Immunol*. 2015;112:53-7.
226. Santner-Nanan B, Peek MJ, Khanam R, Richarts L, Zhu E, Fazekas de St Groth B, et al. Systemic increase in the ratio between Foxp3⁺ and IL-17-producing CD4⁺ T cells in healthy pregnancy but not in preeclampsia. *J Immunol*. 2009;183(11):7023-30.

227. Walsh SW, Nugent WH, Archer KJ, Al Dulaimi M, Washington SL, Strauss JF, 3rd. Epigenetic Regulation of Interleukin-17-Related Genes and Their Potential Roles in Neutrophil Vascular Infiltration in Preeclampsia. *Reprod Sci.* 2022;29(1):154-62.
228. Wang J, Wen ZQ, Cheng XY, Mei TY, Chen ZF, Su LX. siRNA-mediated knockdown of T-bet and ROR γ t contributes to decreased inflammation in pre-eclampsia. *Mol Med Rep.* 2017;16(5):6368-75.
229. Murray EJ, Gumusoglu SB, Santillan DA, Santillan MK. Manipulating CD4+ T Cell Pathways to Prevent Preeclampsia. *Front Bioeng Biotechnol.* 2021;9:811417.
230. Duncan JW, Nemeth Z, Hildebrandt E, Granger JP, Ryan MJ, Drummond HA. Interleukin-17 induces hypertension but does not impair cerebrovascular function in pregnant rats. *Pregnancy Hypertens.* 2021;24:50-7.
231. Liu S, Sun Y, Tang Y, Hu R, Zhou Q, Li X. IL-25 promotes trophoblast proliferation and invasion via binding with IL-17RB and associated with PE. *Hypertens Pregnancy.* 2021;40(3):209-17.
232. Shields CA, Tardo GA, Wang X, Giachelli C, Cornelius DC. IL-25 Supplementation Induces M2 Macrophage Polarization, Reduces Blood Pressure, and Improves Fetal Weight in Placental Ischemic Rats. *Faseb j.* 2022;36 Suppl 1.
233. Bashiri A, Halper KI, Orvieto R. Recurrent Implantation Failure-update overview on etiology, diagnosis, treatment and future directions. *Reproductive Biology and Endocrinology.* 2018;16(1):121.
234. Sheikhsari G, Soltani-Zangbar MS, Pourmoghadam Z, Kamrani A, Azizi R, Aghebati-Maleki L, et al. Oxidative stress, inflammatory settings, and microRNA regulation in the recurrent implantation failure patients with metabolic syndrome. *Am J Reprod Immunol.* 2019;82(4):e13170.
235. Rundell K, Panchal B. Preterm Labor: Prevention and Management. *Am Fam Physician.* 2017;95(6):366-72.
236. Ito M, Nakashima A, Hidaka T, Okabe M, Bac ND, Ina S, et al. A role for IL-17 in induction of an inflammation at the fetomaternal interface in preterm labour. *J Reprod Immunol.* 2010;84(1):75-85.
237. Hosseini S, Shokri F, Ansari Pour S, Jeddi-Tehrani M, Nikoo S, Yousefi M, et al. A shift in the balance of T17 and Treg cells in menstrual blood of women with unexplained recurrent spontaneous abortion. *J Reprod Immunol.* 2016;116:13-22.
238. Jabalie G, Ahmadi M, Koushaeian L, Eghbal-Fard S, Mehdizadeh A, Kamrani A, et al. Metabolic syndrome mediates proinflammatory responses of inflammatory cells in preeclampsia. *Am J Reprod Immunol.* 2019;81(3):e13086.
239. Wang WJ, Zhang H, Chen ZQ, Zhang W, Liu XM, Fang JY, et al. Endometrial TGF- β , IL-10, IL-17 and autophagy are dysregulated in women with recurrent implantation failure with chronic endometritis. *Reprod Biol Endocrinol.* 2019;17(1):2.
240. Cowell W, Colicino E, Lee AG, Bosquet Enlow M, Flom JD, Berin C, et al. Data-driven discovery of mid-pregnancy immune markers associated with maternal lifetime stress: results from an urban pre-birth cohort. *Stress.* 2020;23(3):349-58.
241. Owczarek W, Walecka I, Lesiak A, Czajkowski R, Reich A, Zerda I, et al. The use of biological drugs in psoriasis patients prior to pregnancy, during pregnancy and lactation: a review of current clinical guidelines. *Postepy Dermatol Alergol.* 2020;37(6):821-30.
242. Gerosa M, Argolini LM, Artusi C, Chighizola CB. The use of biologics and small molecules in pregnant patients with rheumatic diseases. *Expert Rev Clin Pharmacol.* 2018;11(10):987-98.
243. Warren RB, Reich K, Langley RG, Strober B, Gladman D, Deodhar A, et al. Secukinumab in pregnancy: outcomes in psoriasis, psoriatic arthritis and ankylosing spondylitis from the global safety database. *Br J Dermatol.* 2018;179(5):1205-7.
244. Gallo L, Ruggiero A, Balato A, Megna M, Fabbrocini G. Secukinumab during pregnancy: a case report and review of literature. *J Dermatolog Treat.* 2022;33(1):585-6.

245. Clarke DO, Hilbish KG, Waters DG, Newcomb DL, Chellman GJ. Assessment of ixekizumab, an interleukin-17A monoclonal antibody, for potential effects on reproduction and development, including immune system function, in cynomolgus monkeys. *Reprod Toxicol*. 2015;58:160-73.
246. Egeberg A, Iversen L, Kimball AB, Kelly S, Grace E, Patel H, et al. Pregnancy outcomes in patients with psoriasis, psoriatic arthritis, or axial spondyloarthritis receiving ixekizumab. *J Dermatolog Treat*. 2021:1-7.
247. Cornelius DC, Hogg JP, Scott J, Wallace K, Herse F, Moseley J, et al. Administration of interleukin-17 soluble receptor C suppresses TH17 cells, oxidative stress, and hypertension in response to placental ischemia during pregnancy. *Hypertension*. 2013;62(6):1068-73.
248. Travis OK, White D, Baik C, Giachelli C, Thompson W, Stubbs C, et al. Interleukin-17 signaling mediates cytolytic natural killer cell activation in response to placental ischemia. *Am J Physiol Regul Integr Comp Physiol*. 2020;318(6):R1036-r46.
249. Ravel J, Gajer P, Abdo Z, Schneider GM, Koenig SS, McCulle SL, et al. Vaginal microbiome of reproductive-age women. *Proc Natl Acad Sci U S A*. 2011;108 Suppl 1(Suppl 1):4680-7.
250. Chen C, Song X, Wei W, Zhong H, Dai J, Lan Z, et al. The microbiota continuum along the female reproductive tract and its relation to uterine-related diseases. *Nat Commun*. 2017;8(1):875.
251. Gajer P, Brotman RM, Bai G, Sakamoto J, Schütte UM, Zhong X, et al. Temporal dynamics of the human vaginal microbiota. *Sci Transl Med*. 2012;4(132):132ra52.
252. Srinivasan S, Liu C, Mitchell CM, Fiedler TL, Thomas KK, Agnew KJ, et al. Temporal variability of human vaginal bacteria and relationship with bacterial vaginosis. *PloS one*. 2010;5(4):e10197-e.
253. Farage M, Maibach H. Lifetime changes in the vulva and vagina. *Archives of Gynecology and Obstetrics*. 2006;273(4):195-202.
254. Mitchell CM, Haick A, Nkwopara E, Garcia R, Rendi M, Agnew K, et al. Colonization of the upper genital tract by vaginal bacterial species in nonpregnant women. *Am J Obstet Gynecol*. 2015;212(5):611.e1-.e6119.
255. Moreno I, Codoñer FM, Vilella F, Valbuena D, Martinez-Blanch JF, Jimenez-Almazán J, et al. Evidence that the endometrial microbiota has an effect on implantation success or failure. *Am J Obstet Gynecol*. 2016;215(6):684-703.
256. Khan KN, Fujishita A, Masumoto H, Muto H, Kitajima M, Masuzaki H, et al. Molecular detection of intrauterine microbial colonization in women with endometriosis. *Eur J Obstet Gynecol Reprod Biol*. 2016;199:69-75.
257. Fransiak JM, Werner MD, Juneau CR, Tao X, Landis J, Zhan Y, et al. Endometrial microbiome at the time of embryo transfer: next-generation sequencing of the 16S ribosomal subunit. *J Assist Reprod Genet*. 2016;33(1):129-36.
258. Sola-Leyva A, Andrés-León E, Molina NM, Terron-Camero LC, Plaza-Díaz J, Sáez-Lara MJ, et al. Mapping the entire functionally active endometrial microbiota. *Hum Reprod*. 2021;36(4):1021-31.
259. Baker JM, Chase DM, Herbst-Kralovetz MM. Uterine Microbiota: Residents, Tourists, or Invaders? *Front Immunol*. 2018;9:208.
260. Kim D, Hofstaedter CE, Zhao C, Mattei L, Tanes C, Clarke E, et al. Optimizing methods and dodging pitfalls in microbiome research.
261. Amabebe E, Anumba DOC. Female Gut and Genital Tract Microbiota-Induced Crosstalk and Differential Effects of Short-Chain Fatty Acids on Immune Sequelae. *Front Immunol*. 2020;11:2184.
262. de Goffau MC, Lager S, Sovio U, Gaccioli F, Cook E, Peacock SJ, et al. Human placenta has no microbiome but can contain potential pathogens. *Nature*. 2019;572(7769):329-34.

263. Leiby JS, McCormick K, Sherrill-Mix S, Clarke EL, Kessler LR, Taylor LJ, et al. Lack of detection of a human placenta microbiome in samples from preterm and term deliveries. *Microbiome*. 2018;6(1):196.
264. Carosso A, Revelli A, Gennarelli G, Canosa S, Cosma S, Borella F, et al. Controlled ovarian stimulation and progesterone supplementation affect vaginal and endometrial microbiota in IVF cycles: a pilot study. *J Assist Reprod Genet*. 2020;37(9):2315-26.
265. Aagaard K, Riehle K, Ma J, Segata N, Mistretta T-A, Coarfa C, et al. A Metagenomic Approach to Characterization of the Vaginal Microbiome Signature in Pregnancy. *PLOS ONE*. 2012;7(6):e36466.
266. DiGiulio Daniel B, Callahan Benjamin J, McMurdie Paul J, Costello Elizabeth K, Lyell Deirdre J, Robaczewska A, et al. Temporal and spatial variation of the human microbiota during pregnancy. *Proceedings of the National Academy of Sciences*. 2015;112(35):11060-5.
267. Romero R, Hassan SS, Gajer P, Tarca AL, Fadrosh DW, Nikita L, et al. Correction: The composition and stability of the vaginal microbiota of normal pregnant women is different from that of non-pregnant women. *Microbiome*. 2014;2(1):10.
268. Moreno I, Franasiak JM. Endometrial microbiota—new player in town. *Fertility and Sterility*. 2017;108(1):32-9.
269. Aagaard K, Ma J, Antony KM, Ganu R, Petrosino J, Versalovic J. The placenta harbors a unique microbiome. *Sci Transl Med*. 2014;6(237):237ra65.
270. Sisti G, Kanninen TT, Witkin SS. Maternal immunity and pregnancy outcome: focus on preconception and autophagy. *Genes & Immunity*. 2016;17(1):1-7.
271. O'Hanlon DE, Moench TR, Cone RA. Vaginal pH and microbicidal lactic acid when lactobacilli dominate the microbiota. *PLoS One*. 2013;8(11):e80074.
272. Ojala T, Kankainen M, Castro J, Cerca N, Edelman S, Westerlund-Wikström B, et al. Comparative genomics of *Lactobacillus crispatus* suggests novel mechanisms for the competitive exclusion of *Gardnerella vaginalis*. *BMC Genomics*. 2014;15:1070.
273. Aldunate M, Srbinovski D, Hearps AC, Latham CF, Ramsland PA, Gugasyan R, et al. Antimicrobial and immune modulatory effects of lactic acid and short chain fatty acids produced by vaginal microbiota associated with eubiosis and bacterial vaginosis. *Front Physiol*. 2015;6:164.
274. Campisciano G, Florian F, D'Eustacchio A, Stanković D, Ricci G, De Seta F, et al. Subclinical alteration of the cervical-vaginal microbiome in women with idiopathic infertility. *J Cell Physiol*. 2017;232(7):1681-8.
275. Eckert LO, Moore DE, Patton DL, Agnew KJ, Eschenbach DA. Relationship of vaginal bacteria and inflammation with conception and early pregnancy loss following in-vitro fertilization. *Infect Dis Obstet Gynecol*. 2003;11(1):11-7.
276. Haahr T, Jensen JS, Thomsen L, Duus L, Rygaard K, Humaidan P. Abnormal vaginal microbiota may be associated with poor reproductive outcomes: a prospective study in IVF patients. *Hum Reprod*. 2016;31(4):795-803.
277. Bracewell-Milnes T, Saso S, Nikolaou D, Norman-Taylor J, Johnson M, Thum MY. Investigating the effect of an abnormal cervico-vaginal and endometrial microbiome on assisted reproductive technologies: A systematic review. *Am J Reprod Immunol*. 2018;80(5):e13037.
278. Vergaro P, Tiscornia G, Barragán M, García D, Rodríguez A, Santaló J, et al. Vaginal microbiota profile at the time of embryo transfer does not affect live birth rate in IVF cycles with donated oocytes. *Reprod Biomed Online*. 2019;38(6):883-91.
279. Moore DE, Soules MR, Klein NA, Fujimoto VY, Agnew KJ, Eschenbach DA. Bacteria in the transfer catheter tip influence the live-birth rate after in vitro fertilization. *Fertil Steril*. 2000;74(6):1118-24.
280. Hashimoto T, Kyono K. Does dysbiotic endometrium affect blastocyst implantation in IVF patients? *J Assist Reprod Genet*. 2019;36(12):2471-9.

281. Blaskewicz CD, Pudney J, Anderson DJ. Structure and function of intercellular junctions in human cervical and vaginal mucosal epithelia. *Biol Reprod.* 2011;85(1):97-104.
282. Zeng R, Li X, Gorodeski GI. Estrogen abrogates transcervical tight junctional resistance by acceleration of occludin modulation. *J Clin Endocrinol Metab.* 2004;89(10):5145-55.
283. Elstein M. Functions and physical properties of mucus in the female genital tract. *Br Med Bull.* 1978;34(1):83-8.
284. Amarante-Mendes GP, Adjemian S, Branco LM, Zanetti LC, Weinlich R, Bortoluci KR. Pattern Recognition Receptors and the Host Cell Death Molecular Machinery. *Frontiers in Immunology.* 2018;9.
285. Wira CR, Fahey JV, Sentman CL, Pioli PA, Shen L. Innate and adaptive immunity in female genital tract: cellular responses and interactions. *Immunol Rev.* 2005;206:306-35.
286. Fazeli A, Bruce C, Anumba DO. Characterization of Toll-like receptors in the female reproductive tract in humans. *Human Reproduction.* 2005;20(5):1372-8.
287. Fichorova RN, Cronin AO, Lien E, Anderson DJ, Ingalls RR. Response to *Neisseria gonorrhoeae* by cervicovaginal epithelial cells occurs in the absence of toll-like receptor 4-mediated signaling. *J Immunol.* 2002;168(5):2424-32.
288. Schaefer TM, Fahey JV, Wright JA, Wira CR. Innate immunity in the human female reproductive tract: antiviral response of uterine epithelial cells to the TLR3 agonist poly(I:C). *J Immunol.* 2005;174(2):992-1002.
289. Hirata T, Osuga Y, Hirota Y, Koga K, Yoshino O, Harada M, et al. Evidence for the presence of toll-like receptor 4 system in the human endometrium. *J Clin Endocrinol Metab.* 2005;90(1):548-56.
290. King AE, Horne AW, Hombach-Klonisch S, Mason JI, Critchley HO. Differential expression and regulation of nuclear oligomerization domain proteins NOD1 and NOD2 in human endometrium: a potential role in innate immune protection and menstruation. *Mol Hum Reprod.* 2009;15(5):311-9.
291. Azlan A, Salamonsen LA, Hutchison J, Evans J. Endometrial inflammasome activation accompanies menstruation and may have implications for systemic inflammatory events of the menstrual cycle. *Hum Reprod.* 2020;35(6):1363-76.
292. Kelly P, Meade KG, O'Farrelly C. Non-canonical Inflammasome-Mediated IL-1 β Production by Primary Endometrial Epithelial and Stromal Fibroblast Cells Is NLRP3 and Caspase-4 Dependent. *Front Immunol.* 2019;10:102.
293. Cheng X, Zhang Y, Ma J, Wang S, Ma R, Ge X, et al. NLRP3 promotes endometrial receptivity by inducing epithelial-mesenchymal transition of the endometrial epithelium. *Mol Hum Reprod.* 2021;27(11).
294. Drannik AG, Nag K, Yao XD, Henrick BM, Sallenave JM, Rosenthal KL. Trappin-2/elafin modulate innate immune responses of human endometrial epithelial cells to PolyI:C. *PLoS One.* 2012;7(4):e35866.
295. Carneiro LC, Bedford C, Jacca S, Rosamilia A, de Lima VF, Donofrio G, et al. Coordinated Role of Toll-Like Receptor-3 and Retinoic Acid-Inducible Gene-1 in the Innate Response of Bovine Endometrial Cells to Virus. *Front Immunol.* 2017;8:996.
296. Qu H, Li L, Wang TL, Seckin T, Segars J, Shih IM. Epithelial Cells in Endometriosis and Adenomyosis Upregulate STING Expression. *Reprod Sci.* 2020;27(6):1276-84.
297. Wallace PK, Yeaman GR, Johnson K, Collins JE, Guyre PM, Wira CR. MHC class II expression and antigen presentation by human endometrial cells. *J Steroid Biochem Mol Biol.* 2001;76(1-5):203-11.
298. Wira CR, Rossoll RM. Antigen-presenting cells in the female reproductive tract: influence of sex hormones on antigen presentation in the vagina. *Immunology.* 1995;84(4):505-8.

299. Wira CR, Rossoll RM. Oestradiol regulation of antigen presentation by uterine stromal cells: role of transforming growth factor-beta production by epithelial cells in mediating antigen-presenting cell function. *Immunology*. 2003;109(3):398-406.
300. Lillard JW, Jr., Boyaka PN, Chertov O, Oppenheim JJ, McGhee JR. Mechanisms for induction of acquired host immunity by neutrophil peptide defensins. *Proceedings of the National Academy of Sciences of the United States of America*. 1999;96(2):651-6.
301. Wan M, van der Does AM, Tang X, Lindbom L, Agerberth B, Haeggström JZ. Antimicrobial peptide LL-37 promotes bacterial phagocytosis by human macrophages. *J Leukoc Biol*. 2014;95(6):971-81.
302. King AE, Critchley HO, Kelly RW. Presence of secretory leukocyte protease inhibitor in human endometrium and first trimester decidua suggests an antibacterial protective role. *Mol Hum Reprod*. 2000;6(2):191-6.
303. Wira CR, Fahey JV, Rodriguez-Garcia M, Shen Z, Patel MV. Regulation of mucosal immunity in the female reproductive tract: the role of sex hormones in immune protection against sexually transmitted pathogens. *Am J Reprod Immunol*. 2014;72(2):236-58.
304. Grant KS, Wira CR. Effect of mouse uterine stromal cells on epithelial cell transepithelial resistance (TER) and TNFalpha and TGFbeta release in culture. *Biol Reprod*. 2003;69(3):1091-8.
305. Bourke NM, Achilles SL, Huang SU, Cumming HE, Lim SS, Papageorgiou I, et al. Spatiotemporal regulation of human IFNε and innate immunity in the female reproductive tract. *JCI Insight*. 2022.
306. Patel MV, Ghosh M, Fahey JV, Wira CR. Uterine epithelial cells specifically induce interferon-stimulated genes in response to polyinosinic-polycytidylic acid independently of estradiol. *PLoS One*. 2012;7(4):e35654.
307. Caballero-Campo P, Buffone MG, Benencia F, Conejo-García JR, Rinaudo PF, Gerton GL. A role for the chemokine receptor CCR6 in mammalian sperm motility and chemotaxis. *J Cell Physiol*. 2014;229(1):68-78.
308. Chang GS, Hong Y, Ko KD, Bhardwaj G, Holmes EC, Patterson RL, et al. Phylogenetic profiles reveal evolutionary relationships within the “twilight zone” of sequence similarity. *Proceedings of the National Academy of Sciences*. 2008;105(36):13474.
309. Moreno-Hagelsieb G, Latimer K. Choosing BLAST options for better detection of orthologs as reciprocal best hits. *Bioinformatics*. 2008;24(3):319-24.
310. Kumar S, Stecher G, Li M, Knyaz C, Tamura K. MEGA X: Molecular Evolutionary Genetics Analysis across Computing Platforms. *Mol Biol Evol*. 2018;35(6):1547-9.
311. Kent WJ. BLAT--the BLAST-like alignment tool. *Genome Res*. 2002;12(4):656-64.
312. Talbi S, Hamilton AE, Vo KC, Tulac S, Overgaard MT, Dosiou C, et al. Molecular phenotyping of human endometrium distinguishes menstrual cycle phases and underlying biological processes in normo-ovulatory women. *Endocrinology*. 2006;147(3):1097-121.
313. Gabriel M, Fey V, Heinosalo T, Adhikari P, Rytkönen K, Komulainen T, et al. A relational database to identify differentially expressed genes in the endometrium and endometriosis lesions. *Sci Data*. 2020;7(1):284.
314. Koot YE, van Hooff SR, Boomsma CM, van Leenen D, Groot Koerkamp MJ, Goddijn M, et al. An endometrial gene expression signature accurately predicts recurrent implantation failure after IVF. *Sci Rep*. 2016;6:19411.
315. Knox K, Baker JC. Genomic evolution of the placenta using co-option and duplication and divergence. *Genome Res*. 2008;18(5):695-705.
316. Xiao S, Diao H, Zhao F, Li R, He N, Ye X. Differential gene expression profiling of mouse uterine luminal epithelium during periimplantation. *Reprod Sci*. 2014;21(3):351-62.
317. Hansen VL, Schilkey FD, Miller RD. Transcriptomic Changes Associated with Pregnancy in a Marsupial, the Gray Short-Tailed Opossum *Monodelphis domestica*. *PLoS One*. 2016;11(9):e0161608.

318. Griffith OW, Chavan AR, Protopapas S, Maziarz J, Romero R, Wagner GP. Embryo implantation evolved from an ancestral inflammatory attachment reaction. *Proc Natl Acad Sci U S A*. 2017;114(32):E6566-e75.
319. Guernsey MW, Chuong EB, Cornelis G, Renfree MB, Baker JC. Molecular conservation of marsupial and eutherian placentation and lactation. *Elife*. 2017;6.
320. Marinić M, Mika K, Chigurupati S, Lynch VJ. Evolutionary transcriptomics implicates HAND2 in the origins of implantation and regulation of gestation length. *Elife*. 2021;10.
321. Law CW, Chen Y, Shi W, Smyth GK. voom: Precision weights unlock linear model analysis tools for RNA-seq read counts. *Genome Biol*. 2014;15(2):R29.
322. Langmead B, Salzberg SL. Fast gapped-read alignment with Bowtie 2. *Nat Methods*. 2012;9(4):357-9.
323. Liao Y, Smyth GK, Shi W. featureCounts: an efficient general purpose program for assigning sequence reads to genomic features. *Bioinformatics*. 2014;30(7):923-30.
324. Phipson B, Lee S, Majewski IJ, Alexander WS, Smyth GK. ROBUST HYPERPARAMETER ESTIMATION PROTECTS AGAINST HYPERVARIABLE GENES AND IMPROVES POWER TO DETECT DIFFERENTIAL EXPRESSION. *Ann Appl Stat*. 2016;10(2):946-63.
325. Wagner GP, Kin K, Lynch VJ. Measurement of mRNA abundance using RNA-seq data: RPKM measure is inconsistent among samples. *Theory Biosci*. 2012;131(4):281-5.
326. Sebastian-Leon P, Devesa-Peiro A, Aleman A, Parraga-Leo A, Arnau V, Pellicer A, et al. Transcriptional changes through menstrual cycle reveal a global transcriptional derepression underlying the molecular mechanism involved in the window of implantation. *Mol Hum Reprod*. 2021;27(5).
327. Broekhuizen M, Hitzerd E, van den Bosch TPP, Dumas J, Verdijk RM, van Rijn BB, et al. The Placental Innate Immune System Is Altered in Early-Onset Preeclampsia, but Not in Late-Onset Preeclampsia. *Front Immunol*. 2021;12:780043.
328. Helguera G, Eghbali M, Sforza D, Minosyan TY, Toro L, Stefani E. Changes in global gene expression in rat myometrium in transition from late pregnancy to parturition. *Physiol Genomics*. 2009;36(2):89-97.
329. Goudarzi A, Zhang D, Huang H, Barral S, Kwon Oh K, Qi S, et al. Dynamic Competing Histone H4 K5K8 Acetylation and Butyrylation Are Hallmarks of Highly Active Gene Promoters. *Molecular Cell*. 2016;62(2):169-80.
330. Chen JC, Roan NR. Isolation and Culture of Human Endometrial Epithelial Cells and Stromal Fibroblasts. *Bio Protoc*. 2015;5(20).
331. Gibson DA, Simitsidellis I, Kelepouri O, Critchley HOD, Saunders PTK. Dehydroepiandrosterone enhances decidualization in women of advanced reproductive age. *Fertil Steril*. 2018;109(4):728-34.e2.
332. Lessey BA, Ilesanmi AO, Castelbaum AJ, Yuan L, Somkuti SG, Chwalisz K, et al. Characterization of the functional progesterone receptor in an endometrial adenocarcinoma cell line (Ishikawa): progesterone-induced expression of the alpha1 integrin. *J Steroid Biochem Mol Biol*. 1996;59(1):31-9.
333. Castelbaum AJ, Ying L, Somkuti SG, Sun J, Ilesanmi AO, Lessey BA. Characterization of integrin expression in a well differentiated endometrial adenocarcinoma cell line (Ishikawa). *J Clin Endocrinol Metab*. 1997;82(1):136-42.
334. Glover LE, Bowers BE, Saeedi B, Ehrentraut SF, Campbell EL, Bayless AJ, et al. Control of creatine metabolism by HIF is an endogenous mechanism of barrier regulation in colitis. *Proc Natl Acad Sci U S A*. 2013;110(49):19820-5.
335. Toki T, Shimizu M, Takagi Y, Ashida T, Konishi I. CD10 is a Marker for Normal and Neoplastic Endometrial Stromal Cells. *International Journal of Gynecological Pathology*. 2002;21(1):41-7.
336. Gans C, Bell CJ. Vertebrates, Overview. In: Levin SA, editor. *Encyclopedia of Biodiversity*. New York: Elsevier; 2001. p. 755-66.

337. Tarver JE, dos Reis M, Mirarab S, Moran RJ, Parker S, O'Reilly JE, et al. The Interrelationships of Placental Mammals and the Limits of Phylogenetic Inference. *Genome Biology and Evolution*. 2016;8(2):330-44.
338. Selwood L. Marsupial egg and embryo coats. *Cells Tissues Organs*. 2000;166(2):208-19.
339. Stadtmauer DJ, Wagner GP. Cooperative inflammation: The recruitment of inflammatory signaling in marsupial and eutherian pregnancy. *J Reprod Immunol*. 2020;137:102626.
340. Griffiths M, McIntosh DL, Coles REA. The mammary gland of the echidna, *Tachyglossus aculeatus* with observations on the incubation of the egg and on the newly-hatched young. *Journal of Zoology*. 1969;158(3):371-86.
341. Bazer FW, Spencer TE, Johnson GA, Burghardt RC, Wu G. Comparative aspects of implantation. *REPRODUCTION*. 2009;138(2):195-209.
342. Fazleabas AT, Kim JJ, Strakova Z. Implantation: Embryonic Signals and the Modulation of the Uterine Environment—A Review. *Placenta*. 2004;25:S26-S31.
343. Roberts RM, Ealy AD, Alexenko AP, Han CS, Ezashi T. Trophoblast interferons. *Placenta*. 1999;20(4):259-64.
344. Spencer TE, Johnson GA, Bazer FW, Burghardt RC, Palmarini M. Pregnancy recognition and conceptus implantation in domestic ruminants: roles of progesterone, interferons and endogenous retroviruses. *Reprod Fertil Dev*. 2007;19(1):65-78.
345. Hinds LA, Reader M, Wernberg-Moller S, Saunders NR. Hormonal evidence for induced ovulation in *Monodelphis domestica*. *J Reprod Fertil*. 1992;95(1):303-12.
346. Renfree MB. Maternal recognition of pregnancy in marsupials. *Rev Reprod*. 2000;5(1):6-11.
347. Roberts RM, Green JA, Schulz LC. The evolution of the placenta. *Reproduction*. 2016;152(5):R179-89.
348. Selwood L, Johnson MH. Trophoblast and hypoblast in the monotreme, marsupial and eutherian mammal: evolution and origins. *Bioessays*. 2006;28(2):128-45.
349. Freyer C, Zeller U, Renfree MB. Placental Function in Two Distantly Related Marsupials. *Placenta*. 2007;28(2-3):249-57.
350. Chavan AR, Griffith OW, Wagner GP. The inflammation paradox in the evolution of mammalian pregnancy: turning a foe into a friend. *Curr Opin Genet Dev*. 2017;47:24-32.
351. Mess A, Carter AM. Evolution of the placenta during the early radiation of placental mammals. *Comp Biochem Physiol A Mol Integr Physiol*. 2007;148(4):769-79.
352. Medawar PB. Some immunological and endocrinological problems raised by the evolution of viviparity in vertebrates. *Symp Soc Exp Biol*. 1953;7:320-37.
353. Blackburn DG. SQUAMATE REPTILES AS MODEL ORGANISMS FOR THE EVOLUTION OF VIVIPARITY. *Herpetological Monographs*. 2006;20(1):131-46, 16.
354. von Stebut E, Boehncke WH, Ghoreschi K, Gori T, Kaya Z, Thaci D, et al. IL-17A in Psoriasis and Beyond: Cardiovascular and Metabolic Implications. *Front Immunol*. 2019;10:3096.
355. Miller J, Puravath AP, Orbai AM. Ixekizumab for Psoriatic Arthritis: Safety, Efficacy, and Patient Selection. *J Inflamm Res*. 2021;14:6975-91.
356. Havrdová E, Belova A, Goloborodko A, Tisserant A, Wright A, Wallstroem E, et al. Activity of secukinumab, an anti-IL-17A antibody, on brain lesions in RRMS: results from a randomized, proof-of-concept study. *J Neurol*. 2016;263(7):1287-95.
357. Dekel N, Gnainsky Y, Granot I, Racicot K, Mor G. The role of inflammation for a successful implantation. *Am J Reprod Immunol*. 2014;72(2):141-7.
358. Robinson MW, Harmon C, O'Farrelly C. Liver immunology and its role in inflammation and homeostasis. *Cell Mol Immunol*. 2016;13(3):267-76.
359. Herington JL, Guo Y, Reese J, Paria BC. Gene profiling the window of implantation: Microarray analyses from human and rodent models. *J Reprod Health Med*. 2016;2(Suppl 2):S19-s25.

360. Murphy WJ, Eizirik E, O'Brien SJ, Madsen O, Scally M, Douady CJ, et al. Resolution of the early placental mammal radiation using Bayesian phylogenetics. *Science*. 2001;294(5550):2348-51.
361. Goepfert A, Lehmann S, Wirth E, Rondeau J-M. The human IL-17A/F heterodimer: a two-faced cytokine with unique receptor recognition properties. *Scientific Reports*. 2017;7(1):8906.
362. Novacek MJ. Mammalian evolution: an early record bristling with evidence. *Curr Biol*. 1997;7(8):R489-91.
363. Miska KB, Harrison GA, Hellman L, Miller RD. The major histocompatibility complex in monotremes: an analysis of the evolution of Mhc class I genes across all three mammalian subclasses. *Immunogenetics*. 2002;54(6):381-93.
364. Belov K, Sanderson CE, Deakin JE, Wong ES, Assange D, McColl KA, et al. Characterization of the opossum immune genome provides insights into the evolution of the mammalian immune system. *Genome Res*. 2007;17(7):982-91.
365. Liu D, Hunt M, Tsai IJ. Inferring synteny between genome assemblies: a systematic evaluation. *BMC Bioinformatics*. 2018;19(1):26.
366. Koonin EV. Orthologs, Paralogs, and Evolutionary Genomics 1. *Annual Review of Genetics*. 2005;39:309-38.
367. Gunimaladevi I, Savan R, Sakai M. Identification, cloning and characterization of interleukin-17 and its family from zebrafish. *Fish Shellfish Immunol*. 2006;21(4):393-403.
368. Huang XD, Zhang H, He MX. Comparative and Evolutionary Analysis of the Interleukin 17 Gene Family in Invertebrates. *PLoS One*. 2015;10(7):e0132802.
369. Chavan AR, Griffith OW, Stadtmauer DJ, Maziarz J, Pavlicev M, Fishman R, et al. Evolution of Embryo Implantation Was Enabled by the Origin of Decidual Stromal Cells in Eutherian Mammals. *Mol Biol Evol*. 2021;38(3):1060-74.
370. Lee Y, Clinton J, Yao C, Chang SH. Interleukin-17D Promotes Pathogenicity During Infection by Suppressing CD8 T Cell Activity. *Front Immunol*. 2019;10:1172.
371. Newman AM, Liu CL, Green MR, Gentles AJ, Feng W, Xu Y, et al. Robust enumeration of cell subsets from tissue expression profiles. *Nature Methods*. 2015;12(5):453-7.
372. Laheri S, Ashary N, Bhatt P, Modi D. Oviductal glycoprotein 1 (OVGP1) is expressed by endometrial epithelium that regulates receptivity and trophoblast adhesion. *J Assist Reprod Genet*. 2018;35(8):1419-29.
373. Young SL, Lyddon TD, Jorgenson RL, Misfeldt ML. Expression of Toll-like receptors in human endometrial epithelial cells and cell lines. *Am J Reprod Immunol*. 2004;52(1):67-73.
374. Aboussahoud W, Aflatoonian R, Bruce C, Elliott S, Ward J, Newton S, et al. Expression and function of Toll-like receptors in human endometrial epithelial cell lines. *J Reprod Immunol*. 2010;84(1):41-51.
375. Rawlings TM, Makwana K, Taylor DM, Molè MA, Fishwick KJ, Tryfonos M, et al. Modelling the impact of decidual senescence on embryo implantation in human endometrial assembloids. *Elife*. 2021;10.
376. Garcia-Alonso L, Handfield LF, Roberts K, Nikolakopoulou K, Fernando RC, Gardner L, et al. Mapping the temporal and spatial dynamics of the human endometrium in vivo and in vitro. *Nat Genet*. 2021;53(12):1698-711.
377. Amabebe E, Anumba DOC. The Vaginal Microenvironment: The Physiologic Role of Lactobacilli. *Front Med (Lausanne)*. 2018;5:181-.
378. Boskey ER, Cone RA, Whaley KJ, Moench TR. Origins of vaginal acidity: high D/L lactate ratio is consistent with bacteria being the primary source. *Hum Reprod*. 2001;16(9):1809-13.
379. Witkin SS, Linhares IM. Why do lactobacilli dominate the human vaginal microbiota? *Bjog*. 2017;124(4):606-11.
380. Gong Z, Luna Y, Yu P, Fan H. Lactobacilli inactivate *Chlamydia trachomatis* through lactic acid but not H₂O₂. *PLoS One*. 2014;9(9):e107758.

381. Ng KYB, Mingels R, Morgan H, Macklon N, Cheong Y. In vivo oxygen, temperature and pH dynamics in the female reproductive tract and their importance in human conception: a systematic review. *Human Reproduction Update*. 2018;24(1):15-34.
382. Feo LG. The pH of the human uterine cavity in situ. *Am J Obstet Gynecol*. 1955;70(1):60-4.
383. Ersahin A, Celik O, Acet M, Ersahin S, Acet T, Bozkurt DK, et al. Impact of Endometrioma Resection on Eutopic Endometrium Metabolite Contents: Noninvasive Evaluation of Endometrium Receptivity. *Reprod Sci*. 2017;24(5):790-5.
384. Yurci A, Dokuzeylul Gungor N, Gurbuz T. Spectroscopy analysis of endometrial metabolites is a powerful predictor of success of embryo transfer in women with implantation failure: a preliminary study. *Gynecol Endocrinol*. 2021;37(5):415-21.
385. Preti G, Huggins GR. Cyclical changes in volatile acidic metabolites of human vaginal secretions and their relation to ovulation. *Journal of Chemical Ecology*. 1975;1(3):361-76.
386. Spiegel CA, Amsel R, Eschenbach D, Schoenknecht F, Holmes KK. Anaerobic bacteria in nonspecific vaginitis. *N Engl J Med*. 1980;303(11):601-7.
387. Yeoman CJ, Thomas SM, Miller ME, Ulanov AV, Torralba M, Lucas S, et al. A multi-omic systems-based approach reveals metabolic markers of bacterial vaginosis and insight into the disease. *PLoS One*. 2013;8(2):e56111.
388. Al-Mushrif S, Eley A, Jones BM. Inhibition of chemotaxis by organic acids from anaerobes may prevent a purulent response in bacterial vaginosis. *J Med Microbiol*. 2000;49(11):1023-30.
389. Mirmonsef P, Gilbert D, Zariffard MR, Hamaker BR, Kaur A, Landay AL, et al. The effects of commensal bacteria on innate immune responses in the female genital tract. *Am J Reprod Immunol*. 2011;65(3):190-5.
390. Iljazovic A, Roy U, Gálvez EJC, Lesker TR, Zhao B, Gronow A, et al. Perturbation of the gut microbiome by *Prevotella* spp. enhances host susceptibility to mucosal inflammation.
391. Morrison DJ, Preston T. Formation of short chain fatty acids by the gut microbiota and their impact on human metabolism. *Gut Microbes*. 2016;7(3):189-200.
392. Parada Venegas D, De la Fuente MK, Landskron G, González MJ, Quera R, Dijkstra G, et al. Short Chain Fatty Acids (SCFAs)-Mediated Gut Epithelial and Immune Regulation and Its Relevance for Inflammatory Bowel Diseases. *Front Immunol*. 2019;10:277.
393. Rivière A, Selak M, Lantin D, Leroy F, De Vuyst L. Bifidobacteria and Butyrate-Producing Colon Bacteria: Importance and Strategies for Their Stimulation in the Human Gut. *Front Microbiol*. 2016;7:979.
394. Cummings JH, Pomare EW, Branch WJ, Naylor CP, Macfarlane GT. Short chain fatty acids in human large intestine, portal, hepatic and venous blood. *Gut*. 1987;28(10):1221-7.
395. Park JH, Kotani T, Konno T, Setiawan J, Kitamura Y, Imada S, et al. Promotion of Intestinal Epithelial Cell Turnover by Commensal Bacteria: Role of Short-Chain Fatty Acids. *PLoS One*. 2016;11(5):e0156334.
396. Kelly CJ, Zheng L, Campbell EL, Saeedi B, Scholz CC, Bayless AJ, et al. Crosstalk between Microbiota-Derived Short-Chain Fatty Acids and Intestinal Epithelial HIF Augments Tissue Barrier Function. *Cell Host Microbe*. 2015;17(5):662-71.
397. Kaiko GE, Ryu SH, Koues OI, Collins PL, Solnica-Krezel L, Pearce EJ, et al. The Colonic Crypt Protects Stem Cells from Microbiota-Derived Metabolites. *Cell*. 2016;165(7):1708-20.
398. Roediger WE. Role of anaerobic bacteria in the metabolic welfare of the colonic mucosa in man. *Gut*. 1980;21(9):793-8.
399. Babidge W, Millard S, Roediger W. Sulfides impair short chain fatty acid beta-oxidation at acyl-CoA dehydrogenase level in colonocytes: implications for ulcerative colitis. *Mol Cell Biochem*. 1998;181(1-2):117-24.
400. Valenzano MC, DiGuilio K, Mercado J, Teter M, To J, Ferraro B, et al. Remodeling of Tight Junctions and Enhancement of Barrier Integrity of the CACO-2 Intestinal Epithelial Cell Layer by Micronutrients. *PLoS One*. 2015;10(7):e0133926.

401. Zheng L, Kelly CJ, Battista KD, Schaefer R, Lanis JM, Alexeev EE, et al. Microbial-Derived Butyrate Promotes Epithelial Barrier Function through IL-10 Receptor-Dependent Repression of Claudin-2. *J Immunol*. 2017;199(8):2976-84.
402. Kelly CJ, Colgan SP. Breathless in the Gut: Implications of Luminal O₂ for Microbial Pathogenicity. *Cell Host Microbe*. 2016;19(4):427-8.
403. Gaudier E, Jarry A, Blottière HM, de Coppet P, Buisine MP, Aubert JP, et al. Butyrate specifically modulates MUC gene expression in intestinal epithelial goblet cells deprived of glucose. *Am J Physiol Gastrointest Liver Physiol*. 2004;287(6):G1168-74.
404. Thangaraju M, Cresci GA, Liu K, Ananth S, Gnanaprakasam JP, Browning DD, et al. GPR109A is a G-protein-coupled receptor for the bacterial fermentation product butyrate and functions as a tumor suppressor in colon. *Cancer Res*. 2009;69(7):2826-32.
405. Macia L, Tan J, Vieira AT, Leach K, Stanley D, Luong S, et al. Metabolite-sensing receptors GPR43 and GPR109A facilitate dietary fibre-induced gut homeostasis through regulation of the inflammasome. *Nat Commun*. 2015;6:6734.
406. Cox MA, Jackson J, Stanton M, Rojas-Triana A, Bober L, Laverty M, et al. Short-chain fatty acids act as antiinflammatory mediators by regulating prostaglandin E(2) and cytokines. *World J Gastroenterol*. 2009;15(44):5549-57.
407. Schulthess J, Pandey S, Capitani M, Rue-Albrecht KC, Arnold I, Franchini F, et al. The Short Chain Fatty Acid Butyrate Imprints an Antimicrobial Program in Macrophages. *Immunity*. 2019;50(2):432-45.e7.
408. Arpaia N, Campbell C, Fan X, Dikiy S, van der Veeken J, deRoos P, et al. Metabolites produced by commensal bacteria promote peripheral regulatory T-cell generation. *Nature*. 2013;504(7480):451-5.
409. Zhang M, Zhou Q, Dorfman RG, Huang X, Fan T, Zhang H, et al. Butyrate inhibits interleukin-17 and generates Tregs to ameliorate colorectal colitis in rats. *BMC Gastroenterol*. 2016;16(1):84.
410. Chen L, Sun M, Wu W, Yang W, Huang X, Xiao Y, et al. Microbiota Metabolite Butyrate Differentially Regulates Th1 and Th17 Cells' Differentiation and Function in Induction of Colitis. *Inflamm Bowel Dis*. 2019;25(9):1450-61.
411. Glaubien R, Batra A, Fedke I, Zeitz M, Lehr HA, Leoni F, et al. Histone hyperacetylation is associated with amelioration of experimental colitis in mice. *J Immunol*. 2006;176(8):5015-22.
412. Dai Z, Ramesh V, Locasale JW. The evolving metabolic landscape of chromatin biology and epigenetics. *Nat Rev Genet*. 2020;21(12):737-53.
413. Pybus V, Onderdonk AB. Evidence for a commensal, symbiotic relationship between *Gardnerella vaginalis* and *Prevotella bivia* involving ammonia: potential significance for bacterial vaginosis. *J Infect Dis*. 1997;175(2):406-13.
414. Delgado-Diaz DJ, Tyssen D, Hayward JA, Gugasyan R, Hearps AC, Tachedjian G. Distinct Immune Responses Elicited From Cervicovaginal Epithelial Cells by Lactic Acid and Short Chain Fatty Acids Associated With Optimal and Non-optimal Vaginal Microbiota. *Front Cell Infect Microbiol*. 2019;9:446.
415. Libby EK, Pascal KE, Mordechai E, Adelson ME, Trama JP. Atopobium vaginae triggers an innate immune response in an in vitro model of bacterial vaginosis. *Microbes Infect*. 2008;10(4):439-46.
416. Eade CR, Diaz C, Wood MP, Anastos K, Patterson BK, Gupta P, et al. Identification and characterization of bacterial vaginosis-associated pathogens using a comprehensive cervical-vaginal epithelial coculture assay. *PLoS One*. 2012;7(11):e50106.
417. Draper DL, Landers DV, Krohn MA, Hillier SL, Wiesenfeld HC, Heine RP. Levels of vaginal secretory leukocyte protease inhibitor are decreased in women with lower reproductive tract infections. *Am J Obstet Gynecol*. 2000;183(5):1243-8.
418. Chen L, Shen Y, Wang C, Ding L, Zhao F, Wang M, et al. *Megasphaera elsdenii* Lactate Degradation Pattern Shifts in Rumen Acidosis Models. *Frontiers in microbiology*. 2019;10:162-.

419. van Teijlingen NH, Helgers LC, Zijlstra-Willems EM, van Hamme JL, Ribeiro CMS, Strijbis K, et al. Vaginal dysbiosis associated-bacteria *Megasphaera elsdenii* and *Prevotella timonensis* induce immune activation via dendritic cells. *J Reprod Immunol.* 2020;138:103085.
420. Mirmonsef P, Zariffard MR, Gilbert D, Makinde H, Landay AL, Spear GT. Short-chain fatty acids induce pro-inflammatory cytokine production alone and in combination with toll-like receptor ligands. *Am J Reprod Immunol.* 2012;67(5):391-400.
421. Li Y, Ye Z, Zhu J, Fang S, Meng L, Zhou C. Effects of Gut Microbiota on Host Adaptive Immunity Under Immune Homeostasis and Tumor Pathology State. *Frontiers in Immunology.* 2022;13.
422. Bunker JJ, Flynn TM, Koval JC, Shaw DG, Meisel M, McDonald BD, et al. Innate and Adaptive Humoral Responses Coat Distinct Commensal Bacteria with Immunoglobulin A. *Immunity.* 2015;43(3):541-53.
423. Atarashi K, Tanoue T, Ando M, Kamada N, Nagano Y, Narushima S, et al. Th17 Cell Induction by Adhesion of Microbes to Intestinal Epithelial Cells. *Cell.* 2015;163(2):367-80.
424. Cheng L, Yu H, Yan N, Lai K, Xiang M. Hypoxia-Inducible Factor-1 α Target Genes Contribute to Retinal Neuroprotection. *Frontiers in Cellular Neuroscience.* 2017;11.
425. Lykke MR, Becher N, Haahr T, Boedtkjer E, Jensen JS, Uldbjerg N. Vaginal, Cervical and Uterine pH in Women with Normal and Abnormal Vaginal Microbiota. *Pathogens.* 2021;10(2).
426. Srinivasan S, Morgan MT, Fiedler TL, Djukovic D, Hoffman NG, Raftery D, et al. Metabolic signatures of bacterial vaginosis. *mBio.* 2015;6(2).
427. Yang XP, Ghoreschi K, Steward-Tharp SM, Rodriguez-Canales J, Zhu J, Grainger JR, et al. Opposing regulation of the locus encoding IL-17 through direct, reciprocal actions of STAT3 and STAT5. *Nat Immunol.* 2011;12(3):247-54.
428. Harper MJ. The implantation window. *Baillieres Clin Obstet Gynaecol.* 1992;6(2):351-71.
429. Achache H, Revel A. Endometrial receptivity markers, the journey to successful embryo implantation. *Human Reproduction Update.* 2006;12(6):731-46.
430. Diedrich K, Fauser BC, Devroey P, Griesinger G. The role of the endometrium and embryo in human implantation. *Hum Reprod Update.* 2007;13(4):365-77.
431. Mariee N, Li TC, Laird SM. Expression of leukaemia inhibitory factor and interleukin 15 in endometrium of women with recurrent implantation failure after IVF; correlation with the number of endometrial natural killer cells. *Hum Reprod.* 2012;27(7):1946-54.
432. Gibson DA, Simitsidellis I, Cousins FL, Critchley HOD, Saunders PTK. Intracrine Androgens Enhance Decidualization and Modulate Expression of Human Endometrial Receptivity Genes. *Scientific Reports.* 2016;6(1):19970.
433. Paiva P, Hannan NJ, Hincks C, Meehan KL, Pruysers E, Dimitriadis E, et al. Human chorionic gonadotrophin regulates FGF2 and other cytokines produced by human endometrial epithelial cells, providing a mechanism for enhancing endometrial receptivity. *Human Reproduction.* 2011;26(5):1153-62.
434. Kong X, Li M, Shao K, Yang Y, Wang Q, Cai M. Progesterone induces cell apoptosis via the CACNA2D3/Ca²⁺/p38 MAPK pathway in endometrial cancer. *Oncol Rep.* 2020;43(1):121-32.
435. Holmberg JC, Haddad S, Wünsche V, Yang Y, Aldo PB, Gnainsky Y, et al. An in vitro model for the study of human implantation. *Am J Reprod Immunol.* 2012;67(2):169-78.
436. Tong J, Lv S, Yang J, Li H, Li W, Zhang C. Decidualization and Related Pregnancy Complications. *Maternal-Fetal Medicine.* 2022;4(1).
437. The European IVFMCfESoHR, Embryology, Wyns C, De Geyter C, Calhaz-Jorge C, Kupka MS, et al. ART in Europe, 2017: results generated from European registries by ESHRE†. *Human Reproduction Open.* 2021;2021(3):hoab026.
438. Benner M, Ferwerda G, Joosten I, van der Molen RG. How uterine microbiota might be responsible for a receptive, fertile endometrium. *Hum Reprod Update.* 2018;24(4):393-415.

439. Ahmed O, Robinson MW, O'Farrelly C. Inflammatory processes in the liver: divergent roles in homeostasis and pathology. *Cell Mol Immunol*. 2021;18(6):1375-86.
440. Chavan AR, Bhullar BA, Wagner GP. What was the ancestral function of decidual stromal cells? A model for the evolution of eutherian pregnancy. *Placenta*. 2016;40:40-51.
441. Chavan AR, Wagner GP. The fetal-maternal interface of the nine-banded armadillo: endothelial cells of maternal sinus are partially replaced by trophoblast. *Zoological Lett*. 2016;2:11.
442. Moseley TA, Haudenschild DR, Rose L, Reddi AH. Interleukin-17 family and IL-17 receptors. *Cytokine Growth Factor Rev*. 2003;14(2):155-74.
443. Fallon PG, Ballantyne SJ, Mangan NE, Barlow JL, Dasvarma A, Hewett DR, et al. Identification of an interleukin (IL)-25-dependent cell population that provides IL-4, IL-5, and IL-13 at the onset of helminth expulsion. *J Exp Med*. 2006;203(4):1105-16.
444. Gu C, Wu L, Li X. IL-17 family: cytokines, receptors and signaling. *Cytokine*. 2013;64(2):477-85.
445. Chen B, Khodadoust MS, Liu CL, Newman AM, Alizadeh AA. Profiling Tumor Infiltrating Immune Cells with CIBERSORT. *Methods Mol Biol*. 2018;1711:243-59.
446. Cua DJ, Tato CM. Innate IL-17-producing cells: the sentinels of the immune system. *Nat Rev Immunol*. 2010;10(7):479-89.
447. Enciso M, Aizpurua J, Rodríguez-Estrada B, Jurado I, Ferrández-Rives M, Rodríguez E, et al. The precise determination of the window of implantation significantly improves ART outcomes. *Sci Rep*. 2021;11(1):13420.
448. Iyer S, Acharya KR. Tying the knot: the cystine signature and molecular-recognition processes of the vascular endothelial growth factor family of angiogenic cytokines. *Febs j*. 2011;278(22):4304-22.
449. Schwarz E. Cystine knot growth factors and their functionally versatile proregions. *Biological Chemistry*. 2017;398(12):1295-308.
450. Bhattacharya A, Chatterjee S, Bhaduri U, Singh AK, Sashidhara KV, Guha R, et al. EP300 (p300) mediated histone butyrylation is critical for adipogenesis. *bioRxiv*. 2022:2021.08.01.454641.

Appendix

I. List of Materials, reagents and equipment used in the study

Table I.1: General reagents used with manufacturer details

Reagent	Company	Catalogue number
Cell Isolation and cell culture		
Alamar blue cell viability reagent	Invitrogen	DAL1025
Amphotericin B	Gibco	15290-026
Bovine Serum Albumin	Sigma-Aldrich	A9418-5G
Collagenase IV	Worthington Biochemical	LS004210
Distilled, sterile, nuclease-free water	Gibco	10977-035
DNase I	Sigma-Aldrich	DN25
Dimethyl Sulfoxide (DMSO)	Sigma-Aldrich	D2660-100ML
Ethanol	Honeywell	E7023-500ML
Fetal Bovine Serum (FBS)	Gibco	10270106
Fetal Bovine Serum (charcoal-stripped)	Gibco	A3382101
Hank's balanced saline solution	Gibco	14175-053
HEPES buffer	Gibco	15630056
Keratinocyte serum free media (KSFM)	Gibco	17005042

Keratinocyte serum free media (KSFM) supplements	Gibco	37000015
Minimim Essential Media (MEM)	Gibco	31095029
Non-essential Amino Acids	Sigma-Aldrich	M7145-100ML
Penicillin-Streptomycin	Gibco	15070-063
Phosphate buffered saline (PBS)	Gibco	14190094
Trypsin-EDTA solution	Sigma-Aldrich	t3924-500ml
RNA Isolation, cDNA synthesis and qPCR		
Agarose	Sigma-Aldrich	A9539-500G
High-Capacity cDNA Reverse Transcription Kit	Applied Biosystems	4368814
Isopropanol	Thermo-Fisher Scientific	bp2618-500
PowerUp™ SYBR™ Green Master Mix	Applied Biosystems	A25742
SYBR™ Safe DNA Gel Stain	Invitrogen	S33102
TRIzol™ Reagent	Invitrogen	15596018
Flow Cytometry		
AbC total Antibody Compensation Bead Kit	Invitrogen	A10513
Brefeldin A		
eBioscience™ Foxp3 / Transcription Factor Staining Buffer Set	eBioscience	00-5523-00
Fc block	BD Pharmingen	564220
ELISA		
1-Step Ultra TMB-ELISA	Thermo-Fisher Scientific	34029

Bovine serum albumin (BSA), Cohn fraction V	Avantor	422371X
Sulfuric Acid	Sigma-Aldrich	07208-2.5L
Tween-20	Sigma-Aldrich	P1379-500ML
Western Blotting		
Marvel Original Dried Skimmed Milk	Marvel	N/A
Methanol	TCD stores	MET001
Spectra™ Multicolor Broad Range Protein Ladder	Thermo-Fisher Scientific	26623
PVDF membrane	Bio-Rad	1620177
WesternBright ECL Spray	Advanta	K-12049-D50
Chromatin Immuno-Precipitation (ChIP)		
Formaldehyde	Sigma-Aldrich	F8775-500ML
Glycine	Thermo-Fisher Scientific	BP-381-1
Protein A Sepharose® Cl-4B	Cytiva	17-0963-03
Proteinase K	Sigma-Aldrich	P6556-5MG
PureLink™ RNase A	Invitrogen	12091021
Wizard® SV Gel and PCR Clean-Up System	Promega	A9281
Protein A Sepharose® Cl-4B	Cytiva	17-0963-03
Proteinase K	Sigma-Aldrich	P6556-5MG
PureLink™ RNase A	Invitrogen	12091021
UltraPure™ Salmon Sperm DNA Solution	Invitrogen	15632011
Wizard® SV Gel and PCR Clean-Up System	Promega	A9281

16S-sequencing		
Pathogen Lysis Tubes S	QIAGEN	19091
QIAmp UCP Pathogen Mini kit	QIAGEN	50214
Vaginal Microbiome Whole Cell Mix	ATCC	MSA-2007™

Table 1.2: Cell culture treatments

Reagent	Company	Catalogue number
8-Bromoadenosine 3',5'-cyclic monophosphate	Sigma-Aldrich	B5386
β-Estradiol	Sigma-Aldrich	E2758-250MG
Acriflavine	Sigma-Aldrich	A8126-25G
Bay 11-7082	Merck	196870-10MG
Lipofectamine RNAiMax	Invitrogen	13778030
LPS from E.coli, serotype O55:B5	Enzo	ALX-581-013-L002
Opti-MEM reduced serum medium	Gibco	31985062
Poly(I:C)	Invivogen	tlrl-pic
Progesterone	Tocris	2835
Recombinant IL-17A	Peprtech	200-17
Sodium Acetate	Sigma-Aldrich	S5636-500G
Sodium Butyrate	Sigma-Aldrich	B5887-250MG
Sodium Lactate	Sigma-Aldrich	1614308

Table 1.3: Antibodies and kits used

Reagent	Company	Catalogue number	Application
Alexa Fluor® 488 anti-human IL-17A Antibody	BioLegend	512307	Flow Cytometry
Alexa Fluor® 647 Mouse Anti-Human RORyt	BD Biosciences	563620	Flow cytometry
Human IL-8 (CXCL8) ELISA Kit	Peprotech	900-K18	ELISA
Anti-butyryl-lysine rabbit mAb	PTM Bio	PTM-301RM	ChIP
HIF-1α (D2U3T) Rabbit mAb	CST	14179S	Western Blotting
Monoclonal Anti-β-Actin antibody	Sigma-Aldrich	A5316	Western Blotting
Peroxidase AffiniPure Goat Anti-Mouse (H+L)	Jackson ImmunoResearch	115-035-146	Western Blotting
Peroxidase AffiniPure Goat Anti-Rabbit (H+L)	Jackson ImmunoResearch	111-035-144	Western Blotting
Phospho-NF-κB p65 (Ser536)Rabbit mAb	CST	3033S	Western Blotting
Zombie aqua fixable viability kit	Bio Legend	423101	Flow Cytometry

Table 1.4: Materials used with manufacturer details.

Item	Company	Catalogue number
0.2mL nuclease-free microcentrifuge tubes	Sarstedt	72.737.002
1.5mL nuclease-free microcentrifuge tubes	Thermo-Fisher Scientific	11569914
5,10 and 25mL plastic pipettes	Thermo-Fisher Scientific	Various
10, 20, 200 and 1000µL nuclease free filtered tips	Thermo-Fisher Scientific	Various
10cm petri dishes for tissue culture	Greiner Bio-One	664160
12-well flat bottom tissue culture plates	Greiner Bio-One	665180
24-well flat bottom tissue culture plates	Greiner Bio-One	662160CF
40µm cell strainer	Sarstedt	83.3945.040
70µm cell strainer	Sarstedt	83.3945.070
96-well ELISA plates	Greiner Bio-One	655061
96-well flat bottom tissue culture plates	Sigma-Aldrich	167008
Bioruptor tubes 1.5mL	Diagenode	C30010016
Flow cytometer tubes	VWR	352054
MicroAmp™ Optical 384-Well Reaction Plate	Applied Biosystems	4309849
Scalpels	Fisher	11758353
T75cm cell culture flask	Thermo-Fisher Scientific	11884235

Table I.5: Equipment used with manufacturer details.

Equipment	Company
Bioruptor Pico sonicator and water cooler	Diagenode
ChemiDoc MP Imaging system	BIO-RAD
VersaMax microplate reader	Molecular Devices
LSR Fortessa	BD Biosciences
Mini-PROTEAN® Tetra Cell gel electrophoresis cassette	BIO-RAD
Mini Trans-Blot® Cell blotting cassette	BIO-RAD
NanoDrop™ 2000 Spectrophotometer	Thermo Scientific
QuantStudio5	Applied Biosystems
Techne ³Prime Thermal cycler	Cole Parmer

Table I.6: Software used with manufacturer details or website.

Software/ Website name	Company/Website
BioRender	https://biorender.com/
Ensembl genome browser	EMBL-EBI, https://www.ensembl.org/index.html
Cibersortx	https://cibersortx.stanford.edu/
FASTQC	http://www.bioinformatics.babraham.ac.uk/projects/fastqc/
FlowJo 10.8.1	BD Biosciences
Galaxy Europe	Freiburg Galaxy Team, https://usegalaxy.eu/
Gene Expression Omnibus (GEO)	NCBI, https://www.ncbi.nlm.nih.gov/geo/
GraphPad Prism v8.0.1	Graphpad Software Inc.
Image Lab v6.1	BIO-RAD

Integrative Genomics Viewer	Broad Institute, igv.org/app
MEGA X v10.1.8	https://www.megasoftware.net/
National Center for Biotechnology Information (NCBI)	NIH, https://www.ncbi.nlm.nih.gov/
PyMOD v3.0.2	http://schubert.bio.uniroma1.it/pymod/index.html
PyMOL	Schrödinger, Inc.
QuantStudio5, Design and Analysis Software v1.5.2	Applied Biosystems
RStudio v4.2.0	https://www.rstudio.com/
SoftMax Pro v7.0.3	Molecular Devices
The Human Protein Atlas	https://www.proteinatlas.org/
University of California Santa Cruz (UCSC) genome browser	University of California Santa Cruz, https://genome-euro.ucsc.edu/index.html

II. Ethical statement for the human sample collection

Ethical statement approval for collecting biopsies to obtain hEEC and hESC cells

	<p>An tOspidéal Náisiúnta Máthreachais The National Maternity Hospital <i>Founded in 1894</i></p> <p>Sráid Holles, Baile Átha Cliath 2 • Holles Street, Dublin 2, D02 YH24 Telephone: (01) 6375100. Fax: (01) 6766623. Web: www.nmh.ie</p>	 <p>Máistir/Master: Dr. Rhona Mahony</p>
<p>PRIVATE AND CONFIDENTIAL</p>		
<p>Prof. Mary Wingfield Consultant Obstetrician and Gynaecologist Merrion Fertility Clinic National Maternity Hospital Mount Street Dublin 2</p>		
<p>Thursday 18th October 2018</p>		
<p>Our ref: EC 19.2018</p>		
<p>Re: Evaluating the Microbiome in Endometriosis</p>		
<p>Dear Mary,</p>		
<p>Thank you for submitting the above project. It was considered by the Ethic Committee on Monday 15th October 2018. I am pleased to inform you that it has received ethical approval.</p>		
<p>Best of luck with the study.</p>		
<p>Kind regards,</p>		
<p>Yours sincerely,</p>		
		
<p>Dr. John Murphy Chairman, Ethics Research Committee</p>		

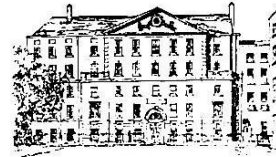
Ethical statement approval for collecting biopsies from the ART cohort



An tOspidéal Náisiúnta Máithreachais The National Maternity Hospital

Founded in 1894

Sráid Holles, Baile Átha Cliath 2 • Holles Street, Dublin 2, D02 YH21
Telephone: (01) 6373100. Fax: (01) 6766623. Web: www.nmh.ie



Máistir/Master: Dr. Rhona Mahony

PRIVATE AND CONFIDENTIAL

Dr. David Crosby,
Clinical Research Fellow,
The National Maternity Hospital,
Holles Street,
Dublin 2.

17th October 2016

Our ref: **EC 27.2016**

Re: **Endometrium, Implantation and Pregnancy.**

Dear Dr. Crosby,

The above study has now been approved.

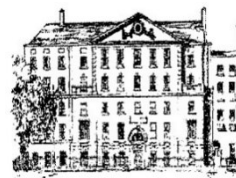
One small point if you could perhaps in the information leaflet inform people that some samples will need to leave the hospital to go to the Conway Institute for analysis.

Many thanks,
Kind regards,
Yours sincerely,

Dr. John Murphy
Chairman,
Ethics Research Committee

III. Written consent forms for human sample authorisation

Written consent form for biopsies authorisation to obtain hEEC and hESC cells



Consent Form

Title of Research Project:

Endometriosis and the microbiome

I have read the information leaflet attached.

I understand what taking part in this study entails.

I am aware that I am under no obligation to take part in the study and that if I choose not to, this will not alter my care in any way.

I agree to undergo sampling of endometrial blood during menstruation.

I agree to provide urine samples.

I agree to a blood test being taken and used for this research study.

I agree to have the following samples taken during my surgery for research purposes: endometrial biopsy.

I agree to the samples obtained being retained for the duration of the study period (maximum 10 years).

I agree to give access to the following results from my records: Age, hormone levels, pregnancy history, gynaecology history, medical history and hormonal medications used. I understand that all data will be anonymised. I have had the opportunity to discuss this study with

_____.

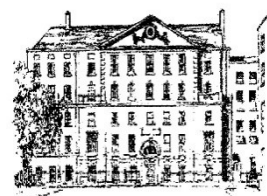
I also understand that I may leave this study at any time and without any explanation and that this will not influence my care.

I am happy to participate in this study.

Participant's name and signature: _____ Date:

MFC staff member's signature: _____ Date:

Written consent form for collecting biopsies from the ART cohort



Consent Form

Title of Research Project: Endometrium, implantation and pregnancy

I have read the information leaflet attached.

I understand what taking part in this study entails.

I am aware that I am under no obligation to take part in the study and that if I choose not to, this will not alter my care in any way.

I agree to undergo an endometrial scratch biopsy.

I agree to my endometrial scratch biopsy being used for this research study.

I agree to a blood test being taken and used for this research study.

I agree to an ultrasound scan being performed.

I agree that Merrion fertility Clinic staff may access my medical records at the clinic but that all data will be anonymised. I have had the opportunity to discuss this study with

_____.

I am happy to participate in this study.

Participant's name and signature: _____ Date:

MFC staff member's signature: _____ Date:
